Diss. ETH No. 17287

Wnt/frizzled signaling during *Xenopus laevis* pronephric kidney organogenesis

A dissertation submitted to the
Swiss Federal Institute of Technology (ETH) Zürich

for the degree of
Doctor of Natural Sciences

Presented by
Christophe Héligon

DEA biologie et santé
Université de Rennes 1

Born December 4, 1977
Citizen of France

Accepted on recommendation of

Prof. Dr. André Brändli, examiner
Prof. Dr. Dario Neri, co-examiner
Prof. Dr. Christoph Niehrs, co-examiner

2007

Table of Contents

Summary

In the present thesis, I took advantage of the *Xenopus* animal model to focus on Wnt and Frizzled (Fzd) gene functions during kidney organogenesis. Vertebrate kidney development is characterized by the formation of three distinct kidneys: the pronephros, the mesonephros, and the metanephros. While the pronephros is a simple structure composed of 1 to 3 nephrons, the metanephros is complex and can contain up to one million nephrons in humans. In mammals, most experimental studies have focused on the more complex metanephros. An alternative model to study kidney organogenesis is provided by the frog, *Xenopus laevis*. *Xenopus* embryos develop a fully functional pronephric kidney within three days. Furthermore, *Xenopus* pronephros is readily accessible to gene manipulation and marker gene expression analysis. Hence, I used here the *Xenopus* pronephros as a model to study the functions of Wnt/Fzd signaling during vertebrate kidney organogenesis. The Wnt gene family encodes for secreted glycoproteins, which bind and activate seven-pass transmembrane receptor of the Fzd gene family. Downstream of Fzd three distinct intracellular signaling pathways are activated leading to cell specification, differentiation and/or polarization. Wnt4, Wnt9b, and Wnt11 have been implicated in different steps of mouse kidney organogenesis. Interestingly, both in mouse and in *Xenopus*, Wnt4 function is required for renal tubulogenesis, which demonstrates a conserved role for Wnt4 signaling during vertebrate kidney development. Presently, it is not known, which Fzd genes function during vertebrate kidney development to mediate Wnt4 signaling.

Here, I asked here which fzd genes are implicated during pronephric kidney development in *Xenopus*. By whole-mount *in situ* hybridization, I detected that fzd3, fzd6, and fzd8 were expressed in the developing pronephric kidney. Interestingly, fzd3 was detected, similarly to wnt4, in the developing proximal tubule. fzd6 was expressed late along the entire pronephric nephron. Finally, fzd8 was expressed in the developing intermediate, distal, and connecting tubules of the pronephros. Hence, I focused my studies on analyzing fzd3, fzd6, and fzd8 gene functions and the downstream signaling pathways involved during pronephric kidney organogenesis.

I report here, that fzd3 function was required for specification of proximal tubule cells. In the absence of fzd3, no expression of proximal tubule marker genes could be detected. In addition, when expressed ectopically, fzd3 was able to induce ectopic pronephric tissue that would differentiate to proximal tubules. The fzd3 phenotype was reminiscent of the wnt4 knockdown phenotype. Using cell cultures, I was able to demonstrate that fzd3 can interact with wnt4. Taken together, fzd3 is the likely *in vivo* receptor mediating wnt4 signaling during proximal tubule development. Knockdown studies of fzd6 failed to reveal a renal phenotype. Finally, fzd8 knockdowns disrupted maturation of pronephric epithelia. Moreover, ectopic fzd8 expression suppressed the formation of proximal tubules and promoted intermediate and distal tubule cell fates. Interestingly, activation of the canonical Wnt signaling pathway or inhibition

of the planar cell polarity (PCP) pathway blocked terminal differentiation of intermediate, distal, and connecting tubules. In summary, I demonstrated that wnt4 signals via fzd3 to instruct renal precursor cells to acquire proximal tubule fate. In contrast, fzd8 appears to activate the PCP pathway to initiate terminal differentiation of intermediate, distal, and connecting tubules.

In collaboration with the laboratory of Prof. Kühl, I have also been involved in a study focusing on the role of Wnt4 signaling during eye development. Interestingly, we demonstrated that wnt4 functioned upstream of eaf2, activated the PCP pathway and was required for eye organogenesis. Furthermore, I also showed that eaf2 acted downstream of wnt4 during pronephric kidney development. Taken together, eaf2 functions as a downstream target of wnt4 in the developing eye and pronephros.

Finally, I have been involved in a collaboration with the laboratory of Prof. Carmeliet, which led to the establishment of *Xenopus* as a model to study vertebrate lymphangiogenesis.

Résumé

Dans cette thèse, j'ai utilisé le xénope comme animal modèle pour étudier la fonction des familles de gènes Wnt et Frizzled (Fzd) pendant l'organogénèse des reins. Chez les vertébrés, les reins se développent en trois phases correspondant à trois formes distinctes de reins : le pronéphros, le mésonephros et le métanephros. Alors que le pronephros, est une structure simple composée de 1 à 3 néphrons, le métanephros est un organe complexe qui peut contenir un million de nephrons chez l'humain. Le métanephros, bien que complexe, est la principale forme de rein étudiée chez les mammifères. Alternativement, le xénope peut être utilisé comme modèle animal pour l'étude du rein. En effet, les embryons du xénope développent un pronéphros totalement fonctionnel en 3 jours. De plus, la manipulation génétique ainsi que l'analyse du développement du pronéphros à l'aide de marqueurs moléculaires est assez aisée chez le xénope. En conséquence, j'ai utilisé le pronéphros du xénope comme modèle pour étudier le rôle des différents gènes membres de la famille Wnt et Fzd durant la formation des reins. Les gènes de la famille Wnt encodent des gluco-protéines sécrétées. Ces gluco-protéines peuvent interagir à la surface des cellules avec les récepteurs transmembranaires de la famille Fzd. Dans le cytoplasme, trois voies de signalisations distinctes peuvent êtres activées par les protéines Fzd. Ces signaux engendrent soit la spécialisation, la différentiation et/ou la polarisation cellulaire. Wnt4, Wnt9b et Wnt11 sont nécessaires à l'organogenèse du rein chez la souris. Plus encore, Wnt4 est nécessaire à la fois chez la souris et le xénope au début de la tubulogénèse. Ces résultats suggèrent que le rôle joué par les signaux émanant des protéines Wnt est conservé pendant l'organogenèse du rein chez les vertébrés. Actuellement, il n'est pas établi quel Fzd récepteur est utilisé par Wnt4 pendant la tubulogénèse du rein.

Ici, j'ai donc tenté d'identifier quel gène Fzd peut jouer un rôle pendant le développement du pronephros de xénope. Par hybridisation *in situ*, j'ai établi que fzd3, fzd6 et fzd8 sont exprimées dans le pronephros durant son développement. Notablement, fzd3 est exprimé dans le tubule proximal d'une façon similaire à wnt4. fzd6 est exprimé tardivement tout au long de l'épithélium du pronephros. Finalement, fzd8 est exprimé dans les tubules intermédiaires, distaux et connectant pendant l'organogénèse du rein.

Je rapporte ici, que fzd3 est nécessaire à la spécification des cellules du compartiment tubulaire proximal. En effet, en l'absence de fzd3, aucune cellule n'acquiert le caractère proximal. De plus, l'activation ectopic de fzd3 entraine le recrutement de cellules non destinées au compartiment proximal à acquérir un caractère proximal. Le phénotype généré par l'absence de fzd3 est similaire à celui observé par l'absence de wnt4. De plus, des résultats obtenus lors de cultures cellulaires suggèrent que fzd3 est le récepteur de wnt4 pendant le développement du pronephros. En résumé, fzd3 est très probablement le récepteur in vivo par lequel wnt4 signale pendant l'organogénèse du rein. L'absence de fzd6 n'a pas révélé de défauts dans le rein. Finalement, l'inhibition de fzd8 empêche la maturation de l'épithélium pronephric. De

plus, fzd8 est capable de convertir des cellules proximales en cellules plus distales. En outre, l'activation de la voie de signalisation canonical ainsi que l'inhibition de la voie de polarisation dans le plan entrainent le même phénotype que l'absence de fzd8. En résumé, j'ai démontré que wnt4 signal au travers de fzd3 pour spécifier les cellules du pronephros vers le compartiment proximal. Au contraire, fzd8 active la voie de polarisation dans le plan dans les compartiments plus postérieurs pour contrôler leur maturation.

Lors d'une collaboration avec le laboratoire du professeur Kühl, j'ai participé à l'étude du rôle de wnt4 pendant l'organogénèse des yeux. Lors de cette étude, nous avons démontré que wnt4 entraine l'expression de eaf2, l'activation de la polarisation dans le plan et est nécessaire pendant la formation des yeux. De plus, j'ai démontré que wnta entraine l'expression de eaf2 dans le rein. En résumé, eaf2 est un géne cible de wnt4 lors du développement de l'œil et du rein.

Finalement, lors d'une collaboration avec le laboratoire du professeur Carmeliet, nous avons établi que le xénope est un modèle permettant l'étude de l'angiogenèse du système lymphatique.

1. Aims of the thesis

Wnt genes are playing key roles during kidney development. Thus, elucidating their mode of action might provide valuable information for the development of therapeutic strategies aiming to the treatment of patients suffering from end stage renal diseases. The frog, *Xenopus laevis*, is a very accessible model to study gene functions during organogenesis, in particular for pronephric kidney development. Our lab has established over a hundred molecular markers to analyze specification, differentiation, and segmentation of the pronephric kidney. These tools together with other make the *Xenopus laevis* pronephric kidney a powerful model to analyze the underlying mechanisms of kidney organogenesis. Previously, our lab has established that Wnt4 function in nephrogenesis is conserved between mouse and *Xenopus*.

Based on these findings, I plan to study Wnt signaling during kidney development by:

- determining which wnt, frizzled, and sfrp genes are active during pronephric kidney organogenesis.

- elucidating, the functions and pathways activated by wnt signaling genes during pronephric kidney organogenesis.

I anticipated that these studies will provide information on the molecular mechanisms requiring Wnt signaling during kidney organogenesis. The results obtained may help to establish the signaling pathways that drive renal progenitor cells from an undetermined state to a specified and differentiated kidney cell. Hence, this work may generate valuable information that could be employed to generate in vitro defined renal cell types from stem cells for cell replacement therapies.

2. Introduction

2.1. Embryonic development

2.1.1 General principles of embryonic development

Embryonic development is a spectacular process that enables a fertilized egg to form a precisely organized multicellular organism. This process is the result of four concomitant basic cellular mechanisms: proliferation, specialization, interaction and, migration.

Cell proliferation is the serial division of one cell into two daughter cells containing the same genetic information. The resulting daughter cells might later differ, not in their genetic content, but in the genes they express. They express different sets of genes because they went through different cell specialization processes. A cell specializes as a result of sensing, integrating and finally, interpreting the different signals it receives. The major source of signals a cell receives during embryogenesis arises from interactions with other cells of the embryo. Cells interact either directly with the surrounding cells or remotely through emission and reception of signaling molecules. Signaling molecules are usually proteins, which are named inducers, morphogens, or growth factors depending on the effects they trigger. They are expressed in a strictly controlled manner forming local gradients (a few nanometers from the source) or broader gradients (several millimeters) leading to the patterning of the developing organism. The ability to respond to extracellular signals is the key feature enabling cells to coordinate their behavior at the local, organ, and organismic level. The responses to embryonic extracellular signals may trigger cell division, cell specialization, cell migration, or cell signaling.

A beautiful aspect of embryonic development and also an important scientific challenge is that cells have memory. Indeed, during development, a cell senses and integrates different signals which may imprint it. This cellular imprinting is how cells specialize. Because a signal changes the cell's memory, a cell might sense, integrate, and interpret the same signal in a different manner at different time points during embryonic development. Possibly the same signal can specialize a cell once and later specialize it even further. So with each round of cell specialization – signal memorization – cells keep remember what they are and what they are able to become.

Cell memory brings a new layer of complexity to embryonic development as one same signal can drive cells with a different history toward different specialization path but also one same signal can be used several times with different effects on the same cell during development.

One of the best studied animal models that exemplifies cell-cell interaction and cell memory during embryonic development is probably the frog *Xenopus laevis*.

2.1.2. *Xenopus laevis*, a powerful model to study organogenesis

Embryogenesis is occurring internally in higher vertebrates. In contrast, embryonic development occurs externally in lower vertebrates such as amphibians and fish. This fact permits easy access to developing embryos and thus amphibians and fish have become very attractive organisms to study embryogenesis. Historically, the establishment of amphibians as animal models to study embryology was performed in two steps. First, descriptive embryologists starting in the 19th centuryobserved and described precisely the different steps the fertilized egg undergoes until it reaches the adult state. One impressive piece of work describing *Xenopus laevis* development has been published by Nieuwkoop and Faber in 1956 (Nieuwkoop and Faber, 1956). The second contribution to amphibian animal models was brought by experimental embryologists that revealed the cellular interactions occurring during embryogenesis (Spemann and Mangold, 1924; Spemann, 1938). By removing, rearranging, and transplanting groups of cells or tissues during embryogenesis, experimental biologists obtained impressive results like reorganization of the whole embryonic body. Such microsurgery experiments are easiest performed in amphibian embryos, who arise from eggs that are usually 1 mm in diameter. Later, with improved knowledge and techniques, *Xenopus* became a very attractive model to perform more refined studies at the level of gene function during early development and organ formation. Remarkably, the knowledge gained in *Xenopus* has in most cases been relevant to mammalian embryogenesis and organogenesis.

One beauty of the *Xenopus* model is the ability to specifically target certain cell populations during the first stages of development by injecting single blastomeres. The spatial restriction of injected compounds may circumvent possible early effects that would had embryonic lethality and thus preclude analysis of organogenesis. The possibility to study later developmental events has made *Xenopus* an attractive model to study gene or signal functions during organogenesis. In this context, the first form of the embryonic kidneys, the pronephros is particularly accessible to studies in *Xenopus laevis* (Vize et al., 1997; Brändli, 1999). The embryonic cells contributing to the pronephros have been mapped precisely. The pronephros develops laterally in the embryo and is covered by a single layer of epidermis. Hence it is readily observable without further manipulation of the embryo. Finally, scientific reports dealing with the amphibian pronephric kidney can be found as early as the 19th century and since these times a considerable amount of knowledge and tools has been produced to help researchers in studying more fine mechanisms.

2.1.3. Kidney organogenesis

2.1.3.1. Physiological functions of the kidney

As part of the urinary system, the kidneys filter waste products from the blood and excrete them along with water (Woolf, 1997). The nephrons, of which one million are present in a

human kidney, are the basic filtration unit responsible for waste excretion. Blood components with a molecular weight smaller than 70 KiloDaltons are filtered through the glomeruli into the nephrons. There, nutrients like glucose, ions and other molecules needed by the organism are reabsorbed along the renal epithelium. Then, water is also reabsorbed at the level of the collecting ducts. Ultimately, only waste products and unnecessary components of the blood filtrate are discarded in the urine through the ureter. Associated with waste excretion, kidneys fulfill an important function in homeostasis. The regulation of homeostasis of body fluids by kidneys includes the control of three parameters: acid-base balance, blood pressure, and plasma volume. The acid-base balance aims to maintain the blood plasma at a neutral pH of 7.4. This is achieved by excretion of H^+-ions from the filtrate and reabsorption of bicarbonate ions that return to the blood plasma. The blood pressure is regulated by the kidneys via the renin-angiotensin system (Santos and Ferreira, 2007). Briefly, the cells of the juxtaglomerular apparatus can sense blood pressure. When blood pressure decreases, these cells secrete the proteolytic enzyme, renin. In the blood, renin will process angiotensinogen into angiotensin I, which will be in turn converted by angiotensin-converting enzyme into angiotensin II. Angiotensin II then stimulates aldosterone production by the adrenal gland. Aldosterone stimulates an increase in the reabsorption of sodium ions from kidney tubules, which causes an increase in the volume of water that is reabsorbed from the tubule. This increase in water reabsorption increases the volume of blood, which ultimately raises the blood pressure. The plasma volume is dependent on blood osmotic pressure. A lack of water causes the posterior pituitary gland to secrete antidiuretic hormone, which results in water reabsorption in the nephric duct and an increase in urine concentration. In addition to these functions mediated by the nephrons and directly related to the urinary system function, kidneys have also an important role in hormone secretion. The kidneys synthesize and secrete a variety of hormones, including erythropoietin, urodilatin, and vitamin D (Woolf, 1997).

2.1.3.2. Mammalian kidney development

During mammalian development, kidneys are present in three successive forms: the pronephros, the mesonephros and, the metanephros (Saxen and Sariola, 1987; Vize et al., 1997) (Fig. 1). All three kidneys share a similar basic structure, the nephron, and differ mainly in nephron number. Mammalian nephrons are composed of three main compartments: the renal corpuscle, the renal tubule, and the renal duct. The filtrate generated by blood filtration at the level of the corpuscle circulates through the nephric tubules. There, necessary components are reabsorbed through the epithelium and waste products are excreted via the collecting duct for release outside of the body. Renal tubules are segmented into various domains corresponding to different epithelial cell populations that fulfill distinct physiological functions (Fig. 2).

The pronephros is the first kidney formed and consists of just a few nephrons. It derives

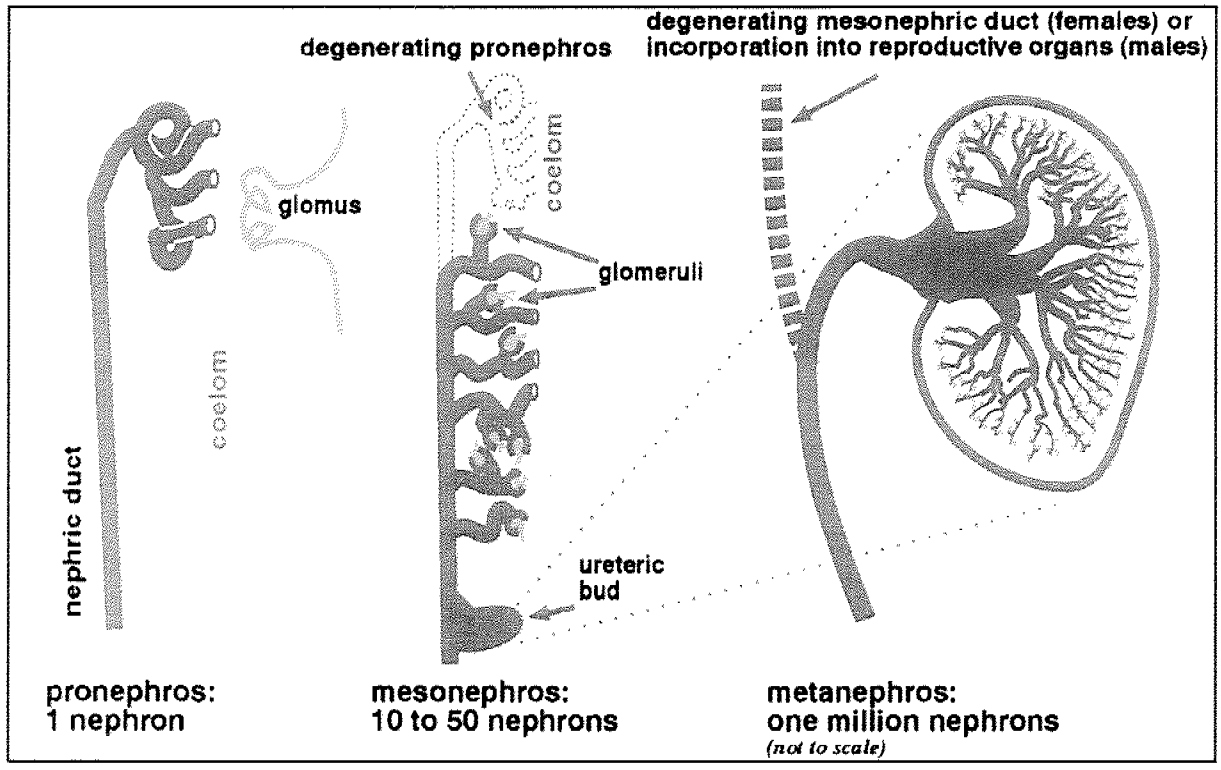

Figure 1: Different forms of vertebrate kidney during development.
The pronephros is the first form of kidney arising from the rostral mesoderm. Later the pronephric duct induces the mesonephros to form in the more caudal adjacent mesoderm. Eventually, the metanephros emerges as a result of an interaction initiated by the ureteric bud level. Figure taken from Vize et al., 1997.

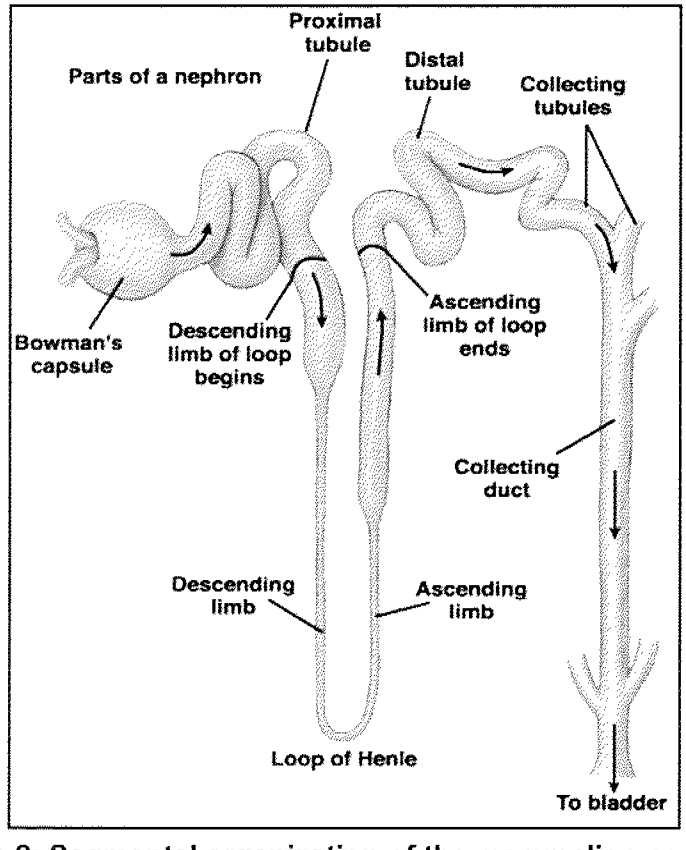

Figure 2: Segmental organization of the mammalian nephron.
Figure taken from http://sedrinne.egloos.com/2402076

from the mesodermal layer of the embryo and does not become functional in mammals. In a second step, the mesonephros arises from an induction event between the pronephric duct and the adjacent nephrogenic mesoderm. Subsequently, the pronephros will degenerate. The mesonephros is, in contrast to the pronephros, functional but still a transitory organ. Indeed, in a third step, the permanent form of the mammalian kidney, the metanephros will develop posterior to the mesonephros that will degenerate. The metanephros is the adult kidney and fulfills the excretory functions necessary to life described above (see 2.1.3.1.).

Development of pronephric and mesonephric kidneys has to date not been extensively studied in mammals. Nevertheless, some genes have been shown to play critical roles during early nephrogenesis. Pax2 homozygous mutant newborn mice lack kidneys, ureters and genital tracts. These defects are attributed to dysgenesis of both ductal and mesenchymal components of the developing urogenital system. The Wolffian and Müllerian ducts, precursors of male and female genital tracts, respectively, develop only partially and degenerate during embryogenesis. The ureters, inducers of the metanephros are absent and therefore kidney development does not take place. Mesenchyme of the nephrogenic cord fails to undergo epithelial transformation and is not able to form tubules in the mesonephros (Torres et al., 1995). In addition, both Pax2 and Pax8 are sufficient to induce the nephric lineage (Bouchard et al., 2002). Lim1 acts downstream of Pax genes and Lim1 KO leads to renal agenesis as in Pax2 KO mice (Kobayashi et al., 2005). The transcription factor odd-skipped related 1 (Osr1) is expressed in mesenchymal precursors within the mesonephric and metanephric kidney and is subsequently downregulated upon tubule differentiation. Mice lacking Osr1 do not form metanephric mesenchyme, and do not express several other factors required for metanephric kidney formation, including Eya1, Six2, Pax2, Sall1 and Gdnf (Wang et al., 2005; James et al., 2006). In addition, maintained expression of Osr1 prevents nephric gene expression and differentiation. Gata3 is expressed in the pronephric anlage, together with Pax2 and Pax8, suggesting that it may be a direct Pax2/8 target gene (Grote et al., 2006). Inactivation of Gata3 results in a massive increase in nephric duct cellularity, which is accompanied by enhanced cell proliferation and aberrant elongation of the nephric duct. At the molecular level, the nephric duct of $Gata3^{-/-}$ embryos is characterized by the loss of Ret expression and signaling (Grote et al., 2006).

In contrast to the earlier kidney forms, the induction and formation of the metanephros are well documented and the signaling networks leading to metanephros formation are emerging. Metanephros development can be divided in three phases: ureteric bud formation, ureteric bud branching, and tubulogenesis (Fig. 3).

Ureteric bud formation

Metanephros organogenesis is initiated by a reciprocal signaling between the posterior end of the nephric duct, or Wolffian duct, and the surrounding nephrogenic mesenchyme, or metanephric mesenchyme, leading to the formation of the ureteric bud (Costantini, 2006). If this initial budding fails to occur no kidney is formed resulting in renal agenesis. If bud formation

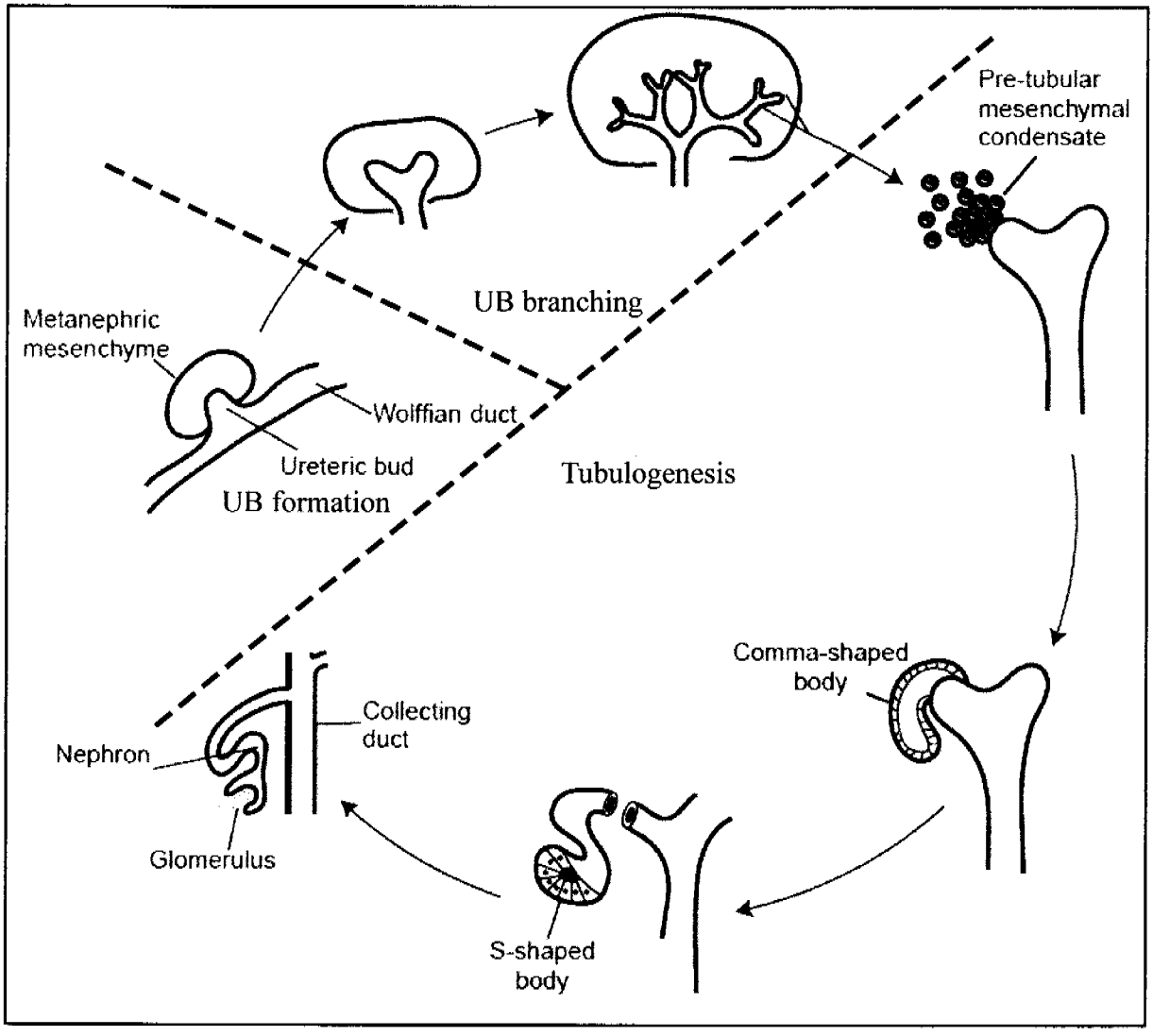

Figure 3: Processes involved in metanephros organogenesis.
The Wolffian duct is induced to form the ureteric bud (UB), which will invade the metanephric mesenchyme. The UB will then grow and branch repeatedly to form the collecting duct system. Adjacent to each bud tip, the metanephric mesenchyme will undergo a cross talk with the UB tip resulting in mesenchymal condensation and tubulogenesis. Figure adapted from Shah et al., 2004.

occurs in the wrong position, the ureter fails to connect properly to the bladder (Mackie and Stephens, 1975; Ichikawa et al., 2002). A clear example of the absence of the ureteric bud is demonstrated by WT1 deficient mice (Kreidberg et al., 1993). In this case, the nephrogenic mesenchyme is induced but no budding occurs, Pax2 expression is lost, and the mesenchyme undergoes apoptosis. Proper outgrowth of the ureteric bud is the result of a complex interplay of signals, where glial-cell-line-derived neurotrophic factor (GDNF) signaling plays a central role (Costantini and Shakya, 2006) (Fig. 4). GDNF is expressed in the metanephric mesenchyme, whereas its receptors c-Ret and GFRα1 are expressed in the whole Wolffian duct. Knockout mice for anyone of these genes display the same renal agenesis phenotype. Renal agenesis results from the absence of the ureteric bud. In those rare case, where kidneys happen to form, they are

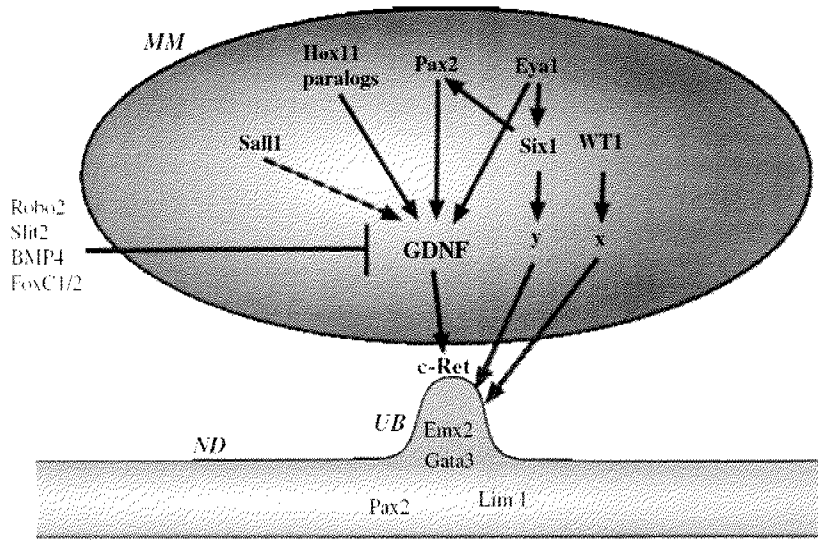

Figure 4: Genetic network involved in ureteric bud formation.
Abbreviations: ND, Nephric duct; UB, ureteric bud; MM, metanephric mesenchyme. Figure taken from Bouchard et al., 2004.

dysplastic (Schuchardt et al., 1994; Moore et al., 1996; Pichel et al., 1996; Sanchez et al., 1996; Cacalano et al., 1998; Enomoto et al., 1998). It is essential for proper ureteric bud outgrowth that GDNF signals are restricted to a particular domain of the Wollfian duct (Vega et al., 1996; Sainio et al., 1997; Shakya et al., 2005). GDNF expression is promoted by several factors expressed in the metanephric mesenchyme like Pax2, Eya1, Sall1, Hox11 (Bouchard, 2004), whereas FoxC1 and Slit2/Robo2 signal to inhibit GDNF expression from the more anterior nephrogenic mesenchyme (Kume et al., 2000; Grieshammer et al., 2004) (Fig. 4). GDNF is the inductive signal promoting ureteric bud outgrowth and its action is counterbalanced by BMP4 signals emerging from the metanephric mesenchyme as well (Miyazaki et al., 2000; Brophy et al., 2001). BMP4 action is in turn inhibited by Gremlin in the posterior metanephric mesenchyme (Michos et al., 2004). Another level of control of bud formation arises from the Wollfian duct itself which expresses Sprouty1, a negative regulator of Ras/Erk MAP kinase, required for GDNF signaling. Absence of Sprouty1 leads to the formation of multiple ureteric buds without alteration of GDNF expression, supporting the idea of a downstream or parallel pathway (Basson et al., 2005). A comprehensive review of KO mice with ureteric bud phenotypes has been published recently (Shah et al., 2004) (Table 1).

Ureteric bud branching

Once the ureteric bud has formed it invades the metanephric mesenchyme, where it will undergo complex growth, branching, and remodeling (Fig. 3). It is important to notice that the continuity of the ureteric bud epithelium and lumen are unaltered during these processes (Meyer et al., 2004). This part of kidney organogenesis is regulated by reciprocal signaling between the ureteric bud and the metanephric mesenchyme.

Heterozygous mice for both Pax2/8 genes display hypoplastic kidneys due to reduced

Table 1: Mouse mutants with defects in ureteric branching morphogenesis and the corresponding branching defects in human disease.

Gene	Location of expression	Mutant mouse phenotype	Human (naturally occurring mutation)
Ureteric bud outgrowth			
Wt1	MM	Bilateral agenesis (Kreidberg et al., 1993)	
Pax2	MM, UB	Bilateral agenesis (Torres et al., 1995)	Renal coloboma syndrome (renal agenesis/hypoplasia, optic nerve coloboma) (Sanyanusin et al., 1995)
Sall1	MM	Agenesis (32%); single hypoplastic kidney (29%); bilateral remnant kidneys (39%) (Nishinakamura et al., 2001)	Townes-Brock syndrome (anal, renal, limb, ear anomalies) (Kohlhase et al., 1998)
Eya1	MM	Bilateral agenesis (100%) (Xu et al., 1999)	Brancho-oto-renal syndrome (branchial fistulae, deafness, renal agenesis) (Abdelhak et al., 1997)
Six1		Bilateral agenesis (Xu et al., 2003)	
Hoxa11/Hoxd11	MM	Variable severity: agenesis to dysplasia. Abnormal branching with elongated primary branches (Davis et al., 1995)	
Lim1	UB	Bilateral agenesis (Shawlot and Behringer, 1995)	
Gdnf	MM	Agenesis caused by lack of UB (Pichel et al., 1996)	
Ret	UB	Bilateral agenesis (58%); unilateral agenesis (31%); decreased branching and undifferentiated MM (11%) (Schuchardt et al., 1996)	
Gfra1	MM, UB	Bilateral agenesis (76%); unilateral rudiment (23%) (Cacalano et al., 1998)	
Foxc1 (Mf1)	MM	Duplicated collecting system (Kume et al., 2000)	
Bmp4	MM	Homozygotes are lethal at E6.5; no mesoderm formation (Winnier et al., 1995). Heterozygotes have a duplicated collecting system (Dunn et al., 1997)	
Unknown			Duplicated collecting system
Early branching			
Gdnf heterozygotes	MM	Dysplasia; 30% fewer nephrons (Cullen-McEwen et al., 2001)	
Fgf7	S	Thirty percent fewer nephrons (Qiao et al., 1999b)	
Fgf10	MM	Hypoplasia (Ohuchi et al., 2000)	
Emx2	MM, UB	Bilateral agenesis secondary to failure of UB branching. Outgrowth normal (Miyamoto et al., 1997)	
Foxd1 (BF2)	S	Hypoplasia (Hatini et al., 1996)	
Rara/Rarb2	S	Fourfold decrease in the number of UB tips; 4-5 versus 8-9 branching iterations when compared with wild type (Mendelsohn et al., 1999)	
Pod1	MM	Hypoplasia and 61% decreased branching (Quaggin et al., 1999)	
Wnt4	MM	Small, dysgenic kidneys; undifferentiated MM interspersed with UB branches (Stark et al., 1994)	
Wnt11	UB	Thirty-six percent fewer nephrons (Majumdar et al., 2003)	
Itga8 (integrin α8)	MM	Bilateral dysgenesis (Muller et al., 1997)	
Kama5 (laminin α5)	MM	Dysgenesis; decreased UB branching (Miner and Li, 2000)	
Heparan sulfate 2-sulfotransferase	MM, UB	Bilateral agenesis (Bullock et al., 1998)	
Unknown			Possibly hypertension
Late branching and maturation			
Tgfb1	MM, UB	Perinatal lethal; kidneys normal (Kulkarni et al., 1993)	
Activin	MM	Perinatal lethal; kidneys normal (Jhavert et al., 1998)	
Bmp2	MM	Embryonic lethal (Zhang and Bradley, 1996)	
Unknown			Possibly hypertension
Branching termination and tubule maintenance			
Hgf	MM	Overexpression leads to cysts (Takayama et al., 1997)	
Tgfa	MM	Overexpression leads to cysts (Jhappan et al., 1990)	
Egfr	MM	Overexpression leads to cysts (Orellana et al., 1995); knockout leads to dilated collecting ducts (Threadgill et al., 1995)	
Tgfb2	MM	Cysts (Sanford et al., 1997)	
Gpc3 (glypican 3)	MM, UB	Enhanced branching, medulla degenerates by E15.5; cysts (Cano-Gauci et al., 1999)	Simpson-Golabi-Behmel syndrome (cystic overgrowth) (Pilia et al., 1996)
Pkd1, Pkd2	UB (cilia)		ADPKD (Wu and Somlo, 2000)
Invs (inversin)	UB (cilia)	Cysts (Morgan et al., 2002)	
Kif3a (kinesin)	UB (cilia)	Conditional knockout leads to cysts (Lin et al., 2003)	
Polaris	UB (cilia)	Cysts (Yoder et al., 2002)	

Abbreviations: MM, metanephric mesenchyme; S, stroma; UB, ureteric bud. Table taken from Shah et al., 2004

branching (Narlis et al., 2007). This is likely to be due to downregulation of Lim1 and Wnt11. Lim1 acts downstream of Pax genes and is necessary for induction of the pronephric lineage, proper elongation of the nephric duct, ureteric bud branching as well as tubulogenesis (Kobayashi et al., 2005; Pedersen et al., 2005). Lim1$^{-/-}$ mice display no kidneys (Shawlot and Behringer, 1995; Kobayashi et al., 2005). Pax2 expression is unaffected in Lim1 mutant mice. Using conditional Lim1 KO approaches, it has been reported that Lim1 expression acting downstream

of Pax2 is necessary for ureteric bud branching as ureteric bud are smaller and undergo few branching events in a KO background (Pedersen et al., 2005). In contrast to Pax2, Wnt9b expression is altered in this context and might account for the role of Lim1 in tubulogenesis (see below). Lim1 function seems to be independent of GDNF signaling and vice versa.

Wnt9b is expressed in the Wolffian duct and the whole ureteric bud during metanephrogenesis (Carroll et al., 2005). Disruption of the Wnt9b gene leads to an arrest of ureteric bud branching at the T-shape stage. This seems to be mainly due to impairment of ureteric bud signalling with the condensed metanephric mesenchyme and will be discussed in the next paragraph. GDNF expression is found in the metanephric mesenchyme and later restricted to the metanephric mesenchyme surrounding the ureteric bud tips. Its receptor c-Ret which is first expressed in the entire Wolffian duct, gets restricted to the ureteric bud tips once budding has occurred. Thus, only ureteric bud tip cells can respond to GDNF signals and undergo growth, branching, and remodeling in a GDNF-dependent manner (Shakya et al., 2005). How the expression domains of c-Ret and GDNF get restricted is unknown to date. GDNF signals at the ureteric bud tip induce Wnt11 expression that in turn supports GDNF expression in a positive feedback loop (Majumdar et al., 2003). Absence of Wnt11 leads to hypoplasia of the metanephros, which looks otherwise normal (Majumdar et al., 2003).

Ureteric bud tips are the main place of cell proliferation, whereas the trunks of the ureteric bud branches display poor proliferation rates (Meyer et al., 2004; Shakya et al., 2005). Tip cell proliferation can account for ureteric bud growth but further mechanisms have to be implicated in the branching process. It is not clear whether two sites of proliferation are present in the ureteric bud tip as controversy exists on this point (Meyer et al., 2004; Costantini, 2006). Apoptosis is virtually absent from the branching ureteric bud and as such cannot be considered as an active mechanism in branching (Shakya et al., 2005). In contrast, directed cell migration has been suggested as high cell motility is observed in the ureteric bud (Shakya et al., 2005). Supporting this hypothesis, GDNF is able to induce both proliferation and directed migration of ureteric bud cells in culture (Tang et al., 1998). A second branching mechanism might be a reorganization of cellular cytoskeleton leading to a purse-string like effect on the ureteric bud tip cells. Present locally at the ureteric bud tips, this mechanism could lead to the formation of T-shaped buds. This hypothesis is supported by the observation of wedge-shaped cells at the ureteric bud tips versus presence of cuboidal cells in the trunks (Meyer et al., 2004). Interestingly, Sprouty1 seems to be implicated in the branching mechanism as mice targeted for Sprouty1, in addition to ectopic ureteric buds discussed above, have an irregular and increased rate of branching (Basson et al., 2005). Sprouty effects are mediated by Wnt11.

Tubulogenesis

Branching morphogenesis leading to the formation of the collecting duct and ureter is only one aspect of kidney organogenesis. Another aspect is the induction and formation of kidney tubules in the mesenchyme adjacent to the ureteric bud tips. Tubulogenesis (or nephrogenesis)

starts with mesenchyme-to-epithelial conversion of the metanephric mesenchyme adjacent to the ureteric bud tips and later differentiation of the epithelial cells. The successive phases of tubulogenesis are commonly divided as follows: (1) condensation resulting in pretubular aggregates, (2) epithelialization of these aggregates forming the renal vesicle, (3) tubulogenesis leading the renal vesicles through the comma-shaped and the S-shaped bodies, and finally, (4) maturation resulting in the fully differentiated nephron (Fig. 5) (Yu et al., 2004). Most known gene functions and signaling pathways implicated in tubulogenesis are required during phases

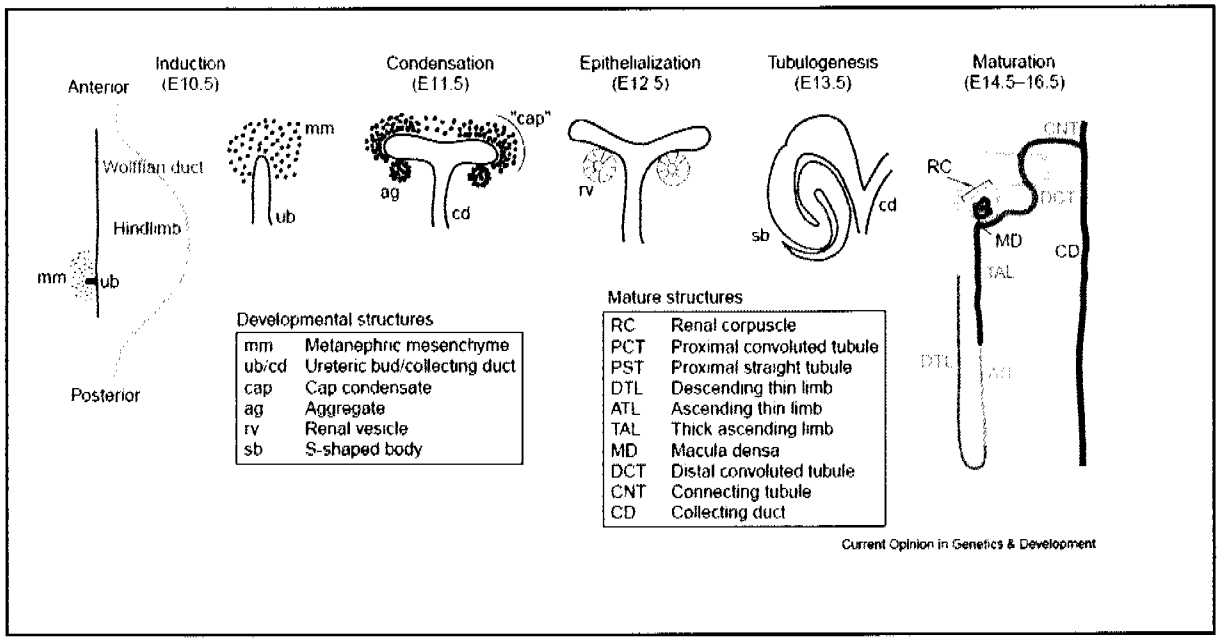

Figure 5: Scheme depicting the different stages of metanephric tubulogenesis. Tubulogenesis (or nephrogenesis) occurs in the metanephric mesenchyme adjacent to the UB tips after branching has been initiated. First, condensation is visualized by formation of cell aggregates. Then, the aggregates undergo mesenchyme-to-epithelial transformation giving rise to the renal vesicle. This epithelial structure will then be subjected to morphogenetic movments to form a tubule that will fuse with the tip of UB to form a continuous lumen. Eventually, the tubule will mature and acquire the cellular and molecular properties of a mature functional nephron. Figure taken from Yu et al., 2004.

1 or 2.

The WT1 gene, which is also expressed early during nephrogenesis, was shown to be required for metanephric development (Pritchard-Jones et al., 1990; Pelletier et al., 1991; Kreidberg et al., 1993). WT1 expression is found in the condensing mesenchyme and later derivatives as well as in glomerular structures (Pritchard-Jones et al., 1990). Mice KO for WT1 show renal agenesis resulting from metanephric mesenchyme apoptosis and absence of ureteric bud formation (Kreidberg et al., 1993). Another gene expressed early in the condensed mesenchyme is Wnt4 (Stark et al., 1994). Mice KO for Wnt4 have no nephron forming in the condensed mesenchyme. Closer examination of the rudimentary kidneys showed that mesenchyme-to-epithelial conversion does not occur (Stark et al., 1994). Despite nephron agenesis, early steps of ureteric bud branching occurred normally and Pax2 and WT1 expression

was present suggesting the Wnt4 functions downstream of WT1 and Pax2. This indicates that Wnt4, and thus nephron formation are not strictly necessary for ureteric bud branching morphogenesis. Recently, it was shown that Wnt4 expression is directly regulated by Pax2 gene function (Torban et al., 2006).

Wnt9b is another Wnt gene implicated in tubulogenesis. In contrast to Wnt4 and Wnt11, Wnt9b expression is found in the whole ureteric bud (Carroll et al., 2005). $Wnt9b^{-/-}$ mice display renal agenesis (Carroll et al., 2005). Wnt9b acts as a paracrine signal of the ureteric bud on the metanephric mesenchyme to induce renal vesicle formation through the control of Fgf8, Pax8, and Wnt4 expression in pretubular aggregates. In addition it is important to notice that the expression of Pax2, Eya1, Six2, and WT1 is unaffected in the metanephric mesenchyme of $Wnt9b^{-/-}$ mice.

The Six1 transcription factor is expressed in the metanephric mesenchyme where it is required for proper ureteric bud growth and tubulogenesis upstream of Pax2, Sall1, and GDNF (Li et al., 2003; Xu et al., 2003). Six1 function depends directly on Eya, a protein tyrosine phophatase (Li et al., 2003). The requirement of Six1 for tubulogenesis is independent of the ureteric bud phenotype as $Six1^{-/-}$ metanephric mesenchyme cocultures with spinal chords do not induce tubulogenesis as they do in a WT background (Xu et al., 2003).

In contrast, little is known about the maturation phase of tubulogenesis. Nevertheless, recent studies have shed some light. Mice harboring only one allele of Pax2 and Pax8 display a drastic inhibition of Lim1 and increased apoptosis in the metanephric mesenchyme (Narlis et al., 2007). Later, ureteric bud branches less likely as a result of Wnt11 downregulation. In this heterozygous background, the distal convoluted segment is absent or strongly reduced revealing a later role for Pax2/8 genes during the maturation step. In addition, Notch signaling has been implicated in nephron segments differentiation (Cheng et al., 2007). Notch1 and Notch2 are expressed in renal vesicles and conditional deletion of Notch2 lead to absence of glomerulus and proximal tubules. Ectopic expression of Notch1 can promote proximal tubule fates and inhibit distal tubule fates.

2.1.3.2. *Xenopus* pronephros development

In contrast to the metanephros with up to one million nephrons in humans, the pronephros is a relatively simple organ containing just a few nephrons (one in *Xenopus*) (Saxen and Sariola, 1987). Despite its simplicity, the pronephros has a nephron organization similar to the more complex kidney forms (Fig. 6). Recent studies have refined previous models of the pronephros (Saxen and Sariola, 1987; Vize et al., 1997; Brändli, 1999) and demonstrated that the *Xenopus* pronephros is composed of a filtration unit termed corpuscule (or glomerulus), a proximal tubule, an intermediate tubule, and a connecting tubule, which connects to the rectal diverticulum and cloaca (Raciti, 2007). Based on comparative gene expression analysis, it was revealed that the same tubular segments are present both in the *Xenopus* pronephros and in mammalian metanephros. This includes the connecting tubule, but not more distal parts of the

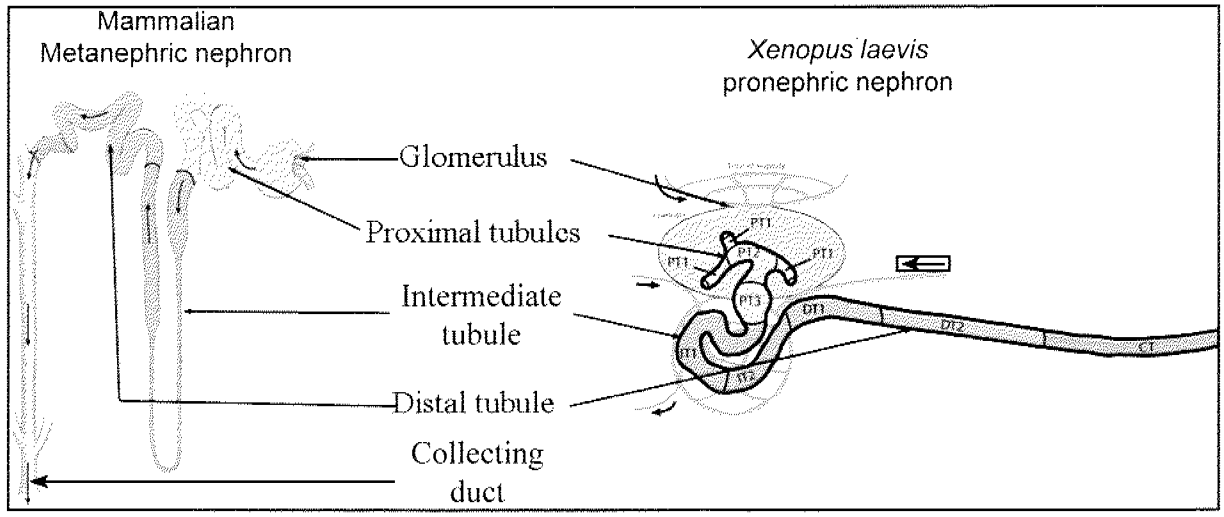

Figure 6: Comparison between mammalian metanephric and *Xenopus* pronephric nephron segmentation.
The organization of the two nephrons is very similar. The blood filtrate from the glomerulus goes through the proximal tubules subdivided in three subsegments (S1, S2, S3 in mammals, PT1, PT2, PT3 in *Xenopus*). Then it enters the intermediate tubule. Next, the filtrate passes the distal and connecting tubules. In Mammals the filtrate is transfered to the collecting duct before excretion. This later segment is absent from *Xenopus* pronephros based on marker genes expression (Raciti, 2007). Abbreviations:PT, proximal tubules; IT, intermediate tubules; DT, distal tubules; CT, Connecting tubule.
Figure adapted from Raciti, 2007.

collecting duct system (Fig. 6). The collecting duct system's main physiologic role in mammals is to reabsorb water. This function might not be required in *Xenopus* tadpoles as they live in fresh water.

Like later kidney forms, the pronephros derives from the intermediate mesoderm lateral to the anterior somites (Nieuwkoop and Faber, 1956; Vize et al., 1997; Brändli, 1999). Pronephros formation is very similar to metanephric tubulogenesis both on the cellular and molecular levels. Indeed, during pronephros formation the intermediate mesenchyme below the somites 3 to 7 undergoes mesenchyme-to-epithelial conversion and later maturation – differentiation – of the epithelial cells to give rise to a functional segmented renal epithelium (Vize et al., 1997). Cell condensation can be morphologically observed at stage 22. A lumen surrounded by an epithelium appears at stage 30/31. During this process the most distal domain of the pronephric anlage elongates caudally parallel to the somites to fuse with the rectal diverticulum at about stage 37. At this point, the heart starts to beat and the pronephros becomes functional (Nieuwkoop and Faber, 1956).

At the molecular level, the first signs of nephric lineage specification are observed much earlier at stage 13 when pax8 and lim1 start to be expressed (Taira et al., 1994; Heller and Brändli, 1999). Pax8 knockdown using morpholino antisense leads to pronephros agenesis (Ghanbari, 2003). Similarly, lim1 function is required for pronephric development (Chan et al., 2000). Slightly later, pax2 expression is detected (Heller and Brändli, 1997) but its function is dispensable (Ghanbari, 2003). At around stage 20, wnt4 expression is detected in the anterior

part of the pronephric anlage, just before cell condensation (Saulnier et al., 2002). Wnt4 function is necessary for tubulogenesis (Saulnier et al., 2002). Another component of the wnt signaling pathway, fzd8, is expressed from stage 20 on in the most caudal part of kidney anlage and later gets restricted to the intermediate and distal segments of the pronephros. fzd8 gene knockdown interferes with pronephros development (Satow et al., 2004). In this context, distal pronephric segments fail to undergo terminal differentiation and, in some cases, loss of proximal pronephric cell marker genes is observed. Ultimately, fzd8 gene knockdown leads to edema formation.

Interestingly, the role of Wnt genes has been largely investigated in the context of the developing kidney and showed to play critical functions conserved among species. Still elusive is the molecular context and signal transduction triggered downstream of those Wnt proteins.

2.2. Wnt signaling

Cell-to-cell communication is vital throughout the development of multicellular organisms. One way in which communication is achieved is through the secretion of signaling molecules that are received by neighboring responding cells. The Wnt family of signaling proteins participates in multiple developmental events during embryogenesis and has also been implicated in adult tissue homeostasis. Wnt signals are pleiotropic, with effects that include mitogenic stimulation, cell fate specification, and differentiation. Wnt signals are also often involved in disease, in particular cancer, reinforcing the concept that cancer is a form of development gone awry (Nusse, 2005; Clevers, 2006).

The interaction of Wnt proteins with their receptors on the cell surface is the first step in transducing an extracellular signal into intracellular responses (Wodarz and Nusse, 1998; Cong et al., 2004b). Frizzled proteins, which are members of the family of seven-pass transmembrane receptors, have been identified as Wnt receptors (Bhanot et al., 1996; Yang-Snyder et al., 1996). Together with Fzd proteins, the Wnt/β-catenin pathway requires single-pass transmembrane proteins that belong to a subfamily of Low-Density Lipoprotein (LDL) Receptor-related Proteins (LRPs): LRP5 and LRP6 (He et al., 2004). In addition to Wnts and Frizzled, there are many other extracellular and cell surface molecules that regulate Wnt signaling. For example, the extracellular secreted frizzled-related protein (SFRP), Dickkopf (Dkk), and SOST/Sclerostin can inhibit the Wnt signaling, whereas Norrin and R-spondin as well as some SFRPs activate it, and the cell surface molecules Ror, Ryk and Kremen bind to Wnt, LRPs and/or Dkk and regulate the intracellular signaling. This complexity makes it difficult to analyze the direct relationship between ligands and receptors.

The complexity is also met intracellulary, where three intracellular Wnt signaling pathways have been described (Huelsken and Behrens, 2002; Gordon and Nusse, 2006). First reported, the activation of the canonical or β-catenin dependent pathway activation prevents β-catenin degradation by the proteasome. β-catenin accumulates and translocates to the nucleus, where it can activate together with Lef/Tcf transcription factors target gene expression. The planar cell polarity (PCP) pathway acts directly on the cytoskeleton as well as on gene transcription to polarize the cell. Finally, the calcium-dependent pathway is thought to act via G-proteins, protein kinase C (PKC), CAM kinase, and NF-AT to induce changes in gene transcription.

Here after, I will describe in greater detail the structure and functions associated with Wnts, Frizzled, SFRP proteins, and the different Wnt-activated signaling pathways.

2.2.1. The Wnt gene family

Wingless (wg) in *Drosophila* and Wnt1 (first called int-1) are the founding members of the Wnt

gene family. the wg gene was first found in *Drosophila*, where mutant alleles had frequent wing absence and notum duplication or lethal segment polarity phenotypes (Sharma and Chopra, 1976; Nusslein-Volhard and Wieschaus, 1980). Working on the origin of mammary cancer, Nusse and Varmus (1982) found retroviral insertional mutations in mouse tumors at the Wnt1 (int-1) gene, later to be identified as the mouse homolog of wg (Baker, 1987; Rijsewijk et al., 1987).

Table 2: List of human, mouse and Xenopus laevis Wnt, frizzled, and SFRP genes.

gene	human	mouse	*Xenopus laevis*	
Wnt1	7855	22408	*X56845*	
Wnt2	7472	22413	378675	
Wnt2B	7482	22414	*U66288*	
Wnt3	7473	22415	*M55054*	
Wnt3A	89780	22416	*L07538*	
Wnt4	54361	22417	397706	
Wnt4B				
Wnt5A	7474	22418	*M55056*	
Wnt5B	81029	22419	*X73510*	
Wnt6	7475	22420	378676	
Wnt7A	7476	22421	378677	
Wnt7B	7477	22422	*L07534*	
Wnt7C			378678	
Wnt8A	7478	20890	397970	
Wnt8B	7479	22423	*XLU22173*	
Wnt9A	7483	216795	-	
Wnt9B	7484	22412	-	
Wnt10A	80326	22409	378674	
Wnt10B	7480	22410	-	
Wnt11	7481	22411	399441	
Wnt-16	51384	93735	-	

gene	human	mouse	*Xenopus laevis*	
Fzd1	8321	14362	373817	
Fzd2	2535	57265	399141	
Fzd3	7976	14365	399190	
Fzd4	8322	14366	399192	
Fzd5	7855	14367	373834	
Fzd6	8323	14368		
Fzd7	8324	14369	378787	
Fzd8	8325	14370	373690	399367
Fzd9	8326	14371		
Fzd10	11211	93897	387604	387605

SFRP1	6422	20377	394302	
SFRP2	6423	20319	380355	
SFRP3	2487	20378	779159	399085
SFRP4	6424	20379		
SFRP5	6425	54612	399205	
crescent			398184	
sizzled			398029	

Each gene is represented with the GeneID, if available. Otherwise, the GenBank accession number is given (*italic*). The Wnt4B gene is known in zebrafish only, whereas Wnt7C has been described in *Xenopus* only. Crescent and sizzled genes are not found in mammalian genomes.

In the human genome, the Wnt gene family is comprised of nineteen members (Table 2) ranging in molecular weight from 39 kDa (WNT7a) to 46 kDa (WNT10a). Homologous genes have been identified in various multicellular organisms ranging from the sea anemone *Nematostella vectensis* (five Wnt genes in its genome) to mammals (Kusserow et al., 2005). Wnts have been defined by amino acid sequence homology rather than by functional properties (Nusse and Varmus, 1992; Miller, 2002). Human Wnt proteins share 27% to 83% aminoacid sequence identity, have an amino terminal signal peptide, and a characteristic conserved pattern of 23 or 24 cysteine residues (Fig. 7). The conserved cysteine residues present in all the Wnts suggests that Wnt proteins have several intramolecular disulfide bonds necessary for their function. This hypothesis has not been proven to date because Wnt proteins are highly insoluble

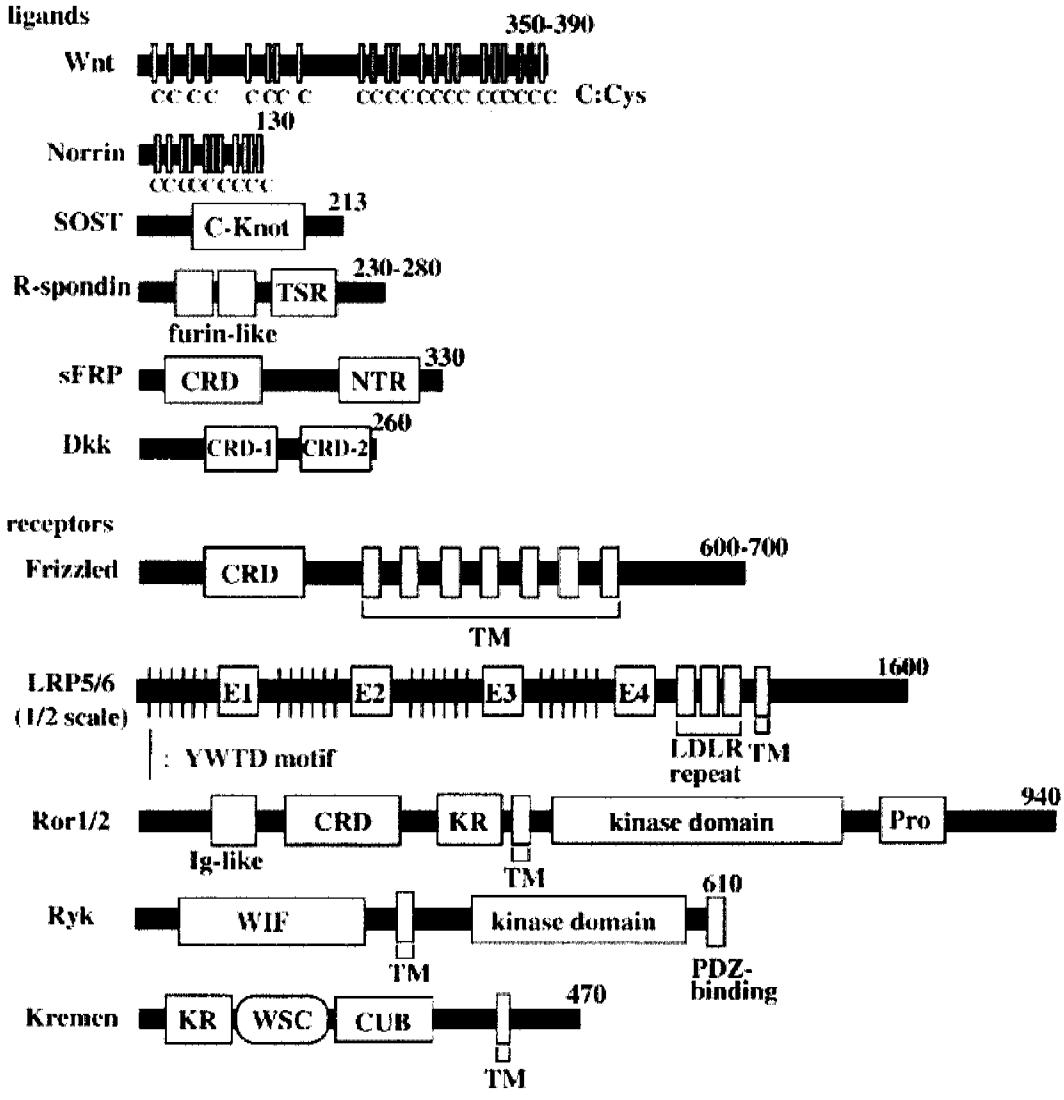

Figure 7: Structure of Wnt signaling ligands and receptors.
The range of amino acid residues foung in the proteins of each gene family is indicated at the upper right extremity of the structure. Abbreviations: C-Knot, Cysteine knot motif; TSR, Thrombospondin type I domain; CRD, cysteine rich domain; NTR, Netrin-like domain; TM, Transmembrane domain; E, EGF-like domain; KR, kringle domain; Pro, proline-rich domain ; WIF, Wnt-inhibitory factor domain; WSC, cell wall integrity and stress response component domain; CUB, C1q-Uegf-BMP-1 domain. Figure taken from Kikuchi et al., 2006.

and no active Wnt could be purified until recently (Willert et al., 2003). The solubility issue was unexpected but can be at least partially explained by post-translational acetylation (palmitoyl acid on Cys77 and palmitoleic acid on Ser209 in murine Wnt3A) (Willert et al., 2003; Takada et al., 2006; Kurayoshi et al., 2007). Wnt palmitoylation on Cys77 is necessary for its function and may in addition tether a certain portion of the secreted protein to the membrane of the producing cell and in this way lead to a local increase of Wnt protein concentration (Willert et al., 2003). N-glycosylations are another kind of post-translational modification that have been reported for Wnt proteins (Wnt-1, -3a, -5a, -5b, -6 and, -7b) (Smolich et al., 1993). In contrast to the palmitoylation, N-glycosylation seems to be dispensable for signaling, but critical for

secretion (Mason et al., 1992; Kurayoshi et al., 2007).

Wnt secretion has been largely underinvestigated compared to the later Wnt-induced signaling cascades. As it has been reported for other proteins, glycosylation might be involved in targeting Wnt proteins to the appropriate exocytic route (Tanaka et al., 2002) and it might also affect the extracellular spreading of Wnt proteins (Vincent and Dubois, 2002; Eaton, 2006). Trafficking of extracellular Wnts is dependent on extracellular matrix components, in particular heparin sulfate proteoglycans (HSPGs). HSPGs are also believed to play a role in the release of Wnt proteins from the surface of the producing cell (Eaton, 2006).

Critical aspects of Wnt secretion are the previously described lipid modifications. For instance, only the serine attached palmitoleic acid, but not the cystein linked palmitoylation, is necessary for correct Wnt intracellular targeting and secretion (Hausmann and Basler, 2006). The acetyltransferase porcupine, a putative multipass transmembrane protein of the membrane-bound O-acetyltransferase superfamily, seems to be catalyzing both types of Wnt acetylations (Kadowaki et al., 1996; Thorpe et al., 1997; Hofmann, 2000; Tanaka et al., 2000; Caricasole et al., 2002). Wnt secretion is dependent on porcupine function (van den Heuvel et al., 1989; van den Heuvel et al., 1993) and blocking acetylation on Ser209 of Wnt3A phenocopies loss of porcupine (Takada et al., 2006). More recently found, Wntless (WLS) (also named Evenness interrupted (Evi) or Sprinter), encoding a multipass transmembrane protein, is essential and dedicated to Wnt protein secretion (Banziger et al., 2006; Bartscherer et al., 2006; Goodman et al., 2006). How and where WLS interacts with Wnt during the secretion process is still unclear (Banziger et al., 2006; Bartscherer et al., 2006). One possibility is that WLS functions in loading Wnt proteins onto lipoprotein particles or in forming Wnt multimers. Indeed, it was recently proposed that Wnts may be loaded onto lipoprotein particles to facilitate long-range signaling (Panakova et al., 2005; Eaton, 2006). Wnt proteins might also form multimers and thereby overcome their hydrophobicity and potentiate their own signaling capacity (Miller, 2002). Secreted Wnt proteins are either tethered to the producing cell membrane via their acetyl groups or circulating in the extracellular space. There, they might interact with components of the extracellular matrix like HSPGs (Eaton, 2006), with circulating proteins like SFRPs, or with receptor proteins at the cell surface to trigger signals.

Wnt genes have been first classified into two groups (Table 3) based on their ability to induce (1) transformation of the mouse mammary epithelial cell line C57MG (Wong et al., 1994), (2) β-catenin stabilization, and (3) axis duplication in *Xenopus* embryos (McMahon and Moon, 1989; Sokol et al., 1991; Du et al., 1995) (Table 3). Wnt genes able to function in these assays, where then classified as Wnts acting in the canonical pathway. This included Wnt1, Wnt2, Wnt3A, and others. In contrast, other Wnt proteins (such as Wnt4 and Wnt5A) were thought to be unable to act in these assays. This turns out to be partially wrong as the ability of Wnt gene products to activate canonical signaling reflects their ability to form an appropriate ternary Wnt-Frizzled-LRP complex (He et al., 1997; Liu et al., 2005; Mikels and Nusse, 2006). Thus, initiation of canonical signaling by Wnt proteins depends not only on intrinsic Wnt

properties but also on the presence of the proper receptors at the cell surface.

Gene	Induces axis duplication
WNT1	Yes
WNT2	Yes
WNT2B	-
WNT3	-
WNT3A	Yes
WNT4	No
WNT5A	No
WNT5B	-
WNT6	No
WNT7A	-
WNT7B	Yes
WNT8A	Yes
WNT8B	Yes
WNT10A	-
WNT10B	-
WNT11	Yes / No
WNT16	-

Table 3: Capacity of Wnt genes to induce axis duplication in *Xenopus laevis*.
WNT11 was reported to induce axis duplication by Ku *et al.*, 1993, but as not able to do so in the hands of Du *et al.*, 1995.

2.2.2. The frizzled gene family

The *frizzled* locus in *Drosophila melanogaster* functions to coordinate the cytoskeleton of epidermal cells to produce a parallel array of cuticular hair and bristles (Gubb and Garcia-Bellido, 1982; Vinson and Adler, 1987). The locus turned out to contain one gene only, termed frizzled (fzd), encoding for a putative seven-pass transmembrane domain protein (Vinson et al., 1989; Adler et al., 1990). Fzd proteins were first suggested as Wnt receptors in *Drosophila* (Adler, 1992; Wong and Adler, 1993; Krasnow et al., 1995; Strutt et al., 1997) and *C. elegans* (Herman et al., 1995; Sawa et al., 1996). Direct evidence showing that Frizzled proteins are receptors for Wnt came from *Drosophila* and human cell cultures (Bhanot et al., 1996; Cadigan et al., 1998) and from studies in *Xenopus laevis* embryos (Yang-Snyder et al., 1996; He et al., 1997). Following the identification of Fzd as Wnt receptors, the study of Fzd genes took off. New Fzd genes were identified in several organisms (Wang et al., 1996). To date, Fzd genes have been characterized from *C. elegans* (whose genome contains three Fzd genes: lin-17, mom-5 and, mig-1) to mammals (ten FZD genes in the human genome). For details, see the

Wnt homepage (http://www.stanford.edu/~rnusse/wntwindow.html).

Fzd genes encode seven-pass transmembrane proteins of the G-protein-coupled receptor (GPCR) superfamily. The size of human Fzd proteins is ranging from 537 amino acids (FZD4) to 706 amino acids (FZD6). All Fzd proteins share the following structural similarities: a signal peptide sequence at the amino terminus, a conserved extracellular domain containing ten invariably spaced cysteines (called the cysteine-rich domain, CRD) necessary for Wnt binding (Dann et al., 2001; Povelones and Nusse, 2005), a seven-pass transmembrane region, and a cytoplasmic domain with little homology among members of the family (Wang et al., 1996; Wang et al., 2006a). The amino termini of Fzd proteins contain sequence motifs for potential sites of N-glycosylation, but no glycosylation of Fzd proteins has been demonstrated to date. Frizzleds appear to lack the cysteinyl residue present in some GPCRs just C-terminal to the seventh transmembrane domain that can serve as a site of reversible palmitoylation leading to a fourth intracellular loop (Bouvier et al., 1995). The C-terminal cytoplasmic tail is poorly conserved among the different Fzds. Their length ranges from 24 residues in FZD1 to 212 residues in FZD6. Two motifs have been identified within the C-terminus of Fzds. First, the C-terminal PDZ domain binding motif Ser/Thr-Xxx-Val (Kay and Kehoe, 2004) is present in most Fzd proteins (Fzd1, -2, -4, -5, -7, -8, and -10), but absent from Fzd-3, -6, and -9. The second motif, KTXXXW, is present in all Fzd proteins and is necessary but not sufficient to signal through the canonical/β-catenin pathway (Umbhauer et al., 2000; Cong et al., 2004b).

Studies aimed at establishing Fzd gene/Wnt pathway relationships based on a combination of empiric results and bioinformatic analysis failed to demonstrate any preference to a particular Wnt signaling pathway (Wang et al., 2006a). Interestingly, studies using Fzd mutants, like chimeric constructs and point mutations, demonstrated the importance of the intracellular loops I and III as well as the KTXXXW motif in the C-terminus for canonical Wnt signaling. The C-terminus has also been proposed to serve a function in targetting the receptor to the proper membrane compartment of polarized cells during protein synthesis (Wu et al., 2004). In contrast to the C-terminus, the intracellular loops are quite well conserved among different Fzd members (Wang et al., 2006a). Thus, if intracellular domains have to account, partially or completely, for pathway specificity the intracellular loops probably play an important role. Wnt glycoproteins are the main ligands for Fzd proteins and have been described in 2.2.1. The Wnt-Fzd ligand-receptor relationship has been well characterized in *Drosophila* with Kd values of about 10^{-8} M (Bhanot et al., 1996; Rulifson et al., 2000; Wu and Nusse, 2002). Nevertheless, the Wnt-Fzd specificity is poorly understood in mammals due to the larger number of Wnt and Fzd genes and the difficulty to obtain active Wnt protein preparations. Recently, two new gene families unrelated to Wnt, have been found to act as ligands for Fzd proteins: Norrin and R-spondin. Norrin is a secreted protein with a cysteine-knot motif, encoded by the Norrie disease gene (Berger et al., 1992a; Berger et al., 1992b). The Norrie disease is a X-linked congenital retinal dysfunction that, in most cases, presents with blindness at birth. The link to Wnt signaling was made due to implication of Norrin gene mutations in familial exudative vitreoretinopathy

(FEVR), which is a developmental disorder characterized by incomplete vascularization of the peripheral retina (Pendergast and Trese, 1998). Fzd4 gene is also implicated in a form a FEVR, which presents with similar vascular phenotypes as Norrin mutations (Robitaille et al., 2002). Studies based on this observation have revealed that Norrin specifically binds to Fzd4 but not to Fzd8 and that Norrin activates the β-catenin pathway through Fzd4 and LRP5 (Xu et al., 2004). The R-spondin gene family contains four members (R-spondin 1-4) that encode for secreted proteins that contain two cystein-rich, furin-like domains and one thrombospondin type I domain (Chen et al., 2002; Kamata et al., 2004). R-spondin genes activate β-catenin-dependent Wnt signaling and can synergize with Wnt ligands in this pathway (Kazanskaya et al., 2004). R-spondin can interact with LRP6 and Fzd extracellular domains, but is not sufficient to form a ternary complex with LRP6 and Fzd8 (Nam et al., 2006).

Inside the cell, frizzled proteins undergo interactions with downstream signaling molecules. One of the best characterized proteins is the cytoplasmic protein Dishevelled (Dvl/Dsh) which is implicated in both canonical and planar cell polarity pathway (Perrimon and Mahowald, 1987; Klingensmith et al., 1994; Theisen et al., 1994). Recent evidence suggests also a role in calcium-dependent Wnt signaling (Sheldahl et al., 2003). The Dvl family contains three members in mammals (Dvl-1, -2, -3) encoding for phosphoproteins composed of three domains: DIX, PDZ, and DEP. These domains serve as multiple sites of protein/protein interactions for Wnt signaling as well as in other pathways (Wharton, 2003; Malbon and Wang, 2006). Wnt binding to Fzd at the cell surface can lead to recruitment of Dvl to the cell surface, where it interacts with Fzd (Wong et al., 2003), and to its phosphorylation (Yanagawa et al., 1995; Gonzalez-Sancho et al., 2004). The DEP domain is necessary to activate planar cell polarity signaling through JNK and RhoA, whereas the DIX and PDZ domains are dispensable (Li et al., 1999b). All three Dvl domains are necessary to activate canonical Wnt signaling. Dvl proteins are key components of the Wnt signaling pathway as they may play the role of a switch between the different Wnt pathways. In addition, as members of the GPCR superfamily, Fzd proteins can interact with G proteins. Bioinformatic approaches enable the prediction of the coupling specificity of GPCR to their G proteins (Moller et al., 2001). Using the 7 TMHMM program , Fzds were subjected to analysis for probable coupling G proteins (Wang et al., 2006a). This analysis suggests that Fzd2, -4, -6, -9, and -10 can interact only with Go/i-type of G proteins. In contrast, Fzd5 and -8 associate only with Gq. Fzd1 and -7 can interact with Go/i as well as Gq. Finally, Fzd3 is the only one able to interact with Gs and can also do so with Go/i and Gq.

2.2.3. The Secreted Frizzled-Related Protein (SFRP) gene family

The first SFRP protein, frzb1, was identified simultaneously by two laboratories as an inhibitor of canonical Wnt signaling pathway that was secreted by Speman's organizer cells in the frog embryo (Leyns et al., 1997; Wang et al., 1997). Later, other SFRP genes where reported and

five are known to be present in the human genome (Jones and Jomary, 2002). SFRP genes have been reported down to the sponge *Lubomirskia baicalensis* where one gene was found (Wiens et al., 2007).

SFRP genes encode for secreted proteins containing a N-terminal signal peptide followed by a frizzled-like CRD, and a C-terminal netrin domain (Leyns et al., 1997; Rattner et al., 1997; Wang et al., 1997). Both domains have been reported to bind Wnt proteins independently (Lin et al., 1997; Uren et al., 2000). The presence of two binding sites for Wnt proteins with different affinities has been postulated to be responsible for biphasic modulation of Wnt signaling (Uren et al., 2000). The netrin domain would enhance Wnt activity by presenting Wnt proteins to their receptors in an appropriate manner, whereas the lower affinity CRD would trap Wnt proteins and so inhibit their Fzd receptor binding.

2.2.4. Wnt signaling pathways

Binding of Wnt proteins to their cell surface receptors elicits different intracellular responses: the canonical/β-catenin, the planar cell polarity (PCP) or, the calcium-dependent pathway (Fig. 8). The reasons for this differential response are unknown and might be due to the Wnt itself and its ability to form a binary Wnt-Frizzled or a ternary Wnt-Frizzled-LRP complex as well as the presence of the appropriate intracellular components. The formation of a ternary receptor Wnt-Fzd-LRP complex is necessary to induce canonical Wnt signaling, whereas the binary receptor complex is sufficient to signal through the PCP or the calcium-dependent pathway. The three pathways also require common intracellular proteins that interact with the receptor complex, namely, Dvl and G proteins. Downstream of these common proteins the three different pathways seem to be non-overlapping, even if they can still modulate one another.

2.2.4.1. The canonical Wnt signaling pathway

The canonical signaling pathway is initiated with the formation of the ternary Wnt-Fzd-LRP protein complex at the cell surface. During this early event the LRP5/6 intracellular "tails" are activated by several phosphorylation events in a caseine kinase-1γ dependent manner (Davidson et al., 2005; Zeng et al., 2005). This complex will then recruits the cytoplasmic Dvl protein to the intracellular portion of the receptor complex and induces Dvl phosphorylation. Dvl can directly interact with Fzd proteins. However, it remains unclear whether this interaction occurs during canonical signaling (Wong et al., 2003). Similarly, it is unclear how Dvl phosphorylation is controlled and how it acts in Wnt signaling. It has been reported that caseine kinase 1ε, caseine kinase 2, and PAR1 can mediate Dvl phosphorylation (Willert et al., 1997; Sun et al., 2001; Cong et al., 2004a; Ossipova et al., 2005). Both Dvl and LRP5/6 in their phosphorylated forms can bind to Axin, a member of the β-catenin phosphorylation complex. In the absence of Wnt, the β-catenin phosphorylation complex is composed of Axin, GSK3β, adenomatous Polyposis

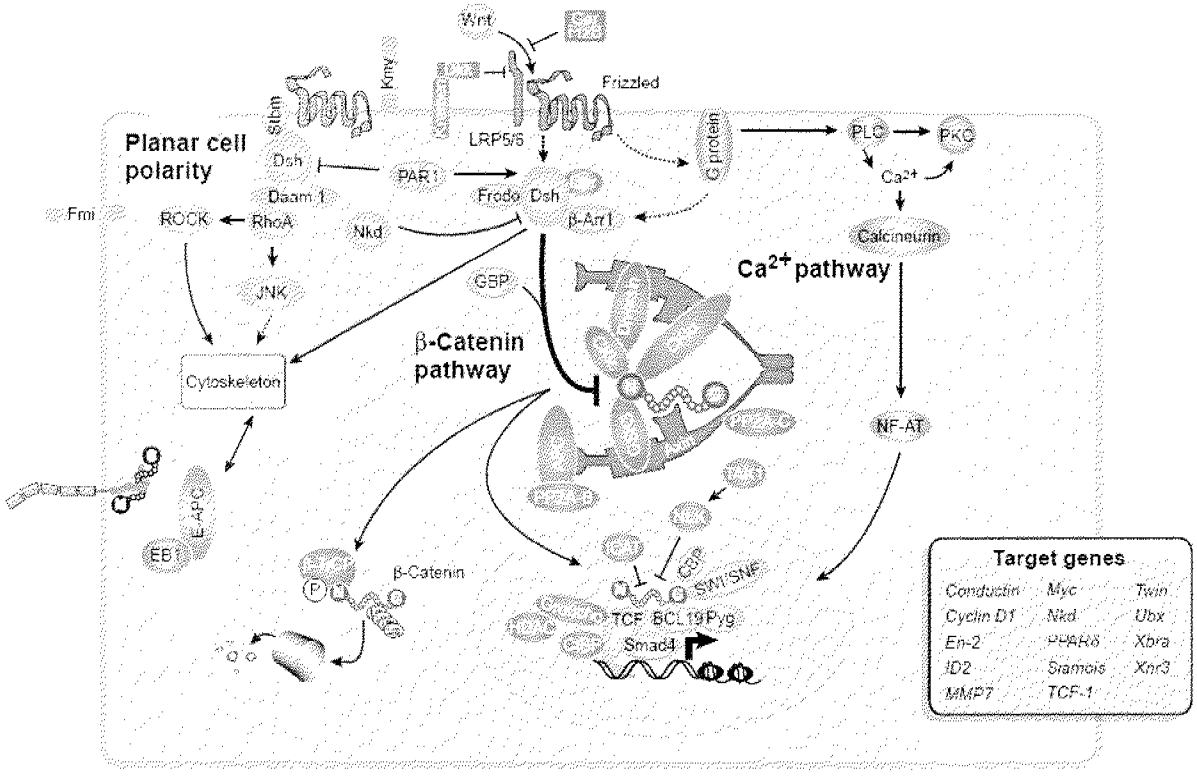

Figure 8: Wnt/Fzd signaling pathways.
Wnt binds to its cell surface receptor, Frizzled, or the receptor complex, Frizzled-LRP, to trigger non-canonical pathways (planar cell polarity, orange; or calcium-depedent, green) or β-catenin pathway (blue) activation, respectively. Activation of the planar cell polarity pathway induces changes in the cell cytoskeleton leading to acquisition of a polarity in the plane. Activation of the canonical or β-catenin dependent pathway inhibits β-catenin degradation by the proteasome, which leads to β-catenin accumulation and translocation to the nucleus. There, it acts as a transcriptional co-activator along with transcription factors of the LEF/TCF gene family. The other non-canonical pathway is calcium-dependent and acts through trimeric G proteins, phospholipase C (PLC), protein kinase C (PKC) and calcineurin to activate NF-AT transcription factor. Figure taken from Huelsken et al., 2002.

Coli (APC), and other proteins. It phosphorylates β-catenin that, in turn, gets ubiquitinated and targeted for degradation. Canonical Wnt signaling downstream of Dvl/LRP may cause the sequestration of Axin and inhibit its function in the phosphorylation complex. It is also known that Dvl can bind Axin and inhibits its function (Fagotto et al., 1999; Kishida et al., 1999; Li et al., 1999a; Smalley et al., 1999). In turn, β-catenin is stabilized leading to its accumulation in the cytoplasm and translocation to the nucleus where it acts as a co-activator of Lef/Tcf transcription factors to induce target genes expression (Brunner et al., 1997; van de Wetering et al., 1997; Daniels and Weis, 2005). While there are four Lef/Tcf family members in vertebrates, only one is known in *Drosophila*. In absence of nuclear localized β-catenin, Lef/Tcf transcription factors interact with Groucho and the histone deacetylase to form a transcription inhibition complex repressing expression of Wnt target genes (Cavallo et al., 1998; Chen et al., 1999; Daniels and Weis, 2005). β-catenin interacts with several other proteins in the nucleus (Gordon and Nusse, 2006). A pair of proteins, Legless (Lgs) and Pygopus (Pygo), is of particular interest as they are

necessary and seem to be dedicated to canonical Wnt signaling (Kramps et al., 2002; Parker et al., 2002; Thompson et al., 2002). Lgs can bind β-catenin directly and as such serve as an adaptor to recruit Pygo to the transcription complex. Then, Pygo functions as a necessary co-activator of transcription. Other proteins are involved in regulating canonical Wnt signaling at the level of the nucleus, such as the MAP kinase like protein NLK/Nemo or APC, which has in the nucleus a different function from the cytoplasmic one. The details of intranuclear regulation have been recently reviewed (Moon et al., 2004; Nusse, 2005; Clevers, 2006; Gordon and Nusse, 2006).

Once the β-catenin/Tcf-dependent transcription complex is formed, it induces expression of target genes, which is determined by the Tcf recognition sequence (ADATCAAAGG) in their promoters (van de Wetering et al., 1997). The availability of these binding sites is determined by the developmental identity of the cell and its physiological status. For a comprehensive overview of TCF target genes identified in diverse biological systems see the Wnt homepage (http://www.stanford.edu/~rnusse/wntwindow.html). The genes induced are then dependent on the cell state. Canonical Wnt signaling has been shown to play critical roles in cell differentiation and stem cell maintenance (Willert et al., 2003; Kleber and Sommer, 2004).

2.2.4.2. The non-canonical Wnt signaling pathways

The calcium-dependent Wnt pathway

Wnt binding to Fzd proteins at the cell surface can lead to the release of intracellular calcium through G proteins (Slusarski et al., 1997a; Sheldahl et al., 1999; Westfall et al., 2003). This signaling pathway is Dvl-dependent and activates calmodulin-dependent protein kinase II (CamKII) and protein kinase C (PKC) (Sheldahl et al., 1999; Kuhl et al., 2000; Sheldahl et al., 2003). Then downstream of CamKII, calcineurin dephosphorylates the transcription factor NF-AT which leads to an accumulation of NF-AT in the nucleus (Saneyoshi et al., 2002). Few target genes have been identified downstream of NF-AT to date and the main function of the calcium-dependent pathway has been linked to inhibition of the canonical Wnt pathway (Westfall et al., 2003; Mikels and Nusse, 2006). Both Wnt5A and Wnt11 have been reported to activate this pathway *in vivo* (Slusarski et al., 1997b; Kuhl et al., 2000; Westfall et al., 2003). During development, the calcium-dependent pathway is triggered by Wnt5A and required for proper patterning of the dorsoventral embryonic axis by inhibiting canonical Wnt signaling on the ventral side (Slusarski et al., 1997b; Kuhl et al., 2000). The calcium-dependent Wnt pathway is also involved in cell type specification in the myoblast lineage (Chin et al., 1998; Anakwe et al., 2003).

The Planar Cell Polarity pathway

The planar cell polarity (PCP) pathway has been largely elucidated in *Drosophila,* where it is involved in bristle and hair orientation (Vinson et al., 1989). Later, it was shown to be mostly

identical in vertebrates (Strutt, 2003). In the PCP pathway, Wnt acts through frizzled receptors and Dvl to activate Jun-N-terminal kinase (JNK), RhoA, and Nemo-like kinase (NLK) pathways (Li et al., 1999b; Habas et al., 2001; Smit et al., 2004). PCP activation eventually leads to rearrangement of the cytoskeleton to induce cell polarity in the plane. Here, Dvl function is mediated by its DEP domain, which is dispensable for canonical Wnt signal transduction (Penton et al., 2002). In this situation, Dvl is hyperphosphorylated and translocates to the cell membrane (Penton et al., 2002). Dvl interacts with Daam1 to activate the small GTPase RhoA (Habas et al., 2001; Aspenstrom et al., 2006). Regulation of the PCP pathway can occur at the cell membrane level, where the Strabismus/Prickle complex inhibits PCP signaling by trapping Dvl (Carreira-Barbosa et al., 2003; Jenny et al., 2003; Takeuchi et al., 2003; Veeman et al., 2003; Das et al., 2004). The PCP pathway is also able to inhibit canonical Wnt signaling through its NLK branch (Ishitani et al., 1999; Ishitani et al., 2003; Kanei-Ishii et al., 2004; Smit et al., 2004; Thorpe and Moon, 2004; Kurahashi et al., 2005).

2.2.5. Wnt signaling functions during vertebrate embryonic development

Mouse knockout studies of the Wnt and Fzd gene families are complicated by the number of homologs and the promiscuity of Wnt–Fzd interactions. Nevertheless, it is the most appropriate approach to study Wnt and Fzd genes function during development (Table 4) (van Amerongen and Berns, 2006). Indeed, the analysis of downstream Wnt pathway components is obstructed by the fact that multiple upstream signaling pathway may converge on these proteins. Therefore, the observed knockout phenotypes do not necessarily represent only Wnt pathway defects. This is illustrated by the phenotype of glycogen synthase kinase-3β (Gsk3β) knockout mice. Although Gsk3β was known to be involved in a vast array of signal transduction pathways in addition to the canonical Wnt pathway, Gsk3β-knockout mice were unexpectedly found to suffer from severe defects in nuclear factor of kappa light chain gene enhancer in B-cells (NF-κB) signaling (Hoeflich et al., 2000). Although they opened a new area of research, these data contributed little to our understanding of the *in vivo* effects of Gsk3β loss on Wnt signal transduction. Most of our knowledge on the *in vivo* roles of Wnt signaling pathways during development is derived from more accessible embryonic models like fish and amphibians.

Wnt signaling pathways are implicated in major steps of embryonic development from embryonic axis patterning to cell differentiation. β-catenin accumulation into the dorsal vegetal side of the developing frog embryo (Nieuwkoop center) is necessary to pattern embryonic anterio-posterior and dorso-ventral axis (Heasman et al., 1994; Funayama et al., 1995; Heasman et al., 2000). This suggested a possible role for canonical signaling, but the mechanism leading to β-catenin accumulation remained unclear for years. Recently, Wnt11 dependent signaling has been shown to be necessary for the formation of this signaling center (Tao et al., 2005). While similar β-catenin accumulation is observed in zebrafish during axis patterning its likely

that another Wnt is responsible for it as Wnt11/*silberblick* mutant embryos do not have an early axis patterning phenotype (Heisenberg et al., 2000). At the same time as canonical signaling induces dorsal structures, Wnt5 activates non-canonical Wnt/Calcium signals on the ventral side of the embryo to inhibit dorsalization (Kuhl et al., 2001; Westfall et al., 2003).

Later, Wnt planar cell polarity signaling is implicated in convergent extension during gastrulation. Gastrulation is a mechanism involving organized cells migration leading to the formation of the three embryonic layers (ectoderm, mesoderm, and endoderm). During this process polarization in the plan of the embryonic cells is necessary for proper cell migration and intercalation (Heisenberg et al., 2000; Tada and Smith, 2000; Carreira-Barbosa et al., 2003; Takeuchi et al., 2003; Veeman et al., 2003). Interference with PCP signaling components leads to impaired gastrulation revealing an important role of PCP signaling during gastrualtion. Finally, Wnt signals are implicated in different aspects of organogenesis (Anakwe et al., 2003; Vainio, 2003; de Iongh et al., 2006; van Amerongen and Berns, 2006; de Lau et al., 2007; Malaterre et al., 2007). It is out of the scope to review all knockout phenotypes affecting organogenesis in detail, but a number of them are associated with defects in kidney organogenesis. This includes, Wnt4, Wnt9b, and Wnt11 which are required for metanephros organogenesis. Wnt4 is expressed in the condensing mesenchymal cells. Mice lacking Wnt4 fail to form pretubular aggregates (Stark et al., 1994). Wnt9b is expressed in the inductive epithelia of the ureteric bud and is essential for the development of mesonephric and metanephric tubules. Wnt9b acts upstream of Wnt4 and is required for the earliest inductive response of the mesenchyme to the induction from the ureteric bud (Carroll et al., 2005). Wnt11 is specifically expressed in the tips of the branching ureteric epithelium. Mutation of the *Wnt11* gene results in ureteric branching morphogenesis defects and consequent kidney hypoplasia in newborn mice. Wnt11 functions, in part, by maintaining normal expression levels of the gene encoding glial cell-derived neurotrophic factor (Gdnf) (Majumdar et al., 2003). In addition, the role during kidney organogenesis of other Wnt signaling components, which are expressed during metanephric kidney organogenesis, is not yet established. This is the case of Wnt6, which expression is detected in the ureteric bud, of Wnt2b, that is expressed in the presumptive stromal cell population (Lin et al., 2001). Fzd2, 3, 4, 5, 6, 7, 9 and 10 genes expression is also found during kidney organogenesis (Wang et al., 1996; Wang et al., 1999; Malik and Shivdasani, 2000). Notably, knockout mice have been produced for all of the Frizzled but no kidney phenotype has been reported (Table 4) (Ishikawa et al., 2001; Wang et al., 2001; Wang et al., 2002; Guo et al., 2004; Hsieh et al., 2005; Ranheim et al., 2005; Zhao et al., 2005; Wang et al., 2006b).

Table 4: Phenotype of conventional Wnt- and Fzd-knockout mice.

Gene knockout	Phenotype	References
Wnt1	Mid- and hindbrain deficiencies (hypomorphic allele: *Swaying*)	(Thomas and Capecchi, 1990) (McMahon and Bradley, 1990) (Thomas et al., 1991)
Wnt2	Abnormal placental development	(Monkley et al., 1996)
Wnt2B	Viable, no phenotype detected	T. Yamaguchi, personal communication
Wnt3	Failure in A–P axis formation before gastrulation (no primitive streak formed)	(Liu et al., 1999)
Wnt3A	Truncated A–P axis (loss of caudal somites and tailbud) Disrupted notochord and CNS dysmorphologies Paraxial mesoderm defects Loss of hippocampus Defects in somitogenesis and vertebral patterning Laterality defects (hypomorphic allele: *Vestigial Tail*)	(Takada et al., 1994) (Yoshikawa et al., 1997) (Lee et al., 2000) (Ikeya and Takada, 2001) (Nakaya et al., 2005) (Greco et al., 1996)
Wnt4	Failure in kidney tubule formation Failure in müllerian duct formation and sex reversal Male gonad determination	(Stark et al., 1994) (Vainio et al., 1999) (Jeays-Ward et al., 2004)
Wnt5A	Truncated A–P axis (with incomplete outgrowth of distal limbs, genitals and tail) Impaired distal lung morphogenesis Abnormal pituitary gland shape Defective pancreatic insulin-cell migration	(Yamaguchi et al., 1999) (Li et al., 2002) (Cha et al., 2004) (Kim et al., 2005)
Wnt5B	Viable	S. Takada and A. McMahon, personal Communication
Wnt6	Viable	A. Kispert, personal communication
Wnt7A	A–P and dorsoventral (D–V) patterning defects with limb and female reproductive tract abnormalities Failure in müllerian duct regression in males Delayed synaptic maturation in cerebellum (hypomorphic allele: *Postaxial hemimelia*)	(Parr and McMahon, 1995) (Miller and Sassoon, 1998) (Parr and McMahon, 1998) (Hall et al., 2000) (Parr et al., 1998)
Wnt7B	Abnormal placental development Lung hypoplasia due to defects in mesenchymal proliferation	(Parr et al., 2001) (Shu et al., 2002)
Wnt8A	Viable	T. Yamaguchi and A. McMahon, personal Communication
Wnt8B	Viable, no phenotype detected	J. Mason, personal communication
Wnt9A	Skeletal abnormalities and synovial chondroid metaplasia	(Spater et al., 2006)
Wnt9B	Defects in urogenital development (vestigial kidneys and absence of reproductive duct)	(Carroll et al., 2005)
Wnt10A	Unknown	
Wnt10B	Accelerated myogenic differentiation of myoblasts and increased activation of adipogenic genes upon muscle regeneration	(Vertino et al., 2005)
Wnt11	Kidney hypoplasia due to ureteric branching defects	(Majumdar et al., 2003)
Wnt16	Viable	J. Yu and A. McMahon, personal communication
Fzd1	Viable	J. Nathans, personal communication
Fzd2	Viable	J. Nathans, personal communication
Fzd3	Defects in axon tracts in the forebrain	(Wang et al., 2002)
Fzd4	Progressive cerebellar, auditory and esophageal dysfunction Infertility due to impaired corpora lutea formation and function	(Wang et al., 2001) (Hsieh et al., 2005)
Fzd5	Defects in yolk sac and placental angiogenesis	(Ishikawa et al., 2001)
Fzd6	Defects in hair patterning	(Guo et al., 2004)
Fzd7	Viable	J. Nathans, personal communication
Fzd8	Viable	J. Nathans, personal communication
Fzd9	Defects in B-cell development at pre-B-cell stage Hippocampal and visuospatial learning defects	(Ranheim et al., 2005) (Zhao et al., 2005)
Fzd10	Unknown	

References

Abdelhak S, Kalatzis V, Heilig R, Compain S, Samson D, Vincent C, Levi-Acobas F, Cruaud C, Le Merrer M, Mathieu M, Konig R, Vigneron J, Weissenbach J, Petit C, Weil D. 1997. Clustering of mutations responsible for branchio-oto-renal (BOR) syndrome in the eyes absent homologous region (eyaHR) of EYA1. Hum Mol Genet 6:2247-2255.

Adler PN. 1992. The genetic control of tissue polarity in Drosophila. Bioessays 14:735-741.

Adler PN, Vinson C, Park WJ, Conover S, Klein L. 1990. Molecular structure of frizzled, a Drosophila tissue polarity gene. Genetics 126:401-416.

Anakwe K, Robson L, Hadley J, Buxton P, Church V, Allen S, Hartmann C, Harfe B, Nohno T, Brown AM, Evans DJ, Francis-West P. 2003. Wnt signalling regulates myogenic differentiation in the developing avian wing. Development 130:3503-3514.

Aspenstrom P, Richnau N, Johansson AS. 2006. The diaphanous-related formin DAAM1 collaborates with the Rho GTPases RhoA and Cdc42, CIP4 and Src in regulating cell morphogenesis and actin dynamics. Exp Cell Res 312:2180-2194.

Baker NE. 1987. Molecular cloning of sequences from wingless, a segment polarity gene in Drosophila: the spatial distribution of a transcript in embryos. Embo J 6:1765-1773.

Banziger C, Soldini D, Schutt C, Zipperlen P, Hausmann G, Basler K. 2006. Wntless, a conserved membrane protein dedicated to the secretion of Wnt proteins from signaling cells. Cell 125:509-522.

Bartscherer K, Pelte N, Ingelfinger D, Boutros M. 2006. Secretion of Wnt ligands requires Evi, a conserved transmembrane protein. Cell 125:523-533.

Basson MA, Akbulut S, Watson-Johnson J, Simon R, Carroll TJ, Shakya R, Gross I, Martin GR, Lufkin T, McMahon AP, Wilson PD, Costantini FD, Mason IJ, Licht JD. 2005. Sprouty1 is a critical regulator of GDNF/RET-mediated kidney induction. Dev Cell 8:229-239.

Berger W, Meindl A, van de Pol TJ, Cremers FP, Ropers HH, Doerner C, Monaco A, Bergen AA, Lebo R, Warburg M, et al. 1992a. Isolation of a candidate gene for Norrie disease by positional cloning. Nat Genet 1:199-203.

Berger W, van de Pol D, Warburg M, Gal A, Bleeker-Wagemakers L, de Silva H, Meindl A, Meitinger T, Cremers F, Ropers HH. 1992b. Mutations in the candidate gene for Norrie disease. Hum Mol Genet 1:461-465.

Bhanot P, Brink M, Samos CH, Hsieh JC, Wang Y, Macke JP, Andrew D, Nathans J, Nusse R. 1996. A new member of the frizzled family from Drosophila functions as a Wingless receptor. Nature 382:225-230.

Bouchard M. 2004. Transcriptional control of kidney development. Differentiation 72:295-306.

Bouchard M, Souabni A, Mandler M, Neubuser A, Busslinger M. 2002. Nephric lineage specification by Pax2 and Pax8. Genes Dev 16:2958-2970.

Bouvier M, Chidiac P, Hebert TE, Loisel TP, Moffett S, Mouillac B. 1995. Dynamic palmitoylation of G-protein-coupled receptors in eukaryotic cells. Methods Enzymol 250:300-314.

Brändli AW. 1999. Towards a molecular anatomy of the Xenopus pronephric kidney. Int J Dev Biol 43:381-395.

Brophy PD, Ostrom L, Lang KM, Dressler GR. 2001. Regulation of ureteric bud outgrowth by Pax2-dependent activation of the glial derived neurotrophic factor gene.

Development 128:4747-4756.
Brunner E, Peter O, Schweizer L, Basler K. 1997. pangolin encodes a Lef-1 homologue that acts downstream of Armadillo to transduce the Wingless signal in Drosophila. Nature 385:829-833.
Bullock SL, Fletcher JM, Beddington RS, Wilson VA. 1998. Renal agenesis in mice homozygous for a gene trap mutation in the gene encoding heparan sulfate 2-sulfotransferase. Genes Dev 12:1894-1906.
Cacalano G, Farinas I, Wang LC, Hagler K, Forgie A, Moore M, Armanini M, Phillips H, Ryan AM, Reichardt LF, Hynes M, Davies A, Rosenthal A. 1998. GFRalpha1 is an essential receptor component for GDNF in the developing nervous system and kidney. Neuron 21:53-62.
Cadigan KM, Fish MP, Rulifson EJ, Nusse R. 1998. Wingless repression of Drosophila frizzled 2 expression shapes the Wingless morphogen gradient in the wing. Cell 93:767-777.
Cano-Gauci DF, Song HH, Yang H, McKerlie C, Choo B, Shi W, Pullano R, Piscione TD, Grisaru S, Soon S, Sedlackova L, Tanswell AK, Mak TW, Yeger H, Lockwood GA, Rosenblum ND, Filmus J. 1999. Glypican-3-deficient mice exhibit developmental overgrowth and some of the abnormalities typical of Simpson-Golabi-Behmel syndrome. J Cell Biol 146:255-264.
Caricasole A, Ferraro T, Rimland JM, Terstappen GC. 2002. Molecular cloning and initial characterization of the MG61/PORC gene, the human homologue of the Drosophila segment polarity gene Porcupine. Gene 288:147-157.
Carreira-Barbosa F, Concha ML, Takeuchi M, Ueno N, Wilson SW, Tada M. 2003. Prickle 1 regulates cell movements during gastrulation and neuronal migration in zebrafish. Development 130:4037-4046.
Carroll TJ, Park JS, Hayashi S, Majumdar A, McMahon AP. 2005. Wnt9b plays a central role in the regulation of mesenchymal to epithelial transitions underlying organogenesis of the mammalian urogenital system. Dev Cell 9:283-292.
Cavallo RA, Cox RT, Moline MM, Roose J, Polevoy GA, Clevers H, Peifer M, Bejsovec A. 1998. Drosophila Tcf and Groucho interact to repress Wingless signalling activity. Nature 395:604-608.
Cha KB, Douglas KR, Potok MA, Liang H, Jones SN, Camper SA. 2004. WNT5A signaling affects pituitary gland shape. Mech Dev 121:183-194.
Chan TC, Takahashi S, Asashima M. 2000. A role for Xlim-1 in pronephros development in Xenopus laevis. Dev Biol 228:256-269.
Chen G, Fernandez J, Mische S, Courey AJ. 1999. A functional interaction between the histone deacetylase Rpd3 and the corepressor groucho in Drosophila development. Genes Dev 13:2218-2230.
Chen JZ, Wang S, Tang R, Yang QS, Zhao E, Chao Y, Ying K, Xie Y, Mao YM. 2002. Cloning and identification of a cDNA that encodes a novel human protein with thrombospondin type I repeat domain, hPWTSR. Mol Biol Rep 29:287-292.
Cheng HT, Kim M, Valerius MT, Surendran K, Schuster-Gossler K, Gossler A, McMahon AP, Kopan R. 2007. Notch2, but not Notch1, is required for proximal fate acquisition in the mammalian nephron. Development 134:801-811.
Chin ER, Olson EN, Richardson JA, Yang Q, Humphries C, Shelton JM, Wu H, Zhu W, Bassel-Duby R, Williams RS. 1998. A calcineurin-dependent transcriptional pathway controls skeletal muscle fiber type. Genes Dev 12:2499-2509.
Clevers H. 2006. Wnt/beta-catenin signaling in development and disease. Cell 127:469-480.
Cong F, Schweizer L, Varmus H. 2004a. Casein kinase Iepsilon modulates the signaling

specificities of dishevelled. Mol Cell Biol 24:2000-2011.
Cong F, Schweizer L, Varmus H. 2004b. Wnt signals across the plasma membrane to activate the beta-catenin pathway by forming oligomers containing its receptors, Frizzled and LRP. Development 131:5103-5115.
Costantini F. 2006. Renal branching morphogenesis: concepts, questions, and recent advances. Differentiation 74:402-421.
Costantini F, Shakya R. 2006. GDNF/Ret signaling and the development of the kidney. Bioessays 28:117-127.
Cullen-McEwen LA, Drago J, Bertram JF. 2001. Nephron endowment in glial cell line-derived neurotrophic factor (GDNF) heterozygous mice. Kidney Int 60:31-36.
Daniels DL, Weis WI. 2005. Beta-catenin directly displaces Groucho/TLE repressors from Tcf/Lef in Wnt-mediated transcription activation. Nat Struct Mol Biol 12:364-371.
Dann CE, Hsieh JC, Rattner A, Sharma D, Nathans J, Leahy DJ. 2001. Insights into Wnt binding and signalling from the structures of two Frizzled cysteine-rich domains. Nature 412:86-90.
Das G, Jenny A, Klein TJ, Eaton S, Mlodzik M. 2004. Diego interacts with Prickle and Strabismus/Van Gogh to localize planar cell polarity complexes. Development 131:4467-4476.
Davidson G, Wu W, Shen J, Bilic J, Fenger U, Stannek P, Glinka A, Niehrs C. 2005. Casein kinase 1 gamma couples Wnt receptor activation to cytoplasmic signal transduction. Nature 438:867-872.
Davis AP, Witte DP, Hsieh-Li HM, Potter SS, Capecchi MR. 1995. Absence of radius and ulna in mice lacking hoxa-11 and hoxd-11. Nature 375:791-795.
de Iongh RU, Abud HE, Hime GR. 2006. WNT/Frizzled signaling in eye development and disease. Front Biosci 11:2442-2464.
de Lau W, Barker N, Clevers H. 2007. WNT signaling in the normal intestine and colorectal cancer. Front Biosci 12:471-491.
Du SJ, Purcell SM, Christian JL, McGrew LL, Moon RT. 1995. Identification of distinct classes and functional domains of Wnts through expression of wild-type and chimeric proteins in Xenopus embryos. Mol Cell Biol 15:2625-2634.
Dunn NR, Winnier GE, Hargett LK, Schrick JJ, Fogo AB, Hogan BL. 1997. Haploinsufficient phenotypes in Bmp4 heterozygous null mice and modification by mutations in Gli3 and Alx4. Dev Biol 188:235-247.
Eaton S. 2006. Release and trafficking of lipid-linked morphogens. Curr Opin Genet Dev 16:17-22.
Enomoto H, Araki T, Jackman A, Heuckeroth RO, Snider WD, Johnson EM, Jr., Milbrandt J. 1998. GFR alpha1-deficient mice have deficits in the enteric nervous system and kidneys. Neuron 21:317-324.
Fagotto F, Jho E, Zeng L, Kurth T, Joos T, Kaufmann C, Costantini F. 1999. Domains of axin involved in protein-protein interactions, Wnt pathway inhibition, and intracellular localization. J Cell Biol 145:741-756.
Funayama N, Fagotto F, McCrea P, Gumbiner BM. 1995. Embryonic axis induction by the armadillo repeat domain of beta-catenin: evidence for intracellular signaling. J Cell Biol 128:959-968.
Ghanbari H. 2003. Elucidation of Pax and Wnt gene functions during pronephric kidney development in *Xenopus*
Diss., Naturwissenschaften ETH Zürich, Nr. 15014, 2003. In: Department of Chemistry and Applied Biosciences. Zürich: Swiss Federal Institute of Technology.
Gonzalez-Sancho JM, Brennan KR, Castelo-Soccio LA, Brown AM. 2004. Wnt proteins

induce dishevelled phosphorylation via an LRP5/6- independent mechanism, irrespective of their ability to stabilize beta-catenin. Mol Cell Biol 24:4757-4768.
Goodman RM, Thombre S, Firtina Z, Gray D, Betts D, Roebuck J, Spana EP, Selva EM. 2006. Sprinter: a novel transmembrane protein required for Wg secretion and signaling. Development 133:4901-4911.
Gordon MD, Nusse R. 2006. Wnt Signaling: Multiple Pathways, Multiple Receptors, and Multiple Transcription Factors. J. Biol. Chem. 281:22429-22433.
Greco TL, Takada S, Newhouse MM, McMahon JA, McMahon AP, Camper SA. 1996. Analysis of the vestigial tail mutation demonstrates that Wnt-3a gene dosage regulates mouse axial development. Genes Dev 10:313-324.
Grieshammer U, Le M, Plump AS, Wang F, Tessier-Lavigne M, Martin GR. 2004. SLIT2-mediated ROBO2 signaling restricts kidney induction to a single site. Dev Cell 6:709-717.
Grote D, Souabni A, Busslinger M, Bouchard M. 2006. Pax 2/8-regulated Gata 3 expression is necessary for morphogenesis and guidance of the nephric duct in the developing kidney. Development 133:53-61.
Gubb D, Garcia-Bellido A. 1982. A genetic analysis of the determination of cuticular polarity during development in Drosophila melanogaster. J Embryol Exp Morphol 68:37-57.
Guo N, Hawkins C, Nathans J. 2004. Frizzled6 controls hair patterning in mice. Proc Natl Acad Sci U S A 101:9277-9281.
Habas R, Kato Y, He X. 2001. Wnt/Frizzled activation of Rho regulates vertebrate gastrulation and requires a novel Formin homology protein Daam1. Cell 107:843-854.
Hall AC, Lucas FR, Salinas PC. 2000. Axonal remodeling and synaptic differentiation in the cerebellum is regulated by WNT-7a signaling. Cell 100:525-535.
Hatini V, Huh SO, Herzlinger D, Soares VC, Lai E. 1996. Essential role of stromal mesenchyme in kidney morphogenesis revealed by targeted disruption of Winged Helix transcription factor BF-2. Genes Dev 10:1467-1478.
Hausmann G, Basler K. 2006. Wnt lipid modifications: not as saturated as we thought. Dev Cell 11:751-752.
He X, Saint-Jeannet JP, Wang Y, Nathans J, Dawid I, Varmus H. 1997. A member of the Frizzled protein family mediating axis induction by Wnt-5A. Science 275:1652-1654.
He X, Semenov M, Tamai K, Zeng X. 2004. LDL receptor-related proteins 5 and 6 in Wnt/beta-catenin signaling: arrows point the way. Development 131:1663-1677.
Heasman J, Crawford A, Goldstone K, Garner-Hamrick P, Gumbiner B, McCrea P, Kintner C, Noro CY, Wylie C. 1994. Overexpression of cadherins and underexpression of beta-catenin inhibit dorsal mesoderm induction in early Xenopus embryos. Cell 79:791-803.
Heasman J, Kofron M, Wylie C. 2000. Beta-catenin signaling activity dissected in the early Xenopus embryo: a novel antisense approach. Dev Biol 222:124-134.
Heisenberg CP, Tada M, Rauch GJ, Saude L, Concha ML, Geisler R, Stemple DL, Smith JC, Wilson SW. 2000. Silberblick/Wnt11 mediates convergent extension movements during zebrafish gastrulation. Nature 405:76-81.
Heller N, Brändli AW. 1997. Xenopus Pax-2 displays multiple splice forms during embryogenesis and pronephric kidney development. Mech Dev 69:83-104.
Heller N, Brändli AW. 1999. Xenopus Pax-2/5/8 orthologues: novel insights into Pax gene evolution and identification of Pax-8 as the earliest marker for otic and pronephric cell lineages. Dev Genet 24:208-219.
Herman MA, Vassilieva LL, Horvitz HR, Shaw JE, Herman RK. 1995. The C. elegans gene lin-44, which controls the polarity of certain asymmetric cell divisions, encodes a Wnt

protein and acts cell nonautonomously. Cell 83:101-110.
Hoeflich KP, Luo J, Rubie EA, Tsao MS, Jin O, Woodgett JR. 2000. Requirement for glycogen synthase kinase-3beta in cell survival and NF-kappaB activation. Nature 406:86-90.
Hofmann K. 2000. A superfamily of membrane-bound O-acyltransferases with implications for wnt signaling. Trends Biochem Sci 25:111-112.
Hsieh M, Boerboom D, Shimada M, Lo Y, Parlow AF, Luhmann UF, Berger W, Richards JS. 2005. Mice null for Frizzled4 (Fzd4-/-) are infertile and exhibit impaired corpora lutea formation and function. Biol Reprod 73:1135-1146.
Huelsken J, Behrens J. 2002. The Wnt signalling pathway. J Cell Sci 115:3977-3978.
Ichikawa I, Kuwayama F, Pope JCt, Stephens FD, Miyazaki Y. 2002. Paradigm shift from classic anatomic theories to contemporary cell biological views of CAKUT. Kidney Int 61:889-898.
Ikeya M, Takada S. 2001. Wnt-3a is required for somite specification along the anteroposterior axis of the mouse embryo and for regulation of cdx-1 expression. Mech Dev 103:27-33.
Ishikawa T, Tamai Y, Zorn AM, Yoshida H, Seldin MF, Nishikawa S, Taketo MM. 2001. Mouse Wnt receptor gene Fzd5 is essential for yolk sac and placental angiogenesis. Development 128:25-33.
Ishitani T, Ninomiya-Tsuji J, Matsumoto K. 2003. Regulation of lymphoid enhancer factor 1/ T-cell factor by mitogen-activated protein kinase-related Nemo-like kinase-dependent phosphorylation in Wnt/beta-catenin signaling. Mol Cell Biol 23:1379-1389.
Ishitani T, Ninomiya-Tsuji J, Nagai S, Nishita M, Meneghini M, Barker N, Waterman M, Bowerman B, Clevers H, Shibuya H, Matsumoto K. 1999. The TAK1-NLK-MAPK-related pathway antagonizes signalling between beta-catenin and transcription factor TCF. Nature 399:798-802.
James RG, Kamei CN, Wang Q, Jiang R, Schultheiss TM. 2006. Odd-skipped related 1 is required for development of the metanephric kidney and regulates formation and differentiation of kidney precursor cells. Development 133:2995-3004.
Jeays-Ward K, Dandonneau M, Swain A. 2004. Wnt4 is required for proper male as well as female sexual development. Dev Biol 276:431-440.
Jenny A, Darken RS, Wilson PA, Mlodzik M. 2003. Prickle and Strabismus form a functional complex to generate a correct axis during planar cell polarity signaling. Embo J 22:4409-4420.
Jhappan C, Stahle C, Harkins RN, Fausto N, Smith GH, Merlino GT. 1990. TGF alpha overexpression in transgenic mice induces liver neoplasia and abnormal development of the mammary gland and pancreas. Cell 61:1137-1146.
Jhaveri S, Erzurumlu RS, Chiaia N, Kumar TR, Matzuk MM. 1998. Defective whisker follicles and altered brainstem patterns in activin and follistatin knockout mice. Mol Cell Neurosci 12:206-219.
Jones SE, Jomary C. 2002. Secreted Frizzled-related proteins: searching for relationships and patterns. Bioessays 24:811-820.
Kadowaki T, Wilder E, Klingensmith J, Zachary K, Perrimon N. 1996. The segment polarity gene porcupine encodes a putative multitransmembrane protein involved in Wingless processing. Genes Dev 10:3116-3128.
Kamata T, Katsube K, Michikawa M, Yamada M, Takada S, Mizusawa H. 2004. R-spondin, a novel gene with thrombospondin type 1 domain, was expressed in the dorsal neural tube and affected in Wnts mutants. Biochim Biophys Acta 1676:51-62.
Kanei-Ishii C, Ninomiya-Tsuji J, Tanikawa J, Nomura T, Ishitani T, Kishida S, Kokura K,

Kurahashi T, Ichikawa-Iwata E, Kim Y, Matsumoto K, Ishii S. 2004. Wnt-1 signal induces phosphorylation and degradation of c-Myb protein via TAK1, HIPK2, and NLK. Genes Dev 18:816-829.

Kay BK, Kehoe JW. 2004. PDZ domains and their ligands. Chem Biol 11:423-425.

Kazanskaya O, Glinka A, del Barco Barrantes I, Stannek P, Niehrs C, Wu W. 2004. R-Spondin2 is a secreted activator of Wnt/beta-catenin signaling and is required for Xenopus myogenesis. Dev Cell 7:525-534.

Kikuchi A, Yamamoto H, Kishida S. 2006. Multiplicity of the interactions of Wnt proteins and their receptors. Cell Signal.

Kim HJ, Schleiffarth JR, Jessurun J, Sumanas S, Petryk A, Lin S, Ekker SC. 2005. Wnt5 signaling in vertebrate pancreas development. BMC Biol 3:23.

Kishida S, Yamamoto H, Hino S, Ikeda S, Kishida M, Kikuchi A. 1999. DIX domains of Dvl and axin are necessary for protein interactions and their ability to regulate beta-catenin stability. Mol Cell Biol 19:4414-4422.

Kleber M, Sommer L. 2004. Wnt signaling and the regulation of stem cell function. Curr Opin Cell Biol 16:681-687.

Klingensmith J, Nusse R, Perrimon N. 1994. The Drosophila segment polarity gene dishevelled encodes a novel protein required for response to the wingless signal. Genes Dev 8:118-130.

Kobayashi A, Kwan KM, Carroll TJ, McMahon AP, Mendelsohn CL, Behringer RR. 2005. Distinct and sequential tissue-specific activities of the LIM-class homeobox gene Lim1 for tubular morphogenesis during kidney development. Development 132:2809-2823.

Kohlhase J, Wischermann A, Reichenbach H, Froster U, Engel W. 1998. Mutations in the SALL1 putative transcription factor gene cause Townes-Brocks syndrome. Nat Genet 18:81-83.

Kramps T, Peter O, Brunner E, Nellen D, Froesch B, Chatterjee S, Murone M, Zullig S, Basler K. 2002. Wnt/wingless signaling requires BCL9/legless-mediated recruitment of pygopus to the nuclear beta-catenin-TCF complex. Cell 109:47-60.

Krasnow RE, Wong LL, Adler PN. 1995. Dishevelled is a component of the frizzled signaling pathway in Drosophila. Development 121:4095-4102.

Kreidberg JA, Sariola H, Loring JM, Maeda M, Pelletier J, Housman D, Jaenisch R. 1993. WT-1 is required for early kidney development. Cell 74:679-691.

Kuhl M, Geis K, Sheldahl LC, Pukrop T, Moon RT, Wedlich D. 2001. Antagonistic regulation of convergent extension movements in Xenopus by Wnt/beta-catenin and Wnt/Ca2+ signaling. Mech Dev 106:61-76.

Kuhl M, Sheldahl LC, Malbon CC, Moon RT. 2000. Ca(2+)/calmodulin-dependent protein kinase II is stimulated by Wnt and Frizzled homologs and promotes ventral cell fates in Xenopus. J Biol Chem 275:12701-12711.

Kulkarni AB, Huh CG, Becker D, Geiser A, Lyght M, Flanders KC, Roberts AB, Sporn MB, Ward JM, Karlsson S. 1993. Transforming growth factor beta 1 null mutation in mice causes excessive inflammatory response and early death. Proc Natl Acad Sci U S A 90:770-774.

Kume T, Deng K, Hogan BL. 2000. Murine forkhead/winged helix genes Foxc1 (Mf1) and Foxc2 (Mfh1) are required for the early organogenesis of the kidney and urinary tract. Development 127:1387-1395.

Kurahashi T, Nomura T, Kanei-Ishii C, Shinkai Y, Ishii S. 2005. The Wnt-NLK signaling pathway inhibits A-Myb activity by inhibiting the association with coactivator CBP and methylating histone H3. Mol Biol Cell 16:4705-4713.

Kurayoshi M, Yamamoto H, Izumi S, Kikuchi A. 2007. Post-translational palmitoylation and glycosylation of Wnt-5a are necessary for its signalling. Biochem J 402:515-523.

Kusserow A, Pang K, Sturm C, Hrouda M, Lentfer J, Schmidt HA, Technau U, von Haeseler A, Hobmayer B, Martindale MQ, Holstein TW. 2005. Unexpected complexity of the Wnt gene family in a sea anemone. Nature 433:156-160.

Lee SM, Tole S, Grove E, McMahon AP. 2000. A local Wnt-3a signal is required for development of the mammalian hippocampus. Development 127:457-467.

Leyns L, Bouwmeester T, Kim SH, Piccolo S, De Robertis EM. 1997. Frzb-1 is a secreted antagonist of Wnt signaling expressed in the Spemann organizer. Cell 88:747-756.

Li C, Xiao J, Hormi K, Borok Z, Minoo P. 2002. Wnt5a participates in distal lung morphogenesis. Dev Biol 248:68-81.

Li L, Yuan H, Weaver CD, Mao J, Farr GH, 3rd, Sussman DJ, Jonkers J, Kimelman D, Wu D. 1999a. Axin and Fratl interact with dvl and GSK, bridging Dvl to GSK in Wnt-mediated regulation of LEF-1. Embo J 18:4233-4240.

Li L, Yuan H, Xie W, Mao J, Caruso AM, McMahon A, Sussman DJ, Wu D. 1999b. Dishevelled proteins lead to two signaling pathways. Regulation of LEF-1 and c-Jun N-terminal kinase in mammalian cells. J Biol Chem 274:129-134.

Li X, Oghi KA, Zhang J, Krones A, Bush KT, Glass CK, Nigam SK, Aggarwal AK, Maas R, Rose DW, Rosenfeld MG. 2003. Eya protein phosphatase activity regulates Six1-Dach-Eya transcriptional effects in mammalian organogenesis. Nature 426:247-254.

Lin F, Hiesberger T, Cordes K, Sinclair AM, Goldstein LS, Somlo S, Igarashi P. 2003. Kidney-specific inactivation of the KIF3A subunit of kinesin-II inhibits renal ciliogenesis and produces polycystic kidney disease. Proc Natl Acad Sci U S A 100:5286-5291.

Lin K, Wang S, Julius MA, Kitajewski J, Moos M, Jr., Luyten FP. 1997. The cysteine-rich frizzled domain of Frzb-1 is required and sufficient for modulation of Wnt signaling. Proc Natl Acad Sci U S A 94:11196-11200.

Lin Y, Liu A, Zhang S, Ruusunen T, Kreidberg JA, Peltoketo H, Drummond I, Vainio S. 2001. Induction of ureter branching as a response to Wnt-2b signaling during early kidney organogenesis. Dev Dyn 222:26-39.

Liu G, Bafico A, Aaronson SA. 2005. The mechanism of endogenous receptor activation functionally distinguishes prototype canonical and noncanonical Wnts. Mol Cell Biol 25:3475-3482.

Liu P, Wakamiya M, Shea MJ, Albrecht U, Behringer RR, Bradley A. 1999. Requirement for Wnt3 in vertebrate axis formation. Nat Genet 22:361-365.

Mackie GG, Stephens FD. 1975. Duplex kidneys: a correlation of renal dysplasia with position of the ureteral orifice. J Urol 114:274-280.

Majumdar A, Vainio S, Kispert A, McMahon J, McMahon AP. 2003. Wnt11 and Ret/Gdnf pathways cooperate in regulating ureteric branching during metanephric kidney development. Development 130:3175-3185.

Malaterre J, Ramsay RG, Mantamadiotis T. 2007. Wnt-Frizzled signalling and the many paths to neural development and adult brain homeostasis. Front Biosci 12:492-506.

Malbon CC, Wang HY. 2006. Dishevelled: a mobile scaffold catalyzing development. Curr Top Dev Biol 72:153-166.

Malik TH, Shivdasani RA. 2000. Structure and expression of a novel frizzled gene isolated from the developing mouse gut. Biochem J 349 Pt 3:829-834.

Mason JO, Kitajewski J, Varmus HE. 1992. Mutational analysis of mouse Wnt-1 identifies two temperature-sensitive alleles and attributes of Wnt-1 protein essential for transformation of a mammary cell line. Mol Biol Cell 3:521-533.

McMahon AP, Bradley A. 1990. The Wnt-1 (int-1) proto-oncogene is required for development of a large region of the mouse brain. Cell 62:1073-1085.

McMahon AP, Moon RT. 1989. Ectopic expression of the proto-oncogene int-1 in Xenopus embryos leads to duplication of the embryonic axis. Cell 58:1075-1084.

Mendelsohn C, Batourina E, Fung S, Gilbert T, Dodd J. 1999. Stromal cells mediate retinoid-dependent functions essential for renal development. Development 126:1139-1148.

Meyer TN, Schwesinger C, Bush KT, Stuart RO, Rose DW, Shah MM, Vaughn DA, Steer DL, Nigam SK. 2004. Spatiotemporal regulation of morphogenetic molecules during in vitro branching of the isolated ureteric bud: toward a model of branching through budding in the developing kidney. Dev Biol 275:44-67.

Michos O, Panman L, Vintersten K, Beier K, Zeller R, Zuniga A. 2004. Gremlin-mediated BMP antagonism induces the epithelial-mesenchymal feedback signaling controlling metanephric kidney and limb organogenesis. Development 131:3401-3410.

Mikels AJ, Nusse R. 2006. Purified Wnt5a protein activates or inhibits beta-catenin-TCF signaling depending on receptor context. PLoS Biol 4:e115.

Miller C, Sassoon DA. 1998. Wnt-7a maintains appropriate uterine patterning during the development of the mouse female reproductive tract. Development 125:3201-3211.

Miller JR. 2002. The Wnts. Genome Biol 3:REVIEWS3001.

Miner JH, Li C. 2000. Defective glomerulogenesis in the absence of laminin alpha5 demonstrates a developmental role for the kidney glomerular basement membrane. Dev Biol 217:278-289.

Miyamoto N, Yoshida M, Kuratani S, Matsuo I, Aizawa S. 1997. Defects of urogenital development in mice lacking Emx2. Development 124:1653-1664.

Miyazaki Y, Oshima K, Fogo A, Hogan BL, Ichikawa I. 2000. Bone morphogenetic protein 4 regulates the budding site and elongation of the mouse ureter. J Clin Invest 105:863-873.

Moller S, Vilo J, Croning MD. 2001. Prediction of the coupling specificity of G protein coupled receptors to their G proteins. Bioinformatics 17 Suppl 1:S174-181.

Monkley SJ, Delaney SJ, Pennisi DJ, Christiansen JH, Wainwright BJ. 1996. Targeted disruption of the Wnt2 gene results in placentation defects. Development 122:3343-3353.

Moon RT, Kohn AD, De Ferrari GV, Kaykas A. 2004. WNT and beta-catenin signalling: diseases and therapies. Nat Rev Genet 5:691-701.

Moore MW, Klein RD, Farinas I, Sauer H, Armanini M, Phillips H, Reichardt LF, Ryan AM, Carver-Moore K, Rosenthal A. 1996. Renal and neuronal abnormalities in mice lacking GDNF. Nature 382:76-79.

Morgan D, Eley L, Sayer J, Strachan T, Yates LM, Craighead AS, Goodship JA. 2002. Expression analyses and interaction with the anaphase promoting complex protein Apc2 suggest a role for inversin in primary cilia and involvement in the cell cycle. Hum Mol Genet 11:3345-3350.

Muller U, Wang D, Denda S, Meneses JJ, Pedersen RA, Reichardt LF. 1997. Integrin alpha8beta1 is critically important for epithelial-mesenchymal interactions during kidney morphogenesis. Cell 88:603-613.

Nakaya MA, Biris K, Tsukiyama T, Jaime S, Rawls JA, Yamaguchi TP. 2005. Wnt3a links left-right determination with segmentation and anteroposterior axis elongation. Development 132:5425-5436.

Nam JS, Turcotte TJ, Smith PF, Choi S, Yoon JK. 2006. Mouse cristin/R-spondin family proteins are novel ligands for the Frizzled 8 and LRP6 receptors and activate beta-catenin-dependent gene expression. J Biol Chem 281:13247-13257.

Narlis M, Grote D, Gaitan Y, Boualia SK, Bouchard M. 2007. Pax2 and Pax8 regulate branching morphogenesis and nephron differentiation in the developing kidney. J Am Soc Nephrol 18:1121-1129.

Nieuwkoop PD, Faber J. 1956. Normal table of Xenopus laevis (Daudin): a systematical and chronological survey of the development from the fertilized egg till the end of metamorphosis.: North-Holland Publishing Company, Amsterdam.

Nishinakamura R, Matsumoto Y, Nakao K, Nakamura K, Sato A, Copeland NG, Gilbert DJ, Jenkins NA, Scully S, Lacey DL, Katsuki M, Asashima M, Yokota T. 2001. Murine homolog of SALL1 is essential for ureteric bud invasion in kidney development. Development 128:3105-3115.

Nusse R. 2005. Wnt signaling in disease and in development. Cell Res 15:28-32.

Nusse R, Varmus HE. 1992. Wnt genes. Cell 69:1073-1087.

Nusslein-Volhard C, Wieschaus E. 1980. Mutations affecting segment number and polarity in Drosophila. Nature 287:795-801.

Ohuchi H, Hori Y, Yamasaki M, Harada H, Sekine K, Kato S, Itoh N. 2000. FGF10 acts as a major ligand for FGF receptor 2 IIIb in mouse multi-organ development. Biochem Biophys Res Commun 277:643-649.

Orellana SA, Sweeney WE, Neff CD, Avner ED. 1995. Epidermal growth factor receptor expression is abnormal in murine polycystic kidney. Kidney Int 47:490-499.

Ossipova O, Dhawan S, Sokol S, Green JB. 2005. Distinct PAR-1 proteins function in different branches of Wnt signaling during vertebrate development. Dev Cell 8:829-841.

Panakova D, Sprong H, Marois E, Thiele C, Eaton S. 2005. Lipoprotein particles are required for Hedgehog and Wingless signalling. Nature 435:58-65.

Parker DS, Jemison J, Cadigan KM. 2002. Pygopus, a nuclear PHD-finger protein required for Wingless signaling in Drosophila. Development 129:2565-2576.

Parr BA, Avery EJ, Cygan JA, McMahon AP. 1998. The classical mouse mutant postaxial hemimelia results from a mutation in the Wnt 7a gene. Dev Biol 202:228-234.

Parr BA, Cornish VA, Cybulsky MI, McMahon AP. 2001. Wnt7b regulates placental development in mice. Dev Biol 237:324-332.

Parr BA, McMahon AP. 1995. Dorsalizing signal Wnt-7a required for normal polarity of D-V and A-P axes of mouse limb. Nature 374:350-353.

Parr BA, McMahon AP. 1998. Sexually dimorphic development of the mammalian reproductive tract requires Wnt-7a. Nature 395:707-710.

Pedersen A, Skjong C, Shawlot W. 2005. Lim 1 is required for nephric duct extension and ureteric bud morphogenesis. Dev Biol 288:571-581.

Pelletier J, Schalling M, Buckler AJ, Rogers A, Haber DA, Housman D. 1991. Expression of the Wilms' tumor gene WT1 in the murine urogenital system. Genes Dev 5:1345-1356.

Pendergast SD, Trese MT. 1998. Familial exudative vitreoretinopathy. Results of surgical management. Ophthalmology 105:1015-1023.

Penton A, Wodarz A, Nusse R. 2002. A mutational analysis of dishevelled in Drosophila defines novel domains in the dishevelled protein as well as novel suppressing alleles of axin. Genetics 161:747-762.

Perrimon N, Mahowald AP. 1987. Multiple functions of segment polarity genes in Drosophila. Dev Biol 119:587-600.

Pichel JG, Shen L, Sheng HZ, Granholm AC, Drago J, Grinberg A, Lee EJ, Huang SP, Saarma

M, Hoffer BJ, Sariola H, Westphal H. 1996. Defects in enteric innervation and kidney development in mice lacking GDNF. Nature 382:73-76.

Pilia G, Hughes-Benzie RM, MacKenzie A, Baybayan P, Chen EY, Huber R, Neri G, Cao A, Forabosco A, Schlessinger D. 1996. Mutations in GPC3, a glypican gene, cause the Simpson-Golabi-Behmel overgrowth syndrome. Nat Genet 12:241-247.

Povelones M, Nusse R. 2005. The role of the cysteine-rich domain of Frizzled in Wingless-Armadillo signaling. Embo J 24:3493-3503.

Pritchard-Jones K, Fleming S, Davidson D, Bickmore W, Porteous D, Gosden C, Bard J, Buckler A, Pelletier J, Housman D, et al. 1990. The candidate Wilms' tumour gene is involved in genitourinary development. Nature 346:194-197.

Qiao J, Uzzo R, Obara-Ishihara T, Degenstein L, Fuchs E, Herzlinger D. 1999. FGF-7 modulates ureteric bud growth and nephron number in the developing kidney. Development 126:547-554.

Quaggin SE, Schwartz L, Cui S, Igarashi P, Deimling J, Post M, Rossant J. 1999. The basic-helix-loop-helix protein pod1 is critically important for kidney and lung organogenesis. Development 126:5771-5783.

Raciti D. 2007. A large-scale gene discovery screen identifies over hundred solute carrier (SLC) genes with organ specific expression patterns in the *Xenopus* embryo. In: Department of Chemistry and Applied Biosceinces. Zürich: Swiss Federal Institute of Technology.

Ranheim EA, Kwan HC, Reya T, Wang YK, Weissman IL, Francke U. 2005. Frizzled 9 knock-out mice have abnormal B-cell development. Blood 105:2487-2494.

Rattner A, Hsieh JC, Smallwood PM, Gilbert DJ, Copeland NG, Jenkins NA, Nathans J. 1997. A family of secreted proteins contains homology to the cysteine-rich ligand-binding domain of frizzled receptors. Proc Natl Acad Sci U S A 94:2859-2863.

Rijsewijk F, Schuermann M, Wagenaar E, Parren P, Weigel D, Nusse R. 1987. The Drosophila homolog of the mouse mammary oncogene int-1 is identical to the segment polarity gene wingless. Cell 50:649-657.

Robitaille J, MacDonald ML, Kaykas A, Sheldahl LC, Zeisler J, Dube MP, Zhang LH, Singaraja RR, Guernsey DL, Zheng B, Siebert LF, Hoskin-Mott A, Trese MT, Pimstone SN, Shastry BS, Moon RT, Hayden MR, Goldberg YP, Samuels ME. 2002. Mutant frizzled-4 disrupts retinal angiogenesis in familial exudative vitreoretinopathy. Nat Genet 32:326-330.

Rulifson EJ, Wu CH, Nusse R. 2000. Pathway specificity by the bifunctional receptor frizzled is determined by affinity for wingless. Mol Cell 6:117-126.

Sainio K, Suvanto P, Davies J, Wartiovaara J, Wartiovaara K, Saarma M, Arumae U, Meng X, Lindahl M, Pachnis V, Sariola H. 1997. Glial-cell-line-derived neurotrophic factor is required for bud initiation from ureteric epithelium. Development 124:4077-4087.

Sanchez MP, Silos-Santiago I, Frisen J, He B, Lira SA, Barbacid M. 1996. Renal agenesis and the absence of enteric neurons in mice lacking GDNF. Nature 382:70-73.

Saneyoshi T, Kume S, Amasaki Y, Mikoshiba K. 2002. The Wnt/calcium pathway activates NF-AT and promotes ventral cell fate in Xenopus embryos. Nature 417:295-299.

Sanford LP, Ormsby I, Gittenberger-de Groot AC, Sariola H, Friedman R, Boivin GP, Cardell EL, Doetschman T. 1997. TGFbeta2 knockout mice have multiple developmental defects that are non-overlapping with other TGFbeta knockout phenotypes. Development 124:2659-2670.

Santos RA, Ferreira AJ. 2007. Angiotensin-(1-7) and the renin-angiotensin system. Curr Opin Nephrol Hypertens 16:122-128.

Sanyanusin P, Schimmenti LA, McNoe LA, Ward TA, Pierpont ME, Sullivan MJ, Dobyns

WB, Eccles MR. 1995. Mutation of the PAX2 gene in a family with optic nerve colobomas, renal anomalies and vesicoureteral reflux. Nat Genet 9:358-364.
Satow R, Chan TC, Asashima M. 2004. The role of Xenopus frizzled-8 in pronephric development. Biochem Biophys Res Commun 321:487-494.
Saulnier DM, Ghanbari H, Brändli AW. 2002. Essential function of Wnt-4 for tubulogenesis in the Xenopus pronephric kidney. Dev Biol 248:13-28.
Sawa H, Lobel L, Horvitz HR. 1996. The Caenorhabditis elegans gene lin-17, which is required for certain asymmetric cell divisions, encodes a putative seven-transmembrane protein similar to the Drosophila frizzled protein. Genes Dev 10:2189-2197.
Saxen L, Sariola H. 1987. Early organogenesis of the kidney. Pediatr Nephrol 1:385-392.
Schuchardt A, D'Agati V, Larsson-Blomberg L, Costantini F, Pachnis V. 1994. Defects in the kidney and enteric nervous system of mice lacking the tyrosine kinase receptor Ret. Nature 367:380-383.
Schuchardt A, D'Agati V, Pachnis V, Costantini F. 1996. Renal agenesis and hypodysplasia in ret-k- mutant mice result from defects in ureteric bud development. Development 122:1919-1929.
Shah MM, Sampogna RV, Sakurai H, Bush KT, Nigam SK. 2004. Branching morphogenesis and kidney disease. Development 131:1449-1462.
Shakya R, Watanabe T, Costantini F. 2005. The role of GDNF/Ret signaling in ureteric bud cell fate and branching morphogenesis. Dev Cell 8:65-74.
Sharma RP, Chopra VL. 1976. Effect of the Wingless (wg1) mutation on wing and haltere development in Drosophila melanogaster. Dev Biol 48:461-465.
Shawlot W, Behringer RR. 1995. Requirement for Lim1 in head-organizer function. Nature 374:425-430.
Sheldahl LC, Park M, Malbon CC, Moon RT. 1999. Protein kinase C is differentially stimulated by Wnt and Frizzled homologs in a G-protein-dependent manner. Curr Biol 9:695-698.
Sheldahl LC, Slusarski DC, Pandur P, Miller JR, Kuhl M, Moon RT. 2003. Dishevelled activates Ca2+ flux, PKC, and CamKII in vertebrate embryos. J Cell Biol 161:769-777.
Shu W, Jiang YQ, Lu MM, Morrisey EE. 2002. Wnt7b regulates mesenchymal proliferation and vascular development in the lung. Development 129:4831-4842.
Slusarski DC, Corces VG, Moon RT. 1997a. Interaction of Wnt and a Frizzled homologue triggers G-protein-linked phosphatidylinositol signalling. Nature 390:410-413.
Slusarski DC, Yang-Snyder J, Busa WB, Moon RT. 1997b. Modulation of embryonic intracellular Ca2+ signaling by Wnt-5A. Dev Biol 182:114-120.
Smalley MJ, Sara E, Paterson H, Naylor S, Cook D, Jayatilake H, Fryer LG, Hutchinson L, Fry MJ, Dale TC. 1999. Interaction of axin and Dvl-2 proteins regulates Dvl-2-stimulated TCF-dependent transcription. Embo J 18:2823-2835.
Smit L, Baas A, Kuipers J, Korswagen H, van de Wetering M, Clevers H. 2004. Wnt activates the Tak1/Nemo-like kinase pathway. J Biol Chem 279:17232-17240.
Smolich BD, McMahon JA, McMahon AP, Papkoff J. 1993. Wnt family proteins are secreted and associated with the cell surface. Mol Biol Cell 4:1267-1275.
Sokol S, Christian JL, Moon RT, Melton DA. 1991. Injected Wnt RNA induces a complete body axis in Xenopus embryos. Cell 67:741-752.
Spater D, Hill TP, O'Sullivan R J, Gruber M, Conner DA, Hartmann C. 2006. Wnt9a signaling is required for joint integrity and regulation of Ihh during chondrogenesis. Development 133:3039-3049.

Spemann H. 1938. Embryonic development and induction. New Haven, Connecticut: Yale University Press.

Spemann H, Mangold H. 1924. Über die Induktion von Embryonalanlagen durch die Implantation artfremder Organisatoren. Arch. f. mikroskop. Anat. u. Entwicklungsmech. 100:599-638.

Stark K, Vainio S, Vassileva G, McMahon AP. 1994. Epithelial transformation of metanephric mesenchyme in the developing kidney regulated by Wnt-4. Nature 372:679-683.

Strutt D. 2003. Frizzled signalling and cell polarisation in Drosophila and vertebrates. Development 130:4501-4513.

Strutt DI, Weber U, Mlodzik M. 1997. The role of RhoA in tissue polarity and Frizzled signalling. Nature 387:292-295.

Sun TQ, Lu B, Feng JJ, Reinhard C, Jan YN, Fantl WJ, Williams LT. 2001. PAR-1 is a Dishevelled-associated kinase and a positive regulator of Wnt signalling. Nat Cell Biol 3:628-636.

Tada M, Smith JC. 2000. Xwnt11 is a target of Xenopus Brachyury: regulation of gastrulation movements via Dishevelled, but not through the canonical Wnt pathway. Development 127:2227-2238.

Taira M, Otani H, Jamrich M, Dawid IB. 1994. Expression of the LIM class homeobox gene *XLIM-1* in pronephros and CNS cell lineages of *Xenopus* embryos is affected by retinoic acid and exogastrulation. Development 120:1525-1536.

Takada R, Satomi Y, Kurata T, Ueno N, Norioka S, Kondoh H, Takao T, Takada S. 2006. Monounsaturated fatty acid modification of Wnt protein: its role in Wnt secretion. Dev Cell 11:791-801.

Takada S, Stark KL, Shea MJ, Vassileva G, McMahon JA, McMahon AP. 1994. Wnt-3a regulates somite and tailbud formation in the mouse embryo. Genes Dev 8:174-189.

Takayama H, LaRochelle WJ, Sabnis SG, Otsuka T, Merlino G. 1997. Renal tubular hyperplasia, polycystic disease, and glomerulosclerosis in transgenic mice overexpressing hepatocyte growth factor/scatter factor. Lab Invest 77:131-138.

Takeuchi M, Nakabayashi J, Sakaguchi T, Yamamoto TS, Takahashi H, Takeda H, Ueno N. 2003. The prickle-related gene in vertebrates is essential for gastrulation cell movements. Curr Biol 13:674-679.

Tanaka K, Kitagawa Y, Kadowaki T. 2002. Drosophila segment polarity gene product porcupine stimulates the posttranslational N-glycosylation of wingless in the endoplasmic reticulum. J Biol Chem 277:12816-12823.

Tanaka K, Okabayashi K, Asashima M, Perrimon N, Kadowaki T. 2000. The evolutionarily conserved porcupine gene family is involved in the processing of the Wnt family. Eur J Biochem 267:4300-4311.

Tang MJ, Worley D, Sanicola M, Dressler GR. 1998. The RET-glial cell-derived neurotrophic factor (GDNF) pathway stimulates migration and chemoattraction of epithelial cells. J Cell Biol 142:1337-1345.

Tao Q, Yokota C, Puck H, Kofron M, Birsoy B, Yan D, Asashima M, Wylie CC, Lin X, Heasman J. 2005. Maternal wnt11 activates the canonical wnt signaling pathway required for axis formation in Xenopus embryos. Cell 120:857-871.

Theisen H, Purcell J, Bennett M, Kansagara D, Syed A, Marsh JL. 1994. dishevelled is required during wingless signaling to establish both cell polarity and cell identity. Development 120:347-360.

Thomas KR, Capecchi MR. 1990. Targeted disruption of the murine int-1 proto-oncogene resulting in severe abnormalities in midbrain and cerebellar development. Nature 346:847-850.

Thomas KR, Musci TS, Neumann PE, Capecchi MR. 1991. Swaying is a mutant allele of the proto-oncogene Wnt-1. Cell 67:969-976.

Thompson B, Townsley F, Rosin-Arbesfeld R, Musisi H, Bienz M. 2002. A new nuclear component of the Wnt signalling pathway. Nat Cell Biol 4:367-373.

Thorpe CJ, Moon RT. 2004. nemo-like kinase is an essential co-activator of Wnt signaling during early zebrafish development. Development 131:2899-2909.

Thorpe CJ, Schlesinger A, Carter JC, Bowerman B. 1997. Wnt signaling polarizes an early C. elegans blastomere to distinguish endoderm from mesoderm. Cell 90:695-705.

Threadgill DW, Dlugosz AA, Hansen LA, Tennenbaum T, Lichti U, Yee D, LaMantia C, Mourton T, Herrup K, Harris RC, et al. 1995. Targeted disruption of mouse EGF receptor: effect of genetic background on mutant phenotype. Science 269:230-234.

Torban E, Dziarmaga A, Iglesias D, Chu LL, Vassilieva T, Little M, Eccles M, Discenza M, Pelletier J, Goodyer P. 2006. PAX2 activates WNT4 expression during mammalian kidney development. J Biol Chem 281:12705-12712.

Torres M, Gomez-Pardo E, Dressler GR, Gruss P. 1995. Pax-2 controls multiple steps of urogenital development. Development 121:4057-4065.

Umbhauer M, Djiane A, Goisset C, Penzo-Mendez A, Riou JF, Boucaut JC, Shi DL. 2000. The C-terminal cytoplasmic Lys-thr-X-X-X-Trp motif in frizzled receptors mediates Wnt/beta-catenin signalling. Embo J 19:4944-4954.

Uren A, Reichsman F, Anest V, Taylor WG, Muraiso K, Bottaro DP, Cumberledge S, Rubin JS. 2000. Secreted frizzled-related protein-1 binds directly to Wingless and is a biphasic modulator of Wnt signaling. J Biol Chem 275:4374-4382.

Vainio S, Heikkila M, Kispert A, Chin N, McMahon AP. 1999. Female development in mammals is regulated by Wnt-4 signalling. Nature 397:405-409.

Vainio SJ. 2003. Nephrogenesis regulated by Wnt signaling. J Nephrol 16:279-285.

van Amerongen R, Berns A. 2006. Knockout mouse models to study Wnt signal transduction. Trends Genet.

van de Wetering M, Cavallo R, Dooijes D, van Beest M, van Es J, Loureiro J, Ypma A, Hursh D, Jones T, Bejsovec A, Peifer M, Mortin M, Clevers H. 1997. Armadillo coactivates transcription driven by the product of the Drosophila segment polarity gene dTCF. Cell 88:789-799.

van den Heuvel M, Harryman-Samos C, Klingensmith J, Perrimon N, Nusse R. 1993. Mutations in the segment polarity genes wingless and porcupine impair secretion of the wingless protein. Embo J 12:5293-5302.

van den Heuvel M, Nusse R, Johnston P, Lawrence PA. 1989. Distribution of the wingless gene product in Drosophila embryos: a protein involved in cell-cell communication. Cell 59:739-749.

Veeman MT, Slusarski DC, Kaykas A, Louie SH, Moon RT. 2003. Zebrafish prickle, a modulator of noncanonical Wnt/Fz signaling, regulates gastrulation movements. Curr Biol 13:680-685.

Vega QC, Worby CA, Lechner MS, Dixon JE, Dressler GR. 1996. Glial cell line-derived neurotrophic factor activates the receptor tyrosine kinase RET and promotes kidney morphogenesis. Proc Natl Acad Sci U S A 93:10657-10661.

Vertino AM, Taylor-Jones JM, Longo KA, Bearden ED, Lane TF, McGehee RE, Jr., MacDougald OA, Peterson CA. 2005. Wnt10b deficiency promotes coexpression of myogenic and adipogenic programs in myoblasts. Mol Biol Cell 16:2039-2048.

Vincent JP, Dubois L. 2002. Morphogen transport along epithelia, an integrated trafficking problem. Dev Cell 3:615-623.

Vinson CR, Adler PN. 1987. Directional non-cell autonomy and the transmission of polarity

information by the frizzled gene of Drosophila. Nature 329:549-551.
Vinson CR, Conover S, Adler PN. 1989. A Drosophila tissue polarity locus encodes a protein containing seven potential transmembrane domains. Nature 338:263-264.
Vize PD, Seufert DW, Carroll TJ, Wallingford JB. 1997. Model systems for the study of kidney development: use of the pronephros in the analysis of organ induction and patterning. Dev Biol 188:189-204.
Wang HY, Liu T, Malbon CC. 2006a. Structure-function analysis of Frizzleds. Cell Signal 18:934-941.
Wang Q, Lan Y, Cho ES, Maltby KM, Jiang R. 2005. Odd-skipped related 1 (Odd 1) is an essential regulator of heart and urogenital development. Dev Biol 288:582-594.
Wang S, Krinks M, Lin K, Luyten FP, Moos M, Jr. 1997. Frzb, a secreted protein expressed in the Spemann organizer, binds and inhibits Wnt-8. Cell 88:757-766.
Wang Y, Guo N, Nathans J. 2006b. The Role of Frizzled3 and Frizzled6 in Neural Tube Closure and in the Planar Polarity of Inner-Ear Sensory Hair Cells. J. Neurosci. 26:2147-2156.
Wang Y, Huso D, Cahill H, Ryugo D, Nathans J. 2001. Progressive cerebellar, auditory, and esophageal dysfunction caused by targeted disruption of the frizzled-4 gene. J Neurosci 21:4761-4771.
Wang Y, Macke JP, Abella BS, Andreasson K, Worley P, Gilbert DJ, Copeland NG, Jenkins NA, Nathans J. 1996. A large family of putative transmembrane receptors homologous to the product of the Drosophila tissue polarity gene frizzled. J Biol Chem 271:4468-4476.
Wang Y, Thekdi N, Smallwood PM, Macke JP, Nathans J. 2002. Frizzled-3 is required for the development of major fiber tracts in the rostral CNS. J Neurosci 22:8563-8573.
Wang YK, Sporle R, Paperna T, Schughart K, Francke U. 1999. Characterization and expression pattern of the frizzled gene Fzd9, the mouse homolog of FZD9 which is deleted in Williams-Beuren syndrome. Genomics 57:235-248.
Westfall TA, Brimeyer R, Twedt J, Gladon J, Olberding A, Furutani-Seiki M, Slusarski DC. 2003. Wnt-5/pipetail functions in vertebrate axis formation as a negative regulator of Wnt/beta-catenin activity. J Cell Biol 162:889-898.
Wharton KA, Jr. 2003. Runnin' with the Dvl: proteins that associate with Dsh/Dvl and their significance to Wnt signal transduction. Dev Biol 253:1-17.
Wiens M, Belikov SI, Kaluzhnaya OV, Adell T, Schroder HC, Perovic-Ottstadt S, Kaandorp JA, Muller WEG. 2007. Regional and modular expression of morphogenetic factors in the demosponge Lubomirskia baicalensis. Micron In Press.
Willert K, Brink M, Wodarz A, Varmus H, Nusse R. 1997. Casein kinase 2 associates with and phosphorylates dishevelled. Embo J 16:3089-3096.
Willert K, Brown JD, Danenberg E, Duncan AW, Weissman IL, Reya T, Yates JR, 3rd, Nusse R. 2003. Wnt proteins are lipid-modified and can act as stem cell growth factors. Nature 423:448-452.
Winnier G, Blessing M, Labosky PA, Hogan BL. 1995. Bone morphogenetic protein-4 is required for mesoderm formation and patterning in the mouse. Genes Dev 9:2105-2116.
Wodarz A, Nusse R. 1998. Mechanisms of Wnt signaling in development. Annu Rev Cell Dev Biol 14:59-88.
Wong GT, Gavin BJ, McMahon AP. 1994. Differential transformation of mammary epithelial cells by Wnt genes. Mol Cell Biol 14:6278-6286.
Wong HC, Bourdelas A, Krauss A, Lee HJ, Shao Y, Wu D, Mlodzik M, Shi DL, Zheng J. 2003. Direct binding of the PDZ domain of Dishevelled to a conserved internal

sequence in the C-terminal region of Frizzled. Mol Cell 12:1251-1260.
Wong LL, Adler PN. 1993. Tissue polarity genes of Drosophila regulate the subcellular location for prehair initiation in pupal wing cells. J Cell Biol 123:209-221.
Woolf AS. 1997. The kidney. In: Thorogood P, editor. Embryos, genes and birth defects. John Wiley & Sons. pp 303-327.
Wu CH, Nusse R. 2002. Ligand receptor interactions in the Wnt signaling pathway in Drosophila. J Biol Chem 277:41762-41769.
Wu G, Markowitz GS, Li L, D'Agati VD, Factor SM, Geng L, Tibara S, Tuchman J, Cai Y, Park JH, van Adelsberg J, Hou H, Jr., Kucherlapati R, Edelmann W, Somlo S. 2000. Cardiac defects and renal failure in mice with targeted mutations in Pkd2. Nat Genet 24:75-78.
Wu J, Klein TJ, Mlodzik M. 2004. Subcellular localization of frizzled receptors, mediated by their cytoplasmic tails, regulates signaling pathway specificity. PLoS Biol 2:E158.
Xu PX, Adams J, Peters H, Brown MC, Heaney S, Maas R. 1999. Eya1-deficient mice lack ears and kidneys and show abnormal apoptosis of organ primordia. Nat Genet 23:113-117.
Xu PX, Zheng W, Huang L, Maire P, Laclef C, Silvius D. 2003. Six1 is required for the early organogenesis of mammalian kidney. Development 130:3085-3094.
Xu Q, Wang Y, Dabdoub A, Smallwood PM, Williams J, Woods C, Kelley MW, Jiang L, Tasman W, Zhang K, Nathans J. 2004. Vascular development in the retina and inner ear: control by Norrin and Frizzled-4, a high-affinity ligand-receptor pair. Cell 116:883-895.
Yamaguchi TP, Bradley A, McMahon AP, Jones S. 1999. A Wnt5a pathway underlies outgrowth of multiple structures in the vertebrate embryo. Development 126:1211-1223.
Yanagawa S, van Leeuwen F, Wodarz A, Klingensmith J, Nusse R. 1995. The dishevelled protein is modified by wingless signaling in Drosophila. Genes Dev 9:1087-1097.
Yang-Snyder J, Miller JR, Brown JD, Lai CJ, Moon RT. 1996. A frizzled homolog functions in a vertebrate Wnt signaling pathway. Curr Biol 6:1302-1306.
Yoder BK, Tousson A, Millican L, Wu JH, Bugg CE, Jr., Schafer JA, Balkovetz DF. 2002. Polaris, a protein disrupted in orpk mutant mice, is required for assembly of renal cilium. Am J Physiol Renal Physiol 282:F541-552.
Yoshikawa Y, Fujimori T, McMahon AP, Takada S. 1997. Evidence that absence of Wnt-3a signaling promotes neuralization instead of paraxial mesoderm development in the mouse. Dev Biol 183:234-242.
Yu J, McMahon AP, Valerius MT. 2004. Recent genetic studies of mouse kidney development. Curr Opin Genet Dev 14:550-557.
Zeng X, Tamai K, Doble B, Li S, Huang H, Habas R, Okamura H, Woodgett J, He X. 2005. A dual-kinase mechanism for Wnt co-receptor phosphorylation and activation. Nature 438:873-877.
Zhang H, Bradley A. 1996. Mice deficient for BMP2 are nonviable and have defects in amnion/chorion and cardiac development. Development 122:2977-2986.
Zhao C, Aviles C, Abel RA, Almli CR, McQuillen P, Pleasure SJ. 2005. Hippocampal and visuospatial learning defects in mice with a deletion of frizzled 9, a gene in the Williams syndrome deletion interval. Development 132:2917-2927.

3. Results

3.1. Analysis of Wnt, Frizzled, and SFRP genes expression during pronephric kidney development in *Xenopus laevis*.

3.2. Comparative analysis of Fzd6 gene expression during embryogenesis and kidney organogenesis in *Xenopus* and mouse

3.3. *Xenopus* fzd3 and fzd8 gene functions are required for pronephric kidney development

3.4. Non-canonical Wnt-4 signaling and EAF2 are required for eye development in *Xenopus laevis*

3.1. Analysis of Wnt, Frizzled, and SFRP genes expression during pronephric kidney development in *Xenopus laevis*.

Christophe Héligon, Vasilios Dabouras, and André W. Brändli*

Institute of Pharmaceutical Sciences, Department of Chemistry and Applied Biosciences, ETH Zürich, Zürich, Switzerland.

* Author for correspondence:
Institute of Pharmaceutical Sciences
Department of Chemistry and Applied Biosciences
ETH Zürich
CH-8093 Zürich
Switzerland
Tel.: +41-44 633 7421
FAX: Brändli@pharma.ethz.ch
Correspondence to: brandli@pharma.ethz.ch

Unpublished manuscript

Abstract

Wnt4, Wnt9b, and Wnt11have been identified as key Wnt genes regulating metanephric kidney development in the mouse. In *Xenopus laevis*, it was shown that wnt4 function is required for the formation of pronephric proximal tubules. Furthermore, it was also found that fzd8, a wnt receptor, function is necessary for differentiation of the distal compartment of the pronephric nephron. Here, we studied the expression of Wnt, frizzled and SFRP genes during Xenopus laevis embryogenesis to identify novel regulators of pronephric kidney development. We report the identification of sfrp2 and fzd6 genes as potential candidate genes, which display temporal and spatial expression in the developing pronephric kidney.

Introduction

Wnt, frizzled, and SFRP genes encode ligands, transmembrane receptors, and secreted wnt binding proteins, respectively, that play critical roles in the activation of Wnt signalling pathways at the cell surface. In mouse, Wnt genes have been shown to act at different stages of kidney organogenesis from ureteric bud branching to tubulogenesis. Wnt11 synergises with glial-cell-line-derived neurotrophic factor (GDNF) signalling to regulate ureteric bud branching events (Majumdar et al., 2003). Wnt9b is required for initiation of metanephric mesenchyme condensation (Carroll et al., 2005). Wnt4 is necessary both in mouse and *Xenopus* during early steps of renal tubulogenesis (Stark et al., 1994; Saulnier et al., 2002). In $Wnt4^{-/-}$ mice, the metanephric mesenchyme does not undergo mesenchyme-to-epithelial transformation (Stark et al., 1994). In *Xenopus laevis*, wnt4 pronephros expression is first detected to the anterior half of the pronephric anlage and later restricted to the most proximal tubular segments. Loss-of-function studies revealed the absence of the proximal tubules in wnt4 deficient *Xenopus laevis* embryos (Saulnier et al., 2002). At present, it is not known which Fzd genes and which Wnt signaling pathway(s) are responsible for Wnt4, Wnt9b, and Wnt11 function during mouse kidney organogenesis. SFRP genes have also been suggested as regulators of metanephric development (Yoshino et al., 2001). To elucidate the mechanism(s) of Wnt action during kidney development in *Xenopus laevis*, we decided to first determine which wnt, frizzled and sfrp genes are expressed in the developing pronephros. Many *Xenopus laevis* cDNAs encoding orthologs of the human Wnt, Frizzled, and SFRP are known. The expression of these genes during pronephric development (stages 13 to 37) has however not been fully documented. Furthermore, a few genes have not been identified in *Xenopus laevis* yet. Hence, we performed database searches to identify wnt, fzd, and sfrp genes and performed whole-mount *in situ* hybridizations to determine the expression of these genes during pronephric kidney development. Databases searches lead to the identification of two fzd6 genes and one new sfrp2 gene. By whole-mount in situ hybridization we determined that wnt4, wnt11, fzd3, fzd6, fzd8, crescent, and sfrp2 genes are potential regulators of pronephric development.

Experimental procedures

Database searches and sequence analysis

Xenopus laevis expressed sequence tags (ESTs) were identified by performing blast searches of public databases at the NCBI website (http://www.ncbi.nlm.nih.gov/BLAST/). The deduced amino acid sequences of the following human genes were used as baits: WNT1 (GenBank Acc. No. NP_005421); WNT2 (NP_003382); WNT2B (NP_004176); WNT3 (NP_110380); WNT3A (NP_149122); WNT4 (NP_110388); WNT5A (NP_003383); WNT5B (NP_110402); WNT6 (NP_006513); WNT7A (NP_004616); WNT7B (NP_478679); WNT8A (NP_490645); WNT8B (NP_003384); WNT9A (NP_003386); WNT9B (NP_003387); WNT10A (NP_079492); WNT10B (NP_003385); WNT11 (NP_004617); WNT16 (NP_476509); FZD1 (NP_003496); FZD2 (NP_001457); FZD3 (NP_059108); FZD4 (NP_036325); FZD5 (NP_003459); FZD6 (NP_003497); FZD7 (NP_003498); FZD8 (NP_114072); FZD9 (NP_003499); FZD10 (NP_009128); SFRP1 (NP_003003); SFRP2 (NP_003004); SFRP3 (NP_001454); SFRP4 (NP_003005); SFRP5 (NP_003006). Double-stranded DNA sequencing was either performed in-house or by Primm srl, Italy. Assembly of nucleotide sequence traces, analysis of nucleotide and protein sequences was performed using the DNAStar Lasergene software package (version 6.0). Amino acid sequence alignments were performed with MegAlign (DNAStar) using the Clustal W algorithm and the PAM250 residue weight table. cDNAs were checked for the presence of introns using the GENSCAN software (http://genes.mit.edu/GENSCAN.html).

*W*hole-mount *in situ* hybridization, sectioning of embryos, and imaging

Albino *Xenopus* embryos were obtained from *in vitro* fertilizations (Brändli and Kirschner, 1995) and staged as described previously (Nieuwkoop and Faber, 1994). Protocols for RNA probe synthesis and *in situ* hybridization to whole-mount embryos can be found elsewhere (Harland, 1991; Helbling et al., 1998; Helbling et al., 1999). Digoxigenin-labeled ribo probes were synthesized from linearized plasmids encoding *Xenopus laevis* wnt1 (GenBank acc. No. BC082627) ; wnt2b (U66288) ; wnt3A (M55054) ; wnt4 (BC087460) ; wnt5A (M55056) ; wnt6 (L07532) ; wnt7B (AF026894) ; wnt8A (X57234) ; wnt 8B (U22173) ; wnt11 (L23542) ; fzd1 (AF231711) ; fzd2 (BC110756) ; fzd3 (AJ001754) ; fzd4 (AJ251750) ; fzd5 (AF300716) ; fzd6a (BJ062929) ; fzd6b (CA790600) ; fzd7 (AJ243323) ; fzd8a (AF017177) ; fzd8b (AF033110) ; fzd10b (BC072128) ; frzA/sfrp1 (AF049908) ; sfrp2a (BC044687) ; sfrp2b (BJ031116) ; frzb1/sfrp3 (U68059) ; sfrp5 (AW765850); crescent (AF260729) ; sizzled (AF059570). Sense strand controls were prepared from all plasmids and tested negative by *in situ* hybridization. For histological analysis, embryos stained in whole mount were embedded in 4% low-melt agarose and sectioned at 20 μm using a Leica VT1000S vibrating blade microtome as described previously (Eid and Brändli, 2001). Photographs were taken digitally with axiocam color cameras (Zeiss)

mounted either on a Stereo Lumar.V12 stereoscopic microscope or an Axioskop 2 mot plus light microscope. Pictures were acquired using AxioVision 4.5 (Zeiss) software. Composite figures were organized and labeled using Adobe Photoshop 9 and Adobe InDesign 4 software.

Results

Search for pronephric *Xenopus laevis* wnt candidate genes

Wnt gene family is comprised of 19 genes in humans. At the time of initiation of the project, no *Xenopus laevis* cDNAs had been described for wnt9a, -9b, -10b, and -16. In contrast, wnt7C and wnt11b is only found in *Xenopus* but not in mammalians' genome. Unfortunately, database searches failed to identify Xenopus cDNAs encoding orthologs of human wnt9a, wnt9b, wnt10b and wnt16. Next, we determined the embryonic expression of the following wnt genes: wnt1, wnt2b, wnt3A, wnt4, wnt5A, wnt6, wnt7B, wnt8A, wnt 8B, and wnt11.

Wnt gene expression was elucidated by whole mount in situ hybridization. Wnt genes encode for secreted glycoproteins with a short to medium diffusion range, which made us consider both pronephric as well as genes expressed in the vicinity of the pronephros as candidate genes. Our approach could only confirm wnt4 as a genuine wnt gene with expression in the pronephros (Fig. 1A, B). None of the other *Xenopus laevis* wnt genes were detected during any stage of pronephric development treated here (data not shown). In addition, Wnt11 was expressed in the developing somites adjacent to the pronephric anlage (Fig. 1C, D).

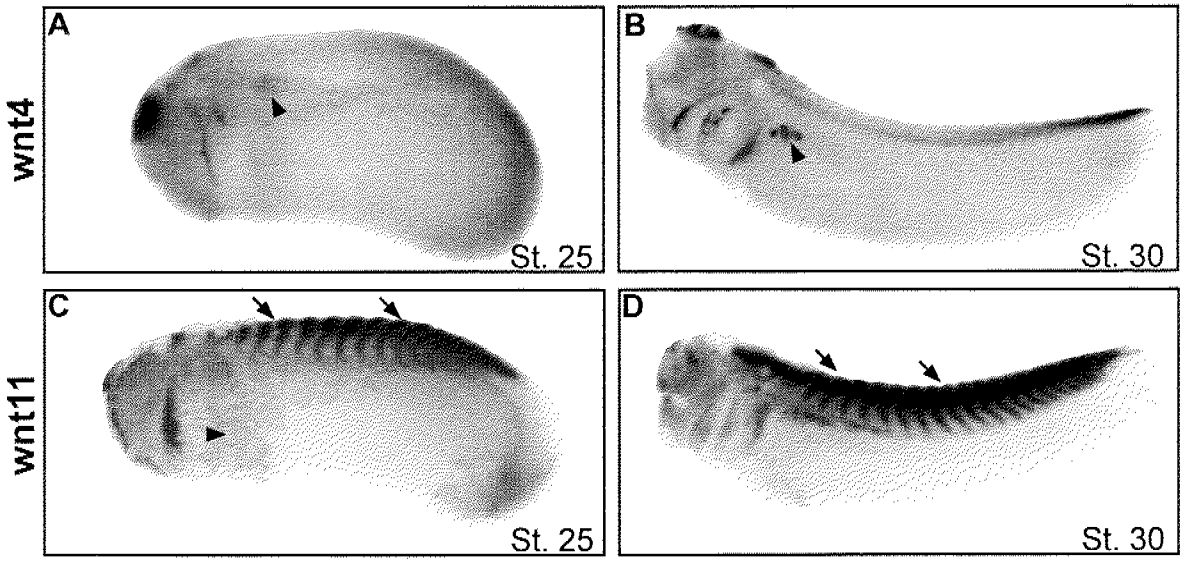

Figure 1: embryonic expression of wnt4 and wnt11 in or in tne vicinity of the developing pronephric kidney.
Albino embryos were allowed to develop to the indicated stage, fixed, and processed for gene expression analysis by whole-mount *in situ* hybridization. (A, B) Wnt4 expression was first detected in the anterior half of the pronephric anlage (A, arrowhead) and later restricted to the most proximal tubules (B, arrowhead). (C, D) Wnt11 is expressed in tissues adjacent to the pronephros (epidermis, arrowhead; somites, arrows) during pronephric kidney development.

Identification of *Xenopus laevis* frizzled candidate genes

Mammalian genomes contain typically 10 Fzd genes. No *Xenopus laevis* orthologs to human FZD6 and FZD9 were known at the beginning of this project. Database searches led to the identification of two *Xenopus* fzd6, but no Fzd9 cDNAs. The *Xenopus laevis* fzd6 genes are expressed in the entire pronephros from stage 29 onwards (Fig. 2E, F). The sequence analysis and expression of fzd6 is described in detail in next chapter (see 3.2.).

With regard to known *Xenopus laevis* fzd genes, fzd3 and fzd8 were expressed into the proximal and distal segments of the pronephric kidney, respectively (Fig. 2C-D, I-J). We completed the survey by analyzing expression of the other fzd genes by whole-mount *in situ* hybridization. The analysis suggested that fzd1 and fzd7 could qualify as candidate genes. fzd1 and fzd7 shared similar expression patterns with fzd8, whose expression was detected in intermediate and distal segments of the pronephric anlage and nephron (Fig. 2A-B, G-H). Transverse sections indicated however that the expression of fzd1 and fzd7 was not associated with the pronephros but with cells superficial to the pronephric anlage (Fig. 3).

Identification of *Xenopus laevis* secreted frizzled related protein candidate genes

Mammalian genomes contain typically 5 sfrp genes. In *Xenopus laevis*, SFRP4 and SFRP5 orthologs have not been described to date. Interestingly, the crescent gene is present in *Xenopus* but absent from mammalian genomes. A pseudogene similar to sizzled has been found in the human genome (GeneID: 651995). Database searches let to the identification of new *Xenopus* genes for sfrp2 and sfrp5. We failed to identify *Xenopus laevis* cDNAs encoding sfrp4. The sfrp5 cDNA was subsequently reported by others (Pilcher and Krieg, 2002). The new sfrp2 gene is pseudoallelic to sfrp2 (Pera and De Robertis, 2000) and therefore named sfrp2b. sfrp2b shared the same expression pattern as sfrp2 previously described (Fig. 4) (Pera and De Robertis, 2000). The sfrp2 genes were strongly expressed in dorsal structures and the epidermis as well as in the developing pronephros. Finally, we also studied crescent expression which was previously reported as being expressed during pronephric kidney development (Fig. 4) (Pera and De Robertis, 2000; Shibata et al., 2000).

Discussion

We performed here EST database searches to identify *Xenopus laevis* genes encoding wnt, fzd and sfrp genes. Using human reference sequences we discovered a number of new genes: fzd6a, fzd6b, sfrp2b, and sfrp5. Expression of fzd6a, fzd6b, sfrp2a, and sfrp2b was detected in the developing pronephros from stage 29 onwards. In summary, wnt4, fzd3, fzd6a, fzd6b, fzd8a, fzd8b, sfrp2a, sfrp2b and crescent genes are presently known to be expressed in the developing pronephros. Their expression pattern has been mapped onto the pronephric model developed by Daniela Raciti and Luca Regiani (Fig. 5) (Raciti, 2007). Interestingly, wnt4, fzd3, crescent,

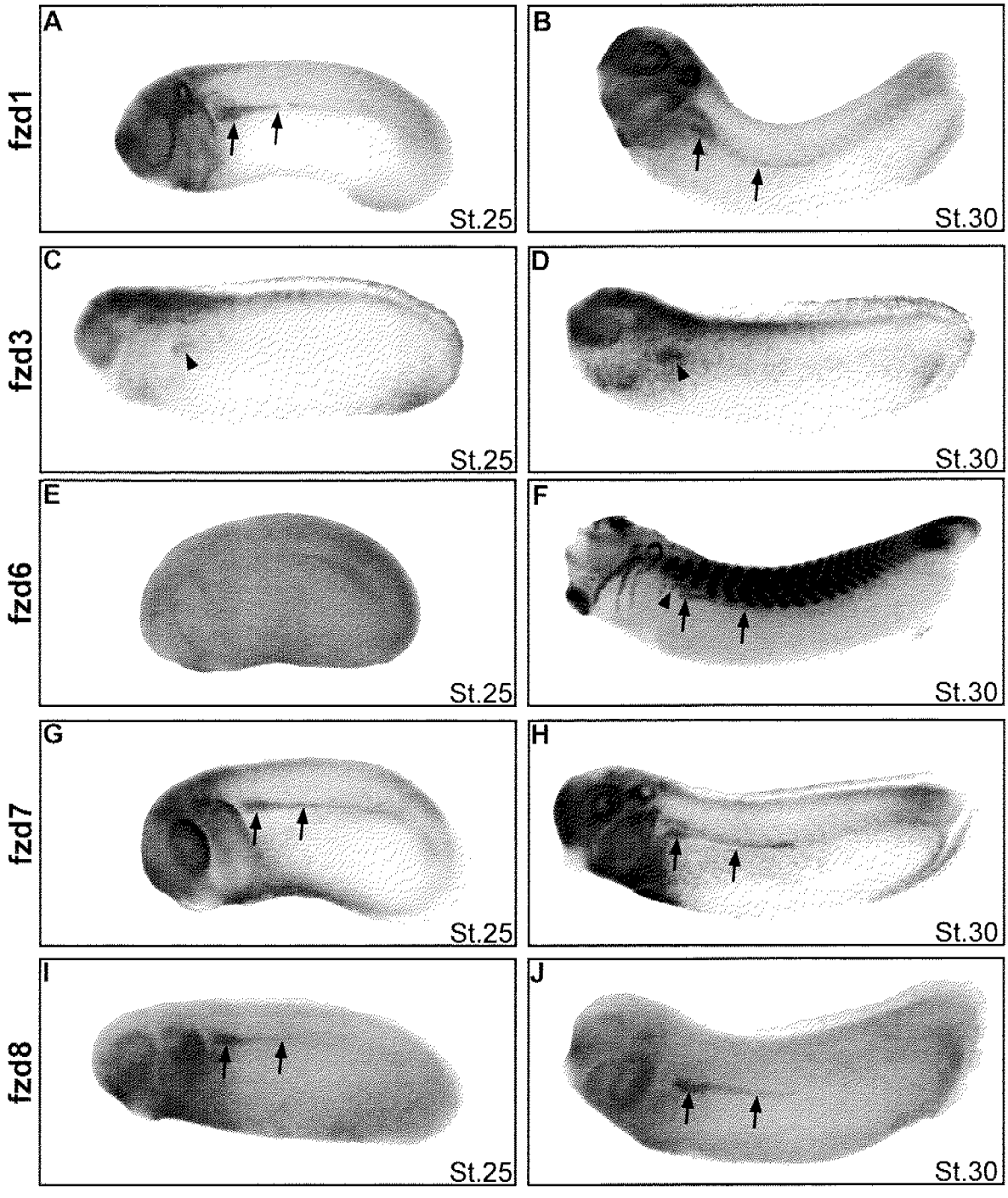

Figure 2: Embryonic expression of selected fzd genes.
Fzd genes expression was analyzed by whole mount *in situ* hybridization. (A, B, G-J) fzd1, fzd7, and fzd8 are expressed in similar patterns suggesting expression in the developing intermediate and distal tubule segments of the pronephros (arrows). (C, D) fzd3 expression is first detected in an anterior subdomain of the pronephric anlage (arrowhead) and is later found in the proximal segments (arrowhead). (E, F) fzd6 gene expression is not detected in the pronephric anlage during early nephrogenesis (E), but later along the entire pronephric nephron (arrowhead, proximal segmetns; arrows, intermediate and distal segments).

and sfrp2 genes share a very similar pattern of expression in the proximal tubule segments and might interact with each other to contribute to the previously described role of wnt4 during

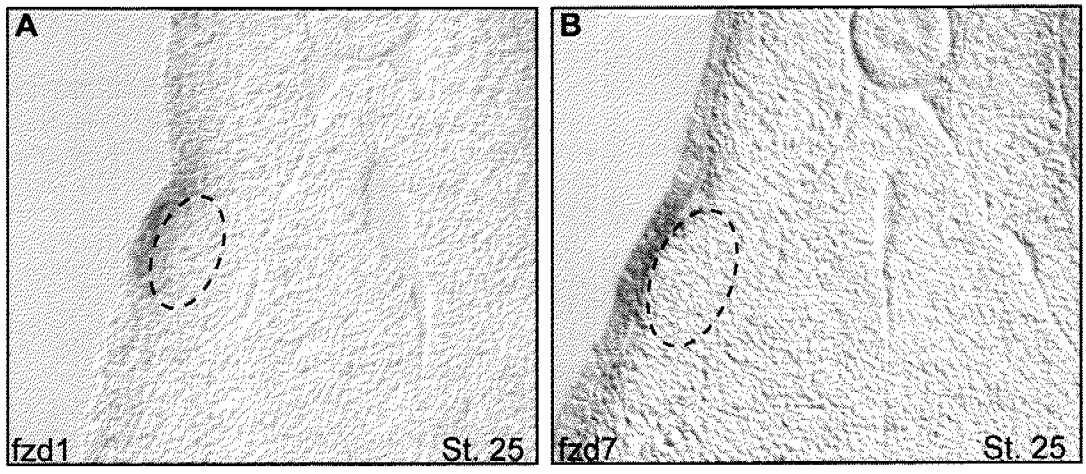

Figure 3: Transverse sections through embryos stained by whole-mount *in situ* hybridization for fzd1 and fzd7 expression.
(A, B) Expression of both genes is confined to epidermal cells but not to the pronephric anlage.

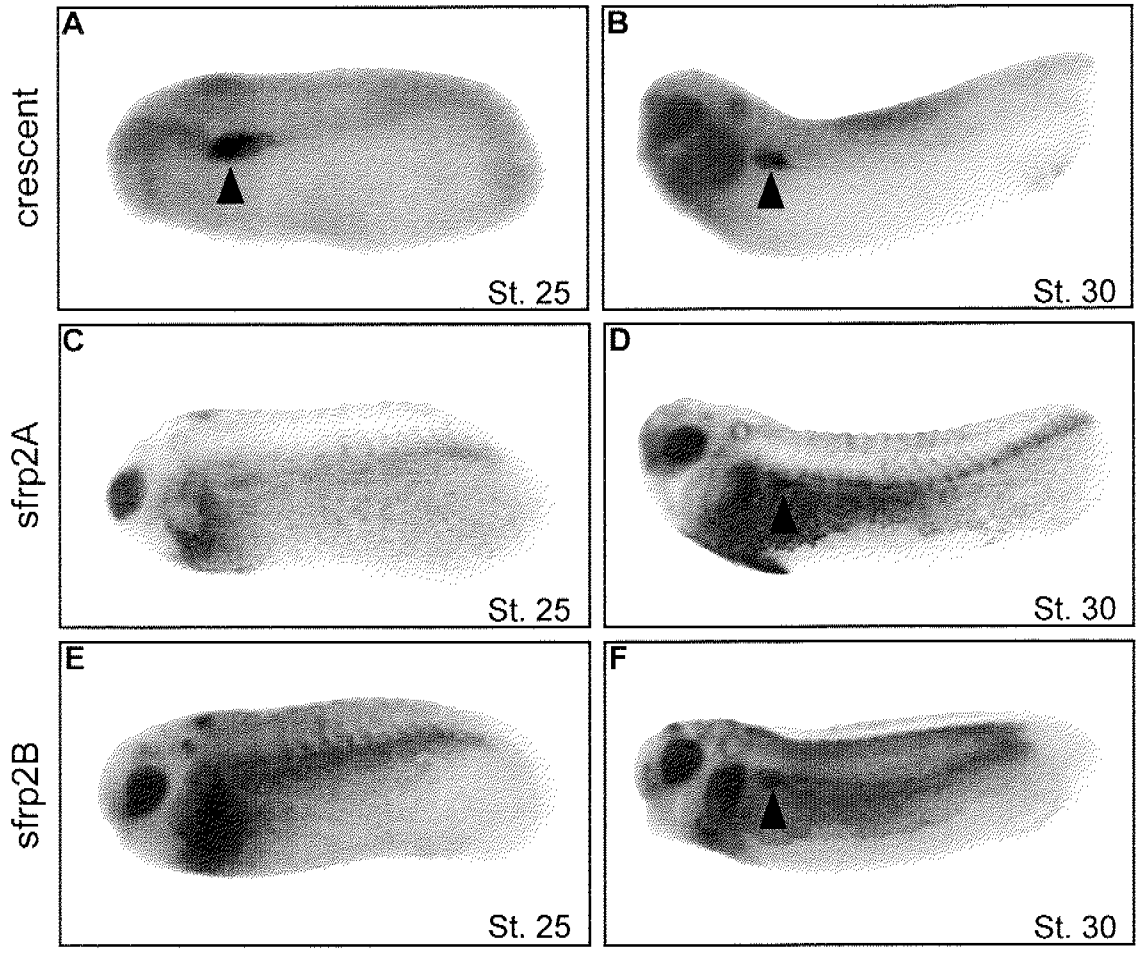

Figure 4: Expression of sfrp genes with pronephric expression.
Gene expression was assessed by whole-mount *in situ* hybridization. (A, B) crescent is first detected in the pronephric anlage and later restricted to the most proximal segments of the pronephros (arrowheads). (C-F) sfrp2A and sfrp2B expression is detected in the developing pronephros from stage 30 onward (arrow heads).

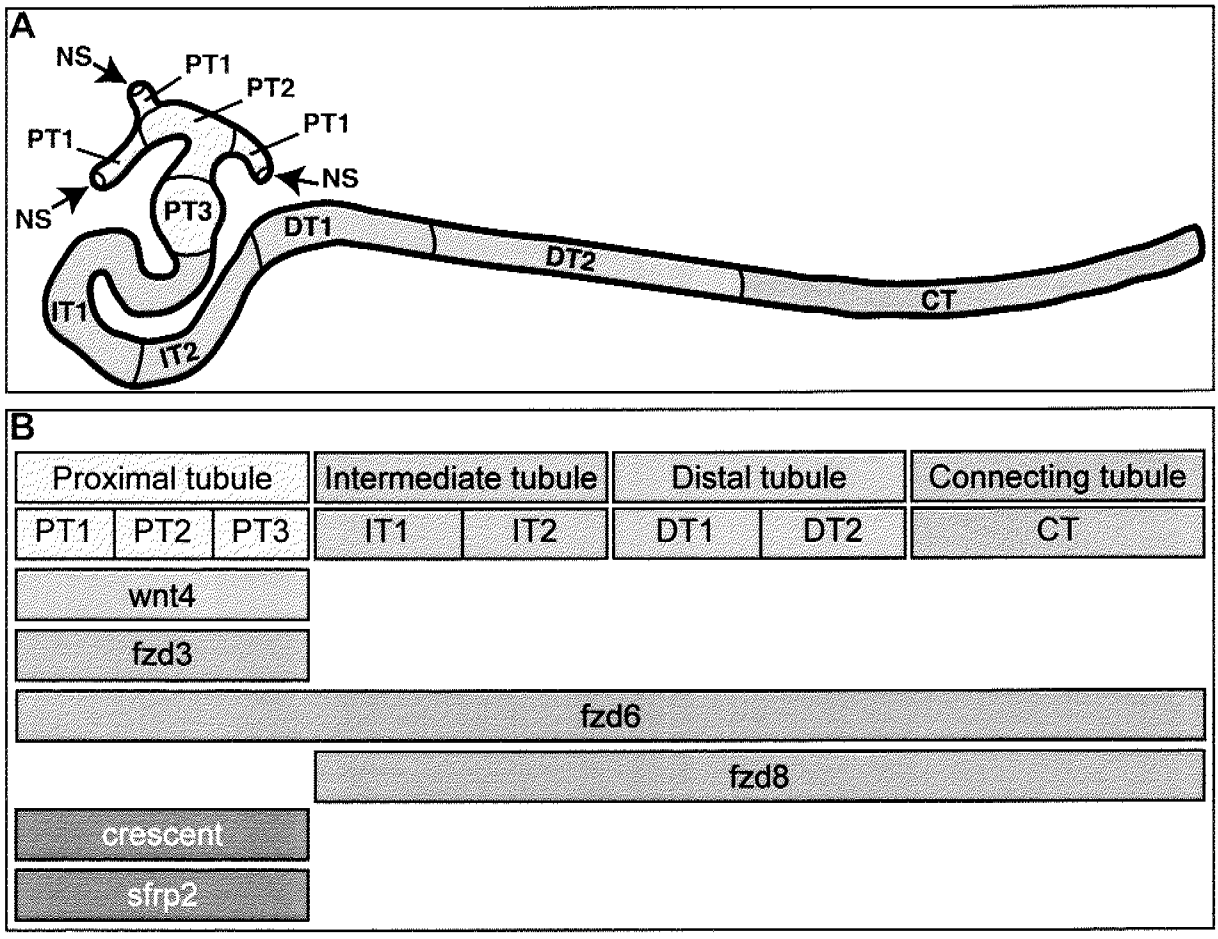

Figure 5: Schematic representation of Wnt, Fzd, and SFRP gene expression during pronephros development.
The expression of wnt, fzd, and sfrp genes was mapped on the scheme of the pronephros proposed by Daniela Raciti (Raciti, 2007). (A) Schematic representation of the tubular portion of the *Xenopus* pronephric kidney. A stage 35/36 pronephric kidney is shown with the four tubular compartments color coded. Each tubule is further subdivided into distinct segments: proximal tubule (yellow; PT1, PT2, PT3), intermediate tubule (green; IT1, IT2), distal tubule (orange; DT1, DT2), and connecting tubule (grey; CT). The nephrostomes (NS) are ciliated peritoneal funnels that connect the coelomic cavity to the nephron. (B) Expression domains of wnt (red), fzd (purple), and sfrp genes (blue) along the proximodistal axis of the developing pronephric nephron. The expression domains were mapped between stage 25 and 35/36. The localization of the expression domains is shown below the corresponding segments.

proximal tubule development (Saulnier et al., 2002). Notably, no wnt ligand has been detected in the distal parts of the pronephric nephron, whereas fzd6a/b and fzd8a/b genes are expressed there. Potentially, the *Xenopus laevis* wnt9a, wnt9b, wnt10b, or wnt16 genes could fulfill roles as ligands for these receptors. This is specially true for wnt9a, which was recently described to be expressed along the entire pronephric nephron from stage 32 on (Garriock et al., 2007). Interestingly this expression pattern resembles the one of fzd6 genes. In their study, Garriock and collaborators have reported, that one WNT11 gene is present in the human genome, whereas chicken, frog and zebrafish genomes contain two WNT11-like genes (Garriock et al., 2007). Based on nucleotide sequence identity, they propose to rename *Xenopus* wnt11-related gene

wnt11 as it is the closets ortholog to the human wnt11. The actual *Xenopus* Wnt11 would then be renamed wnt11b. Xenopus Wnt11b is the closest Wnt gene to zebrafish Wnt11/silberblick and the newly found chicken Wnt11b. *Xenopus* fzd8b gene is necessary for differentiation of the pronephric distal nephron as well as to a certain extent for proximal tubule formation (Satow et al., 2004). No wnt ligand has clearly been identified for fzd8. Wnt9a might therefore account for activation of wnt signaling via fzd8 at stage 30 or later. Despite no direct evidence for an early requirement of fzd8 function in pronephric development, one could also consider wnt-independent fzd8 signaling to occur in pronephros prior to wnt9a onset of expression. Wnt11, sfrp2a, sfrp2b and crescent functions during pronephric kidney development were addressed in the laboratory (Monica Walker; unpublished data). In no case, an antisense morpholino based gene knockdown could establish a pronephric function for these genes. However, it is important to mention that now a great number of novel pronephric marker genes have been established (Raciti, 2007), which could be used to reevaluate wnt and sfrp gene function in pronephric kidney development. With regard to fzd genes, gain- and loss-of-function studies are necessary to assess their role in pronephric kidney development in detail (see chapter 3.2 and 3.3). In summary, our studies have showed that wnt4, fzd3, fzd6a, fzd6b, fzd8a, fzd8b, sfrp2a, sfrp2b, and crescent are expressed during pronephric kidney development.

Acknowledgments

We would like to thank N. Ueno and the NIBB/NIG *Xenopus laevis* EST project for the fzd6a clone. This work was supported by grants of the European Community (EuReGene LSHG-CT-2004-005085) and Swiss National Science Foundation (3100A0-101964) to AWB.

References

Brändli AW, Kirschner MW. 1995. Molecular cloning of tyrosine kinases in the early Xenopus embryo: identification of Eck-related genes expressed in cranial neural crest cells of the second (hyoid) arch. Dev Dyn 203:119-140.

Carroll TJ, Park JS, Hayashi S, Majumdar A, McMahon AP. 2005. Wnt9b plays a central role in the regulation of mesenchymal to epithelial transitions underlying organogenesis of the mammalian urogenital system. Dev Cell 9:283-292.

Eid SR, Brändli AW. 2001. Xenopus Na,K-ATPase: primary sequence of the beta2 subunit and in situ localization of alpha1, beta1, and gamma expression during pronephric kidney development. Differentiation 68:115-125.

Garriock RJ, Warkman AS, Meadows SM, D'Agostino S, Krieg PA. 2007. Census of vertebrate Wnt genes: Isolation and developmental expression of Xenopus Wnt2, Wnt3, Wnt9a, Wnt9b, Wnt10a, and Wnt16. Dev Dyn 236:1249-1258.

Harland RM. 1991. In situ hybridization: an improved whole-mount method for Xenopus embryos. Methods Cell Biol 36:685-695.

Helbling PM, Saulnier DM, Robinson V, Christiansen JH, Wilkinson DG, Brändli AW. 1999. Comparative analysis of embryonic gene expression defines potential interaction sites for Xenopus EphB4 receptors with ephrin-B ligands. Dev Dyn 216:361-373.

Helbling PM, Tran CT, Brändli AW. 1998. Requirement for EphA receptor signaling in the segregation of Xenopus third and fourth arch neural crest cells. Mech Dev 78:63-79.

Majumdar A, Vainio S, Kispert A, McMahon J, McMahon AP. 2003. Wnt11 and Ret/Gdnf pathways cooperate in regulating ureteric branching during metanephric kidney development. Development 130:3175-3185.

Nieuwkoop PD, Faber J. 1994. Normal table of *Xenopus laevis* (Daudin): a systematical and chronological survey of the development from the fertilized egg till the end of metamorphosis. New York & London: Garland Publishing, Inc.

Pera EM, De Robertis EM. 2000. A direct screen for secreted proteins in Xenopus embryos identifies distinct activities for the Wnt antagonists Crescent and Frzb-1. Mech Dev 96:183-195.

Pilcher KE, Krieg PA. 2002. Expression of the Wnt inhibitor, sFRP5, in the gut endoderm of Xenopus. Gene Expr Patterns 2:369-372.

Raciti D. 2007. A large-scale gene discovery screen identifies over hundred solute carrier (SLC) genes with organ specific expression patterns in the *Xenopus* embryo. In: Department of Chemistry and Applied Biosceinces. Zürich: Swiss Federal Institute of Technology.

Satow R, Chan TC, Asashima M. 2004. The role of Xenopus frizzled-8 in pronephric development. Biochem Biophys Res Commun 321:487-494.

Saulnier DM, Ghanbari H, Brändli AW. 2002. Essential function of Wnt-4 for tubulogenesis in the Xenopus pronephric kidney. Dev Biol 248:13-28.

Shibata M, Ono H, Hikasa H, Shinga J, Taira M. 2000. Xenopus crescent encoding a Frizzled-like domain is expressed in the Spemann organizer and pronephros. Mech Dev 96:243-246.

Stark K, Vainio S, Vassileva G, McMahon AP. 1994. Epithelial transformation of metanephric mesenchyme in the developing kidney regulated by Wnt-4. Nature 372:679-683.

Yoshino K, Rubin JS, Higinbotham KG, Uren A, Anest V, Plisov SY, Perantoni AO. 2001. Secreted Frizzled-related proteins can regulate metanephric development. Mech Dev 102:45-55.

3.2. Comparative analysis of Fzd6 gene expression during embryogenesis and kidney organogenesis in *Xenopus* and mouse

Christophe Héligon[1], Lars Geffers[2], Gregor Eichele[2], and André W. Brändli[1*]

[1] Institute of Pharmaceutical Sciences, Department of Chemistry and Applied Biosciences, ETH Zürich, Zürich, Switzerland.

[2] Max Planck Institute for Biophysical Chemistry, Department of Genes and Behavior, Göttingen, Germany

* Author for correspondence:
Institute of Pharmaceutical Sciences
Department of Chemistry and Applied Biosciences
ETH Zürich
CH-8093 Zürich
Switzerland
Tel.: +41-44 633 7421
FAX: Brändli@pharma.ethz.ch
Correspondence to: brandli@pharma.ethz.ch

Unpublished manuscript

Abstract

Frizzled (Fzd) genes encode for seven-pass transmembrane receptor type of proteins that transduce Wnt protein signals into the cell. Mammalian genomes typically contain ten Fzd genes. In *Xenopus laevis*, eight Fzd orthologs have been found to date. Here we report the identification of two novel *Xenopus laevis* Fzd6 genes, fzd6a and fzd6b, and one *Xenopus tropicalis* fzd6 gene. By *in situ* hybridization, we show that the two pseudoallelic *Xenopus laevis* fzd6 genes show the same expression patterns. Initially, fzd6 was expressed in the animal hemisphere of pre-gastrula embryos. During neurulation, fzd6 transcripts were detected in the neural tube. Later during organogenesis, fzd6 was expressed in a complex pattern mainly restricted to the epithelial structures of the *Xenopus* embryo. In the pronephros, fzd6 expression coincided with renal epithelialization and was maintained later on. *Xenopus* fzd6 was also expressed in adult mesonephric kidneys and in the mesonephric A6 cell line. In the mouse, Fzd6 expression was confined to developing epithelial structures. Notably, both mesonephric and metanephric epithelia expressed Fzd6 during embryogenesis. In the adult kidney, Fzd6 expression was restricted to distal segments of the nephron. In contrast to the mouse, no vascular expression of fzd6 could be detected in *Xenopus* embryos. In summary, vertebrate Fzd6 genes show expression in developing epithelia.

Introduction

Secreted glycoproteins of the Wnt family are morphogens playing key roles in embryonic development as well as adult life (Logan and Nusse, 2004; Clevers, 2006). Requirement for Wnt signals during development has been demonstrated from *Caenorhabditis elegans* to mammals (Giudice, 2001; Korswagen, 2002; Logan and Nusse, 2004; Clevers, 2006). Wnt proteins can activate different signaling pathways, which include the canonical and one of the two non-canonical pathways, through binding to frizzled (Fzd) proteins (Huelsken and Birchmeier, 2001; Huelsken and Behrens, 2002). *Frizzled* genes were first shown to be involved in bristle and hair polarity in Drosophila (Adler et al., 1987). They were subsequently shown to encode seven-pass transmembrane receptor-type proteins of the G-protein coupled receptor superfamily (Vinson et al., 1989). Fzd genes have later been cloned from organisms ranging from humans, where ten Fzd genes exist in the genome, to *Caenorhabditis elegans* (Wang et al., 1996), which contain three Fzd genes. Fzd genes are Wnt co-receptors at the cell surface that are necessary to activate intracellular signaling pathways (Logan and Nusse, 2004). In vertebrates, the instrumental role of Fzd genes in Wnt signaling links them to multiple developmental processes like stem cells maintenance, early embryogenesis as well as organogenesis (Logan and Nusse, 2004; Clevers, 2006). The number of Fzd genes and their potential capacity to functionally compensate raises the problem of redundancy that has complicated loss-of-function studies to date.

The human frizzled-6 (FZD6) gene has been characterized and its expression has been reported to occur in multiple fetal and adult tissues as well as in cancer cell lines (Tokuhara et al., 1998). Functional characterization of FZD6 has been performed in cell cultures and has demonstrated a repressive effect of FZD6 (Golan et al., 2004). The repressive activity is attributable to a FZD6-transmitted signal that blocks canonical Wnt signaling at a step downstream of the β-catenin destruction complex. The study also suggests an antagonistic FZD6 signaling acting via the Wnt-$Ca2^{+}$ pathway to activate TAK1-NLK-mediated LEF/TCF phosphorylation which results in the abolishment of TCF/LEF capacity to bind to Wnt-responsive promoters (Golan et al., 2004). In the mouse, Frizzled-6 (Fzd6) expression has been reported in a number of recent publications (Wang et al., 1996; Borello et al., 1999; Sarkar and Sharpe, 1999; Guo et al., 2004; Wang et al., 2006b), but the data is still incomplete. Expression of Fzd6 in adult brain, eye, heart, kidney, liver, lung and spleen was determined by RNase protection assays (Wang et al., 1996); in embryonic somites, ectoderm, metanephric ducts, gut, notochord, and tooth epithelia by *in situ* hybridization (Borello et al., 1999; Sarkar and Sharpe, 1999); in skin and vasculature using a lacZ reporter gene (Guo et al., 2004). More recently, Fzd6 expression was also mapped to the inner-ear sensory epithelium (Wang et al., 2006a). Fzd6-deficient mice have been produced and harbor solely a macroscopic hair patterning phenotype indicating a requirement for Fzd6 function in epithelial cell polarity (Guo et al., 2004). Fzd3/Fzd6 double mutant mice revealed a redundant role for the two genes in neural tube closure as well as in the establishment of planar cell polarity of inner-ear sensory hair cells (Wang et al., 2006a). In

Xenopus laevis, no fzd6 genes have been described to date. Here, we report the identification of X*enopus laevis* cDNAs encoding two closely related fzd6 proteins, termed fzd6a and fzd6b. Next, we determined the expression patterns of fzd6 in *Xenopus* embryos. For comparative purposes, we also established the spatial expression of Fzd6 in the E14.5 mouse embryo and in the mouse E17.5 and adult kidney. We found that *Xenopus* and mouse Fzd6 genes were expressed in complex but similar patterns with high levels of expression in tissues undergoing epithelialization.

Experimental procedures

Database searches, sequencing, and sequence analysis

Xenopus laevis fzd6 cDNAs (fzd6a, (GenBank Acc. No. BJ062929); fzd6b, (CA790600)) were identified by searching public expressed sequence tag (EST) databases at National Center for Biotechnology Information (NCBI) (http://www.ncbi.nlm.nih.gov/BLAST/) using the amino acid sequence of human FZD6 (GenBank Acc.No. AB012911). A *Xenopus tropicalis* fzd6 gene model was identified in a search for orthologs of human FZD6 within the *Xenopus tropicalis* genome project, V4 release (http://genome.jgi-psf.org/cgi-bin/runAlignment?db=Xentr4&advanced=1). Double-stranded DNA sequencing was either performed in-house or by Primm srl, Italy. Assembly of nucleotide sequence traces, analysis of nucleotide and protein sequences was performed using the DNAStar Lasergene software package (version 6.0). The Xenopus fzd6 cDNAs were assessed for the presence of intron sequences using the GENSCAN software (http://genes.mit.edu/GENSCAN.html). Amino acid sequence alignments were performed with MegAlign (DNAStar) using the Clustal W algorithm and the PAM250 residue weight table. The alignments were then used to construct phylogenetic trees with the Neighbor-Joining algorithm (Saitou and Nei, 1987). Potential transmembrane domains were predicted based on sequence hydrophobicity using Kyte-Doolittle method. Signal peptide predictions were performed using SignalP 3.0 software (http://www.cbs.dtu.dk/services/SignalP/). For phylogenetic analysis the following sequences were used: human FZD3 (GenBank Acc. No. AJ272427); human FZD7 (AB010881); mouse Fzd3 (U43205); mouse Fzd6 (MMU43319); mouse Fzd7 (MMU43320); *Xenopus laevis* fzd3 (AJ001754); *Xenopus laevis* fzd7 (AF159106); *Xenopus laevis* smoothened (AF302766). All full-length cDNAs encoding *Xenopus* fzd6a contained a 1159 base pairs long intron located as indicated on Figure 1. Several partial fzd6a cDNAs lacking the intron were identified in public EST databases.

Handling of *Xenopus* embryos

Xenopus embryos were obtained, *in vitro* fertilized, and cultured as described (Brändli and Kirschner, 1995). Staging was performed according to Nieuwkoop & Faber (1956).

Dissection of kidneys from adult *Xenopus* frogs

Adult *Xenopus laevis* frogs were sacrificed by lethal narcosis, which was induced by bathing in 0.5 g/l of Tricaine (Sigma). The kidneys were removed by dissection, immediately frozen in liquid nitrogen, and stored at -80°C.

Extraction of total RNA from *Xenopus* embryos

Total RNA from *Xenopus* eggs, embryos of the indicated stages, and adult kidneys were extracted using TriZol reagent (Gibco BRL) following the manufacturer's instructions. DNase I (Invitrogen) was used to deplete the resulting samples from potentially contaminating genomic DNA.

***Xenopus* A6 cell culture and RNA extraction**

A6 cells, which were established from mesonephric kidneys of an adult male *Xenopus laevis* frog (Rafferty, 1969) were obtained from the ATCC Cell Repository (No. CCL-102). Cells were cultured at 26°C in Leibovitz medium(L-15) adjusted for amphibian tonicity (AL-15) 60% L-15 supplemented with 10% heat-inactivated fetal bovine serum (FBS). Cells were allowed to differentiate by culturing them for 14 days in 0.4 mm polyethylene terephthalate (PET) FALCON™ cell culture inserts (4.2 cm^2 BD 353090) at a seeding density of $2.5x10^5$ cells per insert. Prior to RNA extraction, cells were washed twice in 70% PBS and scraped with a rubber policeman in RLT-buffer (Qiagen) supplemented with β-mercaptoethanol. Total RNA was extracted using the RNeasy Mini Kit (Qiagen) according to the manufacturer's instructions. Total RNA quality and concentration were assessed using the Agilent Bioanalyzer and the Nanodrop spectrometer, respectively.

Reverse transcription and polymerase chain reaction (RT-PCR)

Single-stranded cDNAs were synthesized from 1 μg of total RNA using Superscript III reverse transcriptase (Invitrogen) with a polyT primer. Polymerase chain reaction was carried out using Taq DNA polymerase recombinant (Invitrogen) and the following primers: fzd6_forward (5'-TCCTGCCTCTGTGCCTTTGTGTCT-3'), fzd6a_reverse (5'-GTTACACGGGAATCAGAAGACCAA-3'), fzd6b_reverse (5'-TAGCAGAAACGTTTGTTTTCCCTA-3'), ef-1 (5'-CAGATTGGTGCTGGATATGC-3'), ef-2 (5'-ACTGCCTTGATGACGCCTAG-3'). The amplification products were analyzed by electrophoresis on agarose gels.

Whole-mount *in situ* hybridization of *Xenopus* embryos, embryo sectioning, and imaging

Albino *Xenopus* embryos were obtained from *in vitro* fertilizations and staged as described previously (Brändli and Kirschner, 1995). Protocols for RNA probe synthesis and whole-mount *in situ* hybridization of *Xenopus* embryos can be found elsewhere (Harland, 1991; Helbling et al., 1998; Helbling et al., 1999). Plasmids pXL069l23 and pCA790600 containing *Xenopus*

cDNAs for fzd6a (GenBank Acc. No. BJ062929) and fzd6b (CA790600), respectively, were used for the synthesis of antisense riboprobes. Sense strand controls were prepared from all plasmids and tested negative by *in situ* hybridization. Embryos stained in whole-mount were embedded in 4% low-melt agarose and sectioned at 20 μm using a Leica VT1000S vibrating blade microtome as described previously (Heller and Brändli, 1997). Photographs were taken digitally with AxioCam color cameras (Zeiss) mounted either on a Stereo Lumar. V12 stereoscopic microscope or an Axioskop 2 mot plus light microscope. Pictures were acquired using Axio Vision 4.5 (Zeiss). Composite figures were organized and labeled using Adobe Photoshop 9 and Adobe InDesign 4 software.

Collection of mouse tissues, sectioning, *in situ* hybridization and imaging

Mice were anesthetized with isoflurane (Abbott Laboratories) and sacrificed through cervical dislocation. Following a brief wash in cold phosphate-buffered saline, tissues were transferred to ice-cold O.C.T 4583 (Tissue-Tek, Sakura). Subsequently, tissues are transferred to a freezing chamber within 5 min after dissection. The chamber was filled with O.C.T. and placed for 40 sec onto an aluminum block submerged by 2/3 in a dry ice/methylpentane mixture (maintained at -65°C). The chamber was then removed and the tissue was submerged in O.C.T. and oriented appropriately with the aid of a blunt dissecting needle. Following freezing, the chamber was disassembled. O.C.T. blocks containing tissue were placed into plastic bags and are stored at □80°C for several months. The dissected kidney were placed into a dish filled with ice-cold O.C.T. and shortly thereafter the tissue is placed and frozen in the freezing chamber as described above. Gene expression was detected with digoxigenin-tagged RNA probes that were generated from DNA templates. The templates were synthesized by RT-PCR. Frozen sections were performed as follows. One day prior to sectioning, O.C.T. blocks were transferred to a □20°C freezer and then mounted on a cryostat chuck. A Leica cryostat Model CM 3050S was used and sections were cut 20μm or 25μm thick. Fixation, carried out in a Leica Autostainer XL, was in 4% paraformaldehyde for 20 min at room temperature. Subsequently, slides are washed for 5 min in PBS, acetylated and dried by passing them through an ethanol series ending with 100 % ethanol. After drying at 30°C, slides were stored at □80°C in boxes containing a drying agent and sealed with electrical tape. *In situ* hybridizations were performed by the GenePaint robot in an automated manner. Photography was performed using a Leica DM-RXA2 microscope, a motorized Märzhäuser stage, a Leica electronic focusing system and, a Hitachi CCD camera.

Results

Cloning and sequence analysis of *Xenopus* fzd6 genes

Mammalian genomes contain typically ten genes encoding for frizzled gene family members. Eight *Xenopus laevis* frizzled (fzd) genes have been reported to date. We searched *Xenopus*

laevis expressed sequence tag (EST) databases for cDNAs encoding orthologs of human FZD6. This search led to the identification of two cDNAs classes, exemplified by GenBank Acc. No. BJ062929 and CA790600, which are derived from two distinct pseudoallelic *Xenopus laevis* fzd6 genes. We will refer to the two fzd6 genes as fzd6a and fzd6b (Fig. 1). We identified an intron of 1159 bp length in several fzd6a cDNAs, which was absent in other partial fzd6a cDNAs, such as GenBank Acc. No. CB208731. Initially, we identified by sequence analysis two potential in frame start codons for fzd6a and fzd6b genes. We reasoned that nucleotide sequence comparisons with the fzd6 gene from the closely related *Xenopus tropicalis* species may help to identify the correct initiation codon. Thus, we searched for a fzd6 gene in the *Xenopus tropicalis* genome and identified one putative fzd6 gene (Fig. 1). Nucleotide sequence comparison of *Xenopus laevis* fzd6a and fzd6b and *Xenopus tropicalis* fzd6 sequences revealed the presence of only one conserved potential initiation codon. The sequence identity between the ORFs of *Xenopus laevis* fzd6a and fzd6b was 92% at the nucleotide level, which suggests that fzd6a and fzd6b are indeed pseudoalleles. The deduced amino acid sequences of *Xenopus laevis* fzd6a and fzd6b encode proteins of 707 and 708 amino acids, respectively, sharing 91,4% identity. The *Xenopus tropicalis* fzd6 gene encodes a putative 707 amino acid protein. All three *Xenopus* fzd6 proteins display characteristic features of the Fzd protein family: a N-terminal signal peptide, an extracellular cysteine-rich domain, a hydrophobic region containing a putative seven-pass transmembrane domain, and an intracellular variable domain (Fig. 2). The *Xenopus* fzd6 proteins share high amino acid sequence identity to human and mouse Fzd6 proteins (Fig. 2). The deduced *Xenopus laevis* fzd6a and fzd6b, and *Xenopus tropicalis* fzd6 proteins had amino acid identities of 61%, 61.4%, and 62.1% with human FZD6, respectively. As in human FDZ6 (Golan et al., 2004), *Xenopus laevis* and *tropicalis* fzd6 proteins do not contain the typical PDZ-binding motif found in the C-terminal cytoplasmic domain of Fzd proteins. Phylogenetic analysis of human, mouse, and *Xenopus* Fzd sequences was performed and revealed the clustering of *Xenopus laevis* fzd6a, fzd6b and *Xenopus tropicalis* fzd6 with the mammalian Fzd6 proteins (Fig. 3).

Expression of fzd6 during *Xenopus laevis* embryogenesis

Reverse transcription-polymerase chain reactions (RT-PCR) for fzd6 transcripts were carried out to define the temporal expression profile of fzd6 gene expression during *Xenopus* embryogenesis. Total RNA was isolated from unfertilized eggs and embryos ranging from stage 5 to 40. Transcripts were detected in eggs as well as in all analyzed embryonic stages (Fig. 4A). Interestingly, fzd6 transcripts were also detected in adult kidneys and in the renal epithelial A6 cell line (Fig. 4A). Next, we elucidated the spatiotemporal expression of fzd6 by whole-mount *in situ* hybridization. Both *Xenopus laevis* fzd6 genes shared the same expression pattern and therefore only fzd6a will be shown (Fig. 4B-M). fzd6 transcripts were first detected in the animal

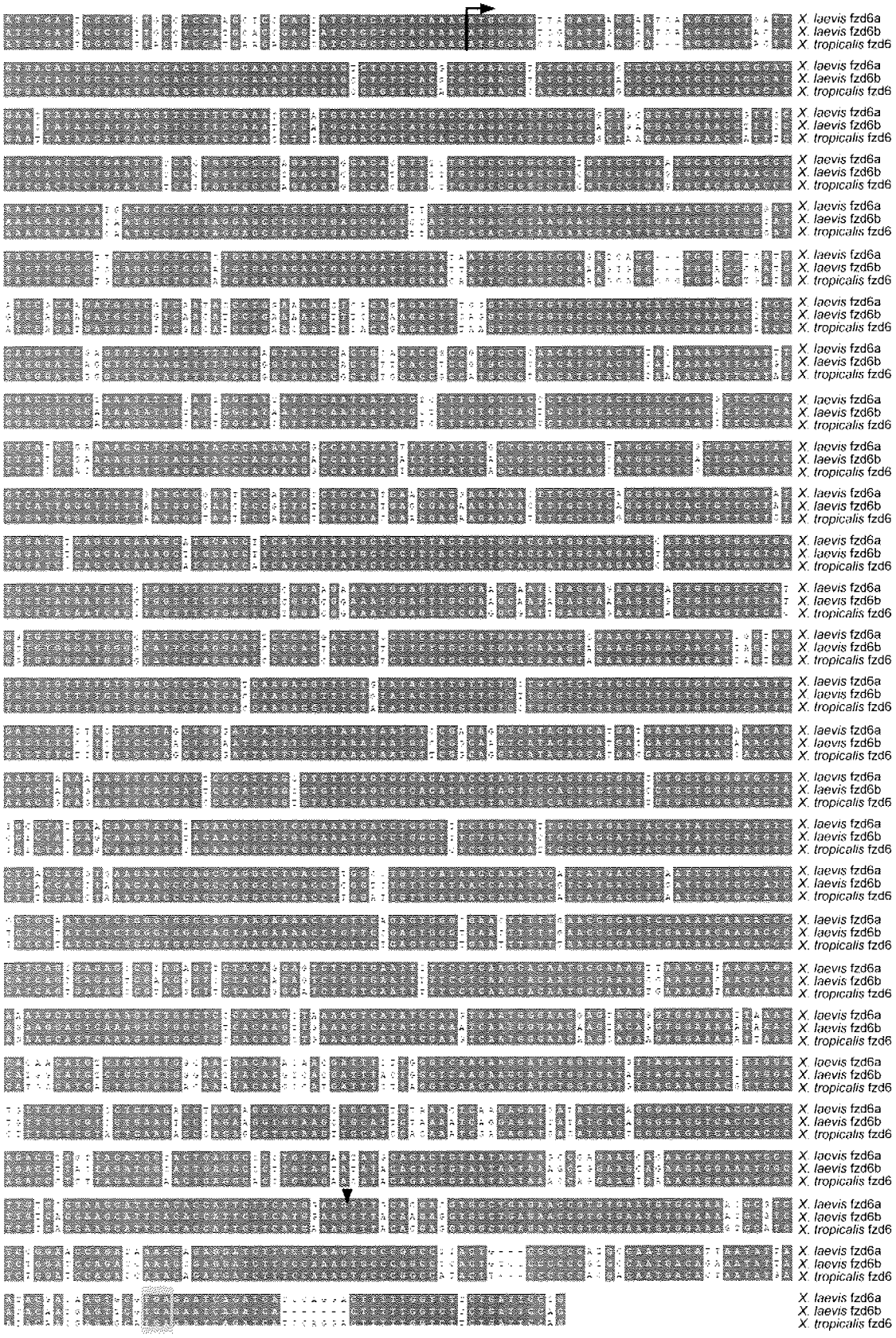

Figure 1: Alignment of *Xenopus* fzd6 nucleotide sequences. The nucleotide sequences of *Xenopus laevis* fzd6a, fzd6b, and *Xenopus tropicalis* fzd6 were aligned using the clustal W algorithm. Conserved nucleotides are boxed in blue. The predicted initiation codons are indicated with an arrow. The predicted stop codons are boxed in red. The intron position found in *Xenopus laevis* fzd6a cDNAs is indicated by an arrowhead. Abbreviation: *X.*, *Xenopus*.

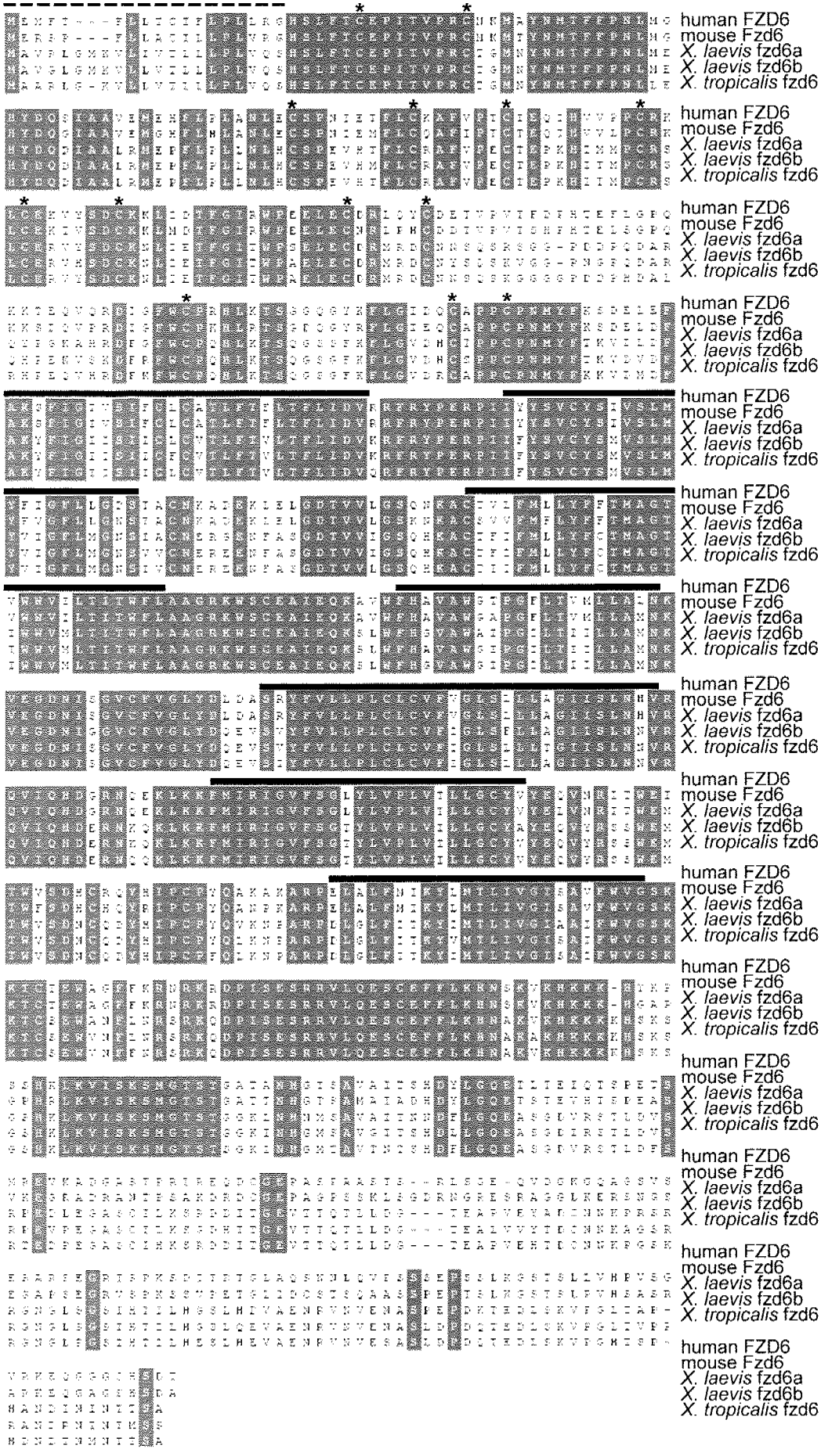
human FZD6
mouse Fzd6
X. laevis fzd6a
X. laevis fzd6b
X. tropicalis fzd6

Figure 2: Alignment of the deduced amino acid sequences of human, mouse, and *Xenopus* Fzd6 proteins.
Amino acid residues conserved throughout all species are boxed in blue. The predicted signal peptides are depicted with a dashed line. The extracellular cysteine-rich domain harbors ten conserved cysteine residues (*). The predicted seven transmembrane domains are highlighted with lines.

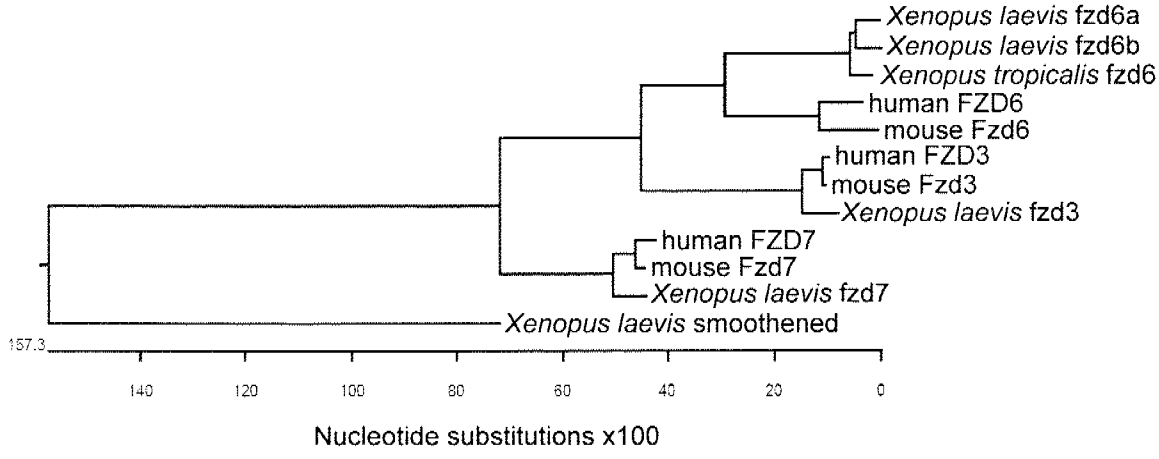

Figure 3: Phylogenetic analysis of vertebrate Fzd3, Fzd6, and Fzd7 genes.
The sequences were aligned by Clustal V method and the phylogenetic tree was constructed using the neighbour joining method. The GenBank accession numbers for the sequences are as follows: human FZD3 (NP_059108), human FZD6 (NP_003497), human FZD7 (NP_003498), mouse Fzd3 (NM_021458), mouse Fzd6 (NM_008056), mouse Fzd7 (NM_008057), *Xenopus laevis* fzd3 (AJ001754), *Xenopus laevis* fzd6a (BJ062929), *Xenopus laevis* fzd6b (CA790600), *Xenopus laevis* fzd7 (AJ243323), and *Xenopus laevis* smoothened (AF302766). The *Xenopus tropicalis* fzd6 gene model was obtained from the Joint Genome Institute (JGI) web server.

hemisphere of pregastrula embryos (Fig. 4B, C), whereas the vegetal hemisphere was devoid of fzd6 expression (Fig. 4D). Later, fzd6 expression was detected in the epidermis as well as in the cement gland and the neural fold (Fig. 4E). This pattern remained until stage 27, when fzd6 expression was detected in organs derived from ectoderm (midbrain, epidermis, neural tube, cement gland, otic vesicle, eye) as well as in mesodermal tissues (somites, notochord, visceral arches, pronephros) (Fig. 4F). At stage 31, ventral fzd6 expression corresponding to the ventral blood islands appeared (Fig. 4G). Transversal section confirmed expression in the epidermis, somites, notochord, and pronephros. Furthermore, expression in the neural tube was revealed (Fig. 4I). At stage 31, fzd6 was expressed in the condensing pronephric tissue undergoing epithelialization to form pronephric tubules (Fig. 4J). At stage 35/36, the previous expression domains remained and the expression levels in ventral blood islands and pronephros increased (Fig. 4H). fzd6 expression in the pronephros was restricted to the renal epithelium as can be seen on transversal sections (Fig. 4K, L). Sections through the head of stage 35/36 embryos confirmed fzd6 expression in the brain, eye, and visceral arches (Fig. 4M).

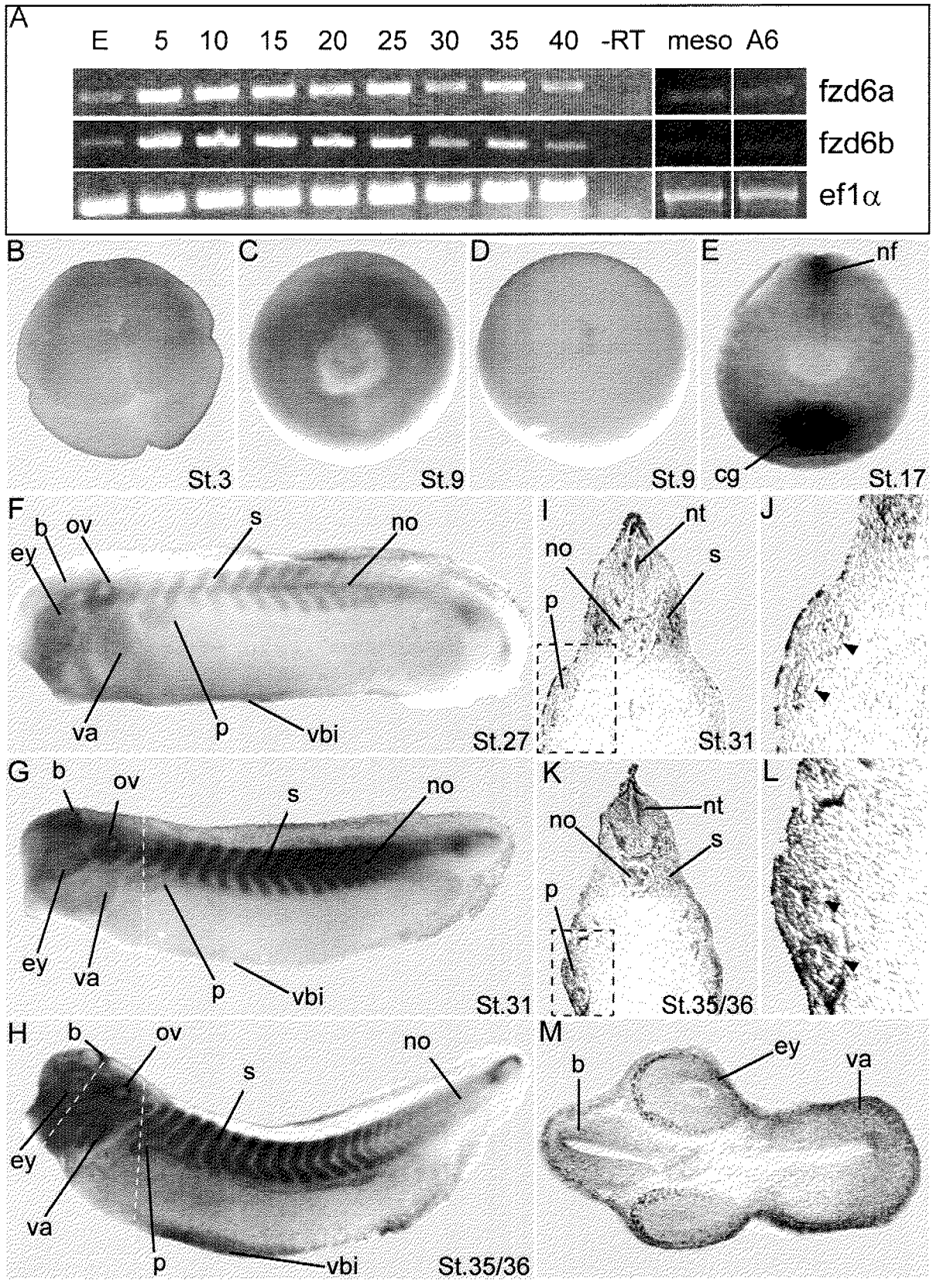
A
E 5 10 15 20 25 30 35 40 -RT meso A6
fzd6a
fzd6b
ef1α
B
St.3
C
St.9
D
St.9
E
nf
cg
St.17
F
b
ov
ey
s
no
va
p
vbi
St.27
I
nt
no
s
p
St.31
J
G
b
ov
s
no
ey
va
p
vbi
St.31
K
nt
no
s
p
St.35/36
L
H
b
ov
no
s
ey
va
p
vbi
St.35/36
M
ey
va
b

Figure 4: *Xenopus* fzd6 gene expression during embryogenesis.
(A) Reverse transcription followed by polymerase chain reaction revealed that fzd6a and fzd6b mRNAs were present maternally and throughout embryogenesis until stage 40. fzd6a and fzd6b mRNAs were also detected in adult kidneys and in renal A6 cells. ef1α (elongation factor-1α) mRNA served as a loading control. (B-M) Embryonic expression of fzd6a as determined by whole-mount *in situ* hybridization. (B) In the 8-cell stage embryo, fzd6a expression was preferentialy in the animal blastomeres. (C, D) In blastula stage embryos, fzd6a mRNA was detected in blastomeres of the animal pole (C) whereas the ventral hemisphere showed no expression (D). (E) During late neurula stages, fzd6a mRNA expression was observed in the neural fold (nf), the cement gland (cg), and the epidermis. (F-H) At tadpole stages, fzd6a expression was observed in ectodermal derivatives like in the brain (b), otic vesicle (ov), notochord (no), eye (ey), visceral arches (va), epidermis as well as in mesodermal derivatives such as somites, pronephros (p), and ventral blood islands (vbi). (I-M)Transversal sections through tadpole stage embryos revealed fzd6a expression in the neural tube (nt), pronephros (arrowheads), epidermis, notochord, somites, ventral blood islands, brain, eyes and visceral arches.

Fzd6 expression in the mouse

For comparative purposes, we investigated the expression of Fzd6 in the E14.5 embryo and in the developing and adult kidney. In E14.5 embryos, Fzd6 transcripts were detected in a complex pattern mainly in tissues undergoing epithelialization (Fig. 5A-C, a-c). Indeed, Fzd6 expression was detected in the epidermis, hair follicles (data not shown), the epithelium of the sensory organs, and epithelia of the digestive, respiratory, and genitourinary systems. Furthermore, Fzd6 expression was also detected in the blood vessels (i.e. scattered pattern in the nervous system), in the somites, and in the spleen (data not shown). Interestingly, Fzd6 expression was detected also in the developing mesonephric and metanephric tubules. To study Fzd6 expression during kidney development in further detail, *in situ* hybridizations were performed on sections of E17.5 and adult mouse kidneys. In the E17.5 metanephric kidney, Fzd6 transcripts are detected in renal epithelia and blood vessels (Fig. 5D). In adult kidneys, Fzd6 transcripts are detected only in the collecting ducts (Fig. 5E).

Discussion

In the present study, we identified novel fzd6 genes from *Xenopus laevis* and *Xenopus tropicalis*. We have established that *Xenopus* fzd6 share the same expression pattern during frog embryonic development, in mesonephros and, in A6 cell line. In addition, we show that Fzd6 expression is highly conserved in vertebrates. Mouse Fzd6 is expressed in various epithelial structures of the E14.5 embryo.This indicates that vertebrate Fzd6 genes are predominantly expressed in epithelial tissues during embryogenesis. Focusing on the kidney, our analysis revealed that the *Xenopus* pronephros and the mouse mesonephros and metanephros express Fzd6 genes in developing renal epithelia. In addition, the blood vessels of metanephric kidneys are positive for Fzd6 transcripts. Interestingly, the embryonic vasculature of *Xenopus* embryos was negative for fzd6 gene expression. However, we found expression in the ventral blood islands. In summary,

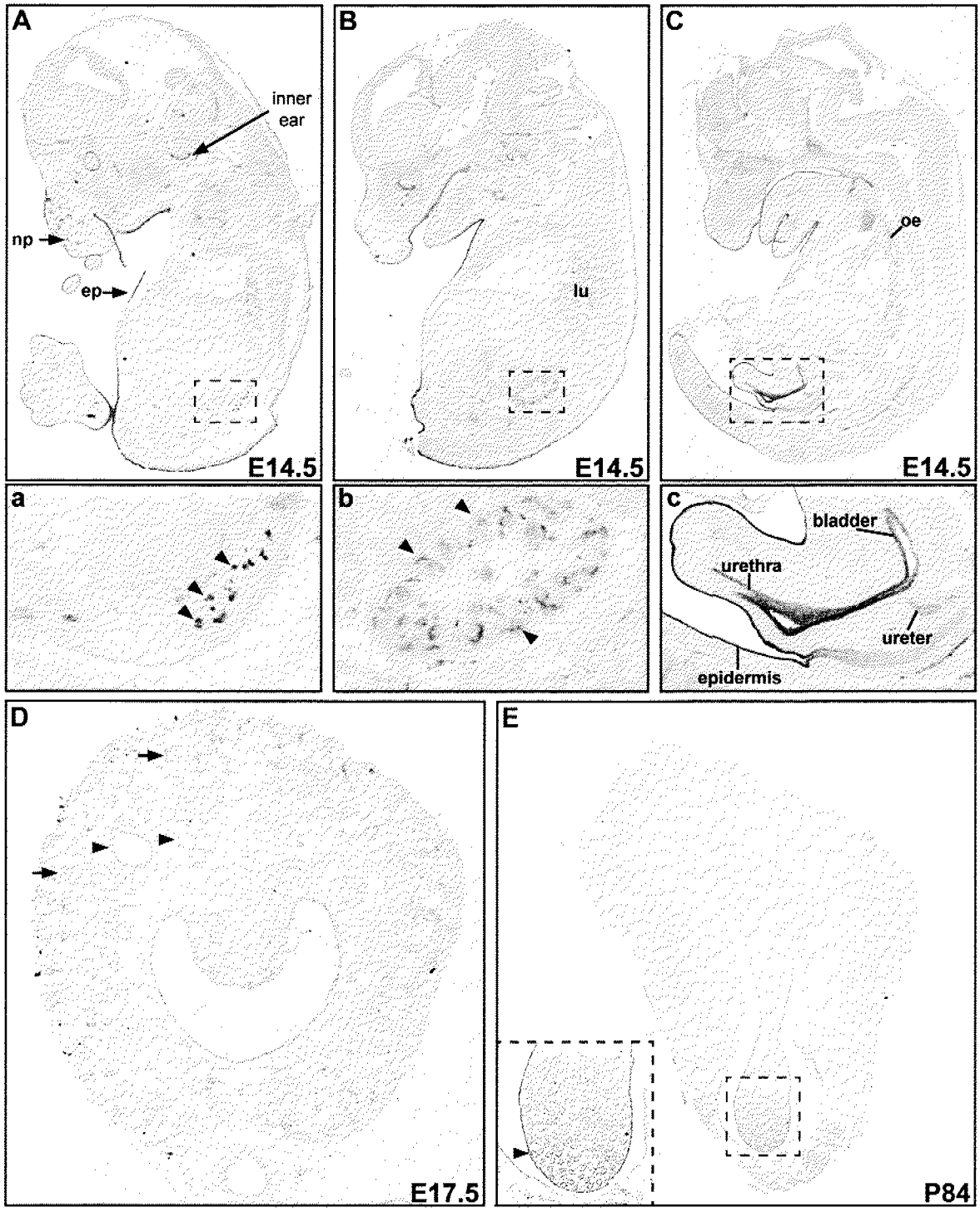

Figure 5: Expression of Fzd6 in the mouse E14.5 embryo, and in the developing and adult kidney. Mouse Fzd6 expression was monitored by *in situ* hybridization on sagital sections of E14.5 embryos (A-C) and transverse sections of E17.5 (D) and adult kidneys (E). (A-C) Fzd6 mRNAs are detected in polarized tissues like the lungs, the epidermis, and the nasal placodes at E14.5. In the developing excretory system, Fzd6 transcripts were found in mesonephric tubules (a, arrowheads), metanephric tubules (b, arrowheads), ureter, urethra, and bladder (c) at E14.5, and in epithelium of metanephric nephrons (arrows) as well as blood vessels (arrowheads) of the E17.5 metanephric kidney (D). In the adult kidney, Fzd6 was expressed in the collecting ducts of adult kidneys (E, arrowhead). Abbreviations: ep, epidermis; lu, lung; np, nasal placodes; oe, oesophagus.

the striking conservation of Fzd6 expression in mammals and amphibians suggests a critical role in the formation of epithelia. It was previously shown that Fzd6 deficient mice present with disorganized hair patterning, while no other phenotype was reported to date (Guo et al., 2004). In Fzd3/Fzd6 double mutant mice additional phenotypes could be observed, which include defects in the organization of the inner ear epithelium as well as failure in neural tube closure (Wang et al., 2006b). These studies illustrate that functional redundancies exist between different Fzd genes *in vivo*. We also performed fzd6 knockdown experiments in *Xenopus laevis* embryos. We failed however to detect any significant developmental defects (C. Héligon and A. Brändli, manuscript in preparation). We conclude that like in the mouse, fzd6 function is dispensable for early embryonic development in *Xenopus*. Fzd6 expression in developing epithelia suggests that Fzd6 could function via the planar cell polarity pathway to polarize epithelial cells. In the mouse, Fzd6 functions together with Fzd3 in the establishment of planar cell polarity of inner ear sensory hair cells (Wang et al., 2006a). Remarkably, fzd3 and fzd6 expression is conserved in the *Xenopus* otic vesicle (Fig. 4; data not shown). Therefore, these two fzd genes could play a similar role in the development of *Xenopus* inner ear. Presently, the Wnt proteins acting as ligands for fzd6 are not known. Interestingly, the expression of *Xenopus* wnt9a was reported to occur during pronephric kidney development (Garriock et al., 2007). Expression occurred throughout the pronephric nephron starting from stage 32 onwards. This coincides both spatially and temporally with the expression of fzd6 during pronephric kidney development as reported here. This suggests that wnt9a may act as an *in vivo* ligand for fzd6 during pronephric kidney development. Future experiments will address this issue in detail.

Acknowledgments

We would like to thank N. Ueno and the NIBB/NIG *Xenopus laevis* EST project for the fzd6a clone. We specially thank R. Lecca and F. Bacchion for total RNA preparations from *Xenopus* A6 cells and adult kidneys. This work was supported by grants of the European Community (EuReGene LSHG-CT-2004-005085) and Swiss National Science Foundation (3100A0-101964) to AWB.

References

Adler PN, Charlton J, Vinson C. 1987. Allelic Variation at the frizzled Locus of Drosophila. Dev Genet 8:99-119.

Borello U, Buffa V, Sonnino C, Melchionna R, Vivarelli E, Cossu G. 1999. Differential expression of the Wnt putative receptors Frizzled during mouse somitogenesis. Mech Dev 89:173-177.

Brändli AW, Kirschner MW. 1995. Molecular cloning of tyrosine kinases in the early Xenopus embryo: identification of Eck-related genes expressed in cranial neural crest cells of the second (hyoid) arch. Dev Dyn 203:119-140.

Clevers H. 2006. Wnt/beta-catenin signaling in development and disease. Cell 127:469-480.

Garriock RJ, Warkman AS, Meadows SM, D'Agostino S, Krieg PA. 2007. Census of vertebrate Wnt genes: Isolation and developmental expression of Xenopus Wnt2, Wnt3, Wnt9a, Wnt9b, Wnt10a, and Wnt16. Dev Dyn 236:1249-1258.

Giudice G. 2001. Conserved cellular and molecular mechanisms in development. Cell Biol Int 25:1081-1090.

Golan T, Yaniv A, Bafico A, Liu G, Gazit A. 2004. The human Frizzled 6 (HFz6) acts as a negative regulator of the canonical Wnt. beta-catenin signaling cascade. J Biol Chem 279:14879-14888.

Guo N, Hawkins C, Nathans J. 2004. Frizzled6 controls hair patterning in mice. Proc Natl Acad Sci U S A 101:9277-9281.

Harland RM. 1991. In situ hybridization: an improved whole-mount method for Xenopus embryos. Methods Cell Biol 36:685-695.

Helbling PM, Saulnier DM, Robinson V, Christiansen JH, Wilkinson DG, Brändli AW. 1999. Comparative analysis of embryonic gene expression defines potential interaction sites for Xenopus EphB4 receptors with ephrin-B ligands. Dev Dyn 216:361-373.

Helbling PM, Tran CT, Brändli AW. 1998. Requirement for EphA receptor signaling in the segregation of Xenopus third and fourth arch neural crest cells. Mech Dev 78:63-79.

Heller N, Brändli AW. 1997. Xenopus Pax-2 displays multiple splice forms during embryogenesis and pronephric kidney development. Mech Dev 69:83-104.

Huelsken J, Behrens J. 2002. The Wnt signalling pathway. J Cell Sci 115:3977-3978.

Huelsken J, Birchmeier W. 2001. New aspects of Wnt signaling pathways in higher vertebrates. Curr Opin Genet Dev 11:547-553.

Korswagen HC. 2002. Canonical and non-canonical Wnt signaling pathways in Caenorhabditis elegans: variations on a common signaling theme. Bioessays 24:801-810.

Logan CY, Nusse R. 2004. The Wnt signaling pathway in development and disease. Annu Rev Cell Dev Biol 20:781-810.

Nieuwkoop PD, Faber J. 1956. Normal table of Xenopus laevis (Daudin): a systematical and chronological survey of the development from the fertilized egg till the end of metamorphosis.: North-Holland Publishing Company, Amsterdam.

Rafferty KA. 1969. Mass culture of amphibian cells: methods and observations concerning the stability of cell type. In: Mizell M, editor. Biology of amphibian tumors. Berlin: Springer-Verlag. pp 52-81.

Saitou N, Nei M. 1987. The neighbor-joining method: a new method for reconstructing phylogenetic trees. Mol Biol Evol 4:406-425.

Sarkar L, Sharpe PT. 1999. Expression of Wnt signalling pathway genes during tooth

development. Mech Dev 85:197-200.

Tokuhara M, Hirai M, Atomi Y, Terada M, Katoh M. 1998. Molecular cloning of human Frizzled-6. Biochem Biophys Res Commun 243:622-627.

Vinson CR, Conover S, Adler PN. 1989. A Drosophila tissue polarity locus encodes a protein containing seven potential transmembrane domains. Nature 338:263-264.

Wang HY, Liu T, Malbon CC. 2006a. Structure-function analysis of Frizzleds. Cell Signal 18:934-941.

Wang Y, Guo N, Nathans J. 2006b. The Role of Frizzled3 and Frizzled6 in Neural Tube Closure and in the Planar Polarity of Inner-Ear Sensory Hair Cells. J. Neurosci. 26:2147-2156.

Wang Y, Macke JP, Abella BS, Andreasson K, Worley P, Gilbert DJ, Copeland NG, Jenkins NA, Nathans J. 1996. A large family of putative transmembrane receptors homologous to the product of the Drosophila tissue polarity gene frizzled. J Biol Chem 271:4468-4476.

3.3. *Xenopus* fzd3 and fzd8 gene functions are required for pronephric kidney development

Christophe Héligon, Didier Saulnier, and André W. Brändli

Institute of Pharmaceutical Sciences, Department of Chemistry and Applied Biosciences, ETH Zurich, 8093 Zurich, Switzerland.

* Author for correspondence:
Institute of Pharmaceutical Sciences
Department of Chemistry and Applied Biosciences
ETH Zürich
CH-8093 Zürich
Switzerland
Tel.: +41-44 633 7421
FAX: Brändli@pharma.ethz.ch
Correspondence to: brandli@pharma.ethz.ch

Unpublished manuscript

Abstract

Wnt genes encode for secreted glycoproteins implicated in several developmental processes. Wnt proteins serve as ligands to the Frizzled (Fzd) cell-surface receptors. Here we report that in Xenopus fzd signaling is critically involved in the regulation of pronephric kidney organogenesis. We first determined the expression of fzd receptors during *Xenopus* pronephric kidney formation and thereby detected differential expression of fzd3, fzd6, and fzd8 in the pronephric kidney. We demonstrated that overexpression of fzd3 resulted in ectopic expression of wnt4 and ectopic proximal tubule development. Blocking fzd3 activity by injecting antisense morpholino oligonucleotides disrupted proximal tubule formation. These findings indicate that fzd3 is both necessary and sufficient for proximal tubule development. Loss of function studies suggested that fzd6 was dispensable for pronephric kidney development.. In contrast, overexpression of fzd8 was sufficient to trigger ectopic intermediate and distal tubule development and suppressed proximal tubulogenesis. Disruption of fzd8 activity impaired expression of late marker genes and blocked epithelial polarization. Expression of early pronephric marker genes was however unaffected. These findings imply a requirement for fzd8 function in terminal differentiation of the distal nephron segments. Finally, we investigated the nature of the Wnt signaling pathways involved in pronephric kidney development. Activation of the canonical Wnt signaling pathway as well as inhibition of Jun N-terminal kinases using pharmacological approaches resulted in the specific loss of distal tubule marker gene expression, while interference with the calcium-dependent pathway did not induce any detectable pronephric defects. Taken together, our studies have revealed distinct roles for fzd3 and fzd8 in pronephric kidney organogenesis.

Introduction

Wnt signaling plays diverse roles in a wide range of developmental processes, such as stem cell maintenance, cell fate decision, control of asymmetric cell division, and patterning of organ primordia (Kleber and Sommer, 2004; Nusse, 2005; Clevers, 2006; de Iongh et al., 2006; de Lau et al., 2007). Wnt genes are expressed in different compartments of the kidney during metanephric development. Wnt4 is confined to the mesenchymal condensates and primitive epithelia derived from the metanephric mesenchyme, while other Wnts (6, 7b, 9b, and 11) are found in the Wolffian duct and/or the ureteric bud tip. Wnt4 is involved in mesenchyme to epithelial conversion during metanephric kidney organogenesis (Stark et al., 1994; Kispert et al., 1998). Disruption of the Wnt4 gene results in hypoplastic kidneys that show no or poor tubulogenesis in mouse. Recents studies indicate that Wnt9b acts upstream of Wnt4 (Carroll et al., 2005). Wnt9b secretion by the invading ureteric bud is required for the induction of the tubulogenic program in the metanephric mesenchyme. Wnt11 function is required for the early steps of branching morphogenesis following the first branching event in the metanephros (Majumdar et al., 2003). Disruption of Wnt11 interferes with Ret/Gdnf signaling causing a reduction in branching events. Finally, Wnt6 and Wnt7b are also known to be expressed in the developing kidney, but their function during kidney organogenesis still remains to be elucidated. In general, early steps of kidney organogenesis are difficult to study in the mammalian metanephric kidney, but can readily be assessed in the pronephric kidneys of amphibians (Vize et al., 1997; Brändli, 1999). In *Xenopus*, interference with wnt4 function blocks pronephric tubule formation (Saulnier et al., 2002). This phenotype is reminiscent to the one observed in Wnt4-deficient mice arguing for a conserved signaling pathway controlling tubulogenesis in pro- and metanephric kidneys.

At the cell surface, different transmembrane receptors are able to transduce Wnt signals (Gordon and Nusse, 2006). Binding of Wnt proteins to seven-pass transmembrane proteins of the Frizzled (Fzd) family can elicit activation of one of three distinct intracellular Wnt signaling pathways. The canonical (or β-catenin-dependent) and the calcium-dependent Wnt pathways are involved in cell fate decision during embryogenesis as well as in adult life (Chin et al., 1998; Kuhl et al., 2001; Nusse, 2005; Clevers, 2006; de Iongh et al., 2006; de Lau et al., 2007; Malaterre et al., 2007). The planar cell polarity (PCP) pathway is known to control the planar polarity of several epithelial structures (Veeman et al., 2003; Wallingford, 2004), including the hair orientation in the mouse epidermis (Guo et al., 2004). Ten Fzd genes are typically present in mammalian genomes, out of them, eight receptors (Fzd2, 3, 4, 5, 6, 7, 9, and 10) were identified to be expressed in the murine metanephric kidney (Wang et al., 1996; Wang et al., 1999; Malik and Shivdasani, 2000). Fzd gene functions during metanephric kidney development in the mouse remain however still elusive. Indeed, knockout mice have been produced for all Fzd genes but no kidney phenotypes has been reported to date (van Amerongen and Berns, 2006). In contrast to the mouse, *Xenopus laevis* fzd8 has been implicated in pronephric kidney development (Satow

et al., 2004). fzd8 expression was reported in the developing duct (Deardorff et al., 1998; Satow et al., 2004). Disruption of fzd8 gene function using antisense morpholino oligonucleotides disrupts differentiation of the pronephric duct (Satow et al., 2004). In the *Xenopus*, fzd3 and fzd6 were found in the developing pronephric kidney (Héligon et al., see chapter 3.2). Their function in pronephric kidney development have however not been explored.

Recently, an extensive analysis of solute carrier gene expression during *Xenopus* embryogenesis revealed that the basic segmental organization of the nephron is largely conserved between *Xenopus* pronephric and mouse metanephric kidneys (Raciti, 2007). This study establishes an updated model of nephron segmentation and introduces a new nomenclature with four tubules: proximal tubule, intermediate tubule, distal tubule, and connecting tubule (Fig. 1). Each tubule compartment may be further subdivided into distinct segments. Moreover, this study establishes new marker genes to study mechanisms underlying nephron segmentation. These tools where used to show that irx3 and sim2 functions are required for intermediate tubule specification and morphogenesis, respectively (Reggiani, 2007).

Here, we analyzed the role of fzd3, fzd6, and fzd8 signaling during *Xenopus laevis* pronephric development. We mapped the fzd gene expression domains to the newly proposed nephron segmentation model. fzd3 expression was confined to the proximal tubules with an expression pattern similar to wnt4. fzd8 was expressed in the intermediate, distal and connecting tubules. Finally, fzd6 is expressed late in all epithelia of the pronephric nephron. We report that loss of fzd3 function impaired proximal tubule development, whereas gain of fzd3 function induced ectopic proximal tubule fates. fzd6 gain- and loss-of-function failed to reveal any role for fzd6 in pronephric kidney development. In contrast, gain of fzd8 function induced intermediate tubule formation in place of proximal tubule. Finally, we demonstrated that activation of canonical Wnt signaling as well as disruption of planar cell polarity signaling prevents distal tubule differentiation in a similar manner to the loss of fzd8 function. In summary, our work demonstrates that different fzd genes fulfill distinct functions during pronephric kidney organogenesis.

Experimental procedures

Gene nomenclature

The standard gene nomenclature suggested by Xenbase (www.xenbase.org) and adopted by the NCBI for *Xenopus* genes is utilized rather than the original gene names to maximize compatibility with data available from other model systems. Where possible, *Xenopus* gene names are the same as the human orthologs.

Manipulation of *Xenopus* embryos

In vitro fertilization, embryo culture, staging, and microinjections were performed as described

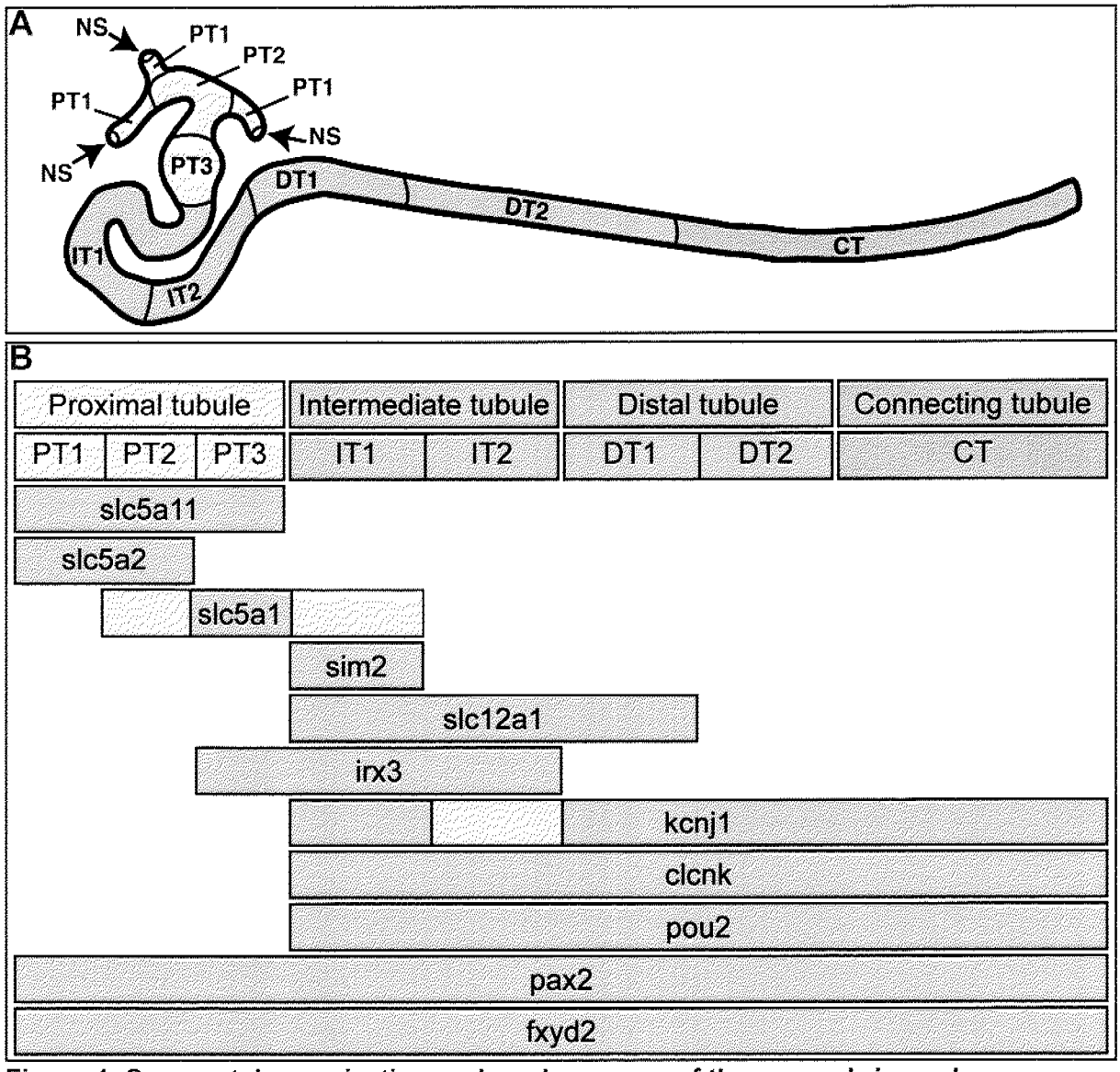

Figure 1. Segmental organization and marker genes of the pronephric nephron.
(A) Schematic representation of the tubular portion of the *Xenopus* pronephric kidney. A stage 35/36 pronephric kidney is shown with the four tubular compartments color coded. Each tubule is further subdivided into distinct segments: proximal tubule (yellow; PT1, PT2, PT3), intermediate tubule (green; IT1, IT2), distal tubule (orange; DT1, DT2), and connecting tubule (grey; CT). The nephrostomes (NS) are ciliated peritoneal funnels that connect the coelomic cavity to the nephron. (B) Expression domains of selected marker genes along the proximodistal axis of the developing pronephric nephron. The expression domains were mapped between stage 25 and 35/36. The localization of the expression domains is shown below the corresponding segments. Blue indicates low levels of marker gene expression.

previously (Brändli and Kirschner, 1995; Helbling et al., 1998; Helbling et al., 1999). RNA encoding the lineage tracer nuclear β-galactosidase (nucβgal) was coinjected at 100 pg per blastomere.

Bathing of *Xenopus* embryos in BIO, MeBIO, or SP600125

For embryo treatment in chemical compounds, embryos were transferred at stage 15 to 0.1xMMR

containing 0.05% DMSO plus 15 μM of BIO or MeBIO, or 25 mM of SP600125 (Alexis, San Diego, CA). Embryos were fixed when control siblings reached stage 35 and processed for *in situ* hybridization.

Experiments with hormone inducible construct

pTHVGR was kindly provided by Jing Yang and Peter Klein. pTHVGR was generated by cloning an activated tcf3 mutant into pCS2-hGRN, which encodes the ligand binding domain of the human glucocorticoid receptor. The resulting fusion protein encodes a N-terminal activated tcf3 and a C-terminal glucocorticoid binding domain. THVGR was used for *in vitro* RNA synthesis. 500 pg of mRNA was subsequently injected at the 8-cell stage in a single V2 blastomere. The embryos were cultured into 0.1xMMR. At stage 15, embryos were transferred into 0.1xMMR containing 10 μg/mL dexamethasone (D1756, Sigma).

Plasmid constructs

The following plasmids containing the complete open reading frame (ORF) of *Xenopus* fzd3 (Shi et al., 1998), fzd6a (Heligon *et al.*, see chapter 3.2), fzd6b (Heligon *et al.*, see chapter 3.2), fzd8a (Itoh et al., 1998), and fzd8b (Deardorff et al., 1998) were constructed by subcloning into pCS2+ (Turner and Weintraub, 1994) for *in vitro* coupled transcription-translation reaction and *in vitro* RNA synthesis: pCS2-fzd3, pCS2-fzd6a, pCS2-fzd6b, pCS2-fzd8a, pCS2-fzd8b. The following plasmids encoding for different HA tagged Wnt proteins to use in cell culture experiments were constructed by replacing DNA encoding for mature ActivinβB sequence of pCS2-HAActivinβB (Piccolo et al., 1999) by DNA encoding for Wnt proteins lacking their signal peptides: pDS23-HAWnt-1 contains mature wnt1 (nucleotides 88 to 1116) (Wolda et al., 1993); pDS24-HAWnt-4 contains mature wnt4 (nucleotides 73 to 1056) (McGrew et al., 1992); pCS2-HAWnt-8 contains mature wnt8 (nucleotides 76 to 1077) (Piccolo et al., 1999); pDS25-HAWnt-11 contains mature wnt11 (nucleotides 76 to 1062) (Ku and Melton, 1993). The following plasmids containing the complete ORF of *Xenopus* fzd3 (Shi et al., 1998), fzd7 (gift from Doris Wedlich), or fzd8a (Itoh et al., 1998) fused in frame with 6 myc repeats were constructed by subcloning into pCS2+MT: pDS28-Fz-3-myc; pDS26-Fz-7-myc; pDS30-Fz-8-myc. The cDNAs were amplified by PCR using the Expand High Fidelity PCR system (Roche Diagnostics) and subcloned into the vector using T4 DNA ligase (Fermentas).

***In situ* hybridizations, sectioning, and TUNEL assays**

Probe synthesis, whole-mount *in situ* hybridization and β-galactosidase staining was carried out as described (Helbling et al., 1998; Helbling et al., 1999). Where necessary, embryos were bleached for 2 hours with 1% hydrogen peroxide-5% formamide-0.5x SSC. Digoxigenin-labeled probes were synthesized from linearized plasmids encoding clcnk (Maulet et al., 1999), fxyd2 (Na,K-ATPase, γ-subunit) (Eid and Brändli, 2001), fzd1 (Brown et al., 2000), fzd2 (Deardorff and Klein, 1999), fzd3 (Shi et al., 1998), fzd4 (Shi and Boucaut, 2000), fzd5 (Sumanas and

Ekker, 2001), fzd6a (Héligon *et al.*, see chapter 3.2), fzd6b (Héligon *et al.*, see chapter 3.2), fzd7 (Djiane et al., 2000), fzd8a (Itoh et al., 1998), fzd8b (Deardorff et al., 1998), fzd10 (Héligon *et al.*, unpublished), irx3 (Bellefroid et al., 1998), kcnj1 (Romk1) (Reggiani, 2007), lim1 (Taira et al., 1994), pax2 (Heller and Brändli, 1997), pax8 (Heller and Brändli, 1999), pou2 (Witta et al., 1995), sim2 (Bordoli and Brändli, unpublished), slc5a1, slc5a2, and slc12a1 (Raciti, 2007), slc5a11 (Eid et al., 2002), wnt4 (McGrew et al., 1992) and wnt11 (Ku and Melton, 1993). Sense strand controls were prepared from all plasmids and tested negative by *in situ* hybridization. Embryos stained in whole mount were sectioned at 30 µm using a vibrating blade microtome as described (Heller and Brändli, 1997). Alternatively, stained embryos were plastic embedded in Durcupan (Fluka) according to the manufacture's instructions, sectioned at 2 or 3 µm using a Ultracut E microtom (Reichert-Jung) and counterstained with 0.1% tuloidin blue in 1% sodium borate and 1% basic fuchsine in distilled water. Whole mount TUNEL staining was performed on stage 20 and 24 embryos as described previously (Hensey and Gautier, 1999).

Morpholino oligonucleotides

Morpholinos (MO) were obtained from Gene Tools, LLC. They were designed to bind to the 5'-UTR or sequences flanking and including the initiating methionine. 25-mer morpholinos were designed according to the manufacturer's recommendations. The MO sequences were as follows (sequence complementary to the start codon is underlined in all cases). Nucleotides differing between fzd8a-MO and fzd8b-MO are highlighted in bold. fz3-MO, 5'-TTAAATAGGCAGCCATGATAAATGC-3'; fz3(mp)-MO (negative control of fz3-MO containing 4 mispairs highlighted in bold), 5'-TTA**G**ATAA**G**CAGC**C**ATGAT**G**AAA**G**C-3'; fzd6(1)-MO, 5'-GGAGGCAGCAGCCAATCAGATCCAT -3'; fzd6(3)-MO, 5'-TCAGAT CCATGGTGTCAGCAGCTAG-3'; fz8a-MO (MO designed to anneal to *Xenopus laevis* fzd8a (Itoh et al., 1998), 5'-GCAGCGACAG**C**GACAGACTCTC**C**AT-3'; fz8b-MO (MO designed to anneal to *Xenopus laevis* fzd8b (Deardorff et al., 1998), nucleotides differing between fz8a-MO and fz8b-MO are highlighted in bold), 5'-GCAGCGACAG**A**TAC**G**GACA**C**TC**C**AT-3'; and standard control (Cont-MO) provided by Gene Tools, 5'-CCTCTTACCTCAGTTACAATTTATA-3'. Typically 5 or 10 ng of MO was injected per blastomere.

Cell cultures and transfections

293 HEK cells were grown in DMEM supplemented with 10% fetal calf serum, 50 µg/ml Gentamycin in the presence of 5% CO_2. Cells were seeded on fibronectin (Roche Diagnostics) coated coverslips. For transfection experiments, 1 µg of the myc-tagged fzd receptor plasmid DNAs (fzd3, -7, -8) or 2.5 µg of the HA-tagged ligand plasmid DNAs (ActivinβB, wnt1, -4, -8, and -11) were applied by calcium phosphate precipitation. At 36 h after transfection cells were fixed with 4% formaldehyde during 15 min, then blocked for 30 min in 1xPBS with 1% bovine serum albumin (BSA) without detergent. Cells were next incubated with a rat anti-HA high-affinity monoclonal antibody (Roche Diagnostics, clone 3F10) for 30 min, extensively washed

in 1xPBS and re-incubated with a secondary rabbit anti-rat-HRP conjugate antibody (DAKO). The signal was subsequently amplified using the Tyramide-Signal-Amplification (TSA)-direct system (NEN Life Science Products). After this step, cells were extensively washed in 1x PBS, refixed for 10 min and blocked in 1x PBS with 1% BSA and 0.3% Triton X-100. Cells were then incubated with a mouse anti-myc monoclonal antibody (line 1-9E10.2, American Type Cell Culture) for 30 min, washed with 1x PBS and followed by a 30 min incubation with a secondary horse anti-mouse-FITC conjugate antibody (Vector). All incubations were performed at room temperature. After the last washing step in 1x PBS, cells were mounted in 87% glycerol and analyzed by confocal laser scanning microscopy.

Confocal microscopy

Confocal images were recorded on an inverted microscope DM IRB/E equipped with a true confocal scanner TCS NT and a PL APO 40x (air) or 63x oil immersion objective (Leica) using an argon-krypton mixed gas laser. Image processing was done on a Silicon Graphic workstation using Imaris software (Bitplane AG).

Photography and computer graphics

Photographs were taken digitally with either a STEMI-2000C stereoscopic microscope (Zeiss) equipped with a Progress 3008 CCD camera (Jenoptik) or an Axiocam color cameras (Zeiss) mounted either on a Stereo Lumar.V12 stereoscopic microscope (Zeiss) or an Axioskop 2 mot plus light microscope (Zeiss). Pictures were acquired using AxioVision 4.5 (Zeiss) software. Composite figures were organized and labeled using Adobe Photoshop 9 and Adobe InDesign 4 software.

Results

***Xenopus* fzd genes are differentially expressed during pronephric kidney development**

We had previously demonstrated that wnt4 is expressed in the developing pronephric anlage and subsequently in pronephric tubules (Saulnier *et al.,* 2002; Fig. 2A, B). We therefore assessed the spatial and temporal expression patterns of several fzd genes during *Xenopus* pronephric development to identify possible receptors for wnt4. Antisense probes for fzd1, fzd2, fzd3, fzd4, fzd5, fzd6, fzd7, fzd8, and fzd10 were used for whole mount *in situ* hybridizations. Expression of fzd1, fzd2, fzd4, fzd5, fzd7, and fzd10 was detected in various developing organ primordial including the otic vesicle, the olfactory bulb, the eyes, the visceral arches, the vasculature, and the brain (data not shown). No expression was however observed in the developing pronephric kidney. These results suggest that a role for these genes in pronephric kidney organogenesis is rather unlikely. In contrast, expression of fzd3, fzd6, and fzd8 was specifically detected in the developing pronephric kidney. *Xenopus* fzd3 transcripts were observed in the pronephric anlage

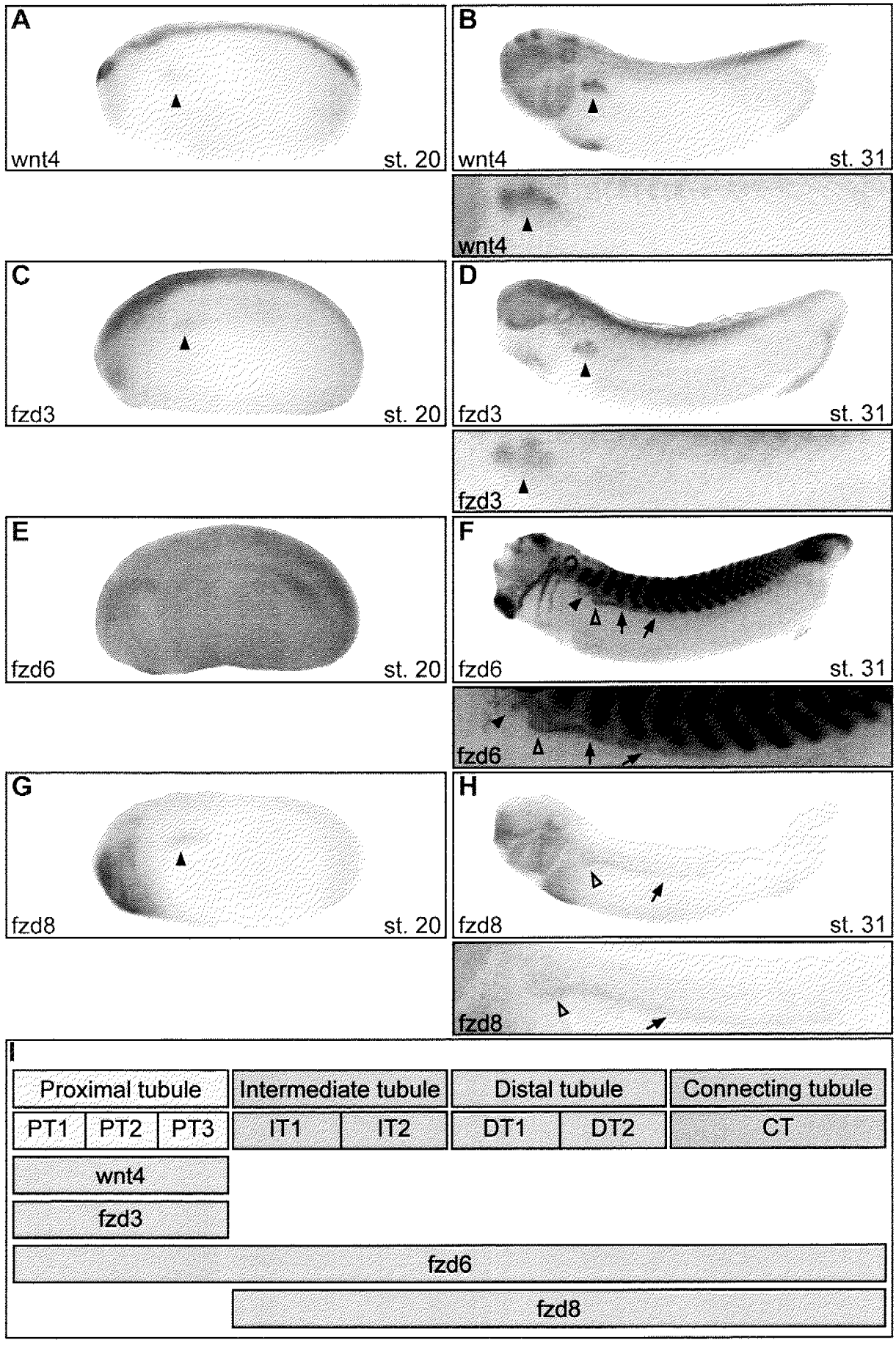
A
wnt4
st. 20
B
wnt4
st. 31
wnt4
C
fzd3
st. 20
D
fzd3
st. 31
fzd3
E
fzd6
st. 20
F
fzd6
st. 31
fzd6
G
fzd8
st. 20
H
fzd8
st. 31
fzd8
I
Proximal tubule
Intermediate tubule
Distal tubule
Connecting tubule
PT1
PT2
PT3
IT1
IT2
DT1
DT2
CT
wnt4
fzd3
fzd6
fzd8

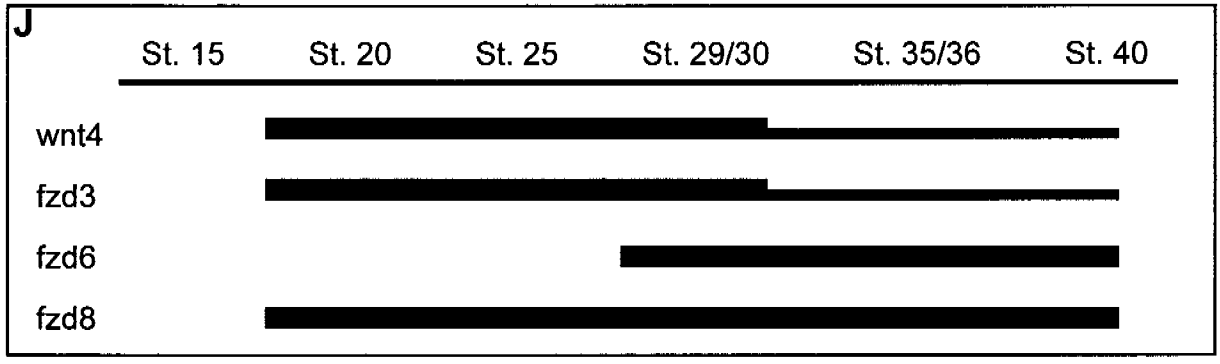

Figure 2: Expression of Wnt4 and Fzd genes during early *Xenopus* embryogenesis. Whole-mount *in situ* hybridizations were performed on albino embryos using dioxygenin-labeled antisense RNA probes. Lateral views are shown. Embryos are oriented with anterior to the left. Enlargments of the pronephric region are shown below stage 31 embryos. (A, B) Wnt4 expression pattern. (A) Stage 20 embryo showing wnt4 transcripts in the central nervous system and in the pronephric anlage (arrowhead). (B) Stage 31 embryo displaying specific wnt4 expression in pronephric proximal tubules (arrowhead). (C, D) Fzd3 expression pattern. (C) Stage 20 embryo showing fzd3 transcripts in the central nervous system, the eye, and the pronephric anlage (arrowhead). (D) At stage 31, pronephric expression of fzd3 is restricted to the proximal tubules (arrowhead). (E, F) Fzd6 expression pattern. (E) Stage 20 embryo showing lack of fzd6 expression in the pronephric anlage. (F) At stage 31, fzd6 expression is detected in the cement gland, the brain, the visceral arches, the otic vesicle, the somites, and the pronephric kidney. Expression in the proximal (arrowhead), intermediate (open arrowhead), and the distal and connecting tubules (arrows) of the pronephric nephron is indicated. (G, H) Fzd8 expression pattern. (G) Stage 20 embryo displaying extensive fzd8 expression in the developing head and in the pronephric anlage (arrowhead). (H) At stage 31, pronephric fzd8 expression is associated with the intermediate (open arrowhead) and distal and connecting (arrow) pronephric nephron segment. (I) Summary of wnt4 and fzd gene expression in the pronephric kidney during embryogenesis. The expression domains were mapped between stage 25 and 35/36. The localization of the expression domains is shown below the corresponding segments. (J) Time course of wnt4 and fzd gene expression during the pronpehric kidney development.

as early as stage 20 (Fig. 2C). The expression of fzd3 becomes subsequently associated with the differentiating proximal tubules (Fig. 2D). From stage 35 on, expression of fzd3 begins to decline concomitant with terminal differentiation of the pronephric kidney (data not shown). Interestingly, the expression of fzd3 during pronephric tubule formation parallels the situation described previously for wnt4 (compare Fig. 2A, B and C, D). Expression of fzd6 could not be detected in the pronephric anlage at stage 20 (Fig. 2E). At stage 31, fzd6 transcripts were however observed in the entire pronephric kidney (Fig. 2F). fzd6 expression in the pronephros remained present until at least stage 40 (data not shown). Expression of fzd8 was also observed in the pronephric anlage as early as stage 20 (Fig. 2G). Later in development, pronephric expression of fzd8 was detected in the intermediate, distal, and connecting tubules but not in proximal tubule (Fig. 2H). From stage 40 on, pronephric expression of fzd8 began to cease (data not shown). In summary, wnt4 and fzd3 were co-expressed during early proximal tubule development suggesting that they could physically interact with each other. In contrast, fzd8 expression was restricted to the distal segments of the pronephros. Finally, expression of fzd6

was late and occurred in all pronephric epithelia along the proximo-distal axis of the nephron.

Disruption of fzd3 function blocks development of proximal tubule

We have previously shown that disruption of *Xenopus* wnt4 gene function results in a specific defect in pronephric kidney organogenesis that is characterized by the loss of proximal tubules (Saulnier et al., 2002). The co-expression of wnt4 and fzd3 observed here suggests that wnt4 might act through fzd3 to promote the formation of proximal tubule. To determine whether fzd3 is necessary for the formation of the pronephric tubules, we used an antisense morpholino oligonucleotide approach to deplete the embryos of fzd3 protein in the pronephric region. First, we demonstrated *in vitro* that fzd3-MO was able to interfere with fzd3 protein synthesis, whereas the control fzd3(mp)-MO could not (Fig. 3A). Then, we injected fzd3-MO in a single or both V2 blastomere of 8-cell stage embryos, whose progeny contribute to the pronephros (Moody and Kline, 1990; Huang et al., 1998). We observed in tadpoles injected unilaterally with fzd3-MO, that they frequently lacked a pronephric kidney. The tadpoles developed otherwise normally (Fig. 4A, B; Table 1). In contrast, 43% (n=89) of the embryos bilaterally injected with fzd3-MO developed edemas from stage 41 onwards (Fig. 4C, D; Table 1). Interestingly, in tadpoles displaying edemas no pronephric tubules could be observed at stage 47. Eventually, all the embryos carrying edemas died at stage 48. Note that fzd3(mp)-MO injections did not cause edema formation (data not shown; Table 1). These results demonstrated that fzd3 function was necessary for water homeostasis and tadpole survival. Furthermore, the results suggest that fzd3 is required for pronephric kidney development.

To investigate the pronephric kidney defects, we injected unilaterally fzd3-MO into single V2 blastomeres and analyzed the expression of pronephric marker genes (Fig. 5; Table 2). The expression domains of the pronephric marker genes used to analyze the mutant embryos are shown in Figure 1. First, inspection of pax2-stained embryos revealed that pronephric cell fate specification occurred, but the proximal tubule appeared to be abnormal (Fig. 5A). In addition, the expression of the pronephric epithelia marker fxyd2 (Na,K-ATPase, γ-subunit) showed that the proximal parts of the pronephros have morphological defects (Fig. 5B; 59%, n=56). We then used nephron segment-specific marker genes to study their expression upon fzd3 depletion. Injection of 5 ng of fzd3-MO caused a strong downregulation of tubular wnt4 expression (Fig. 5C; 62%, n=101). Embryos were also analyzed with the proximal tubule-specific marker genes slc5a1, slc5a2, and slc5a11. fzd3-MO injection caused a complete loss of these markers in 57-62% of the embryos (Fig. 5D; Table 2) suggesting a failure in proximal tubule maturation. Analysis of fzd3-MO injected embryos showed that the intermediate tubule was specified as evidenced by expression of irx3 and sim2 (Fig. 5E; Table 2; data not shown). The intermediate tubule was also able to undergo terminal differentiation indicated by sustained expression of slc12a1 (Fig. 5F; Table2). We noticed however that there was a morphogenesis defect affecting the proximal part of the intermediate tubule. Inspection of embryos for expression clcnk and kcnj1, which are expressed in the intermediate, distal, and connecting tubules, revealed no

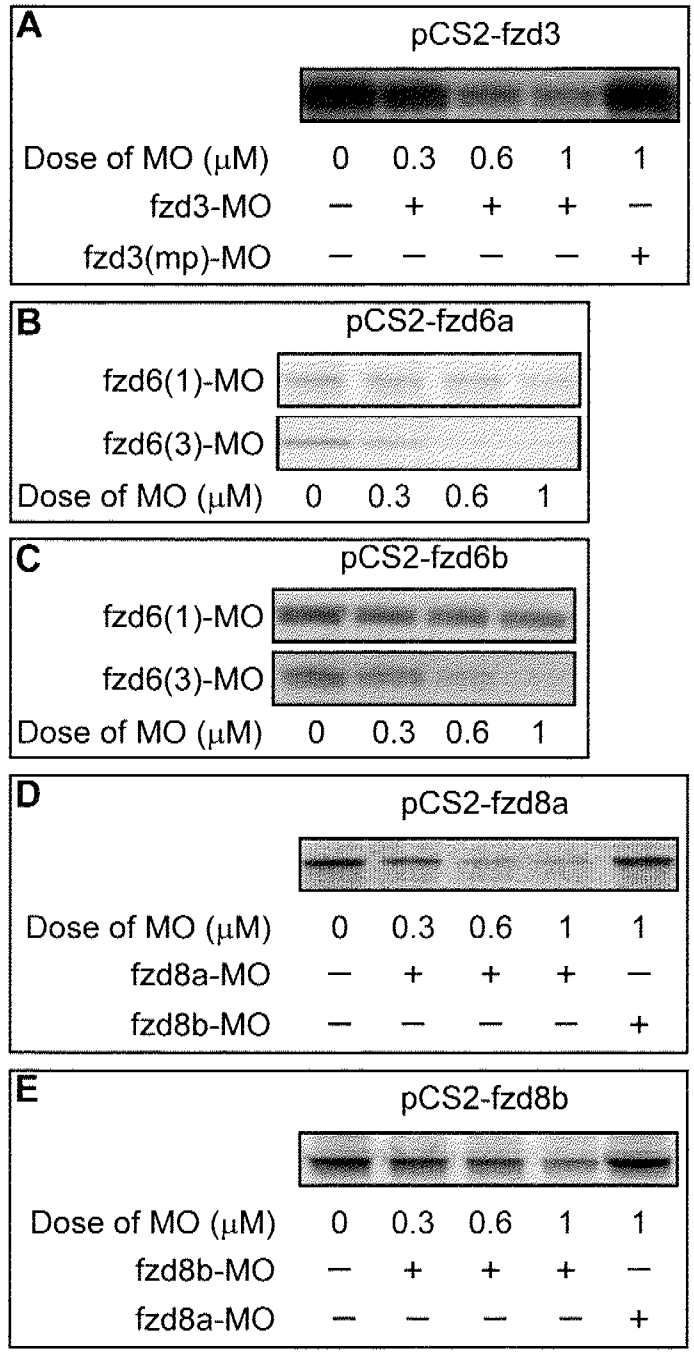

Figure 3: Inhibition of fzd3, fzd6, and fzd8 translation *in vitro* by antisense morpholinos.

Plasmids (500 pg) encoding the ORF of the indicated fzd genes were used as templates in cell-free coupled transcription-translation reactions. Morpholinos (MO) were tested for inhibition of translation at the doses indicated. Cell-free transcription-translation reactions were performed in the presence of [35S]methionine and analyzed by SDS-PAGE/autoradiography. (A) Dose-response analysis of inhibition of fzd3 translation by fzd3-MO. (B) Dose-response analysis of inhibition of fzd6a translation by fzd6(1)-MO and fzd6(3)-MO. (C) Dose-response analysis of inhibition of fzd6b translation by fzd6(1)-MO and fzd6(3)-MO. Note that fzd6(1)-MO is only partially inhibiting translation of fzd6b. (D) Dose-response analysis of inhibition of fzd8a translation by fzd8a-MO. (E) Dose-response analysis of inhibition of fzd8b translation by fzd8b-MO.

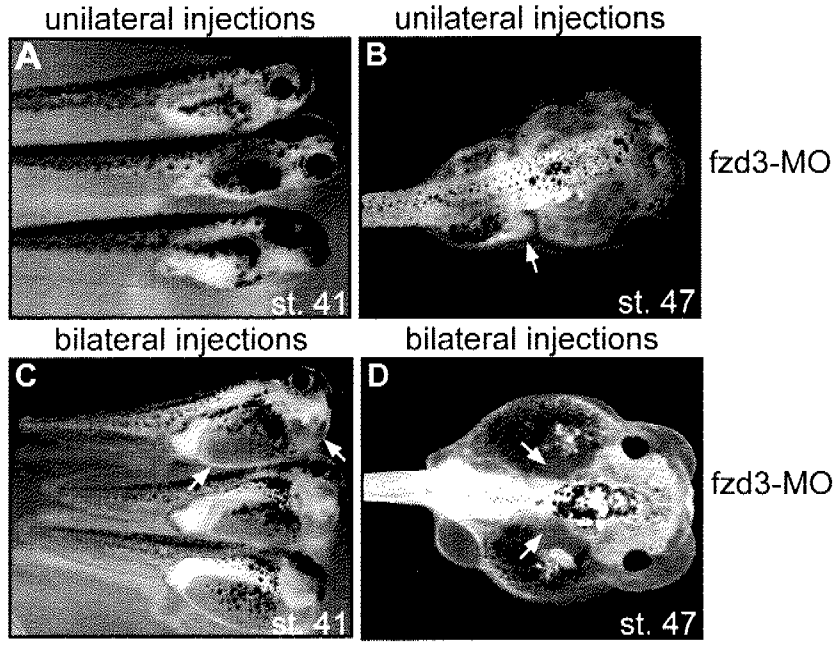

Figure 4: Inhibition of fzd3 translation *in vivo* leads to edema formation.
fzd3-MO (5 ng) were injected into a single or both V2 blastomeres of 8-cell stage embryos. Embryos were monitored for edema formation during development. (A, B) Unilaterally injected embryos failed to develop any signs of edemas at stage 41 and 47. Stage 47 embryos displayed typically only one pronephric kidney (arrow). (C, D) Bilaterally injected embryos developed by stage 41 edemas with ventral and pericardiac fluid accumulations (arrows). At stage 47, embryos displayed severe edemas. Note the bilateral absence of pronephric kidneys (arrows).

Table 1: Bilateral fzd3 depletion leads to edema formation

MO	Type of injection	Edemas at stage 41	Edemas at stage 47	n
fzd3-MO	unilateral	0%	0%	120
	bilateral	43%	43%	89
fzd3(mp)-MO	bilateral	0%	0%	94

A single or both V2 blastomeres of 8-cell stage embryos were injected with 5 ng of either fzd3-MO or fzd3(mp)-MO. Embryos were allowed to develop to stage 48. During development, tadpoles embryos where monitored for edema formation. n, number of embryos injected.

defects other than a mild abnormality in intermediate tubule morphogenesis (Fig. 5G; Table 2). Histological analysis demonstrated a complete absence of epithelialized cells at the level of the proximal tubule on the injected side (Fig. 6). Next, we performed TUNEL staining on fzd3-MO injected embryos to investigate whether loss of fzd3 caused increased apoptosis. We failed however to detect any evidence for enhanced apoptosis (data not shown). In summary, our results suggest that knockdown of fzd3 caused a selective loss of proximal tubule, while other nephron segments remained unaffected. The loss of proximal tubule is likely to underlie the abnormal morphogenesis of the intermediate tubule as has been observed previously in wnt4-deficient embryos (Saulnier et al., 2002)

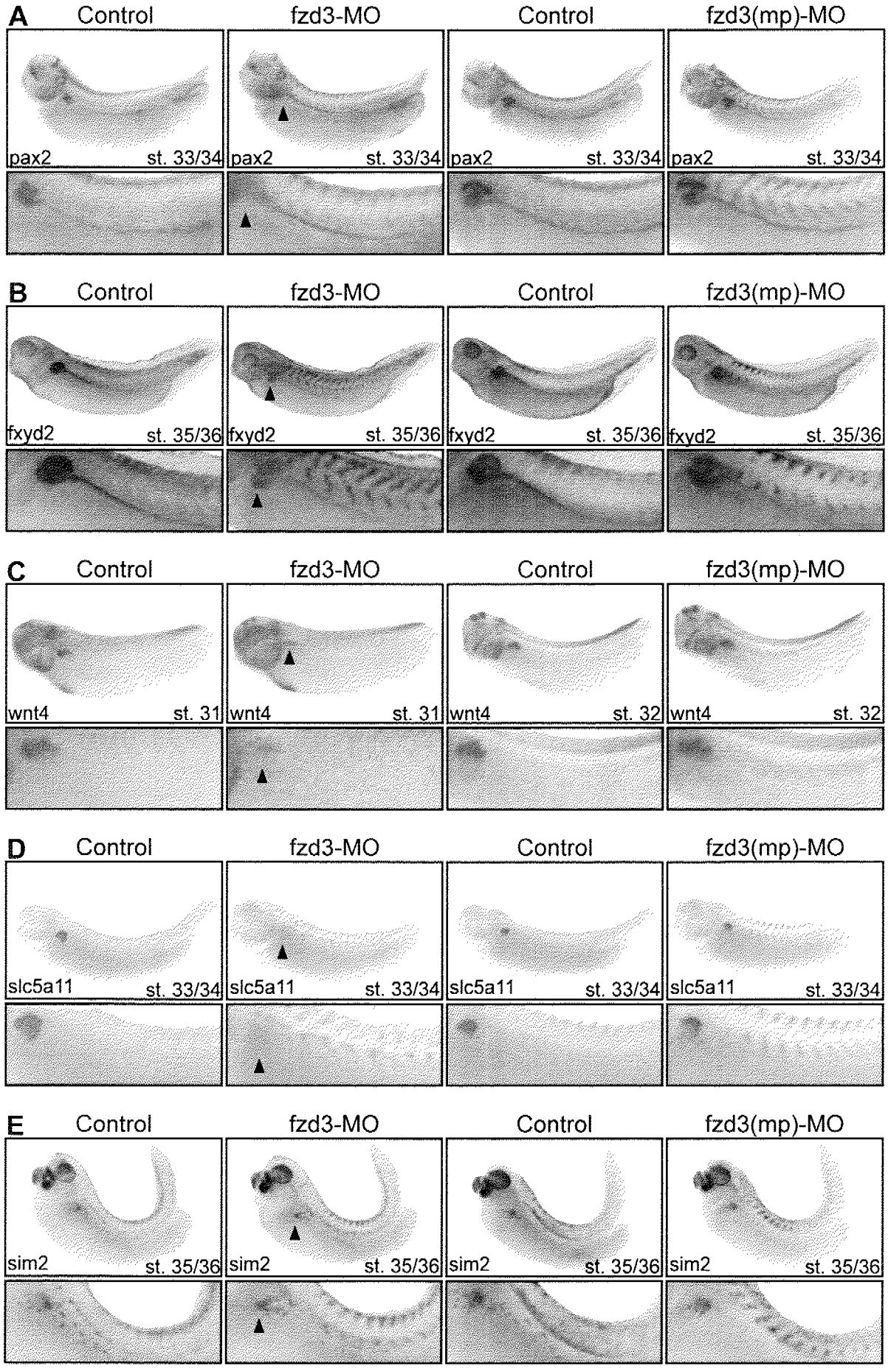
A
Control
fzd3-MO
Control
fzd3(mp)-MO
pax2 st. 33/34
pax2 st. 33/34
pax2 st. 33/34
pax2 st. 33/34
B
Control
fzd3-MO
Control
fzd3(mp)-MO
fxyd2 st. 35/36
fxyd2 st. 35/36
fxyd2 st. 35/36
fxyd2 st. 35/36
C
Control
fzd3-MO
Control
fzd3(mp)-MO
wnt4 st. 31
wnt4 st. 31
wnt4 st. 32
wnt4 st. 32
D
Control
fzd3-MO
Control
fzd3(mp)-MO
slc5a11 st. 33/34
slc5a11 st. 33/34
slc5a11 st. 33/34
slc5a11 st. 33/34
E
Control
fzd3-MO
Control
fzd3(mp)-MO
sim2 st. 35/36
sim2 st. 35/36
sim2 st. 35/36
sim2 st. 35/36

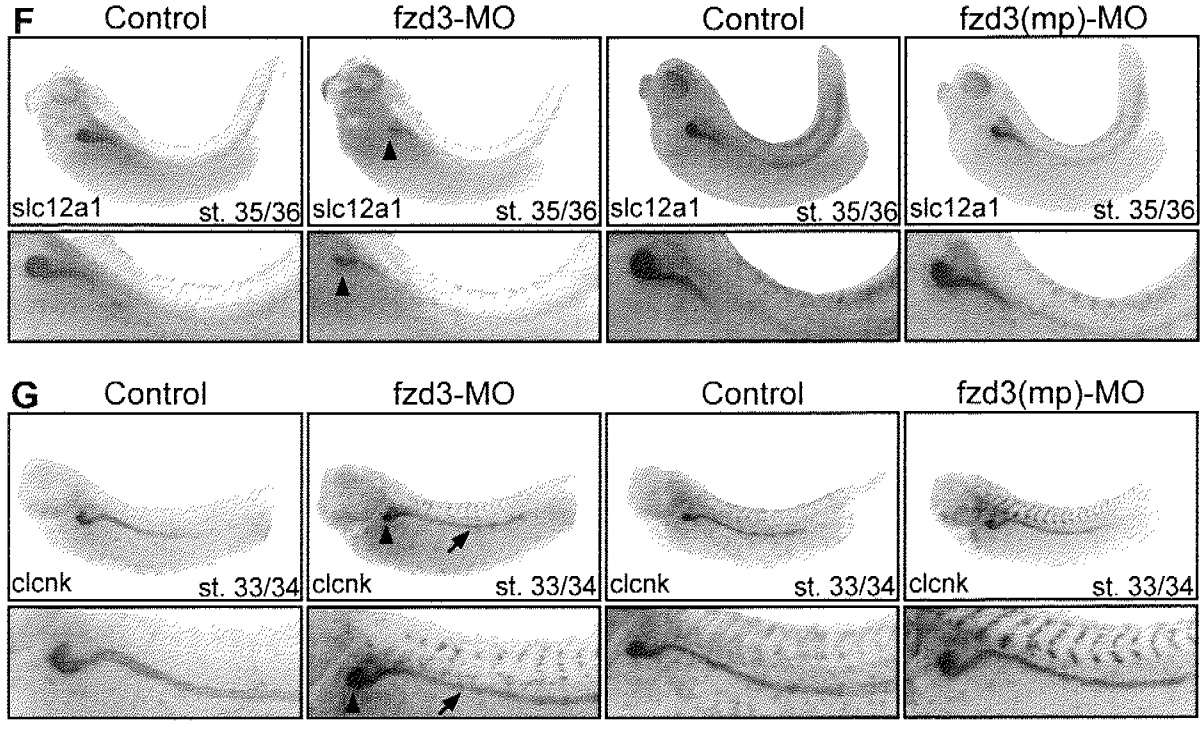

Figure 5. Inhibition of proximal tubule formation by fzd3-MO.
One V2 blastomere per 8-cell stage embryo was coinjected with either 5 ng of fzd3-MO or fzd3(mp)-MO and the lineage tracer nucβgal. Embryos were fixed at indicated stages, processed for nucβgal activity and hybridized with pax2, fxyd2, wnt4, slc5a11, slc12a1, sim2, and clcnk probes as indicated. Close-up views of the pronephric region are shown below each embryo. (A) Abnormal proximal tubular pax2 expression was detected (arrowhead), while distal expression appeared normal (arrows). (B) fxyd2 expression revealed an abnormal proximal tubule morphogenesis. (C) wnt4 expression in the pronephric tubules was strongly reduced on the injected side (arrowheads). (D) Expression of slc5a11 was absent from the injected side (arrowheads). (E) sim2 expression in the intermediate tubule was normal. (F) Expression of the intermediate tubule marker slc12a1 occured, but morphogenesis was affected. (G) Expression of clcnk in intermediate, distal, and connecting tubules was not affected by fzd3 depletion (arrows), but morphogenesis of the proximal part of the intermediate tubule was abnormal.

Table 2: Disruption of fzd3 function causes loss of proximal tubules

MO	Marker gene	Expression domains	Phenotype scored	Frequency	n
fzd3-MO	pax2	PT1 → CT	Abnormal PT morphogenesis	58%	77
	fxyd2	PT1 → CT	Abnormal PT morphogenesis	59%	56
	wnt4	PT1 → PT3	Loss of expression	62%	101
	slc5a1	PT3	Loss of expression	59%	64
	slc5a2	PT1 → PT2	Loss of expression	57%	60
	slc5a11	PT1 → PT3	Loss of expression	62%	94
	sim2	IT1	Loss of expression	20%	49
	irx3	PT3 → IT2	Loss of expression	10%	30
	slc12a1	IT1 → DT1	Loss of expression	13%	64
	clcnk	IT1 → CT	Loss of expression	7%	68
	kcnj1	IT1 → CT	Loss of expression	17%	29
fzd3(mp)-MO	pax2	PT1 → CT	Abnormal PT morphogenesis	2%	49
	fxyd2	PT1 → CT	Abnormal PT morphogenesis	0%	40
	wnt4	PT1 → PT3	Loss of expression	4%	51
	slc5a1	PT3	Loss of expression	5%	40
	slc5a2	PT1 → PT2	Loss of expression	3%	39
	slc5a11	PT1 → PT3	Loss of expression	4%	50
	sim2	IT1	Loss of expression	0%	30
	irx3	PT3 → IT2	Loss of expression	0%	29
	slc12a1	IT1 → DT1	Loss of expression	0%	30
	clcnk	IT1 → CT	Loss of expression	0%	50
	kcnj1	IT1 → CT	Loss of expression	0%	30
Cont-MO	pax2	PT1 → CT	Abnormal PT morphogenesis	0%	75
	wnt4	PT1 → PT3	Loss of expression	0%	50
	slc5a11	PT1 → PT3	Loss of expression	2%	57
	clcnk	IT1 → CT	Loss of expression	2%	60

One V2 blastomere per 8-cell stage embryo was injected with 5 ng of fzd3-MO, fzd3(mp)-MO, or Cont-MO as indicated. Nucβgal mRNA (100 pg) was coinjected as a lineage tracer. Embryos were allowed to develop to stages 30-34, fixed, stained for nucβgal activity, and processed for *in situ* hybridization. The injected sides of embryos were scored for the indicated phenotypes. Every experiment was performed at least twice, except for irx3 and kcnj1. n, total number of embryos scored. Abbreviations: PT, proximal tubule; IT, intermediate tubule; DT, distal tubule; CT, connecting tubule.

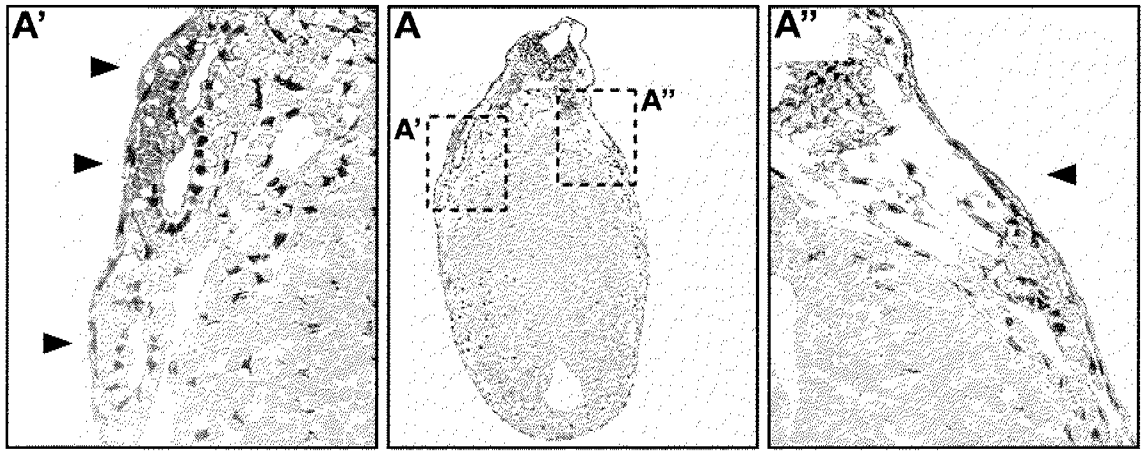

Figure 6. Histological analysis of Fz3-MO injected embryos.
One V2 blastomere of an 8-cell stage embryo was coinjected with 5 ng of fzd3-MO and the lineage tracer nucβgal. Embryos were fixed at stage 33/34, processed for nucβgal activity, and hybridized with slc5a11. For histological analysis, embryos were plastic embedded and transverse sections (3 µm) were cut at the level of the pronephric tubules. Enlargements of the control (A') and injected (A") sides are shown as indicated in (A). Proximal tubule formation was disrupted by fzd3-MO as indicated by the absence of discernable tubules (compare arrowheads in A' and A").

Ectopic expression of fzd3 induces ectopic pronephric proximal tubules

We performed gain-of-function experiments to determine whether fzd3 is not only necessary for proximal tubule formation but can also instructs cells towards the proximal tubule fate. Synthetic mRNA encoding full-length fzd3 was injected into a single V2 blastomere of 8-cell stage embryos. The injected embryos were allowed to develop to stage 30-34, which occurred normally without discernable malformations. Mutant embryos were analyzed by *in situ* hybridization using a panel of pronephric gene markers (Fig. 7; Table 3). First, analysis of pax2 expression, which stains all pronephric epithelia, revealed the presence of multiple ectopic tubules (Fig. 7A; 58%, n=115). Analysis of the expression of the early proximal tubule-specific marker wnt4 revealed multiple ectopic wnt4-expressing tubules on the injected side (Fig. 7B; 55%, n=87), whereas the control side displayed as expected three proximal tubules expressing wnt4. Next, we used late proximal tubule-specific markers (slc5a1, slc5a2, and slc5a11) to demonstrate that the ectopic proximal tubule tissue, typically 8-13%, were able to undergo terminal differentiation (Fig. 7C, D; Table 3). The analysis of injected embryos with intermediate tubule-specific markers demonstrated posterior displacement of the early intermediate markers irx3 (18%, n=39) and sim2 (Fig. 7E; 31%, n=45) as well as of the terminal differentiation marker slc12a1 (Fig. 7F; 32%, n=54). slc12a1 staining revealed however that intermediate tubule morphogenesis was disturbed. Then, injected embryos were analyzed for expression of markers of the intermediate, distal, and connecting tubules such as pou2 and clcnk to test whether the distal nephron was affected. No patterning defects were observed. However, on the injected side the expression domains of the marker genes were again shifted posteriorly

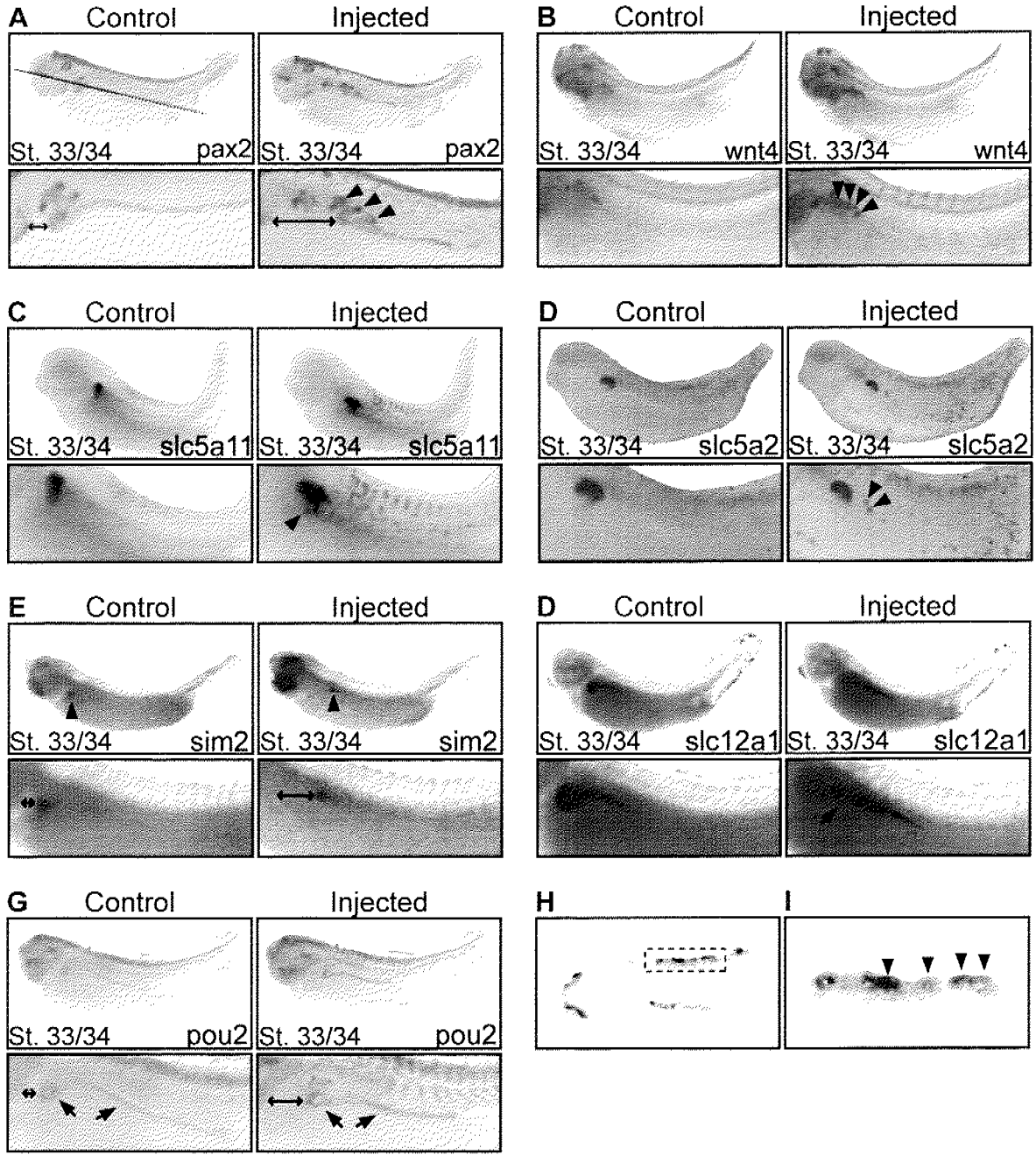
A Control Injected
St. 33/34 pax2
St. 33/34 pax2
B Control Injected
St. 33/34 wnt4
St. 33/34 wnt4
C Control Injected
St. 33/34 slc5a11
St. 33/34 slc5a11
D Control Injected
St. 33/34 slc5a2
St. 33/34 slc5a2
E Control Injected
St. 33/34 sim2
St. 33/34 sim2
D Control Injected
St. 33/34 slc12a1
St. 33/34 slc12a1
G Control Injected
St. 33/34 pou2
St. 33/34 pou2
H
I

Figure 7: fzd3 overexpression induces ectopic pronephric tubule formation.
One V2 blastomere per 8-cell stage embryo was coinjected with mRNA encoding fzd3 (500 pg) and the lineage tracer nucβgal (100 pg). Embryos were grown to stage 34/35, fixed and processed for nucβgal activity. Whole-mount *in situ* hybridizations were performed for pax2 (A), wnt4 (B), slc5a11 (C), slc5a2 (D), sim2 (E), slc12a1 (F), and pou2 (G). Lateral views are shown with anterior to the left. Close-up views of the pronephric region are shown below each embryo. The black bars in A, E, and G measure the distance between the 4th visceral arch and the most anterior marker gene expression domain. (A) Effect of fzd3 overexpression on pax2 expression. The injected side displayed multiple ectopic proximal tubules (arrowheads). The intermediate and distal segments are displaced posteriorly (compare the length of the black bars). (B) Effect of fzd3 overexpression on wnt4. Multiple ectopic proximal tubules were detected on the injected side (arrowheads). (C) Effect of fzd3 overexpression on slc5a11. The injected side displayed ectopic proximal tubules (arrowheads). (D) Effect of fzd3 overexpression on slc5a2. The injected side displayed ectopic proximal tubules (arrowheads). (E) Effects of fzd3 overexpression on sim2 expression. sim2 expression in the intermediate segment appeared overall normal (arrowheads). However, the intermediate segment was shifted more posteriorly in comparison to the control side (compare the length of the black bars). (F) Effect of fzd3 overexpression on slc12a1. The injected embryo displayed slc12a1 expression but morphogenesis is abnormal (arrow). (G) pou2 expression in the intermediate and distal segments appeared overall normal (arrows). However, the intermediate and distal segments were shifted more posteriorly in comparison to the control side (compare the length of the black bars). (H) A horizontal section at the level of the pronephric tubules (plane of section is shown in A) revealed the presence of ectopic tubules on the injected side. (I) Close-up of the boxed region in H. Ectopics tubules are present on the injected side (arrowheads).

Table 3: Overexpression of fzd3 induces ectopic proximal and intermediate tubule formation

Marker gene	Expression domains	Phenotype scored	Frequency	n
pax2	PT1 → CT	Ectopic tubules	58%	115
wnt4	PT1 → PT3	Ectopic PT	55%	87
slc5a1	PT3	Ectopic PT	11%	64
slc5a2	PT1 → PT2	Ectopic PT	8%	60
slc5a11	PT1 → PT3	Ectopic PT	13%	116
sim2	IT1	Displaced IT1	31%	45
irx3	PT3 → IT2	Displaced expression	18%	39
slc12a1	IT1 → DT1	Displaced expression	32%	54
pou2	IT1 → CT	Displaced expression	55%	71
clcnk	IT1 → CT	Displaced expression	54%	88

One V2 blastomere per 8-cell stage embryo was injected with 500 pg fzd3 mRNA. Nuclear β-galactosidase (nucβgal) mRNA (100 pg) was coinjected as a lineage tracer. Embryos were allowed to develop to stage 30-34, fixed, stained for nucβgal activity, and processed for *in situ* hybridization using a panel of pronephric kidney marker genes. The injected sides of embryos were scored for the indicated phenotypes. Every experiment was performed at least twice. n, total number of embryos scored. Abbreviations: PT, proximal tubule; IT, intermediate tubule; DT, distal tubule; CT, connecting tubule.

(Fig. 7G; 55%, n=71 for pou2; 54%, n=88 for clcnk). Finally, a horizontal section of a pax2-stained embryo cut at the level of the ectopic tubules showed that they contain a lumen and are composed of polarized epithelial cells (Fig. 7H, I). Taken together, these results suggested that fzd3 was sufficient to induce the formation of ectopic proximal tubules. As a result of ectopic tubules, more distal parts of the nephron were shifted posteriorly in the embryo.

Fzd6 gene function is dispensable for pronephric kidney development

In order We designed antisense MOs to block fzd6 protein synthesis and investigate the potential roles for fzd6 during pronephros formation. Fzd6(1)-MO and fzd6(3)-MO were first tested for their ability to interfere with fzd6a and fzd6b protein translation *in vitro* (Fig. 3B, C). fzd6(1)-MO is able to block fzd6a protein synthesis in a dose-dependent manner, while fzd6b protein synthesis was only partially inhibited. In contrast, fzd6(3)-MO was able to block both fzd6a and fzd6b protein synthesis in a dose-dependent manner. We then injected fzd6(3)-MO into a single V2 blastomere at the 8-cell stage to deplete fzd6 protein from the developing pronephric kidney. Injections of doses up to 40 ng of fzd6(3)-MO did not cause any discernable embryonic defects as monitored by *in situ* hybridization using pax2, pax8, lim1, fxyd2, slc5a11, and clcnk as marker genes (data not shown). These results suggested that fzd6 function was dispensable for pronephric kidney organogenesis. Next, we tested whether overexpression of fzd6 would affect pronephric development. We injected 1 ng fzd6 mRNA into single V2 blastomeres into the 8-cell stage embryos. Injected embryos developed normally to stage 48 without any discernable morphological defects. Furthermore, when embryos were analyzed by *in situ* hybridization for pronephric marker gene expression (pax2, fxyd2, slc5a11, clcnk), no defects were observed. Taken together, these results suggested that fzd6 protein misexpression into the prospective pronephric region does not affect pronephric kidney development.

Disruption of fzd8 genes function by morpholino oligonucleotides blocks pronephric tubules maturation

To date, two pseudoallelic fzd8 genes have been described in *Xenopus laevis* (Deardorff et al., 1998; Itoh et al., 1998). Based on their submission dates to GenBank, they were renamed here fzd8a (Itoh et al., 1998) and fzd8b (Deardorff et al., 1998). The deduced proteins encoded by fzd8a and fzd8b are comprised of 583 and 581 amino acid residues, respectively, and share an amino acid identity of 97%. Furthermore their expression patterns are virtually identical in particular in regard to intermediate and distal segments of the pronephric kidney. Previously, fzd8 gene function during pronephros development had been studied using an antisense morpholino oligonucleotide strategy (Satow et al., 2004). Importantly, the Xfzd8-Mo used by Satow and collaborators matches perfectly the fzd8b sequence, whereas it has four mismatche relative to fzd8a. In their study, injection of 20 ng of Xfz8-Mo into a V2 blastomere leads to abnormal proximal tubule morphogenesis as visualized by immunohistochemistry using pronephric proximal tubule-specific 3G8 antibody. Furthermore, Xfzd8-Mo injection impairs

final differentiation of the pronephric intermediate, distal and connecting tubules epithelium as visualized by immunohistochemistry using the 4A6 antibody. In contrast, none of the pronephric marker genes used in the study displayed abnormal pronephric expression (Satow et al., 2004). Here, we targeted the fzd8 genes by antisense MOs to investigate whether fzd8a and/ or fzd8b are necessary for pronephros organogenesis. We designed two different morpholino oligonucleotides, fzd8a-MO and fzd8b-MO, targeting fzd8a and fzd8b genes, respectively. First, we demonstrated *in vitro* that fzd8a-MO and fzd8b-MO were able to specifically block fzd8a and fzd8b protein synthesis, respectively. fzd8a translation was blocked by fzd8a-MO in a dose-dependent manner (Fig. 3D). fzd8b-MO did not interfere with fzd8a protein synthesis. On the other hand, fzd8b-MO was able to specifically block fzd8b protein synthesis, whereas fzd8a-MO could not (Fig. 3E). Then, we injected 5 ng of fzd8a-MO and fzd8b-MO in a single or both V2 blastomere of 8-cell stage embryos. We observed in tadpoles bilaterally depleted from fzd8 proteins, that they frequently developed edemas from stage 41 onwards (data not shown; 44%, n=78). Interestingly, in tadpoles displaying edemas no pronephric tubules could be observed at stage 47 (data not shown). Eventually, all the embryos carrying edemas died at stage 48. These results are comparable to the ones obtained by Satow and collaborators when targeting fzd8b (Satow et al., 2004). These results demonstrated that fzd8a and fzd8b functions were necessary for water homeostasis and tadpole survival. Injection of fzd8b-MO at a dose of 5 ng in a single V2 blastomere, but not of 5 ng of fzd8a-MO, caused loss of marker gene expression at low frequencies, typically 13-17% (Table 4). Injection of 5 ng of each morpholino together in a single V2 blastomere led to defects in the expression of pronephric markers with a much higher penetrance, typically 31-62% (Fig. 8; Table 4). The expression of pax2 was not inhibited by fzd8 depletion but revealed abnormal intermediate tubule morphogenesis (Fig. 8A). Next, we analyzed the expression of segment-specific marker genes. wnt4 expression in the proximal tubule was lost on the injected side in 31% (n=48) of the embryos (Fig. 8B). Similarly, slc5a1, slc5a2, and slc5a11 expression was absent in 32-40% of the injected embryos (Fig. 8C; Table 4). Using intermediate tubule-specific markers such as sim2, irx3, and slc12a1, we noticed that their expression was also affected by fzd8 depletion (Fig. 8D, E; Table 4). Interestingly, fzd8 gene knockdown did not affect pou2 expression (Fig. 8F; 0%, n=48), while clcnk expression was lost with a high penetrance (Fig.8G; 62%, n=78). Histological analysis of fzd8 depleted embryos demonstrated the absence of an organized pronephric epithelium on the injected side (Fig. 9). In summary, induction of early pronephric marker genes was not affected by depletion of fzd8 proteins. Expression of pronephric differentiation markers was however lost. The maturation defect was most pronounced for markers of the distal segments of the pronephric nephron.

Ectopic expression of fzd8 induces ectopic pronephric distal segment fates

We performed gain-of-function experiments to assess whether fzd8 is sufficient to trigger ectopic expression of pronephric marker genes. Single V2 blastomeres were injected with

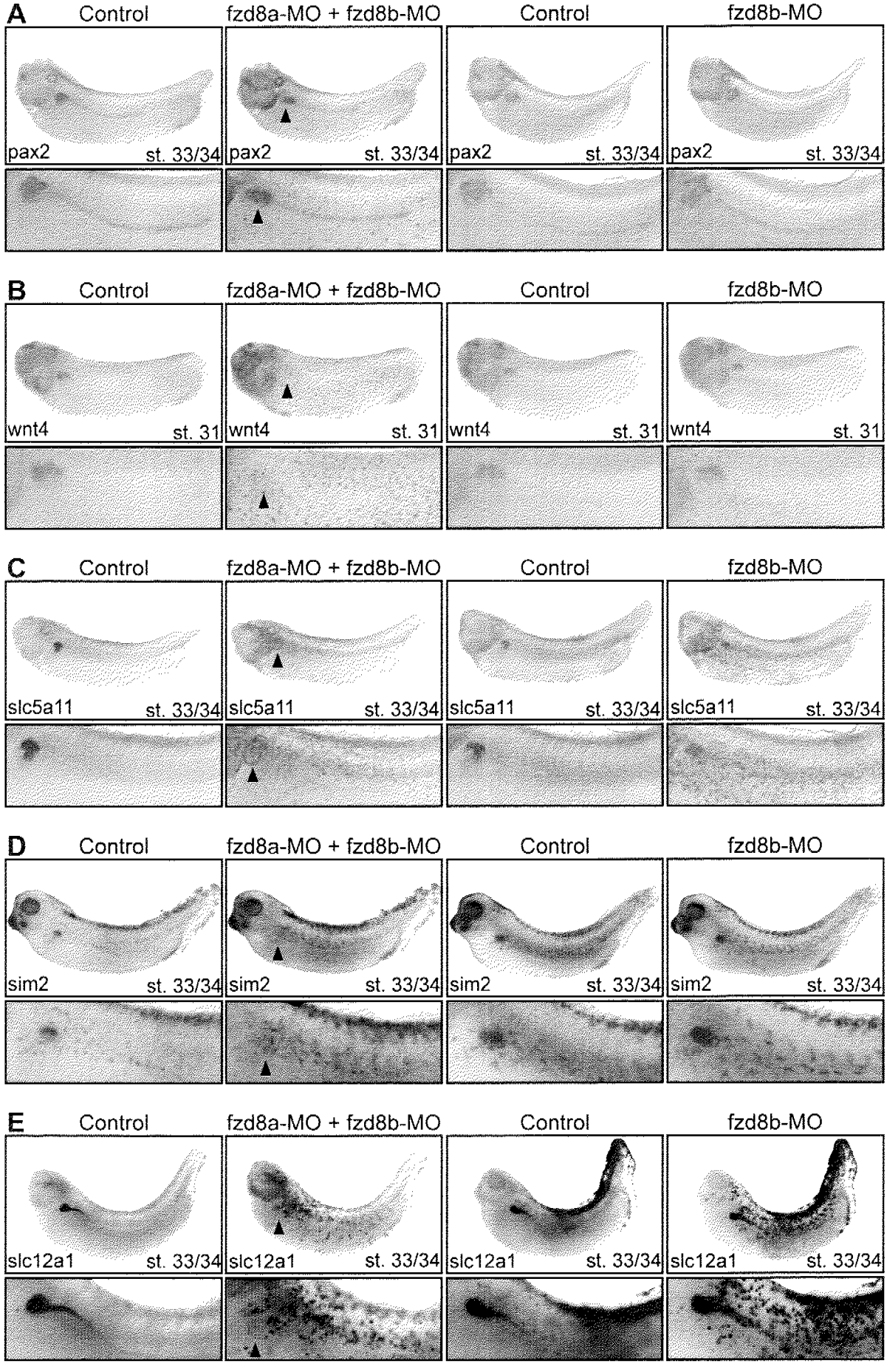
A
Control
fzd8a-MO + fzd8b-MO
Control
fzd8b-MO
pax2 st. 33/34
pax2 st. 33/34
pax2 st. 33/34
pax2 st. 33/34
B
Control
fzd8a-MO + fzd8b-MO
Control
fzd8b-MO
wnt4 st. 31
wnt4 st. 31
wnt4 st. 31
wnt4 st. 31
C
Control
fzd8a-MO + fzd8b-MO
Control
fzd8b-MO
slc5a11 st. 33/34
slc5a11 st. 33/34
slc5a11 st. 33/34
slc5a11 st. 33/34
D
Control
fzd8a-MO + fzd8b-MO
Control
fzd8b-MO
sim2 st. 33/34
sim2 st. 33/34
sim2 st. 33/34
sim2 st. 33/34
E
Control
fzd8a-MO + fzd8b-MO
Control
fzd8b-MO
slc12a1 st. 33/34
slc12a1 st. 33/34
slc12a1 st. 33/34
slc12a1 st. 33/34

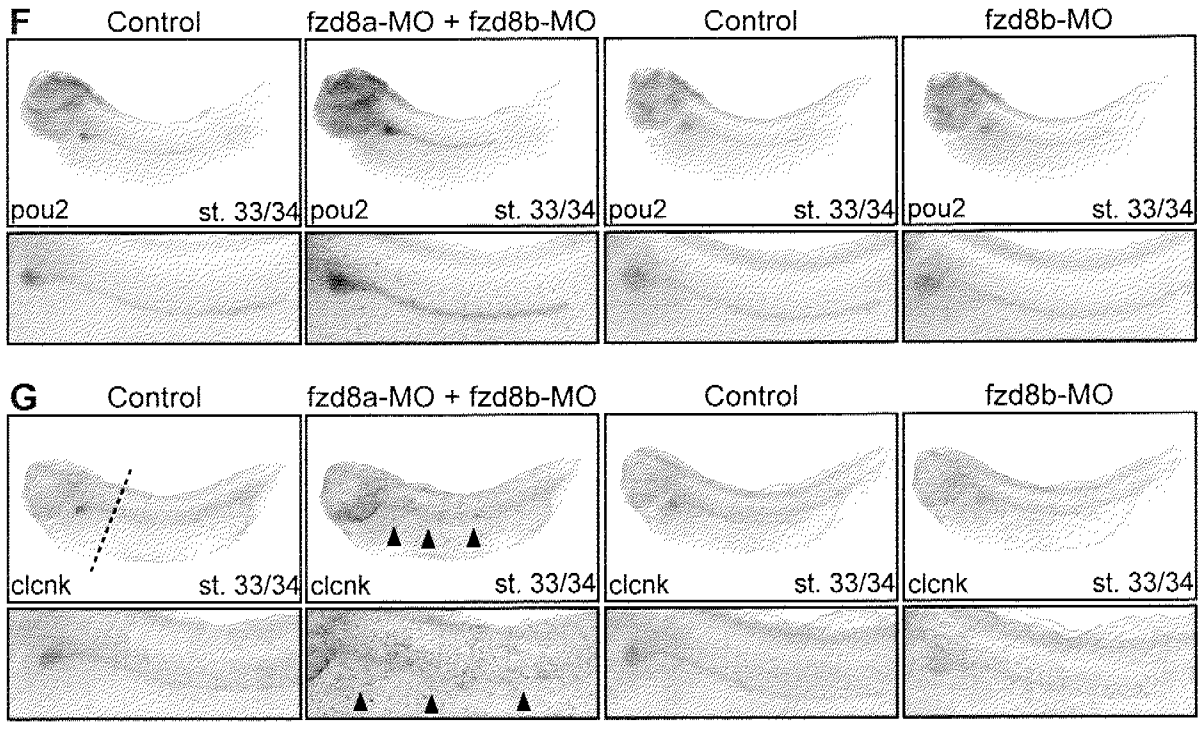

Figure 8: Inhibition of maturation of pronephric epithelia by coinjection of fzd8a-MO and fzd8b-MO.

One V2 blastomere per 8-cell stage embryo was coinjected with either 5 ng of fzd8b-MO or both 5 ng of fzd8a-MO and 5 ng of fzd8b-MO and the lineage tracer nucβgal. Embryos were fixed at stages 31 (B) and 33/34 (A, C-G), processed for nucβgal activity and hybridized for marker gene expression as indicated. Control and injected sides are shown as indicated. Close-up views of the pronephric regions are shown below each embryo. (A) Abnormal intermediate tubule morphogenesis revealed by pax2 expression (arrowheads) was detected upon injection of both fzd8. (B) Embryos injected with both fzd8 MOs showed an absence of pronephric wnt4 staining (arrowheads). (C) The proximal tubule marker slc5a11 was absent in the embryos injected with both MO (arrowheads). (D) Sim2 expression was lost upon injection of both fzd8 MOs (arrowheads). (E) The intermediate tubule marker slc12a1 was absent on the injected side of MO-injected embryos (arrowheads). (F) pou2 expression was unaffected. (G) Analysis of clcnk revealed a failure in distal tubule maturation as clcnk staining was absent on the injected side (arrowheads).

Table 4: Disruption of fzd8 function impairs differentiation of pronephric epithelia

MO	Marker gene	Expression domains	Phenotype	Frequency	n
fzd8a-MO	pax2	PT1 → CT	Abnormal PT morphogenesis	2%	40
	wnt4	PT1 → PT3	Loss of expression	3%	41
	slc5a2	PT1 → PT2	Loss of expression	3%	30
	slc5a11	PT1 → PT3	Loss of expression	6%	50
	slc12a1	IT1 → DT1	Loss of expression	0%	31
	pou2	IT1 → CT	Loss of expression	0%	40
	clcnk	IT1 → CT	Loss of expression	6%	52
fzd8b-MO	pax2	PT1 → CT	Abnormal PT morphogenesis	15%	38
	wnt4	PT1 → PT3	Loss of expression	13%	38
	slc5a2	PT1 → PT2	Loss of expression	13%	31
	slc5a11	PT1 → PT3	Loss of expression	18%	44
	slc12a1	IT1 → DT1	Loss of expression	17%	30
	pou2	IT1 → CT	Loss of expression	0%	37
	clcnk	IT1 → CT	Loss of expression	16%	38
fzd8a-MO + fzd8b-MO	pax2	PT1 → CT	Abnormal PT morphogenesis	37%	49
	wnt4	PT1 → PT3	Loss of expression	31%	48
	slc5a1	PT3	Loss of expression	32%	63
	slc5a2	PT1 → PT2	Loss of expression	38%	56
	slc5a11	PT1 → PT3	Loss of expression	40%	47
	sim2	IT1	Loss of expression	33%	46
	irx3	PT3 → IT2	Loss of expression	35%	34
	slc12a1	IT1 → DT1	Loss of expression	44%	59
	pou2	IT1 → CT	Loss of expression	0%	48
	clcnk	IT1 → CT	Loss of expression	62%	78

One V2 blastomere per 8-cell stage embryo was injected with 5 ng of fzd8a-MO, fzd8b-MO or both MO as indicated. Nucβgal mRNA (100 pg) was coinjected as a lineage tracer. Embryos were allowed to develop to stages 30-34, fixed, stained for nucβgal activity, and processed for *in situ* hybridization. The injected sides of embryos were scored for the indicated phenotypes. Every experiment was performed at least twice, except for irx3. n, total number of embryos scored. Abbreviations: PT, proximal tubule; IT, intermediate tubule; DT, distal tubule; CT, connecting tubule.

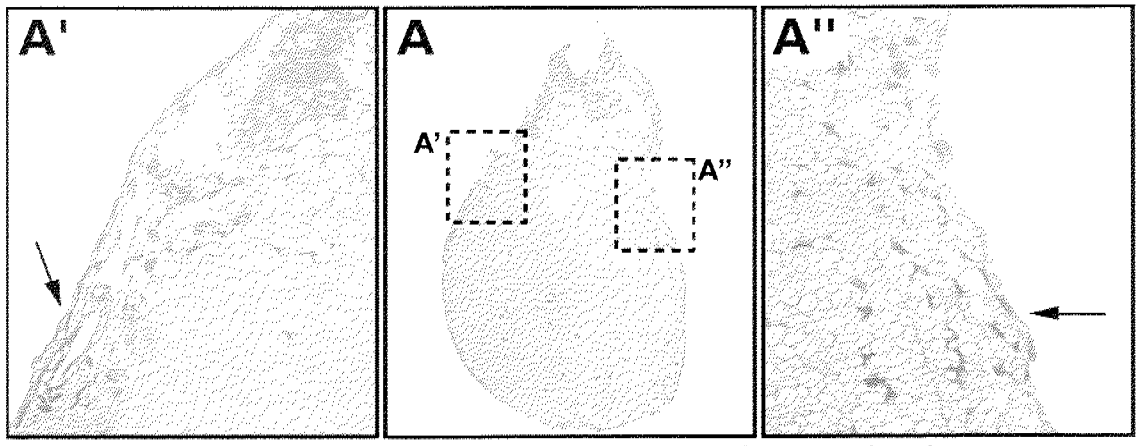

Figure 9: Histological analysis of fzd8a- and fzd8b-MO injected embryos.
One V2 blastomere per 8-cell stage embryo was coinjected with fzd8a-MO (5 ng), fzd8b-MO (5 ng) and the lineage tracer nucβgal. Embryos were fixed at stage 33/34, processed for nucβgal activity and hybridized for clcnk expression. Embryos were plastic embedded and transverse section (2 μm) were cut at the level of the distal tubules. Plane of section is shown in Fig. 8G. (A) Transverse section of a fzd8-depleted embryo. Enlargements of the control (A') and injected (A") sides are shown as indicated. (A') A normal pronephric epithelia was detectable on the control side (arrow). (A") Coinjection of fzd8a- and fzd8b-MO disrupted pronephric development on the injected side. No organized pronephric epithelium was present (arrow).

200 pg of synthetic mRNA encoding full-length fzd8a. The injected embryos were allowed to develop to stages 31-35 and processed for *in situ* hybridization (Fig. 10, Table 5). Injected embryos were analyzed first for pax2 expression (Fig. 10A). Remarkably, pax2 expression in areas corresponding to the proximal tubules was disorganized (61%, n=124). pax2 expression extended ventroanteriorly towards the visceral arches. Moreover, analysis of the tubular expression of wnt4 revealed a loss of expression on the injected side with a frequency of 60% (n=88) (Fig. 10B). Furthermore, we observed that fzd8a injected embryos failed to express proximal tubule markers, such as slc5a1, slc5a2 and slc5a11 (Fig. 10C; Table 5). Analysis of embryos with the intermediate tubule-specific markers sim2, irx3, and slc12a1 demonstrated anterior extension of the expression domains in 52-57% of the injected embryos (Fig. 10D, E; Table 5). Similarly, analysis using other markers such as pou2 and clcnk revealed ectopic staining more anteriorly than on the control side indicating the presence of ectopic intermediate and/or distal tubular tissue on the injected side (Fig. 10F, G; 50%, n=38 for pou2; 47%, n=77 for clcnk). Notably, no morphological defects were observed in the areas corresponding to distal and connecting tubules. Finally, analysis of transverse sections of clcnk-stained embryos revealed that the ectopic tissue was organized into polarized epithelia (Fig. 11). Taken together these results demonstrated that gain of fzd8 function suppressed proximal tubule formation and led to ectopic intermediate tubules extending anteriorly.

Wnt4 can physically interact with fzd3

We have previously shown that *Xenopus* wnt4 was necessary for proximal tubule formation

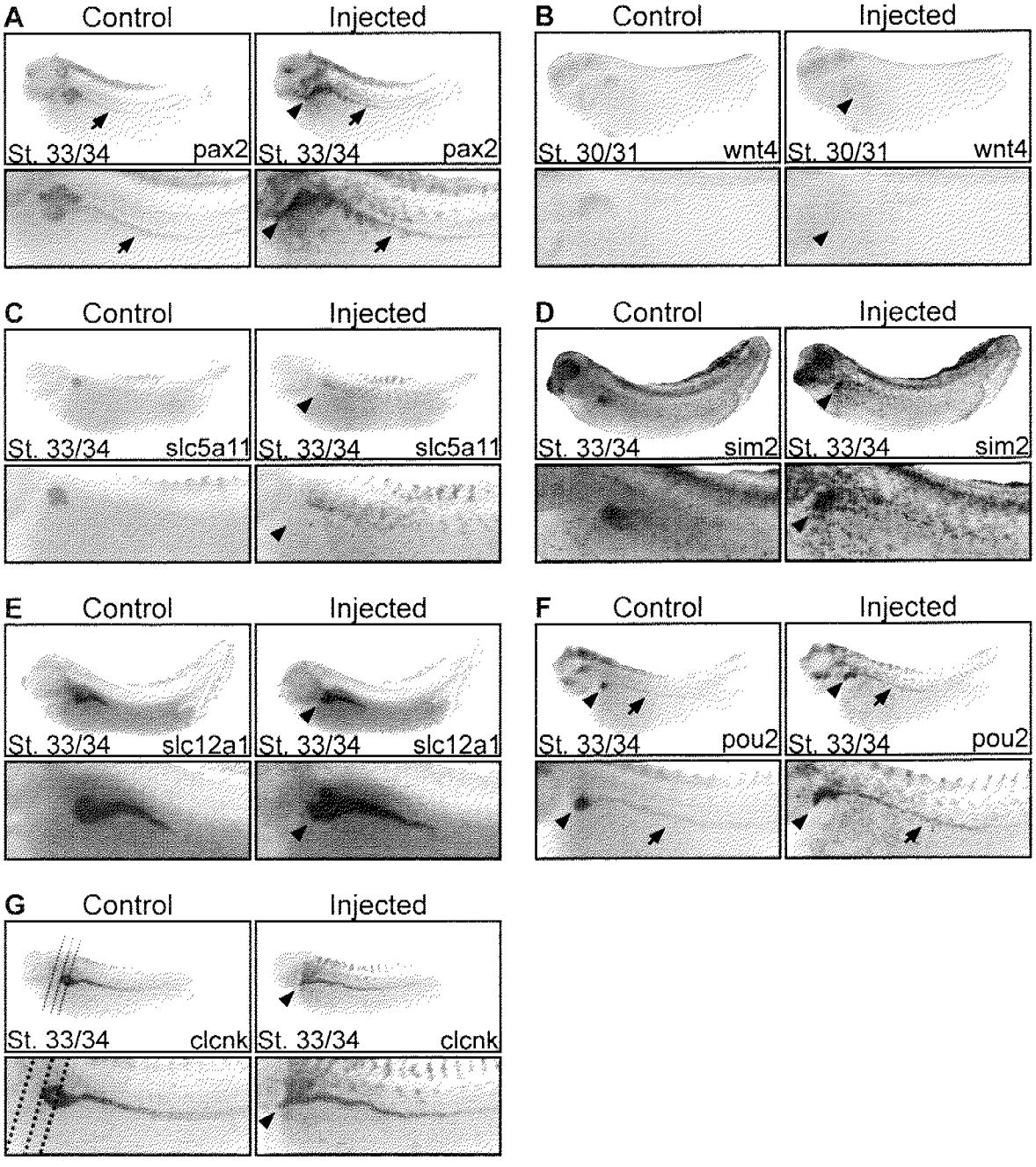

Figure 10: Ectopic fzd8 expression induces ectopic pronephric intermediate tissue. One V2 blastomere per 8-cell stage embryo was coinjected with RNA encoding fzd8a (200 pg) and the lineage tracer nucβgal (100 pg). Embryos were fixed at stages 31 (B) and 33/34 (A, C-G), processed for nucβgal activity, and hybridized with pax2, wnt4, slc5a11, sim2, slc12a1, pou2, and clcnk, as indicated. Close-up views of the pronephric region are shown below each embryo. (A) pax2 expression was perturbed in region corresponding to the proximal tubules. Ectopic pax2 staining extending ventrally towards the visceral arches (arrowheads). Distal tubule elongation was unaffected (arrows). (B) Effect of fzd8a overexpression on wnt4 expression. wnt4 staining was absent on the injected side (arrowheads). (C) slc5a11 expression was absent from the injected side (arrowheads). (D) The expression of sim2 was displaced anteriorly (arrowheads). (E) Ectopic slc12a1 expression was detected anterioventrally (arrowheads). (F) Ectopic pou2 expression was detected on the injected side (arrowheads). Posterior extension of the distal nephron segments was unaffected (arrows). (G) Ectopic expression of clcnk was detected anteriorly (arrowheads).

Table 5: Overexpression of fzd8 induces loss of proximal tubules and ectopic intermediate and distal tubules.

Marker gene	Expression domains	Phenotype	Frequency	n
pax2	PT1 → CT	Abnormal PT morphogenesis	61%	124
wnt4	PT1 → PT3	Loss of expression	60%	88
slc5a1	PT3	Loss of expression	58%	64
slc5a2	PT1 → PT2	Loss of expression	64%	59
slc5a11	PT1 → PT3	Loss of expression	49%	82
sim2	IT1	Anteriorly displaced expression	52%	67
irx3	PT3 → IT2	Anteriorly displaced expression	53%	38
slc12a1	IT1 → DT1	Ectopic expression	57%	92
pou2	IT1 → CT	Ectopic expression	50%	38
clcnk	IT1 → CT	Ectopic expression	47%	77

One V2 blastomere per 8-cell stage embryo was injected with 200 pg fzd8a mRNA. Nuclear β-galactosidase (nucβgal) mRNA (100 pg) was coinjected as a lineage tracer. Embryos were allowed to develop to stage 30-34, fixed, stained for nucβgal activity, and processed for *in situ* hybridization using a panel of pronephric kidney marker genes. The injected sides of embryos were scored for the indicated phenotypes. Every experiment was performed at least twice. n, total number of embryos scored. Abbreviations: PT, proximal tubule; IT, intermediate tubule; DT, distal tubule; CT, connecting tubule.

(Saulnier et al., 2002). In addition, we demonstrated here that fzd3 plays a key role in proximal tubule development. Taken together, this strongly suggested that wnt4 is the endogenous ligand for fzd3. To date, it is unknown whether wnt4 is capable of physically interacting with pronephric fzd receptors. We addressed this question by assessing the qualitative binding preferences of different secreted molecules (β-activin, as a negative control, and four members of the wnt family including wnt4) to fzd receptors using a co-transfection assay. We performed co-transfection experiments in 293 HEK cells to determine whether specific wnt-fzd combinations will trap wnt ligands to the cell surface. A series of *Xenopus* wnt proteins were tagged with haemagglutinin (HA) at the amino terminus. Carboxyterminal fusions of the complete frizzled with a myc epitope were also constructed. Single transfections of the myc-tagged receptors revealed normal plasma membrane localization (data not shown). HA-tagged wnt proteins could be detected in the secretory pathway, when immunostaining was performed on permeabilized cells (Fig. 12A). No significant plasma membrane localization could however be detected, neither on permeabilized (Fig. 12A, white arrowheads) nor on unpermeabilized cells (data not shown). Next, we performed co-transfection experiments of all possible combinations as shown in Fig. 12G. One representative negative example is shown in Fig. 12B. wnt4/fzd8 co-transfection revealed normal fzd8 receptor expression, whereas wnt4 could not be detected at the cell surface. This indicates that fzd8 is apparently not able to retain wnt4 at the plasma

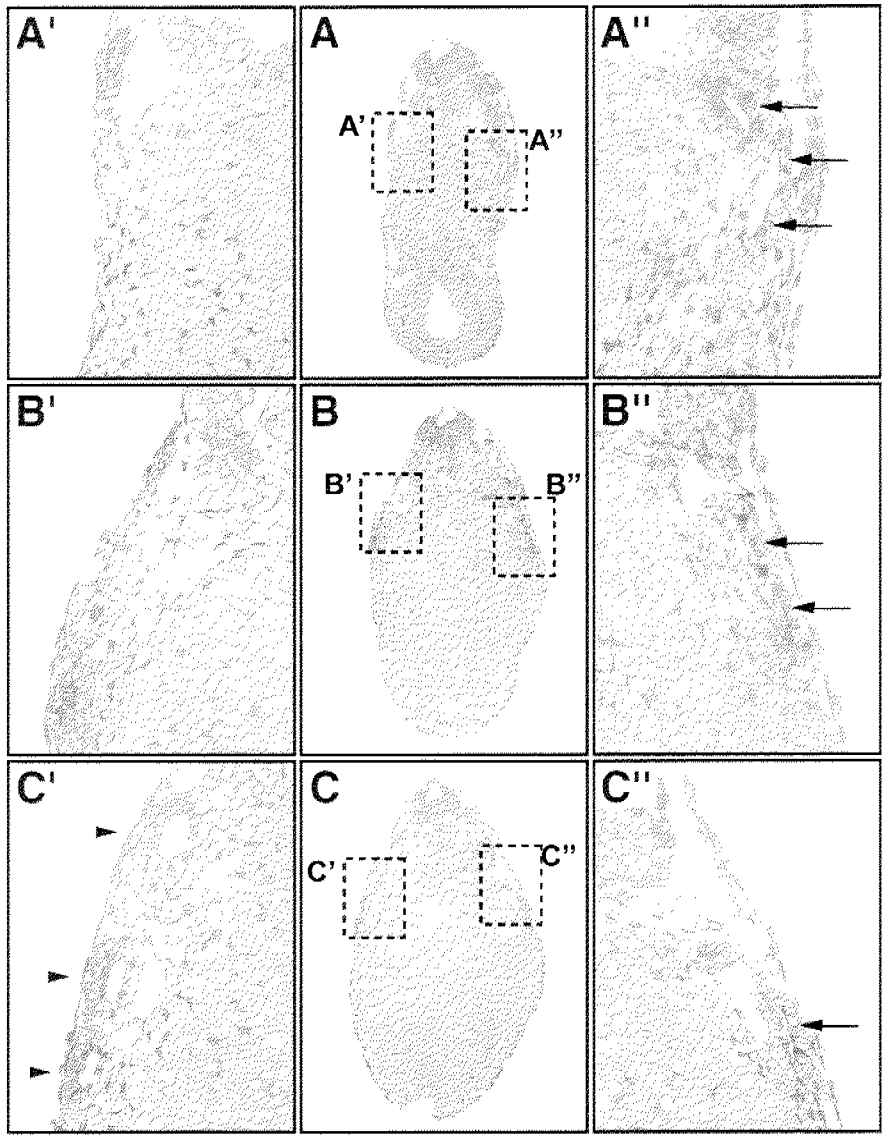

Figure 11. Histological analysis of fzd8 mRNA injected embryos.
One V2 blastomere of an 8-cell stage embryo was coinjected with 200 pg of fzd8a mRNA and the lineage tracer nucβgal. Embryos were fixed at stage 33/34, processed for nucβgal activity and hybridized with clcnk. For histological analysis embryos were plastic embedded and transverse sectioned (2 μm) at the level of the otic vesicle, at the anterior edge of the pronephric kidney, and at the level of the pronephric tubules. Planes of sections are shown in Fig. 10G. Enlargements of the pronephric regions are shown as indicated. (A-C) fzd8 overexpression induces ectopic distal segment tissue (arrows). (A', A") Ectopic epithelialized pronephric tissue could be detected in sections cut at the level of the otic vesicle (arrows). (B', B") Section cut anterior to the pronephros. The injected side shows ectopic pronephric epithelial tissue, whereas no epithelial structures could be detected on the control side (arrows). (C', C") Section cut through the proximal tubule region of the pronephros. Three normal proximal tubules were present on the control side (arrowheads), whereas only one pronephric tubule was detected on the injected side (arrow).

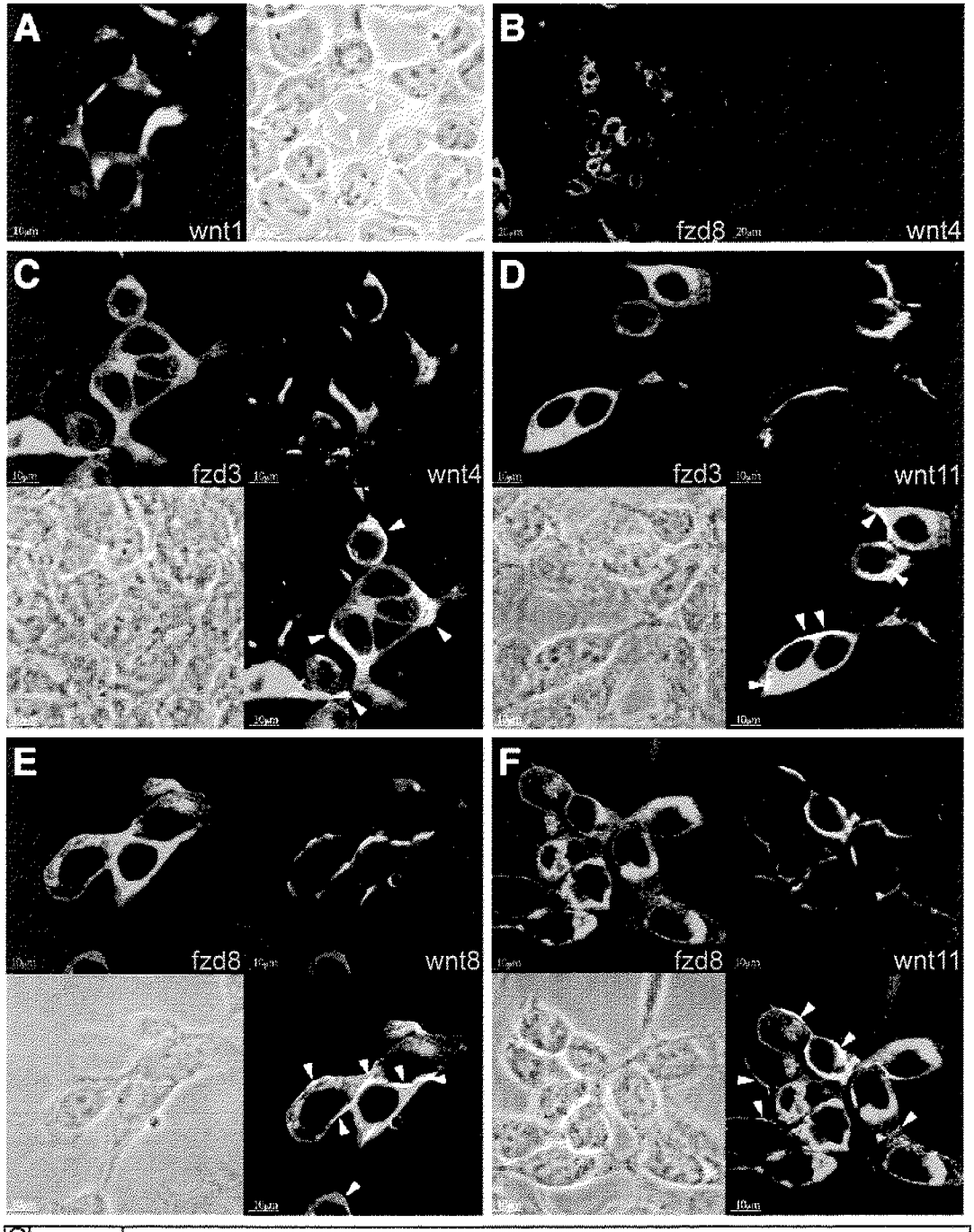

G: myc \ HA	ActivinβB	wnt1	wnt4	wnt8	wnt11
fzd3	—	—	▷	—	▷
fzd7	—	—	—	—	▷
fzd8	—	—	—	▷	▷

Figure 12: Binding preferences of wnt ligands and fzd receptors.
293 HEK cells were transfected alone with myc-tagged variants of various fzd receptors, or various HAtagged wnt ligands (A, data not shown). Co-tranfection experiments with various wnt/fzd combinations are shown in panel B to F. Immunohistochemistry was performed as described in Materials and Methods. Cells were analyzed by confocal microscopy. (A) Transfected Wnt ligands do not bind to the plasma membrane of 293 HEK cells. An example with wnt1 is shown. In permeabilized cells, wnt1 is detected in the secretory pathway (left panel). The overlay of the wnt1 fluorescent signal with the bright field image indicates that wnt1 is not present at the cell surface (right panel, white arrowheads). In unpermeabilized cells, none of the wnt ligands tested displayed a detectable signal (data not shown). (B) Co-transfection of the wnt4 and fzd8 combination. fzd8 is detected at the plasma membrane (right), while no wnt4 signal could be detected at the cell surface (left). (C-F) Binding preferences of various wnt ligands to fzd3 and fzd8 receptors. (C) 293 HEK cells were co-transfected with wnt4 and fzd3. fzd3 (upper left image) and wnt4 (upper right image) signals could be detected. The overlay of both images (bottom right image) shows a clear yellow signal at the plasma membrane indicating that fzd3 is able to retain wnt4 at the cell surface (white arrowheads). The same is also true for the combinations wnt11 and fzd3 (D), wnt8 and fzd8 (E), and wnt11 and fzd8 (F), where a clear colocalization signal was detected (yellow signals, white arrowheads). (G) Summary of the different wnt/fzd combinations tested and results obtained in co-transfection experiments (-: the fzd receptor does not retain the wnt ligand at the plasma membrane; +: the fzd receptor retains the wnt ligand at the plasma membrane).

membrane. Panel C of Fig. 12 shows the results obtained after wnt4/fzd3 co-transfection. wnt4 could be readily detected on the plasma membrane. Furthermore, fzd3 colocalized with wnt4. fzd3 appeared therefore to be capable of physically interacting with wnt4. Similar findings were obtained for wnt11/fzd3 (Fig. 12D), wnt8/fzd8 (Fig. 12E), wnt11/fzd8 (Fig. 12F), and wnt11/fzd7 (data not shown). A summary of the results obtained in the co-tranfection experiments is shown in Fig. 12G. Collectively, our findings demonstrate that each fzd receptor interacts with a subset of wnt proteins, indicating that specific Wnt interactions might occur *in vivo*. Most importantly, fzd3 but not fzd8 interacts with wnt4, indicating that wnt4 is an *in vivo* ligand of fzd3.

Activation of tcf3 signaling induces ectopic pronephric tissue and disorganizes pronephric development

We addressed next the issue of the nature of the Wnt signaling pathways triggered during pronephric kidney organogenesis. Ectopic, premature activation of canonical Wnt signaling in the pronephric primordium might provide information on the instructive potential of canonical Wnt signaling during pronephric kidney development. Activation of canonical Wnt signaling by Wnt mRNA injection causes axis duplication (McMahon and Moon, 1989) and precludes analysis of later developmental processes. In order to overcome this limitation, we took advantage of the conditionally active tcf3 mutant construct THVGR (Yang et al., 2002). Activation of tcf transcription factors is believed to mimic activation of canonical Wnt signaling. The use of tcf3 mutants fused to the ligand-binding domain of the human glucocorticoid receptor (GR) enables the hormone-dependent control of signal activation (Kolm and Sive, 1995; Tada et al., 1997;

Yang et al., 2002). Indeed, in absence of GR ligand, the THVGR fusion protein is thought to interact with the cytoplasmic heat shock protein hsp90 and as such retained into the cytoplasm. Addition of dexamethasone, a GR ligand, to the culture medium and its subsequent binding to THVGR releases the fusion protein from hsp90. Thus, THVGR can translocate to the nucleus where it can function as an active tcf3 transcription factor. Hence, we injected THVGR mRNA in one V2 blastomere at the 8-cell stage, treated the embryos with dexamethasone at various developmental stages, and analyzed pronephric marker gene expression to visualize effects of hormone-induced activation of canonical Wnt signaling on pronephros development (Fig. 13; Table 6). Surprisingly, embryos injected with THVGR mRNA displayed axis duplication in 20-30% of the cases independently of dexamethasone treatment (data not shown). This observation suggests that in this context the glucocorticoid receptor system is to some extent leaky. Hormone treatment was performed at stages 12, 15, 18, 22, and 25. Hormone treatment at stage 12 induced severe developmental defect including increased axis duplication, while activation at stage 18 and later did not affect pronephric development (data not shown). Therefore, we settled on adding dexamethasone at stage 15. Dexamethasone alone did not induce any phenotype (Table 6). Embryos injected with THVGR but not induced by dexamethasone developed a normal pronephric kidney as revealed by pax2, slc5a11, and clcnk expression (Fig.13 A-F; Table 6).Analysis of embryos lacking evidence of secondary axis formation revealed that pax2 expression was expanded and disorganized in the intermediate mesoderm (Fig. 13J; 70%, n=43). This indicates that widespread activation of tcf3-dependent transcription causes ectopic pronephric cell fate specification. We next tested whether the ectopic pronephric tissue could undergo terminal differentiation. The proximal tubule marker slc5a11 showed ectopic patches of expression (Fig. 13K; 32 %, n=38), while the distal tubule marker clcnk showed reduced expression compared to the control side (Fig. 13L; 25 %, n=28). In summary, mid-neurula activation of tcf3-dependent transcription disrupted normal pronephric development leading to the induction of proximal tubular tissue and inhibiting more distal nephron fates.

Inhibition of GSK3β or JNK resulted in a block of distal tubule differentiation

Alternatively, pharmacological agents can be employed to interfere with Wnt signaling pathway functions. Activation of canonical Wnt pathway can be achieved by the inhibition of GSK3β, a member of the β-catenin phosphorylation complex (van Noort et al., 2002; Meijer et al., 2003). BIO is able to inhibit GSK3β leading to activation of the canonical Wnt pathway (Meijer et al., 2003). In contrast, MeBIO, a methylated form of BIO, does not inhibit GSK3β. Treatment of embryos with BIO was performed at developmental stages 12, 15, 18, and 20. BIO treatment at stage 12 caused general embryonic defects, while treatment at stage 18 and later did not induce pronephric defects (data not shown). Therefore, we focused our analysis on embryos treated at stage 15. Control treatment of stage 15 embryos with MeBIO did not cause pronephric defects (Fig. 14A-C; Table 7). Treatment of stage 15 embryos with BIO led to a loss of distal tubule marker clcnk (Fig. 14 F; 100%, n=120). Expression of pax2 and the proximal tubule marker

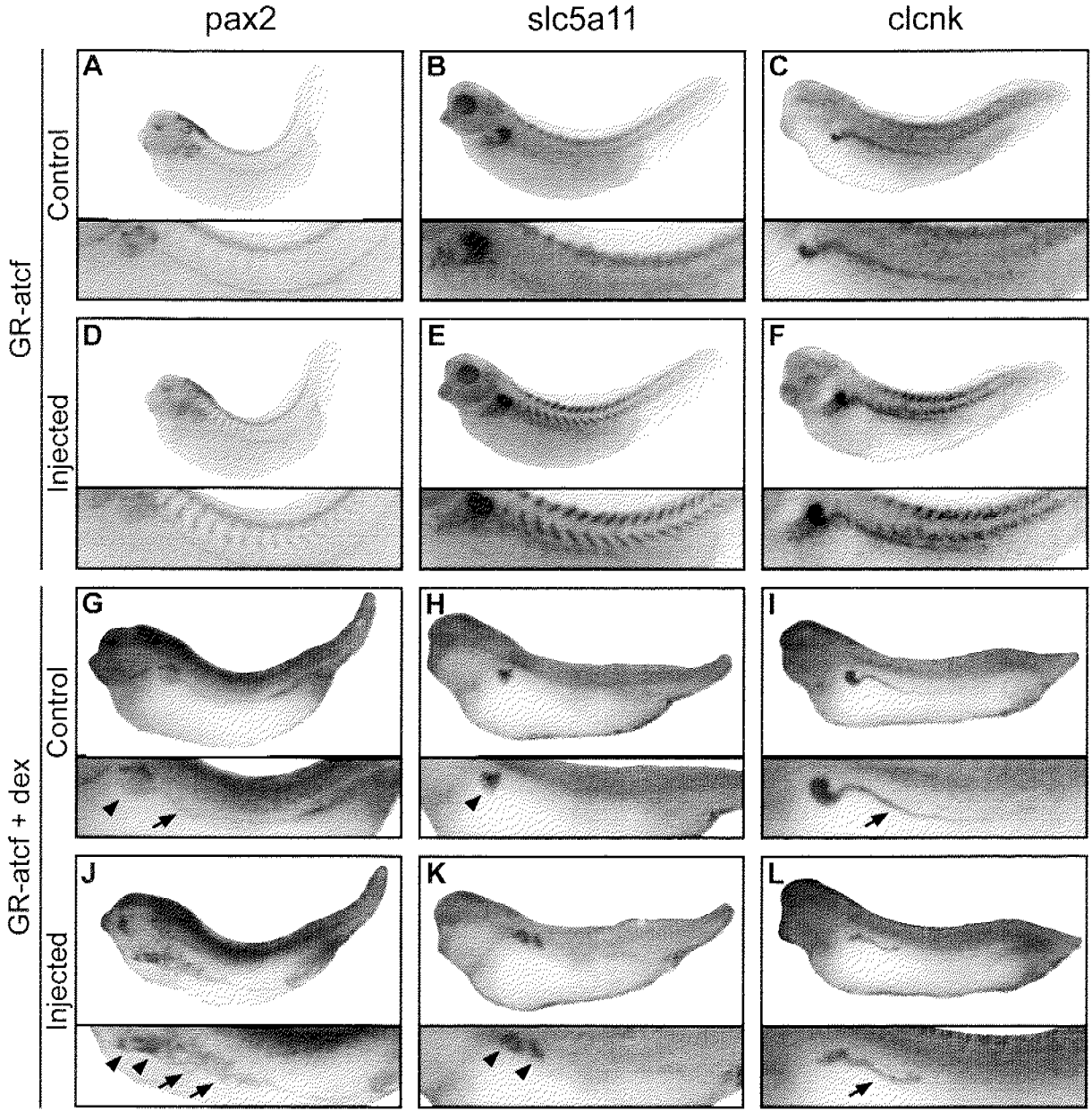

Figure 13: Effects of hormon-dependent activation of canonical wnt signaling pathway on pronephric development.

One V2 blastomere of 8-cell stage embryos was injected with 500 pg GR-atcf mRNA. Nucβgal mRNA (100 pg) was injected as lineage tracer. Embryos were treated or not with dexamethasone at stage 15, allowed to develop until control siblings reached stage 35/36, fixed, stained for nucβgal activity, and processed for *in situ* hybridization. (A-F) Injected embryos not treated in dexamethasone. (A-C) Non injected side of control embryos show no defect in pax2, slc5a11, and clcnk expression. (D-F) Injected side of injected embryos not treated with dexamethasone reveal no defect in pax2, slc5a11, and clcnk expression. (G-I) Control side of injected embryos treated with dexamethasone stained for pax2, slc5a11, and clcnk displayed no abnormal phenotype in the proximal (arrowheads) or distal (arrows) pronephric tubule. (J-L), Injected side of embryos treated in dexamethasone showed an expansion and desorganization of pronephric pax2 expression (arrowheads and arrows), ectopic slc5a11 expression (arrowhead), and reduced clcnk expression (arrow). Arrowheads, proximal tubules; arrows, intermediate, distal, and connecting tubules.

Table 6: Effects of hormone-dependent activated tcf3 signaling on pronephric marker gene expression

mRNA	Dex.	Marker gene	Expression domains	Phenotype	Frequency	n
-	+	pax2	PT1 → CT	Disorganized expression	0%	30
		slc5a11	PT1 → PT3	Ectopic expression	0%	31
		clcnk	IT1 → CT	Reduced expression	0%	31
THVGR	-	pax2	PT1 → CT	Disorganized expression	13%	30
		slc5a11	PT1 → PT3	Ectopic expression	0%	29
		clcnk	IT1 → CT	Reduced expression	0%	30
	+	pax2	PT1 → CT	Disorganized expression	70%	43
		slc5a11	PT1 → PT3	Ectopic expression	32%	38
		clcnk	IT1 → CT	Reduced expression	25%	28

One single V2 blastomere was injected with 500 pg of THVGR synthetic mRNA together with 100 pg of nucβgal mRNA as lineage tracer or with 600 pg of nucβgal mRNA alone as indicated. Embryos were bathed into dexamethasone at stage 15 when indicated. Embryos were allowed to develop to stage 35, fixed, stained for nubβgal, and processed for *in situ* hybridization using a panel of pronephric kidney marker genes. The injected sides of embryos were scored for the indicated phenotype. n, total number of embryos scored. Abbreviations: PT, proximal tubule; IT, intermediate tubule; DT, distal tubule; CT, connecting tubule.

slc5a11was unaffected (Fig. 14D, E; Table 7). The Jun N-terminal kinase (JNK) signaling pathway is activated in the planar cell polarity pathway downstream of Dvl (Li et al., 1999; Huelsken and Behrens, 2002). SP600125 is a JNK specific inhibitor that functions in *Xenopus laevis* (Bennett et al., 2001; Maurus et al., 2005). Interestingly, SP600125 treatment had no effect on pax2 and slc5a11 expression, but caused a loss of clcnk expression (Fig. 14F; 100%, n=120). These results demonstrate that activation of canonical Wnt signaling and inhibition of the JNK pathway disrupt distal nephron differentiation. Interestingly, these phenotypes are similar to the fzd8 knockdown phenotypes.

Disruption of the Wnt/Calcium dependent pathway does not interfere with pronephric development

In order to investigate the role of wnt/calcium-dependent pathway we used two calcineurin inhibitors, cyclosporine A (CsA) and FK506, to shut down this pathway as has been recently reported (Yoshida et al., 2004). Thus, we decided to monitor pronephric kidney development in presence of calcineurin inhibitors using whole-mount *in situ* hybridization (Table 8). Despite incidence of edema in over 50% of the embryos treated with CsA or FK506 pronephric marker gene expression was unaffected in all embryos analyzed. This suggests that the wnt/calcium pathway is dispensable for pronephric kidney development.

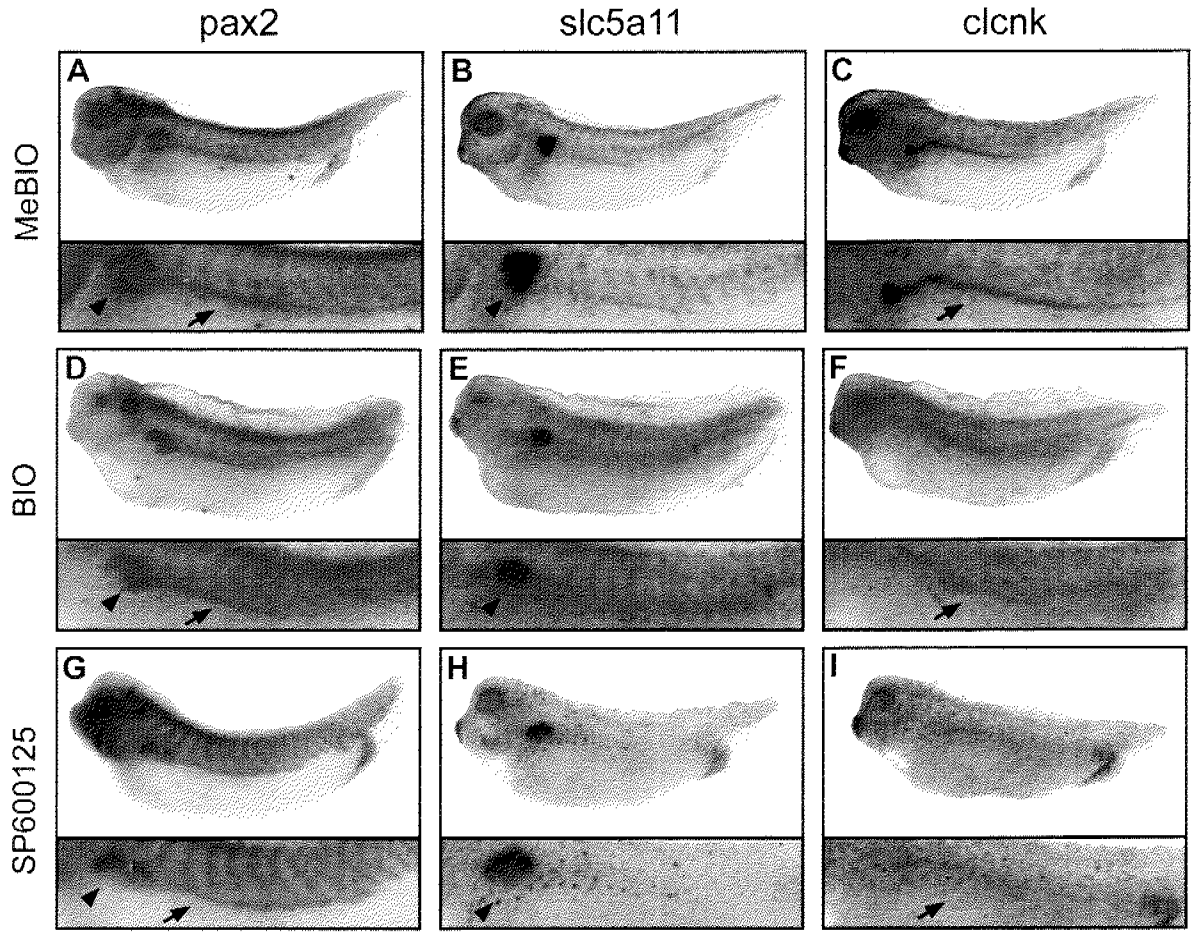

Figure 14: Effects of interference with canonical or PCP Wnt signaling pathways on pronephros development.

(A-F) Embryos were treated with either 15 μM BIO or MeBIO solution from stage 15 onwards, allowed to develop until siblings reached stage 35, fixed, and processed for *in situ* hybridization. (A-C) pax2, slc5a11, and clcnk expression are not affected by treatment with MeBIO. (D-F) pax2 and slc5a11 expression is not affected by treatment with BIO but clcnk expression was lost. (G-I) Embryos were treated with 25 μM SP600125 solution from stage 15 onwards, allowed to develop until control siblings reached stage 35, fixed, and processed for *in situ* hybridization. pax2 and slc5a11 expression is not affected by the treatment while clcnk expression was lost. Proximal tubules are indicated with arrowheads and intermediate, distal, and connecting tubules with arrows.

Table 7: Effects of GSK3β and JNK inhibition on *Xenopus* pronephric marker gene expression

Compound	Embryos displaying			n
	Abnormal pax2 expression (%)	Abnormal slc5a11 expression (%)	Loss of clcnk expression (%)	
DMSO alone	0	0	0	250
BIO	0	8	100	120
MeBIO	0	0	0	150
SP600125	0	10	100	120

Embryos were treated from stage 15 onwards with 0.05% DMSO (vector) alone or together with 25 μM SP600125, 15 μM BIO, or 15 μM MeBIO as indicated. Embryos were allowed to develop until control siblings reached stage 35, fixed, and analyzed for pronephric marker gene expression by whole-mount *in situ* hybridization. BIO is a GSK3β inhibitor, MeBIO is the inactive methylated form of BIO, and SP600125 is a specific JNK inhibitor. n, number of embryos scored.

Table 8: Effects of calcineurin inhibitors on pronephric marker gene expression and edema formation

Compound	Stage	Edema formation	Embryos displaying normal marker gene expression (%)						n
			pax2	slc5a2	slc5a11	slc12a1	clcnk	fxyd2	
DMSO	18	**0%** (n=100)	100	98	100	100	100	100	300
DMSO	29/30	**0%** (n=100)	100	100	100	100	100	100	298
CsA	18	**63%** (n=99)	96	100	100	100	100	100	550
CsA	29/30	**98%** (n=100)	98	98	100	100	100	100	500
FK506	18	**54%** (n=100)	100	100	98	100	100	100	600
FK506	29/30	**100%** (n=98)	100	100	100	100	100	100	550

Embryos were treated from the indicated stages onwards in 0.05% DMSO (vector) alone or together with 500 nM CsA or 50 nM FK506 as indicated. Embryos were allowed to develop to stage 47 and monitored for edema formation or allowed to develop to stages 30/34 and analyzed for pronephric marker genes expression by whole mount in situ hybridization. N, number of embryos scored.

Discussion

Wnt4 has been identified as a conserved key regulator of nephrogenesis in mouse and *Xenopus* (Stark et al., 1994; Saulnier et al., 2002). However, downstream effectors of wnt4 signaling have not been determined to date. In this study, we have established the expression of fzd genes during pronephros development and elucidated their roles in pronephric development. Whole-mount *in situ* hybridization led to the identification of fzd3 expression in the proximal tubule. Interestingly, fzd3 expression parallels the expression of wnt4 in the pronephros (Saulnier et al., 2002). In contrast fzd8 was also expressed in the pronephric anlage but was subsequently restricted to the developing intermediate, distal, and connecting tubules. Finally, we identified fzd6, which was not expressed during early pronephric kidney organogenesis but was expressed later along the entire pronephric nephron. Based on temporal and spatial similarities in expression patterns, it seams likely that fzd3 acts *in vivo* as a receptor of wnt4 during pronephros development. Indeed, we have provided compelling evidence that fzd3 interacts with wnt4 in cell cultures. Finally, disruption of fzd3 function resulted in a block of proximal tubule formation reminiscent of the wnt4 knockdown phenotype described previously (Saulnier et al., 2002). Furthermore, ectopic expression of fzd3 caused a complementary result - the formation of ectopic proximal tubules. In contrast, fzd8 gain- and loss-of-function experiments indicated that fzd8 was necessary for the formation of intermediate, distal, and connecting tubules. Finally, fzd6 appeared not to be essential for nephrogenesis in *Xenopus*.

We will now discuss in detail our findings on the roles of fzd3, fzd6, and fzd8 in the developing pronephric kidney. Interestingly, fzd3 depletion did not affect pronephric cell fate specification as pax2 expression occurred normally. Nevertheless, pax2 staining highlighted defects in proximal tubule morphogenesis. Furthermore, we observed absence of proximal tubule-specific marker genes expression, whereas expression of marker genes of more distal nephron segments were not affected. These results demonstrated an unequivocal requirement for fzd3 function in proximal tubule formation. The loss of proximal tubulse raises the question whether proximal tubule precursor cells undergo apoptosis in absence of fzd3. Indeed, pioneering work on kidney organogenesis has shown in the early 1950's that uninduced murine metanephric mesenchyme undergoes apoptosis (Grobstein, 1953; Grobstein, 1955). To address this issue, we performed TUNEL staining on fzd3-deficient embryos but failed to detect any increase of apoptosis during pronephric kidney development. Interestingly, Fzd3 expression occurs also in the developing mouse metanephros, but Fzd3-deficient mice do not develop an obvious kidney phenotype (Wang et al., 2002). This suggests that the loss of Fzd3 function in the mouse can be functionally compensated by other Fzd genes during metanephric kidney development. We also demonstrated that, ectopic expression of fzd3 was sufficient to induce formation of ectopic differentiated proximal tubules. Interestingly, the ectopic pronephric tubules expressed wnt4, which suggests that wnt4 acts in an autoregulatory loop via fzd3 to promote and/or maintain its own expression. In addition, the ectopic proximal tubules expressed also pax2. Pax2 acts

upstream of Wnt4 during mammalian kidney development (Torban et al., 2006). Our findings suggested now that pax2 might also be a target of wnt4 in *Xenopus*. Alternatively, this could simply indicate that fzd3 overexpression acts on uncommitted pronephric progenitors to specify proximal tubular cell fate. Interestingly, the fzd3 gain-of-function experiments did not suppress globally more distal pronephric cell fates. Rather they were displaced and formed posteriorly. This suggests that only the anterior intermediate mesoderm and its pronephric progenitors were competent to adopt proximal tubule fate in response to ectopic fzd3 expression. Taken together, our findings revealed that fzd3 was necessary and sufficient to instruct pronephric progenitor cells towards cell lineage of the proximal tubule.

Given its expression in the late developing pronephric nephron, we performed fzd6 knockdown and misexpression experiments. Unfortunately, our studies failed to reveal any function for fzd6 in pronephric kidney development. However, our results are in line with recent findings indicating that Fzd6-deficient mice do not have renal defects (Guo et al., 2004).

Finally, we analyzed fzd8 gene function during pronephric kidney development. Previous work had suggested a requirement for fzd8 function in pronephric kidney development (Satow et al., 2004). Satow and collaborators reported a requirement for fzd8 function for pronephric tubule morphogenesis and duct maturation, but failed to identify abnormal marker genes expression. As mentioned above, the antisense MO used in that study was specifically targeted against the fzd8b gene only. In the present study, we targeted both fzd8a and fzd8b genes using two specific MOs. We found that pronephric cell fate specification occurred unaffected in fzd8-depleted embryos but fzd8 was required for the maturation of pronephric epithelia. Importantly, our knockdown experiments indicated that the expression of all tested terminal differentiation marker genes was affected. Interestingly, the early intermediate tubule markers irx3 and sim2 were also affected by fzd8 depletion. In contrast to Satow and collaborators, histological inspection of fzd8-depleted embryos revealed the absence of polarized pronephric epithelia. The absence of polarized epithelia is most probably not due to apoptosis or disrupted somitogenesis, since the early pronephric marker genes pax2 and pou2 were still expressed. Remarkably, typically 31-40% of the fzd8 depleted embryos had defects in proximal tubule formation. This implies that normal development of proximal tubules was dependent on the function of fzd8. fzd8 is however not expressed in the anlage of proximal tubules after stage 25. We cannot exclude the possibility that fzd8 expression occurs throughout the pronephric anlage prior to stage 25. Thus, if fzd8 acts directly on proximal tubule it has to be before stage 25. In summary, depletion of fzd8a and fzd8b impaired pronephric epithelialization and terminal differentiation. Gain-of-function experiments demonstrated that fzd8 was sufficient to induce at the expense of proximal tubules, the development of ectopic intermediate tubule tissue. This caused anterior expansion of the intermediate tubules. The more posterior segments of the distal tubule appear to remain unaffected. Our results suggest that misexpression of fzd8 causes progenitor cells of the intermediate mesoderm to adopt the intermediate tubule fate. Consistent with this observation, expression of proximal tubule marker genes (wnt4, slc5a1, slc5a2, and

slc5a11) was suppressed in the region, where ectopic pronephric intermediate tubules were developing. Interestingly, the loss of wnt4 expression upon overexpression of fzd8 is also consistent with the absence of proximal tubules. Taken together, we demonstrated here that both fzd8a and fzd8b are necessary and sufficient for epithelialization and terminal differentiation of renal intermediate, distal, and connecting tubules. To date, fzd3 and fzd8 are the first frizzled proteins shown to be sufficient to induce ectopic pronephric kidney development in vertebrate embryos and they appear to be at the top of the signaling cascades controlling specific cell fates of the developing pronephric nephron.

We next asked which of the different intracellular Wnt signaling pathways are required and activated during pronephric kidney development. Here, we used different approaches to interfere with wnt signaling pathways. Active of conditionally active tcf3 mutant mid-neurula embryos led to major defects of the developing pronephric kidney as visualized by pax2 expression. This most likely reflects the ability of the canonical Wnt pathway to commit mesodermal cells towards the pronephric cell lineage. The same approach also led to appearance of ectopic proximal tubules but reduced distal tubule formation. This suggests a role for canonical Wnt signaling in promoting proximal tubular cell fates. We also performed experiments to activate the canonical Wnt signaling pathway pharmacologically in mid-neurula embryos by treatment with BIO, a GSK3β inhibitor (Meijer et al., 2003). We observed normal induction of pax2 expression in the pronephros as well as presence of slc5a11 expression in the proximal tubule. However, expression of clcnk, a marker of the intermediate, distal, and connecting tubules was lost. This suggests that ectopic activation of wnt canonical signaling suppresses intermediate and distal tubule differentiation similar to the results obtained after tcf3 activation. Surprisingly, the inhibition of the planar cell polarity pathway component, JNK, by SP600125, resulted in a phenotype similar to what was obtained after GSK3β inhibition. This suggests that JNK function was also required for differentiation of distal nephron segments. Interestingly, these similar results obtained by interfering with two different Wnt pathways are in line with the reported ability of canonical Wnt signaling to inhibit JNK function (Depraetere, 2001; Sun et al., 2001). Subsequently, it was also found that JNK activation can inhibit the wnt canonical pathway (Liao et al., 2006). It is important to keep in mind that the analysis of downstream Wnt pathway components is difficult since multiple upstream signaling pathways converge on these proteins. Interference with the calcium-dependent Wnt pathway failed to impair early pronephric kidney development. Taken together, our studies of intracellular Wnt signaling pathways suggested that the planar cell polarity pathway acts through JNK to promote maturation of the intermediate, distal, and connecting tubules.In contrast, we have provided evidence indicating that canonical Wnt signaling would mediate proximal tubule specification. This notion is further supported by a recent study demonstrating that activation of canonical Wnt pathway is sufficient to induce nephrogenesis in metanephrogenic mesenchymes (Kuure et al., 2007).

In summary, our work suggests that distinct fzd genes act downstream of pax2 to specify distinct cell fates along the nephron. Wnt4 would act in a positive feedback loop through fzd3

to trigger specification of proximal tubule fates, which would be mediated by canonical Wnt signaling. In contrast, fzd8 activation would activate the planar cell polarity pathway to induce the intermediate, distal, and connecting tubule cell fates.

Acknowledgments

We thank Dr. Ali Hemmali-Brivanlou for providing BIO and MeBIO. We also thank Peter Klein for the THVGR plasmid and Randall Moon for the frizzled plasmids. This work was supported by grants of the European Community (EuReGene LSHG-CT-2004-005085) and Swiss National Science Foundation (3100A0-101964) to AWB.

References

Bellefroid EJ, Kobbe A, Gruss P, Pieler T, Gurdon JB, Papalopulu N. 1998. Xiro3 encodes a Xenopus homolog of the Drosophila Iroquois genes and functions in neural specification. Embo J 17:191-203.

Bennett BL, Sasaki DT, Murray BW, O'Leary EC, Sakata ST, Xu W, Leisten JC, Motiwala A, Pierce S, Satoh Y, Bhagwat SS, Manning AM, Anderson DW. 2001. SP600125, an anthrapyrazolone inhibitor of Jun N-terminal kinase. Proc Natl Acad Sci U S A 98:13681-13686.

Brändli AW. 1999. Towards a molecular anatomy of the Xenopus pronephric kidney. Int J Dev Biol 43:381-395.

Brändli AW, Kirschner MW. 1995. Molecular cloning of tyrosine kinases in the early Xenopus embryo: identification of Eck-related genes expressed in cranial neural crest cells of the second (hyoid) arch. Dev Dyn 203:119-140.

Brown JD, Hallagan SE, McGrew LL, Miller JR, Moon RT. 2000. The maternal Xenopus beta-catenin signaling pathway, activated by frizzled homologs, induces goosecoid in a cell non-autonomous manner. Dev Growth Differ 42:347-357.

Carroll TJ, Park JS, Hayashi S, Majumdar A, McMahon AP. 2005. Wnt9b plays a central role in the regulation of mesenchymal to epithelial transitions underlying organogenesis of the mammalian urogenital system. Dev Cell 9:283-292.

Chin ER, Olson EN, Richardson JA, Yang Q, Humphries C, Shelton JM, Wu H, Zhu W, Bassel-Duby R, Williams RS. 1998. A calcineurin-dependent transcriptional pathway controls skeletal muscle fiber type. Genes Dev 12:2499-2509.

Clevers H. 2006. Wnt/beta-catenin signaling in development and disease. Cell 127:469-480.

de Iongh RU, Abud HE, Hime GR. 2006. WNT/Frizzled signaling in eye development and disease. Front Biosci 11:2442-2464.

de Lau W, Barker N, Clevers H. 2007. WNT signaling in the normal intestine and colorectal cancer. Front Biosci 12:471-491.

Deardorff MA, Klein PS. 1999. Xenopus frizzled-2 is expressed highly in the developing eye, otic vesicle and somites. Mech Dev 87:229-233.

Deardorff MA, Tan C, Conrad LJ, Klein PS. 1998. Frizzled-8 is expressed in the Spemann organizer and plays a role in early morphogenesis. Development 125:2687-2700.

Depraetere V. 2001. PAR-1 helps Wnt to get rid of JNK. Nat Cell Biol 3:E158.

Djiane A, Riou J, Umbhauer M, Boucaut J, Shi D. 2000. Role of frizzled 7 in the regulation of convergent extension movements during gastrulation in Xenopus laevis. Development 127:3091-3100.

Eid SR, Brändli AW. 2001. Xenopus Na,K-ATPase: primary sequence of the beta2 subunit and in situ localization of alpha1, beta1, and gamma expression during pronephric kidney development. Differentiation 68:115-125.

Eid SR, Terrettaz A, Nagata K, Brandli AW. 2002. Embryonic expression of Xenopus SGLT-1L, a novel member of the solute carrier family 5 (SLC5), is confined to tubules of the pronephric kidney. Int J Dev Biol 46:177-184.

Gordon MD, Nusse R. 2006. Wnt Signaling: Multiple Pathways, Multiple Receptors, and Multiple Transcription Factors. J. Biol. Chem. 281:22429-22433.

Grobstein C. 1953. Inductive epitheliomesenchymal interaction in cultured organ rudiments of the mouse. Science 118:52-55.

Grobstein C. 1955. Tissue disaggregation in relation to determination and stability of cell

type. Ann N Y Acad Sci 60:1095-1107.
Guo N, Hawkins C, Nathans J. 2004. Frizzled6 controls hair patterning in mice. Proc Natl Acad Sci U S A 101:9277-9281.
Helbling PM, Saulnier DM, Robinson V, Christiansen JH, Wilkinson DG, Brändli AW. 1999. Comparative analysis of embryonic gene expression defines potential interaction sites for Xenopus EphB4 receptors with ephrin-B ligands. Dev Dyn 216:361-373.
Helbling PM, Tran CT, Brändli AW. 1998. Requirement for EphA receptor signaling in the segregation of Xenopus third and fourth arch neural crest cells. Mech Dev 78:63-79.
Heller N, Brändli AW. 1997. Xenopus Pax-2 displays multiple splice forms during embryogenesis and pronephric kidney development. Mech Dev 69:83-104.
Heller N, Brändli AW. 1999. Xenopus Pax-2/5/8 orthologues: novel insights into Pax gene evolution and identification of Pax-8 as the earliest marker for otic and pronephric cell lineages. Dev Genet 24:208-219.
Hensey C, Gautier J. 1999. Developmental regulation of induced and programmed cell death in Xenopus embryos. Ann N Y Acad Sci 887:105-119.
Huang S, Johnson KE, Wang HZ. 1998. Blastomeres show differential fate changes in 8-cell Xenopus laevis embryos that are rotated 90 degrees before first cleavage. Dev Growth Differ 40:189-198.
Huelsken J, Behrens J. 2002. The Wnt signalling pathway. J Cell Sci 115:3977-3978.
Itoh K, Jacob J, S YS. 1998. A role for Xenopus Frizzled 8 in dorsal development. Mech Dev 74:145-157.
Kispert A, Vainio S, McMahon AP. 1998. Wnt-4 is a mesenchymal signal for epithelial transformation of metanephric mesenchyme in the developing kidney. Development 125:4225-4234.
Kleber M, Sommer L. 2004. Wnt signaling and the regulation of stem cell function. Curr Opin Cell Biol 16:681-687.
Kolm PJ, Sive HL. 1995. Efficient hormone-inducible protein function in Xenopus laevis. Dev Biol 171:267-272.
Ku M, Melton DA. 1993. Xwnt-11: a maternally expressed Xenopus wnt gene. Development 119:1161-1173.
Kuhl M, Geis K, Sheldahl LC, Pukrop T, Moon RT, Wedlich D. 2001. Antagonistic regulation of convergent extension movements in Xenopus by Wnt/beta-catenin and Wnt/Ca2+ signaling. Mech Dev 106:61-76.
Kuure S, Popsueva A, Jakobson M, Sainio K, Sariola H. 2007. Glycogen synthase kinase-3 inactivation and stabilization of beta-catenin induce nephron differentiation in isolated mouse and rat kidney mesenchymes. J Am Soc Nephrol 18:1130-1139.
Li L, Yuan H, Xie W, Mao J, Caruso AM, McMahon A, Sussman DJ, Wu D. 1999. Dishevelled proteins lead to two signaling pathways. Regulation of LEF-1 and c-Jun N-terminal kinase in mammalian cells. J Biol Chem 274:129-134.
Liao G, Tao Q, Kofron M, Chen JS, Schloemer A, Davis RJ, Hsieh JC, Wylie C, Heasman J, Kuan CY. 2006. Jun NH2-terminal kinase (JNK) prevents nuclear beta-catenin accumulation and regulates axis formation in Xenopus embryos. Proc Natl Acad Sci U S A 103:16313-16318.
Majumdar A, Vainio S, Kispert A, McMahon J, McMahon AP. 2003. Wnt11 and Ret/Gdnf pathways cooperate in regulating ureteric branching during metanephric kidney development. Development 130:3175-3185.
Malaterre J, Ramsay RG, Mantamadiotis T. 2007. Wnt-Frizzled signalling and the many paths to neural development and adult brain homeostasis. Front Biosci 12:492-

506.

Malik TH, Shivdasani RA. 2000. Structure and expression of a novel frizzled gene isolated from the developing mouse gut. Biochem J 349 Pt 3:829-834.

Maulet Y, Lambert RC, Mykita S, Mouton J, Partisani M, Bailly Y, Bombarde G, Feltz A. 1999. Expression and targeting to the plasma membrane of xClC-K, a chloride channel specifically expressed in distinct tubule segments of Xenopus laevis kidney. Biochem J 340 (Pt 3):737-743.

Maurus D, Heligon C, Burger-Schwarzler A, Brändli AW, Kuhl M. 2005. Noncanonical Wnt-4 signaling and EAF2 are required for eye development in Xenopus laevis. Embo J 24:1181-1191.

McGrew LL, Otte AP, Moon RT. 1992. Analysis of Xwnt-4 in embryos of Xenopus laevis: a Wnt family member expressed in the brain and floor plate. Development 115:463-473.

McMahon AP, Moon RT. 1989. Ectopic expression of the proto-oncogene int-1 in Xenopus embryos leads to duplication of the embryonic axis. Cell 58:1075-1084.

Meijer L, Skaltsounis AL, Magiatis P, Polychronopoulos P, Knockaert M, Leost M, Ryan XP, Vonica CA, Brivanlou A, Dajani R, Crovace C, Tarricone C, Musacchio A, Roe SM, Pearl L, Greengard P. 2003. GSK-3-selective inhibitors derived from Tyrian purple indirubins. Chem Biol 10:1255-1266.

Moody SA, Kline MJ. 1990. Segregation of fate during cleavage of frog (Xenopus laevis) blastomeres. Anat Embryol (Berl) 182:347-362.

Nusse R. 2005. Wnt signaling in disease and in development. Cell Res 15:28-32.

Piccolo S, Agius E, Leyns L, Bhattacharyya S, Grunz H, Bouwmeester T, De Robertis EM. 1999. The head inducer Cerberus is a multifunctional antagonist of Nodal, BMP and Wnt signals. Nature 397:707-710.

Raciti D. 2007. A large-scale gene discovery screen identifies over hundred solute carrier (SLC) genes with organ specific expression patterns in the *Xenopus* embryo. In: Department of Chemistry and Applied Biosceinces. Zürich: Swiss Federal Institute of Technology.

Reggiani L. 2007. Irx, Emx, and Sim transcription factors control distinct aspects of nephrogenesis in Xenopus. In: Department of Chemistry and Applied Biosciences. Zürich: Swiss Federal Institute of Technology.

Satow R, Chan TC, Asashima M. 2004. The role of Xenopus frizzled-8 in pronephric development. Biochem Biophys Res Commun 321:487-494.

Saulnier DM, Ghanbari H, Brändli AW. 2002. Essential function of Wnt-4 for tubulogenesis in the Xenopus pronephric kidney. Dev Biol 248:13-28.

Shi DL, Boucaut JC. 2000. Xenopus frizzled 4 is a maternal mRNA and its zygotic expression is localized to the neuroectoderm and trunk lateral plate mesoderm. Mech Dev 94:243-245.

Shi DL, Goisset C, Boucaut JC. 1998. Expression of Xfz3, a Xenopus frizzled family member, is restricted to the early nervous system. Mech Dev 70:35-47.

Stark K, Vainio S, Vassileva G, McMahon AP. 1994. Epithelial transformation of metanephric mesenchyme in the developing kidney regulated by Wnt-4. Nature 372:679-683.

Sumanas S, Ekker SC. 2001. Xenopus frizzled-5: a frizzled family member expressed exclusively in the neural retina of the developing eye. Mech Dev 103:133-136.

Sun TQ, Lu B, Feng JJ, Reinhard C, Jan YN, Fantl WJ, Williams LT. 2001. PAR-1 is a Dishevelled-associated kinase and a positive regulator of Wnt signalling. Nat Cell Biol 3:628-636.

Tada M, O'Reilly MA, Smith JC. 1997. Analysis of competence and of Brachyury autoinduction by use of hormone-inducible Xbra. Development 124:2225-2234.

Taira M, Otani H, Jamrich M, Dawid IB. 1994. Expression of the LIM class homeobox gene *XLIM-1* in pronephros and CNS cell lineages of *Xenopus* embryos is affected by retinoic acid and exogastrulation. Development 120:1525-1536.

Torban E, Dziarmaga A, Iglesias D, Chu LL, Vassilieva T, Little M, Eccles M, Discenza M, Pelletier J, Goodyer P. 2006. PAX2 activates WNT4 expression during mammalian kidney development. J Biol Chem 281:12705-12712.

Turner DL, Weintraub H. 1994. Expression of achaete-scute homolog 3 in Xenopus embryos converts ectodermal cells to a neural fate. Genes Dev 8:1434-1447.

van Amerongen R, Berns A. 2006. Knockout mouse models to study Wnt signal transduction. Trends Genet 22:678-689.

van Noort M, Meeldijk J, van der Zee R, Destree O, Clevers H. 2002. Wnt signaling controls the phosphorylation status of beta-catenin. J Biol Chem 277:17901-17905.

Veeman MT, Axelrod JD, Moon RT. 2003. A second canon. Functions and mechanisms of beta-catenin-independent Wnt signaling. Dev Cell 5:367-377.

Vize PD, Seufert DW, Carroll TJ, Wallingford JB. 1997. Model systems for the study of kidney development: use of the pronephros in the analysis of organ induction and patterning. Dev Biol 188:189-204.

Wallingford JB. 2004. Closing in on vertebrate planar polarity. Nat Cell Biol 6:687-689.

Wang Y, Macke JP, Abella BS, Andreasson K, Worley P, Gilbert DJ, Copeland NG, Jenkins NA, Nathans J. 1996. A large family of putative transmembrane receptors homologous to the product of the Drosophila tissue polarity gene frizzled. J Biol Chem 271:4468-4476.

Wang Y, Thekdi N, Smallwood PM, Macke JP, Nathans J. 2002. Frizzled-3 is required for the development of major fiber tracts in the rostral CNS. J Neurosci 22:8563-8573.

Wang YK, Sporle R, Paperna T, Schughart K, Francke U. 1999. Characterization and expression pattern of the frizzled gene Fzd9, the mouse homolog of FZD9 which is deleted in Williams-Beuren syndrome. Genomics 57:235-248.

Witta SE, Agarwal VR, Sato SM. 1995. XIPOU 2, a noggin-inducible gene, has direct neuralizing activity. Development 121:721-730.

Wolda SL, Moody CJ, Moon RT. 1993. Overlapping expression of Xwnt-3A and Xwnt-1 in neural tissue of Xenopus laevis embryos. Dev Biol 155:46-57.

Yang J, Tan C, Darken RS, Wilson PA, Klein PS. 2002. Beta-catenin/Tcf-regulated transcription prior to the midblastula transition. Development 129:5743-5752.

Yoshida Y, Kim S, Chiba K, Kawai S, Tachikawa H, Takahashi N. 2004. Calcineurin inhibitors block dorsal-side signaling that affect late-stage development of the heart, kidney, liver, gut and somitic tissue during Xenopus embryogenesis. Dev Growth Differ 46:139-152.

3.4. Non-canonical Wnt-4 signaling and EAF2 are required for eye development in *Xenopus laevis*

Daniel Maurus[1], Christophe Héligon[2], Anja Bürger-Schwärzler[1], André W. Brändli[2], and Michael Kühl[1]*

1 Department of Biochemistry, University of Ulm, Albert-Einstein-Allee 11, D-89081 Ulm, Germany

2 Institute of Pharmaceutical Sciences, Department of Chemistry and Applied Biosciences, Swiss Federal Institute of Technology Zürich, Wolfgang-Pauli-Strasse 10, CH-8093 Zürich, Switzerland

* Author for correspondence:
Michael Kühl
Abt. Biochemie
Universität Ulm
Albert-Einstein-Allee 11
D-89081 Ulm
Germany
Phone: ++49-731-50023283
Fax: ++49-731-50023277
Email: michael.kuehl@medizin.uni-ulm.de

Abstract

Wnt-4 is expressed in developing neural and renal tissue and is required for renal tubulogenesis in mouse and *Xenopus*. The function of Wnt-4 in neural differentiation is unknown so far. Here we demonstrate that Wnt-4 is required for eye development in *Xenopus laevis*. This effect of Wnt-4 depends on the activation of a β-catenin independent, non-canonical Wnt signaling pathway. Furthermore, we report the identification of EAF2, a component of the ELL-mediated RNA polymerase II elongation factor complex, as a target gene of Wnt-4 signaling. EAF2 is specifically expressed in the eye and EAF2 expression was dependent on Wnt-4 function. Loss of EAF2 function results in loss of eyes and loss of Wnt-4 function could be rescued by EAF2. In neuralized animal caps, EAF2 has properties characteristic for an RNA polymerase II elongation factor regulating the expression of the eye specific transcription factor Rx. These data add a new layer of complexity to our understanding of eye development and give further evidence for the importance of non-canonical Wnt pathways in organ development.

Introduction

Specification of cells during development becomes evident by differential gene expression and is regulated by extracellular growth factors. Wnt proteins form a family of secreted glycoproteins which can activate different intracellular signaling pathways. The canonical Wnt/β-catenin pathway involves stabilization of cytoplasmic β-catenin, which can act as a transcriptional co-activator (Logan and Nusse, 2004). Non-canonical Wnt pathways are per definition independent of β-catenin signaling (Kühl et al., 2000a, Veeman et al., 2003). These pathways involve activation of calcium-sensitive enzymes like protein kinase C and calcium calmodulin-dependent kinase II or activation of Jun-N-terminal kinase (JNK) through members of the rho family of small GTPases. This latter pathway is also known as planar cell polarity pathway which is involved in *Drosophila* epithelial cell polarity as well as *Drosophila* eye development (Mlodzik, 1999). In vertebrates, non-canonical Wnt signaling is activated by Wnt-5A, Wnt-11, and Wnt-4 (Du et al., 1995) and regulates dorso-ventral patterning of the embryo, cell migration, and heart development (Veeman et al., 2003). In *Xenopus*, mouse, and chicken embryos Wnt-4 is expressed in distinct expression domains in neural tissues as well as the developing excretory system (McGrew et al., 1992, Parr et al., 1993, Hollyday et al., 1995, Saulnier et al., 2002). Loss of function studies have shown that Wnt-4 is required for kidney organogenesis in mouse and *Xenopus*. Wnt-4 has also been linked to axonal pathfinding in rat embryos (Lyuksyutova et al., 2003). The role for Wnt-4 in regulating gene expression during neural differentiation, however, is poorly defined so far.

The eye derives from anterior neural tissue, the forebrain. The early eye field is characterized by expression of several marker genes including the homeobox transcription factor Rx and the paired box transcription factor Pax-6. During neurulation this initially continous eye field is divided resulting in two lateral expression domains of Rx and Pax-6 by a midline derived inhibitory signal. Pax-6, Rx, and other transcription factors expressed in the developing eye are thought to constitute a positive autoregulatory feedback loop (Zuber et al., 2003). However, upstream signaling pathways and growth factors that contribute to this feedback loop are not known. In a recent report, the Wnt receptor *Xenopus* Frizzled-3 (Fz-3) has been implicated in eye development suggesting that Wnt signaling might play a role during early eye development (Rasmussen et al., 2001). The Wnt ligand activating Fz-3 during eye development, however, is unknown so far.

As the neural functions of Wnt-4 have been poorly investigated to date, we aimed to i) uncover potential roles for Wnt-4 in neural patterning and ii) to identify downstream factors by which Wnt-4 can mediate its effects. Here, we show that Wnt-4 and its downstream factor EAF2 are required for eye development in *Xenopus laevis*. Furthermore, our data implicate non-canonical Wnt signaling in early eye development.

Results

Wnt-4 is required for eye development in Xenopus

During *Xenopus* embryogenesis, Wnt-4 expression starts at the onset of neurogenesis at stage 12,5-13 with two characteristic spots in the anterior brain region that persist until later stages (McGrew et al., 1992 and Fig. 1A-C). Whole mount in situ analyses using marker genes specific for the early eye field (Pax-6, Rx) or the midbrain marker Pax-2 indicate that Wnt-4 is expressed immediately adjacent to the early eye field (Fig. 1D-F) and marks the forebrain/ midbrain boundary. Additionally, Wnt-4 is expressed in the pronephros (Fig. 1C) as well as in the floor plate. To uncover a potential role of Wnt-4 during neural development we persued two independent strategies: We first performed neural specific loss of function analyses for Wnt-4 and, second, we aimed to identify genes that are transcriptionally upregulated by Wnt-4 in neuralized animal caps of *Xenopus* embryos.

In order to analyze the function of Wnt-4 in neural tissues we used a characterized Wnt-4 antisense morpholino oligo (Wnt-4 MO) that has previously been shown to interfere with translation of the endogenous Wnt-4 protein (Saulnier et al., 2002) and has been used to study the function of Wnt-4 during pronephros development. The Wnt-4 MO or a control MO were injected unilaterally into one dorsal-animal blastomere at the 8-cell stage to target the presumptive anterior neural region. 61% of Wnt-4 MO but not control MO injected embryos showed strongly reduced (35%) or absent eyes (26%) at stage 42 of development (Fig. 1 G,I,L) as judged by the size of the retinal pigment epithelium (RPE). This result was confirmed by histological sections (Fig. 1H,J). Whereas normally developed eyes have a multilayered structure, this is missing in Wnt-4 MO treated embryos on the injected side. As a complete loss of RPE is a simple and reliable way to monitor developmental eye defects we used this phenotype to analyze the outcome of further experiments described below. To rescue the Wnt-4 MO induced phenotype, we used an Activin-Wnt-4 fusion construct which consists of the activin derived propeptide and the mature Wnt-4 protein. The Wnt-4 MO does not target RNA coding for this fusion protein and after translation cleavage of the propeptide releases a mature and functional Wnt-4 protein (Saulnier et al., 2002). Coinjecting 50 pg of this RNA with Wnt-4 MO significantly reduced the number of embryos with eye defects on the injected side (Fig. 1K,L). In addition we overexpressed Wnt-4 RNA in dorsal-animal blastomeres of 8-cell stage embryos to analyze Wnt-4 gain-of-function embryos. Most of these embryos displayed defects in gastrulation movements as described earlier by others (Du et al., 1995). However, in rare cases (1-2%) embryos were obtained with ectopic eye structures (Fig. 1M) similar to those injected with the Wnt receptor Fz-3 (Rasmussen et al., 2001) or Pax-6 (Chow et al., 1999).

We next characterized the loss-of-function defects in eye development at the molecular level. Unilateral injection of Wnt-4 MO into dorsal-animal blastomeres resulted in a loss of Rx and Pax-6 expression at stages 13 /14 on the injected side (Fig. 1N-Q). This effect on gene

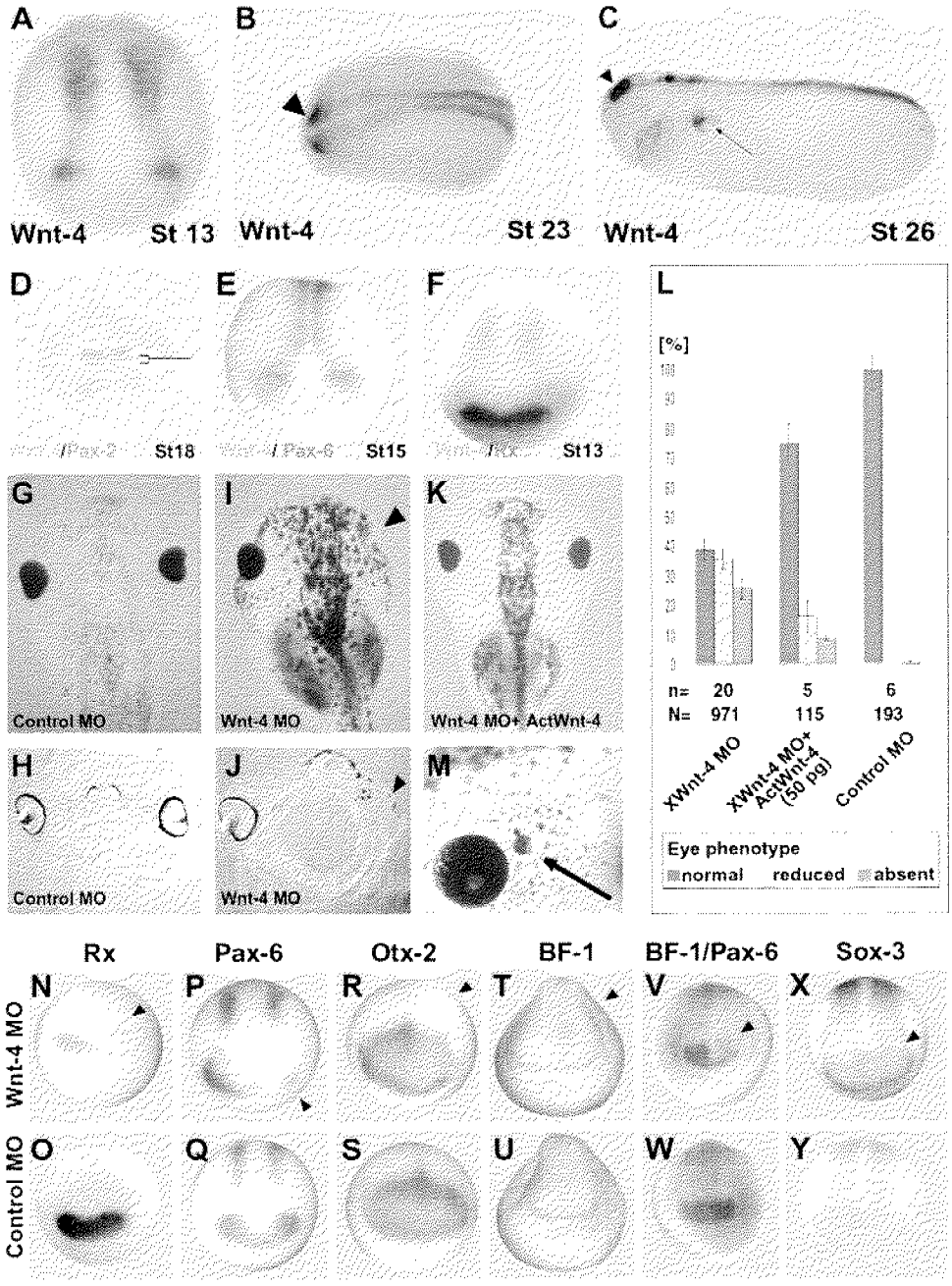
A
Wnt-4
St 13
B
Wnt-4
St 23
C
Wnt-4
St 26
D
St18
E
St15
F
St13
L
[%]
n= 20 5 6
N= 971 115 193
XWnt-4 MO
XWnt-4 MO+ ActWnt-4 (50 pg)
Control MO
Eye phenotype
normal reduced absent
G
Control MO
I
Wnt-4 MO
K
Wnt-4 MO+ ActWnt-4
H
Control MO
J
Wnt-4 MO
M
Rx
Pax-6
Otx-2
BF-1
BF-1/Pax-6
Sox-3
Wnt-4 MO
Control MO
N
P
R
T
V
X
O
Q
S
U
W
Y

Figure 1: Inhibition of Wnt-4 function by an antisense morpholino-oligonucleotide leads to loss of eye structures.
(A-C) Wnt-4 is expresssed in neural tissue as monitored by whole mount *in situ* hybridization of Xenopus laevis embryos of different stages as indicated. Expression of Wnt-4 in neural tissue starts at stage 13. Two characteristic spots in the anterior neural plate persist until later stages (arrowhead). Arrow in C: pronephros expression. (D-F) Mapping of the anterior most neural expression domain of Wnt-4. (D) Double in situ hybridization with the midbrain marker Pax-2, (E) the early eye field marker genes Pax-6 or (F) Rx indicate that Wnt-4 is expressed at the forebrain-midbrain boundary immediately caudally to the eye field. Bracket in (D) indicates the expression of Wnt-4 in the forebrain region that does not overlap with Pax-2. (G,I) Injection of a Wnt-4 MO but not a control MO interferes with eye development as judged by a loss of retinal pigment epithelium. (H,J) Sections of those embryos indicate the complete loss of eyes. (K) Co-injection of Wnt-4 MO and an Activin-Wnt-4 fusion is able to revert the phenotype in a significant manner. (L) Statistical evaluation of experiments. n= number of independent experiments, N = number of embryos scored. Error bars indicate standard error means. (M) Overexpression of Wnt-4 leads to development of ectopic eye structures in rare cases (Arrow). (N-Y) Wnt-4 MO or control MO unilaterally injected embryos were analyzed by whole mount *in situ* hybridization against Rx (N,O), Pax-6 (P,Q), Otx-2 (R,S), BF-1 (T,U), BF-1/Pax-6 simultaneously (V,W) or Sox-3 (X,Y). Loss of Wnt-4 function specifically leads to a loss of Rx and Pax-6 in the early eye field but not of Otx-2,BF-1 or Sox-3. Arrowheads in (I, J, N,P,R,T,V,X) indicate the injected side of the embryo.

expression was specific for Pax-6 and Rx expression as the fore- and midbrain marker gene Otx-2 or the forebrain marker BF-1 were not affected (Fig. 1R-U). Note that Otx-2 is not considered to be an eye marker gene at this stage of development (see Suppl. Fig. 1). Pax-6 expression in the spinal cord (Fig 1P,Q) and the expression of the pan-neural marker Sox-3 were not affected (Fig 1X,Y). These data indicate that Wnt-4 is specifically required for eye specific marker gene expression. At later stages, both the olfactory and the otic placode were established normally (data not shown). In addition, double in situ staining for Pax-6 and BF-1 revealed that a knock-down of Wnt-4 function interfered solely with Pax-6 expression (Fig. 1V,W). As a consequence, the possibility that the loss of eyes is due to defects in gastrulation movements can be excluded. Our findings thus clearly establish a specific requirement for Wnt-4 in early eye development of *Xenopus*.

Wnt-4 exerts its function through a non-canonical Wnt pathway

We next addressed the question of which intracellular signaling pathway is triggered by Wnt-4 during eye development. Wnt-4 has recently been suggested to activate β-catenin independent, non-canonical Wnt signaling pathways, which can be activated by a deletion mutant of dishevelled (dsh), dshΔDIX (Du et al., 1995, Boutros et al. 1998, Veeman et al., 2003). Co-injection of dshΔDIX RNA and Wnt-4 MO resulted in a significant reversal of the Wnt-4 MO phenotype (Fig. 2A,C,E). Injection of GFP RNA had no effect. In contrast, overexpression of β-catenin RNA can mimic signaling via the canonical Wnt/β-catenin pathway. Neural specific overexpression of β-catenin RNA was unable to rescue the Wnt-4 MO phenotype (Fig. 2A,B,E). As an early overexpression of β-catenin might interfere with aspects of early axial and neural

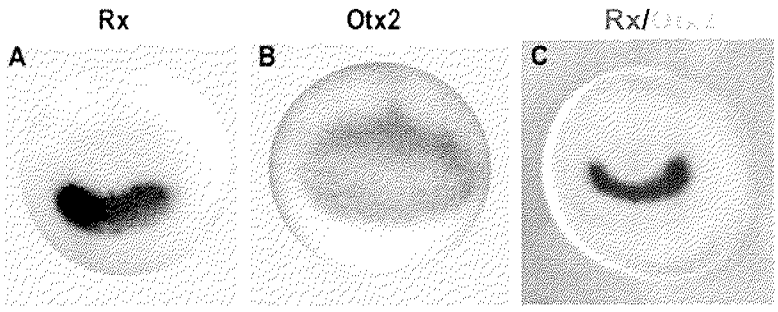

Supplementary Figure 1: Otx2 is a marker for fore- and midbrain at stage 14.
(A,B) Expression of Rx in the early eye field (A) and Otx2 in the fore- and midbrain region (B). Note the weaker expression of Otx2 in the region where Rx is expressed. (C) A double whole mount *in situ* hybridization for Rx and Otx2 at stage 14 is shown. Expression of Rx, an eye specific marker gene, is shown in blue, Otx2 is represented by the red color. Otx2 is not considered to be a eye specific marker gene at stage 14. Panels (A) and (B) are identical to (Figure 1 O and S) of the manuscript. At stage 23/24, however, Otx2 is highly expressed in the eye anlage (see Figure 6 J).

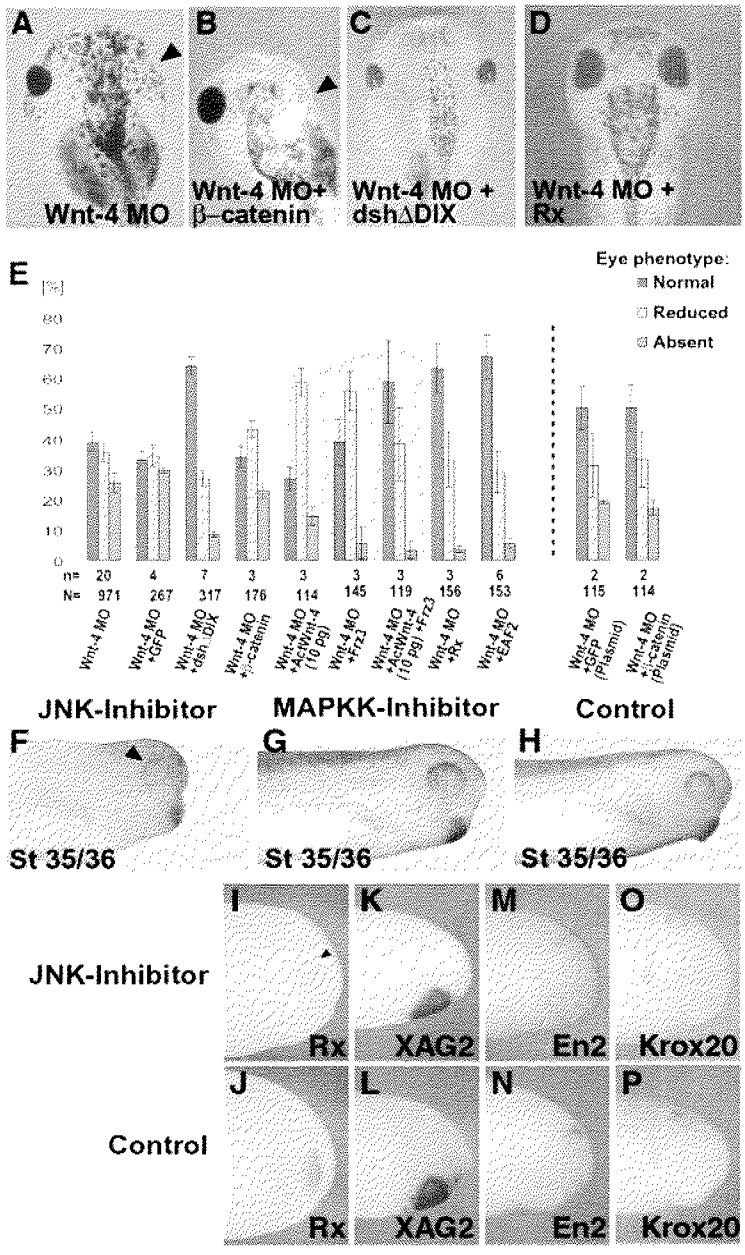

Figure 2: The effect of Wnt-4 is mediated through a β-catenin independent non-canonical Wnt pathway.
(A-C) Injection of dshΔDIX (C) but not β-catenin RNA (B) rescues the eye phenotype of Wnt-4 MO (A) injected embryos. (D) Injection of Rx RNA rescues the eye phenotype of Wnt-4 MO. Arrowheads indicate missing eyes. (E) To quantify the rescue experiments, embryos were characterized according to the phenotype observed as normal, reduced eye or absent eye. Mean values of n experiments are given. N = number of embryos scored. Error bars indicate standard error means. For the β-catenin DNA rescue experiments an independent set of Wnt-4 MO embryos is given for comparison. (F-H) Treatment of embryos with the JNK inhibitor SP600125 from stage 11-22 results in strongly reduced retinal pigment epithelium (arrow-head) at stages 35/36. (G,H) Treatment with the MAPKK inhibitor PD98059 does not affect eye development. (I-P) Marker gene analyzes of JNK inhibitor treated embryos by *in situ* hybridization (stage 24) using different marker genes as indicated.

patterning (Kieckers and Niehrs, 2001) we also overexpressesd β-catenin later in development by means of plasmid injections. CMV-driven β-catenin overexpression after onset of zygotic transcription (Stage 8) did not rescue the Wnt-4 MO phenotype (Fig. 2E). We therefore conclude that Wnt-4 signals through β-catenin independent signaling pathways.

Recently, Wnt-4 has been shown to activate Jun-N-terminal kinase JNK (Cai et al. 2002) as does dshΔDIX (Boutros et al. 1998). In support of a role for JNK activity in Wnt-4 induced non-canonical signaling, treatment of *Xenopus* embryos with the JNK inhibitor SP600125 but not an inhibitor against MAPKK during stages of early eye development (St. 11-22) resulted in a small eye phenotype at stage 30 (Fig. 2F-H). A molecular analysis of this phenotype revealed a downregulation of Rx expression at stage 24 whereas XAG2, a cement gland marker, En-2, a marker for the midbrain-hindbrain border, as well as Krox-20, a hindbrain marker, remained unchanged (Fig. 2I-P). Thus, these data indicate that Wnt-4 regulates eye development in *Xenopus* through a non-canonical Wnt pathway and implicate JNK to be involved in this pathway.

As Fz-3 has been implicated in eye development and in non-canonical Wnt signaling (Rasmussen et al., 2001), we tested whether Fz-3 RNA is able to rescue the Wnt-4 MO phenotype. Indeed, a low amount of Fz-3 RNA (10 pg) reduced the number of eyeless embryos but did not reduce the overall occurence of an eye phenotype. Interestingly, injection of a low dose of Act-Wnt-4 RNA (10 pg) had also only a modest rescueing activity. However, co-injection of Fz-3 a low dose of Act-Wnt-4 RNA (10 pg) synergistically rescued the Wnt-4 MO phenotype (Fig. 2E). Taken together, these data implicate Fz-3 in Wnt-4 mediated signaling.

Finally, we tested the ability of Rx as a potential downstream gene to rescue the Wnt-4 MO phenotype. Therefore we injected Rx RNA together with Wnt-4 MO and monitored eye development. Interestingly, injection of Rx RNA was able to significantly revert the Wnt-4 MO phenotype in *Xenopus* (Fig. 2A,D,E).

Identification of Wnt-4 downstream genes

We performed a PCR-mediated subtractive cDNA screen (Fig. 3) using the animal cap assay

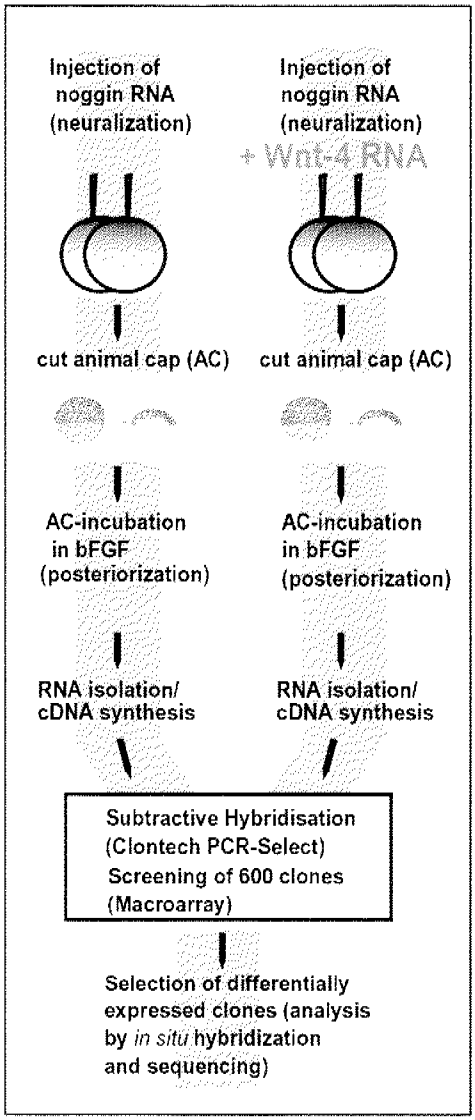

Figure 3: Identification of Wnt-4 target genes by subtractive cDNA cloning.

A Schematic drawing of the subtractive cDNA screen. Animal caps were treated either with noggin and FGF (left branch) or with noggin, FGF, and Wnt-4 (right branch) as indicated. RNA was isolated from these caps and enriched for those RNA species to be upregulated by Wnt-4 following the Clontech protocol. Of those clones obtained, 600 were spotted as a macroarray and rehybridized with radioactively labeled cDNA pools of both samples. Verified clones were sequenced and the spatio-temporal expression was determined by whole mount *in situ* hybridization. See Suppl. Table for a list of identified genes.

to elucidate in an alternative approach the role of Wnt-4 in neural patterning and to identify potential Wnt-4 downstream genes in neural tissue. Animal caps were neuralized by injecting noggin RNA into two cell stage *Xenopus* embryos. FGF was subsequently added to neuralized animal cap cultures resulting in caps expressing anterior as well as posterior neural marker genes. These noggin/FGF treated caps define the default state for the screen and we asked which genes are upregulated by overexpressing Wnt-4 by RNA co-injection into two-cell stage embryos. A subtractive cDNA library was constructed from treated animal caps when controls reached stage 22. This procedure results in a cDNA library consisting of cDNA clones likely to be enriched in the noggin/FGF/Wnt-4 pool versus the noggin/FGF pool. To eliminate false positive clones, inserts of 600 clones were PCR amplified, spotted onto nylon membranes and subsequently hybridized with radioactively labelled cDNA probes derived from both RNA pools. Using this experimental approach we identified 44 genes that were more highly expressed after treatment with Wnt-4. To narrow down the number of genes of potential interest, these clones were sequenced and their spatial expression patterns were determined by in situ hybridization techniques using *Xenopus* embryos at different developmental stages. A list of genes upregulated by Wnt-4 treatment in FGF/noggin treated animal caps is given in Suppl. Tab. 1.

Clone	Gene	GenBank Accession No.	Expression in Eye	Pro-nephros	Floor-plate
A1B	homology with MIZF (Hs)	XP_051422.1			
A1D	cytoskeletal actin type-5	M24769		+	
A3A	pescadillo	AAH43950	+	+	
A4A	XFDL 141	XLU65897			
A5E	homology with MGC68561 protein (Xl)	AAH59966.1			
A5F	homology with OST48 (Cf)	DOGOST48A			
A6B	gp96	AAO21339		+	
A6E	homology with prothymosin alpha (Mm)	NP_032998.1	+		
A7B	homology with presenilin enhancer2 (Dr)	BJ029038		+	
A7D	XTRAP-gamma subunit	AB058505		+	
A9B	homology with phosphoserine phosphatase (Hs)	NP_004568.1			
A9E	DUF87	AB004793	+	+	
A10C	FXR1	U25163			+
A10E	homology with annexin A2	BC046669	+		
B2C	homology with Solute carrier family 2 transporter (Gg)	NP_997061			
B4A	homology with CtBP	BC076800.1			
B9F	EAF2	AJ579576	+	+	
B10A	XHSP105	BC077316			
B12B	homology with MAPK7 (Xl)	BC077412.1			
B12D	XNCp120.1.2 isoform 1	AF150744.1			
C1G	XWSTF	AF412333	+		
D9E	XCHRAC17	AY271302.1	+		
E11F	YB3	X60217		+	

Supplementary Table 1: Genes identified to be upregulated by Wnt-4.
A list of genes is given that have been shown to be upregulated by Wnt-4 in noggin/FGF animal caps. Specific expression domains were determined by whole mount *in situ* hybridization and are indicated if the potential target gene is expressed in the floor plate or the pronephros, two sites of Wnt-4 expression, indicating the validity of the screen. Eye specific expression is indicated as well. Not all isolated genes revealed a specific expression pattern. This might be due to the relative small inserts in these clones. Additional 21 clones revealed no homology in a BLAST comparison and most likely represent untranslated and not well conserved regions. Accession numbers are given as well. Dr: *Drosophila melanogaster*, Mm: *Mus musculus*, Xl: *Xenopus laevis*, Gg: *Gallus gallus*, Cf: *Canis familiaris*.

EAF2 is a Wnt-4 downstream factor and a direct target of non-canonical Wnt signaling

One of the potential downstream genes identified in the screen is the *Xenopus* homolog of EAF2 (Fig. 4A), which is an ELL associated factor and part of the ELL mediated RNA polymerase II elongation factor complex (Li et al. 2003, Simone et al., 2003). In *Xenopus*, EAF2 is expressed maternally in a ubiquitous manner (data not shown). Tissue-specific, zygotic expression of EAF2 starts at stage 18.5 in the developing eye and the posterior neural plate (Fig. 4B). Additional specific expression domains include the pronephric tubule anlage, and at lower levels, the somites and the epiphysis (Fig. 4C,H). The lens does not express EAF2 (Fig. 4D). Parasagittal sections indicate that the expression of EAF2 in the eye is immediately adjacent to the expression of Wnt-4 in the posterior diencephalon at stage 18.5 (data not shown). In both cases, eye and pronephros, Wnt-4 expression timely preceeds that of EAF2 (see Fig. 4E-H for pronephros expression, compare Fig. 4B and 1A for anterior neural expression).

If EAF2 is indeed regulated by Wnt-4 *in vivo*, a loss of Wnt-4 function should result in a reduced or absent expression of EAF2. In Wnt-4 MO injected embryos, EAF2 gene expression is significantly downregulated as determined by semi-quantitative RT-PCR analyses (Fig. 5A). Targeted injections of Wnt-4 MO but not a control MO into single blastomeres, which contribute primarily to anterior neural tissue or the pronephros, indicate that expression of EAF2 in both organs depends on Wnt-4 (Fig. 5B-E). In addition, inhibiting JNK function by SP600125 treatment from stage 11-22 resulted in downregulation of EAF2 expression (Fig. 5F-H). We subsequently addressed the question whether EAF2 is a direct target gene of non-canonical Wnt signaling. Due to the lack of purified Wnt-4 we made use of characterized inducible Frizzled receptors encompassing extracellular and transmembrane domains of the β_2 adrenergic receptor (β_2AR) and intracellular loops of Frizzled receptors (Fig. 5I). These receptors can be stimulated or inhibited by β-adrenergic agonist (isoproterenol) or antagonists (propanolol), respectively. The β_2AR/Rfz-1 chimeric receptor couples to the Wnt/β-catenin pathway whereas the β_2AR/Rfz-2 chimeric receptor couples to non-canonical Wnt signaling (Liu et al., 1999, Liu et al., 2001, Kühl et al., 2000b). These receptors were stably transfected into human embryonic kidney cells (HEK293), challenged with isoproterenol or propanolol, and the expression of human EAF2 was monitored by RT-PCR. Interestingly, hEAF2 was induced by the activated β_2AR/Rfz-2 but not by the β_2AR/Rfz-1 chimeric receptor (Fig. 5J). Upregulation of EAF2 transcription was observed as early as 30 minutes after stimulation of the β2AR/Rfz-2 receptor (Fig. 5K). This

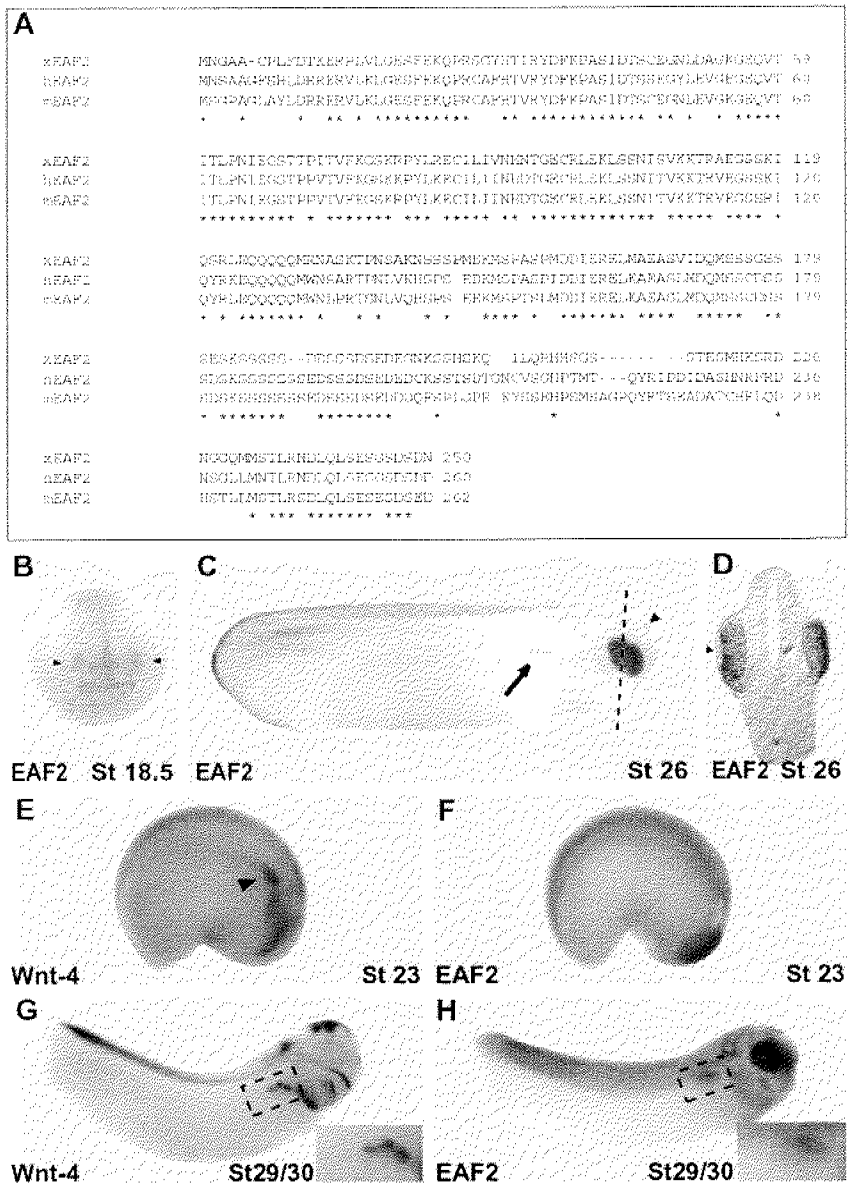

Figure 4: Sequence and expression of *Xenopus* EAF2.

(A) Xenopus EAF2 (xEAF2, GenBank Acc. # AJ579576) codes for a 250 amino acid protein with homologs in humans (hEAF2, GenBank Acc. # NP_060926) and mouse (mEAF2, GenBank Acc. # AAK59701). The amino acid identity between xEAF2 and hEAF2 and mEAF2 was calculated as 64% and 63%, respectively. Asterisks indicate conserved amino acids. (B) During Xenopus embryogenesis, EAF2 is expressed in the developing eye (arrow heads) as early as stage 18.5. (C) At stage 26, EAF2 expression is also detected in the pronephric tubule anlage (arrow) and faintly in the epiphysis (arrowhead). Dotted line indicates level of section shown in (D). (D) Transverse sections indicate that EAF2 is not expressed in the lens (arrowhead). (E-H) Wnt-4 and EAF2 are co-expressed in the pronephric anlage and in developing pronephric tubules. Wnt-4 (E,G) and EAF2 (F,H) transcripts were detected by whole-mount *in situ* hybridization. Embryos are shown in lateral views with anterior to the right and dorsal to the top. Insets show enlargements of the pronephric region. Wnt-4 expression is present in the pronephric anlage (E, arrowhead) of a stage 23 embryo whereas EAF2 expression is not yet detected at this stage (F). At stage 29/30, both Wnt-4 (G) and EAF2 (H) are expressed in the pronephric tubule anlage.

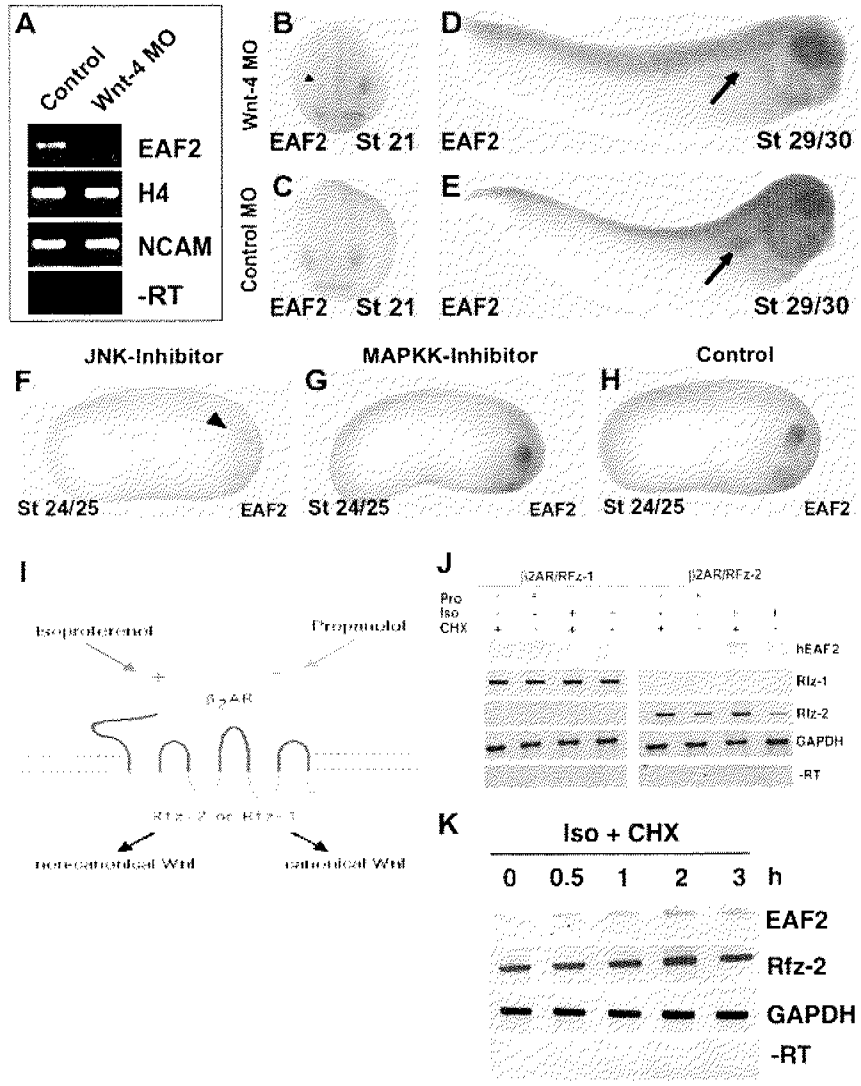

Figure 5: EAF2 is a direct target of non-canonical Wnt signaling.

(A) RT-PCR analysis demonstrate that EAF2 gene expression is downregulated in Wnt-4 loss-of-function embryos confirming the results obtained in the Wnt-4 gain-of-function screen. (B-E) Targeted injection of the Wnt-4 MO (B,D) but not a control MO (C,E) into blastomeres that will give rise to anterior neural tissue (B,C) or the pronephric kidneys (D,E), respectively, indicate that expression of EAF2 in these tissues depends on Wnt-4 gene function at stage 21 or stage 29/30, respectively. Arrowhead in (B) indicates missing expression of EAF2 in the eye anlage after Wnt-4 MO injection. Arrows in (D) and (E) highlight the pronephric anlage. (F-H) Treatment of embryos with the JNK inhibitor but not the MAPKK inhibitor from stage 11-22 leads to a downregulation of EAF2 expression in the eye at stage 24/25. (I) Schematic drawing of inducible Frizzled receptors and their signaling specificity as previously reported. (J) HEK293 cells were stably transfected with inducible β_2AR/Rfz-1 or β_2AR/Rfz-2 receptors, as indicated and verified by RT-PCR for Rfz-1 or Rfz-2 intracellular loops. Activation of β_2AR/Rfz-2 but not β_2AR/Rfz-1 by the β_2-adrenergic agonist isoproterenol (Iso) but not the antagonist propanolol (Pro) leads to activation of EAF2 gene expression as monitored by RT-PCR within 4 hours of treatment. Activation is resistant to treatment with cycloheximide (CHX) indicating that this activation is direct. GAPDH served as loading control. –RT: negative control. K, Time course of EAF2 activation after stimulation as indicated.

activation was resistent to treatment with cycloheximide, an inhibitor of eukaryotic translation. This indicates that activation of EAF2 transcription by a non-canonical Wnt pathway does not require intermediate protein translation and thus is a direct response to stimulation in the choosen cell line. In summary, we have identified EAF2 as a gene regulated by Wnt-4 activity in explant cultures and during embryonic organogenesis.

EAF2 is required for eye development in Xenopus laevis

Recently, it has been demonstrated that RNA polymerase II elongation factors like ELL, Foggy/ Spt5, or Pandora/Spt6 play important roles during development (Guo et al. 2000; Keegan et al. 2002; Eissenberg et al. 2002). We therefore asked, whether EAF2 is required for eye development. We first tested whether an EAF2 MO inhibits translation of EAF2 RNA (5'UTR+EAF2) in an *in vitro* transcription and translation assay (Fig. 6A). The EAF2 MO clearly blocked translation of EAF2 RNA whereas a control MO had no effect. An EAF2 control RNA construct lacking the 5'-UTR (Δ5'UTR+EAF2) was not targeted by the EAF2 MO and was therefore used for rescue experiments. We next injected the EAF2 MO into those blastomeres that will give rise to the eye region. Unilateral injection of EAF2 MO results in 50% of embryos with reduced or absent eyes on the injected side. Loss of complete eye structures was observed in 24% of the embryos (Fig. 6B-D) as judged by loss of RPE. The loss-of-eye phenotype could be rescued by co-injection of an EAF2 construct (Δ5'UTR+EAF2) that is not a target for the EAF2 MO whereas injection of RNA coding for GFP had no effect (Fig. 6D). Molecular analysis indicateed that EAF2 loss-of-function embryos display a loss of Rx, Pax-6, and Otx-2 expression in the eye region consistent with the morphological phenotype (Fig. 6E-J). As EAF2 expression in the eye starts at stage 18.5 we also analyzed expression of marker genes at earlier stages of development (St. 13/14). As expected, we did not observe an effect on marker gene expression at this stage implicating that EAF2 is involved in maintenance of eye specific marker gene expression. Interestingly, overexpression of EAF2 does not result in enlarged or ectopic eye structures (data not shown) implicating a permissive rather than an instructive function of EAF2 during eye development. Taken together, our data clearly indicate that EAF2 function is required for eye development and highlight an essential function of EAF2 during embryonic development. As EAF2 expression in the eye depends on Wnt-4 function and both, Wnt-4 MO and EAF2 MO injections result in the same phenotype, we next analyzed whether EAF2 RNA injection is sufficient to rescue the Wnt4 MO phenotype. Co-injection experiments clearly indicate that EAF2 can revert the effect elicited by Wnt-4 MO (Fig. 2E) indicating that both might act through a common downstream target.

EAF2 functions as an RNA polymerase II elongation factor

We next explored whether EAF2 indeed functions as a component of an RNA polymerase II elongation complex. To address this point, we adopted an established RNA polymerase II elongation assay to the *Xenopus* animal cap system (Guo et al., 2000). We focussed these

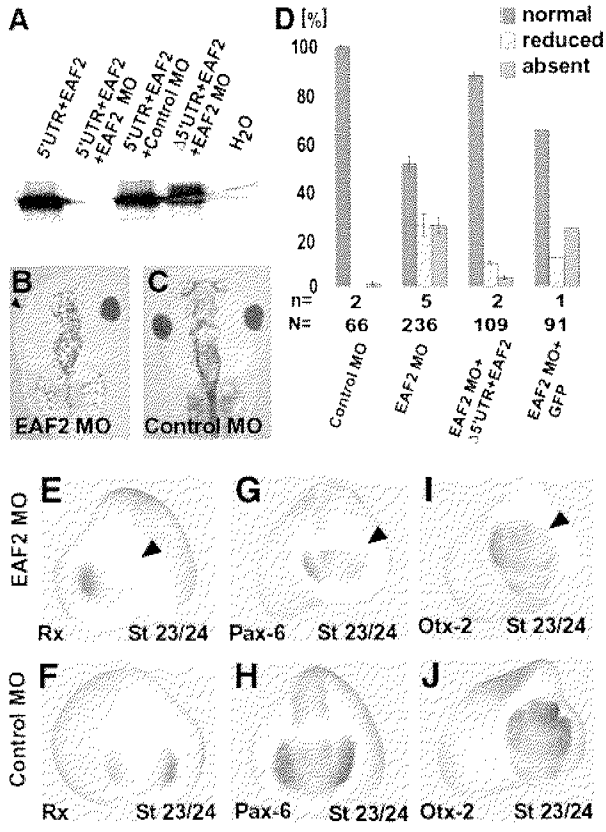

Figure 6: EAF2 is required for eye development.

(A) The EAF2 MO used inhibits translation of EAF2 RNA (5'UTR+EAF2), whereas the control MO does not. An EAF2 construct lacking the 5'UTR (Δ5'UTR+EAF2) is not targeted by the morpholino oligonucleotide. Data of transcription and translation assays resulting in production of [^{35}S]-labelled proteins are shown. (B,C) Unilateral injection of EAF2 MO but not control MO into dorsal animal blastomeres of 8-cell stage embryos results in loss of eyes as indicated by a loss of retinal pigment epithelium (arrow head). (D) Statistical evaluation of phenotypes observed. n = number of independent experiments, N = number of embryos scored. Error bars indicate standard error means. (E-J) Marker gene analysis for Rx, Pax-6 or Otx-2 expression as indicated by whole mount in situ hybridization of unilaterally EAF2 MO injected embryos (E,G,I) or control MO injected embryos (F,H,J). All three marker genes are downregulated in the developing eye. The arrowheads in panels (E,G,I) indicate the injected sides of the embryos.

experiments on the regulation of Rx transcription as Rx was able to rescue Wnt-4 MO injected embryos and Rx expression depends on Wnt-4, EAF2 and JNK. Due to RNA polymerase II pausing and template escape during transcription, a population of RNA transcripts is generated from the Rx gene locus that differs in RNA length in noggin neuralized animal caps. This can be shown by RT-PCR using primers specific for different regions of the generated RNAs (Figure 7A), i.e. the signal for a primer pair proximal to the transcription start site is stronger than the signal for more distal primer pairs although all of them show comparable signals on a DNA template. Overexpression of EAF2 in noggin neuralized caps led to an increase in signal strength for the distal primer, Rx(d) (Figure 7B). The signal for the proximal primer pair, Rx(p) remained unchanged, indicating that EAF2 indeed increases the number of Rx full length transcripts and thus likely functions as an RNA polymerase II elongation factor. This effect on Rx transcription was not observed when GFP RNA was overexpressed instead of EAF2 RNA. We also did not observe an effect of EAF2 on Pax-6 transcription (Figure 7B). This effect of EAF2 on Rx expression thus might explain why EAF2 is able to rescue the Wnt-4 MO phenotpype.

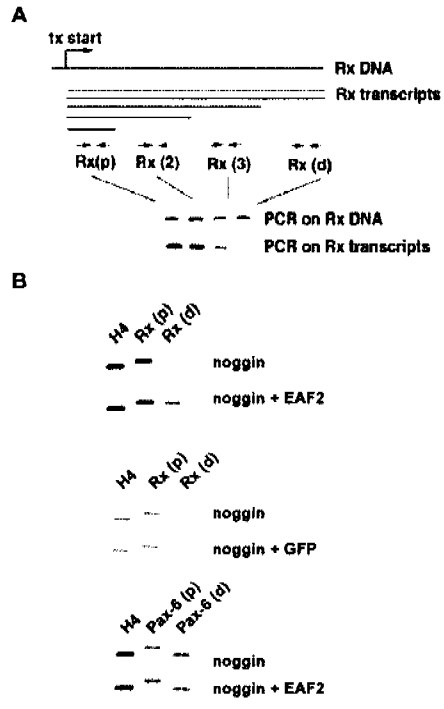

Figure 7: EAF2 has properties of an RNA polymerase II elongation factor.

(A) During transcription, RNA transcripts of different length are generated due to pausing and template escape as indicated in the schematic drawing. Relative occurence of Rx transcripts of different lenghts can be monitored by RT-PCR in noggin neuralized animal caps using different RT-PCR primer sets (Rx (p), Rx (2), Rx(3), Rx(d)). Tx: transcription start site. (B) Overexpression of EAF2 but not GFP RNA in noggin neuralized animal caps leads to an increase in full length transcripts as monitored by the distal Rx primer, Rx(d). H4 served as loading control. Transcription of Pax-6 was not affected by EAF2 overexpression.

Discussion

Detailed studies of transcription factors that are expressed at early stages of eye specification and morphogenesis of the eye have given us great insight into the molecular steps required for eye development (Chow and Lang, 2001). However, the molecular nature of growth factors involved in early eye development has remained largely unknown so far. We here report that Wnt-4 is required for early steps of eye development in *Xenopus laevis*. This finding is based on loss-of-function experiments with subsequent analyses of marker gene expression. Furthermore, our gain-of-function studies led to the identification of a novel Wnt-4 downstream factor, EAF2, which is specifically expressed in the developing eye and which is required for eye development. In this context, Wnt-4 acts through a non-canonical Wnt pathway that is independent of β-catenin but involves activation of JNK.

XWnt-4 is required for Xenopus eye development

Several transcription factors are known to pattern the anterior neural plate of vertebrate embryos and function in eye development (Zuber et al., 2003). These transcription factors regulate each others expression and form a network controling specification of eye fate. Expression of these genes occurs after neural induction but growth factors that initiate their expression or contribute to maintenance of expression are presently unknown. A similiar network of transcription factors is involved in specification of eye fate in *Drosophila,* where signaling by EGFR, Notch, Hedgehog and Wingless has been implicated in eye specification (Royet and Finkelstein, 1997). We have shown here that Wnt-4, a vertebrate member of the Wnt/wingless family of secreted glycoproteins, is required for eye development in a vertebrate embryo, *Xenopus laevis*.

Based on several observations our experiments suggest that Wnt-4 is required for maintenance rather than initial induction of eye specific marker genes. First, expression of Pax-6 or Rx in the anterior neural plate starts during gastrulation at stage 11-12 and is strongly upregulated at stage 12.5 (Zuber et al., 2003). However, neural Wnt-4 expression is not detectable until stage 12.5-13. Thus the initial expression of eye marker genes preceeds the expression of Wnt-4. Second, overexpression of noggin in animal caps was sufficient to induce Pax-6 and Rx in the absence of Wnt-4 expression further supporting the notion that Wnt-4 is not required for Pax-6 or Rx induction (data not shown). However, we observed a loss of Pax-6 and Rx expression in the prospective eye field as early as stage 13 in Wnt-4 MO injected embryos clearly indicating that Wnt-4 function is required at this stage and thus for maintenance of marker gene expression. In rescue experiments we were able to show that Rx is able to rescue the Wnt-4 MO phenotype, whereas initial experiments suggest that Pax-6 is unable to revert the Wnt-4 MO phenotype. Indeed, previous publications placed Rx upstream of Pax-6 in eye development (Zuber et al., 2003, Mathers et al., 1997, Zhang et al., 2000). $Rx^{-/-}$ mice do not develop an optic vesicle and lack expression of Pax-6 and Six-3 whereas $Pax\text{-}6^{-/-}$ mice develop an optic vesicle, which is however abnormally small and malformed (small eye phenotype). Our data implicate Rx as a target for Wnt-4 action which will require analyzes of the *Xenopus* Rx promoter. Experiments aimed at analyzing the *Xenopus* Rx promotor are currently under way.

The effect of Wnt-4 on eye development might be mediated by binding to the Wnt receptor Frizzled-3 (Fz-3). Fz-3 is expressed in the diencephalon and loss of function experiments reveal the requirement of Fz-3 for eye development and eye specific marker gene expression (Rasmussen et al., 2001). Just recently, Fz-3 has been shown to be functionally coupled to Wnt-4 during axonal pathfinding in the rat neural tube (Lyuksyutova et al., 2003). In addition, it has been suggested that Fz-3 is able to activate a non-canonical Wnt pathway (Rasmussen et al., 2001; Kühl et al., 2000a,b). This is consistent with our observation described above that Wnt-4 signals through non-canonical Wnt pathways during eye development and that low doses of Wnt-4 and Fz-3 synergistically rescue the Wnt-4 MO phenotype.

Strikingly, Wnt-4 knock out mice were reported to lack any obvious eye phenotype (Stark et al., 1994). It needs to be noted though that other Wnt members are co-expressed with Wnt-4 in the posterior diencephalon in mice (Parr et al., 1993) but not *Xenopus* (Wolda et al., 1992) including Wnt-7B. This Wnt member was reported not to fall into the class of Wnt proteins that act through β-catenin (Naylor et al., 2000). Accordingly, Wnt-7B was mentioned to activate a non-canonical Wnt signaling pathway (Rosso et al., 2005). Therefore, Wnt-7B may compensate for the loss of Wnt-4 in $Wnt\text{-}4^{-/-}$ mice.

Wnt-4 signals through a non-canonical Wnt pathway

Wnt-4 has recently been shown to act through activation of JNK (Cai et al., 2002) and thus through the Wnt/JNK pathway. Here we provide further evidence for the existence of a Wnt-

4 triggered Wnt/JNK signaling pathway as a deletion mutant of dsh, dshΔDIX, that has been shown to activate non-canonical Wnt and JNK signaling is sufficient to rescue the Wnt-4 MO phenotype. In addition, treatment of embryos with the JNK inhibitor SP600125 during stages of early eye development resulted in eye defects. Thus, a decrease in JNK signaling activity can phenocopy a Wnt-4 loss-of-function situation and activation of JNK signaling can revert the Wnt-4 MO phenotype. Taken together, these findings strongly indicate that Wnt-4 signals through JNK during eye development. This observation is further supported by the finding that $JNK1^{-/-}$, $JNK2^{+/-}$ mutant mice also display an eye phenotype with reduced Pax-6 expression although during later stages of eye development (Weston et al., 2003). In parallel we were able to exclude a role for Wnt/β-catenin signaling during these early stages of eye development as co-injection of Wnt-4 MO and β-catenin RNA or DNA did not rescue the eye specific phenotype. Further supporting our conclusion, Wnt-4 did not posteriorize neuralized animal caps whereas Wnt-3A and β-catenin did (data not shown). This however does not exclude the possibility that Wnt/β-catenin signaling might act at later stages of eye development, i.e. lens development, as recently suggested (Stump et al., 2003).

Non-canonical Wnt signaling has been shown to regulate cell migration processes, i.e. during gastrulation or migration of neuronal precursor cells (Veeman et al., 2003). These processes involve the transmembrane proteins strabismus or prickle to be part of a non-canonical Wnt signaling pathway resembling the *Drosophila* planar cell polarity pathway. However, when we injected a strabismus MO (Darken et al., 2002) into animal neural blastomeres we never observed the loss of eye phenotype which is characteristic for the Wnt-4 MO (data not shown). In addition, our marker gene analyzes also indicate that Wnt-4 MO injection into dorsal animal blastomeres does not interfere with cell movements. In summary, we conclude that the effect of neural Wnt-4 MO injections is on differentiation rather than cell migration.

Wnt-4 as a long range signaling molecule

Wnt-4 is expressed at the forebrain/midbrain boundary and its expression does not overlap with the primary eye field raising the question how Wnt-4 mediates its effect on eye development. As Wnts are lipid modified and as they strongly interact with proteoglycans (Logan and Nusse, 2004) it is widely assumed that they act as short range signaling molecules. However, recent findings also argue for a long range signaling activity of Wnts. Recently, it has been shown that Wnt-3A can induce β-catenin signaling with properties consistent as a long range signaling molecule (Kiecker and Niehrs, 2001) during anterior-posterior patterning of the neural tube. During inner ear development, Wnt-7A is also able to signal over a long distance (Dabdoub et al., 2003). Patterning of the somites occurs by Wnt proteins derived from the adjacent dorsal neural tube as well as the ectoderm at least in part through non-canonical Wnt signaling (Chen et al., 2004). Wnt-4 has also been implicated as a long-range signaling molecule during anterior-posterior guidance of commissural axons in rat embryos (Lyuksyutova et al., 2003). Consistent with this hypothesis, the *Drosophila* homolog wingless also can signal over long distance

(Neumann and Cohen, 1997, Zecca et al., 1996). Our finding that EAF2 can be regulated by Wnt-4 signaling, expression domains of both genes in neural tissue are just adjacent to each other, support the idea of Wnt-4 to signal as a long range molecule.

A potential function of RNA polymerase II elongation for eye development

Using a subtractive cloning strategy we identified EAF2 as a potential downstream factor in neural Wnt-4 signaling, which is known to interact in mammals with the RNA polymerase II elongation factor ELL. Within eucaryotes, several elongation factors exist that regulate the activity of RNA polymerase II. These elongation factors are regulated by interacting proteins and show some specificity with respect to the genes they regulate (Shilatifard et al., 2003). Interfering with RNA polymerase II elongation by specifically targeting individual components of elongation complexes thus might result in specific phenotypes during development. In *Xenopus*, EAF2 is highly enriched in the developing eye with lower expression in the pronephros, the epiphysis and the somites. This expression pattern is conserved between species as the mouse EAF2 homolog is expressed in the eye, the developing kidney and the somites as well (Li et al., 2003). Whether this reflects a conserved function of EAF 2 is currently unknown as knock-out mice for EAF2 are not available. On a functional level, our data demonstrate that EAF2 is essential for normal eye development as EAF2 regulates Rx expression.

How is the function of EAF2 coupled to the function of Wnt-4 during eye development? Whereas we observed a downregulation of eye specific marker genes after knock-down of Wnt-4 function as early as stage 13, eye specific expression of EAF2 starts not earlier than stage 18. Nevertheless EAF2 can rescue the phenotype observed after Wnt-4 MO treatment suggesting an identical molecular target. Indeed we were able to demonstrate that Rx can rescue the Wnt-4 MO phenotype whereas Rx itself is regulated by EAF2. This suggests that Wnt-4 is required for early aspects of eye development in the absence of EAF2 expression. Later, Wnt-4 induces EAF2 which itself is involved in maintaining the expression of eye specific marker genes in a stable feedback loop.

We also analyzed a potential function of EAF2 during pronephros development. Knock-down of pronephric EAF2 gene function resulted in abnormal pronephric development affecting however not only the EAF2 expressing tubules but also the pronephric duct (data not shown). Pronephric defects occurred with high frequency in conjuction with abnormal somitogenesis as revealed by marker gene analysis. As the paraxial mesoderm, which gives rise to the somites, is an important source of signals inducing pronephric development it is likely that the large-scale nature of the pronephric defects is a consequence of disrupting an earlier, EAF2-dependent step essential for paraxial mesoderm differentiation. This precludes at present a detailed analysis of EAF2 function in pronephric development.

In summary, our data provide a first example for a growth factor regulating the expression of an RNA polymerase II elongation factor component. Thereby we also add a new layer of

complexity on the regulation of gene expression by extracellular factors. Having established a link between non-canonical Wnt-4 signaling and EAF2 expression and function, our data also provide a new molecular mechanism how biological effects of non-canonical Wnt signaling might be mediated.

Material and Methods

Embryos

Xenopus embryos were obtained using standard procedures and staged according to Nieuwkoop and Faber (1967).

RNA transcription, microinjections and explant cultures

Capped RNAs were transcribed in vitro using the SP6 or T7 Message Machine Kit (Ambion). For the animal cap assay, embryos were injected at the 2-cell stage and caps were dissected at stage 8. The explants were cultured in LCMR (43 mM NaCl, 0.85 mM KCl, 0.37 mM $CaCl_2$, 0.19 mM $MgCl_2$, 5 mM HEPES pH 7.2) including 0,5% BSA and Penicillin/Streptomycin (Invitrogen, final concentrations: Penicillin 20 U/ml, Streptomycin 20 µg/ml) until uninjected control embryos reached stage 19/20. RNA amounts injected were: noggin 400 pg; XWnt-4 1000 pg. For FGF treatment, bFGF (Promega) was added at a concentration of 200 ng/ml. The JNK inhibitor SP600125 (Alexis) was used at a concentration of 12.5 µM consistent with the inhibitory function of this compound agains JNK in different cell based assays (Bennett et al., 2001). Optimal concentration and timing of inhibitor treatment was evaluated experimentally (see Suppl. Fig. 2). The MAPKK inhibitor PD98059 (Calbiochem) was used at 2 µM.

RNA isolation and RT-PCR analyses

Total RNA was isolated from explanted tissues using Purescript RNA Isolation Kit (Biozym) and subsequently analyzed by RT-PCR. First strand cDNA was synthesized according to the Invitrogen protocol using Superscript II reverse transcriptase. The PCR reaction mixtures were prepared using the Master Amp PCR Core Kit (Epicentre Technologies) and PCR was performed under standard conditions at 55°C annealing temperature. Primer sequences are given in Supplementary Material (Sup_4.pdf).

Whole mount in situ hybridization and histology

For the analyses of marker gene expression by whole mount in situ hybridization, embryos were injected unilaterally into one dorsal animal blastomere at the 8-cell stage and cultured until indicated stages. Embryos were fixed in MEMFA (0.1M MOPS (pH 7,4), 2mM EGTA, 1mM $MgSO_4$, and 4% formaldehyde) for 1.5-2 hours at room temperature, washed in 1X MEM solution and dehydrated in EtOH. Whole mount in situ hybridization was performed according

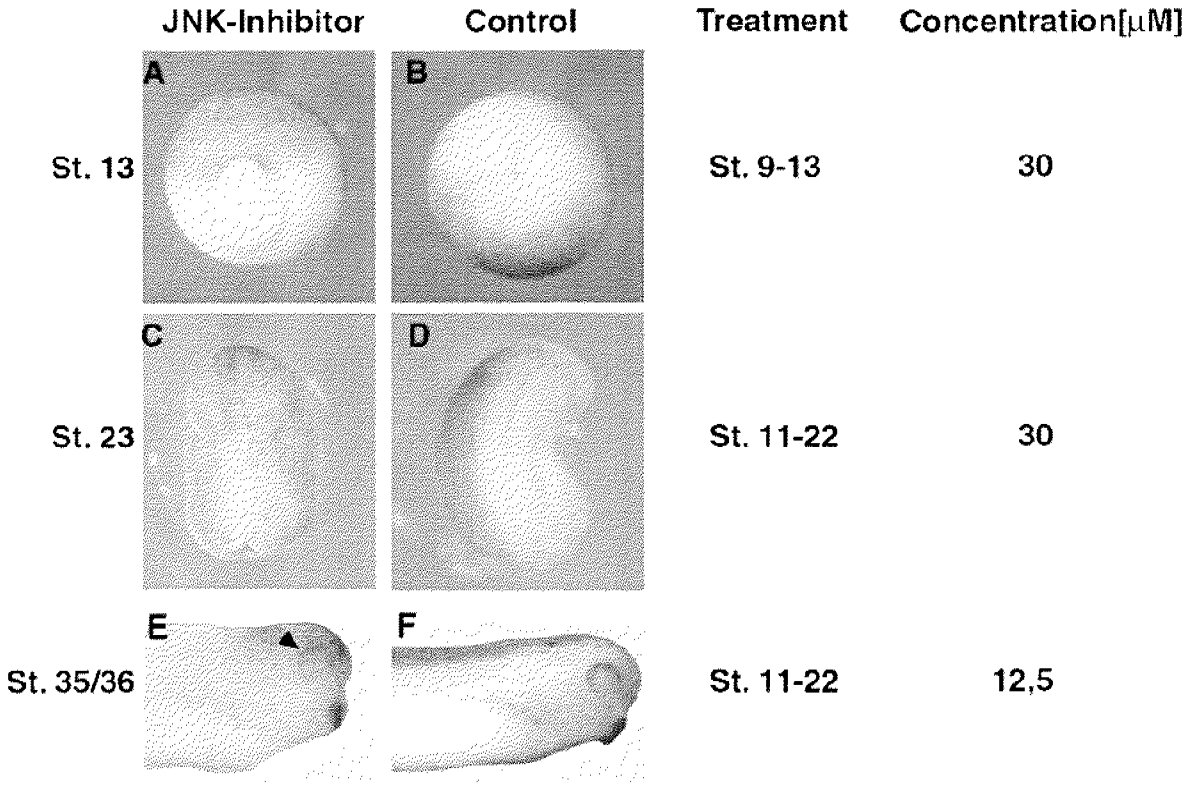

Supplementary Figure 2: The JNK inhibitor SP600125 elicits different phenotypes depending on concentration and timing of treatment.
Embryos were treated during different stages with different concentrations of SP600125 as indicated. (A,B) Treatment between stage 9 and 13 (30 µM) results in gastrulation defects at stage 13. (C,D) Treatment between stage 11 and 22 with a high concentration (30 µM) results in an open neural plate phenotype at stage 23. (E,F) Treatment with a lower concentration (12.5 µM) between stage 11 and 22 results in small eyes (arrow head) at stage 35/36. Panels (E) and (F) are identical to Figure 2 (F) and (H) of the manuscript.

to a standard protocol. For histology, embryos were refixed in MEMFA for 1-2h and embedded in gelatine/BSA. Vibratome sections were cut at 30µm thickness and coverglass mounted with 90% glycerol, 10% 0.1M Tris-Cl (pH 7,4).

Wnt- 4 and EAF2 antisense morpholino oligonucleotides (MO)

The Wnt-4 MO was used as published (Saulnier et al., 2002). A standard MO with the base composition 5'CCTCTTACCTCAGTTACAATTTATA-3' or a Wnt-4 4-base mismatch morpholino oligo (Saulnier et al., 2002) was used as a control. The EAF2 MO used was a 25-mer morpholino oligo with the base composition 5'-AGCTGCTCCATTCATCCTGCCGGCC-3'. The functionality of the EAF2 MO was tested using the transcription and translation assay TNT-Kit (Promega). The 5'UTR+EAF2 construct consists of the whole open reading frame and additional 10 bp of the 5'UTR. Those 10 bp are missing in the Δ5'UTR+EAF2 construct. Oligos were resuspended in sterile water and injected unilaterally into a single blastomere at the 8-cell stage in doses of 5 ng per embryo. One dorsal-animal blastomere was selected to target anterior neural tissue, while a ventral vegetal blastomere was selected to target the developing

pronephric kidney. For rescue experiments, 5 ng of Wnt-4 MO were injected together with different RNAs or DNA as indicated. Amounts of RNA were: dshΔDIX: 50 pg, β-catenin RNA: 150 pg, β-catenin DNA: 100 pg, EAF2: 1 ng, Activin-Wnt-4: 10 or 50pg, Fz-3: 10 pg, Rx: 200 pg, Pax-6: 200 pg. The β-catenin RNA induced secondary axes when overexpressed on the ventral side of 4-cell stage embryos indicating the functionality of the RNA used.

Subtractive cDNA Screen

In order to identify Wnt-4 downstream genes activated in neuralized animal caps we followed the protocols of the following Clontech kits: SMART PCR cDNA synthesis kit, PCR-Select cDNA subtraction Kit and PCR-Select Differential screening kit. The original identified EAF2 clone contained 950 bp of the 3'UTR and we completed the EAF2 sequence by a RACE procedure (GeneRacer Kit, Invitrogen). The 5' RACE primer used was: 5'-GAT CTG CCA GGC ACT GAG GGA ATT T-3' using an annealing temperature of 65°C resulting in a 1800 bp fragment with the 5'-UTR and the open reading frame. The full sequence of EAF2 was deposited under the accession number AJ579576. A related EST clone was found in the data base with the accession number CA988261 which likely represents an allelic variation.

RNA polymerase II elongation assay

For the RNA poylmerase II elongation assay animal caps were neuralized by injection of 400 pg of noggin RNA at 2 cell stage. Caps were cut at stage 8 and cultured until stage 20 in 1x MBSH (10 mM HEPES (pH 7.5), 88 mM NaCl, 2.5 mM KCl, 0.33 mM $Ca(NO_3)_2$, 0.41 mM $CaCl_2$, 0.82 mM $MgSO_4$, 2.4 mM $NaHCO_3$). Length of RNA transcripts was monitored by RT-PCR. Primer sequences are given in Supplementary Material.

Cell culture

Human embryonic kidney cells (HEK293) were stably transfected with expression plasmids coding for β_2AR/Rfz-1 or β_2AR/Rfz-2. Correct expression of these constructs was verified by RT-PCR using primers specific for Rfz-1 or Rfz-2 intracellular loops. To activate or inactivate these receptors, cells were treated with the β_2-adrenergic agonist isoproterenol (100 μM) or the β_2-adrenergic antagonist propanolol (30 μM) and gene expression was analyzed by RT-PCR. Primers are given in Supplementary Material. Cycloheximide was used at 500 ng/ml simultaneously to agonist/antagonist treatment. Functionality of the cycloheximide used was tested in a TNT assay.

Supplementary Materials and Methods

Primer sequences for RT-PCR analyses
The sequences of the oligonucleotide primers used for RT-PCR are the following: H4-F: CGG GAT AAC ATT CAG GGT ATC ACT, H4-R: ATC CAT GGC GGT AAC TGT CTT CCT, N-CAM-F: GCC CCT CTT GTG GAT CTT AGT GA, N-CAM-R: ACA GCG GCA GGA GTA GCA GTT C, Otx2-F: CCA GTC ATC TCG AGC AGC ACA, Otx2-R: CAG GAG GCC GTT TGG TCT TTG, En-2-F: ACC TTC ATC AGG TCC GAG ATC, En-2-R: CCG TCC TTT GAA GTG GTC GCC, Krox20-F: AAC CGC CCC AGT AAG ACC, Krox20-R: GTG TCA GCC TGT CCT GTT AG, Xlhbox9-F:GCC CCT GCG CAA TCT GAA C, Xlhbox9-F: CAG CAG CGG CTC AGA CTT GAG, EAF2_RT_L: 5'-TGT GAT GGA GGG AAA GGA TT -3', EAF2_RT_R: 5'- TGG AAA GTG AGT CAG CTA GCA A -3'.

Primer sequences for the RNA polymerase II assay
Length of RNA transcripts was monitored by RT-PCR using the following primer pairs: Rx(p)_L = RxeloRT1_L: 5'- ATT TGC AGC CTG CTC TGA CT -3', Rx(p)_R = RxeloRT1_R: 5'- TCC TGG ACT CCT GAG CAG AT -3', RxeloRT2_L: 5'- CAG AAG GAA CCG GAC AAC AT -3', RxeloRT2_R: 5'- TGG ATA AAG TTG GGG TGA GC -3', RxeloRT3_L: 5'- TTG GCA AGC CTT GGT AAA AC -3', RxeloRT3_R: 5'- AGA GAC CTG GCT TCA AGC TG -3', Rx(d)_L = RxeloRT4_L: 5'- TCA ACA ACA AGC TGC AGG AC -3', Rx(d)_R = RxeloRT4_R: 5'- CTG GGA TCC GTT ATC TGG AA -3', Xpax- 6_prox_L: 5'- AGG AAG GAG CAA GGA GGA AG –3', Xpax6_prox_R: 5'- CAT CTG CTG ATC AAC GCC TA – 3', Xpax6_dist_L: 5'- GTA AAT GGG CGG AGC TAT GA -3', Xpax6_dist_R: 5' - TGA TGC AGT CCT TCC AAC AG – 3'.

Cell culture
Primers used to monitor gene expression in HEK293 cells were: hEAF2_RT_L: 5'- CGA GCG GGT TCT CAA GTT AG -3', hEAF2_RT_R: 5'- GTC CTG GCT GAA TTC CAC AT -3', β2AR/Rfz1_F: 5'- GCG GAC ATG CGG CGA TTC AGC -3', β2AR/Rfz2_F: 5'- CGC GCC ATG CAG CGA TTC CGC -3', β2AR/Rfz1/2_R: 5'- GCG GTT GTC CTG GAT CAC GTG -3', GAPDH_L: 5'- AGC CAC ATC GCT TCA GAC ACC -3', GAPDH_R: 5'- GTA CTC AGC GGC CAG CAT CG -3'.

Acknowledgements

We thank Drs R.T. Moon, C. Niehrs, T. Pieler, C. Malbon, M. Andreazzoli, and T. Hollemann for providing cDNA clones. We also like to thank D. Weber, J. Brohl, P. Dietmann and M. Läsche for technical support and A. Nolte for sequencing. M.K. is supported by the Deutsche Forschungsgemeinschaft (SFB 497, Tp A6) and A.W.B. by the Swiss National Science Foundation (No. 3100A0-101964).

References

Bennett BL, Sasaki DT, Murra BW, O'Leary EC, Sakata ST, Xu W, Leistern JC, Motiwala A, Pierce S, Satoh Y, Bhagwat, SS, Manning AM, Anderson DW (2001) SP600125, an anthrapyrazolone inhibitor of Jun N-terminal kinase. *Proc Natl Acad Sci USA* **98**: 13681-13686

Boutros M, Paricio N, Strutt DI, Mlodzik M (1998) Dishevelled activates JNK and discriminates between JNK pathways in planar polarity and wingless signaling. ***Cell* 94**: 109-118

Cai Y, Lechner MS, Nihalani D, Prindle MJ, Holzman LB, Dressler GR (2002) Phosphorylation of Pax2 by the c-Jun N-terminal Kinase and Enhanced Pax2-dependent Transcription Activation. ***J Biol Chem* 277**: 1217-1222

Chen AE, Ginty DD, Fan CM (2004) Protein kinase A signaling via CREB controls myogenesis induced by Wnt proteins, Nature, Nov. 28, epub ahead of print

Chow RL, Lang RA (2001) Early Eye Development in Vertebrates. ***Annu Rev Cell Dev Biol* 17**: 255-296

Chow RL, Altmann CR, Lang RA, Hemmati-Brivanlou A (1999) Pax6 induces ectopic eyes in a vertebrate. ***Development* 126**: 4213-4222

Dabdoub A, Donohue MJ, Brennan A, Wolf V, Montcouquiol M, Sassoon DA, Hseih JC, Rubin JS, Salinas PC, Kelley MW (2003) Wnt signaling mediates reorientation of outer hair cell stereociliary bundles in the mammalian cochlea. ***Development* 130**: 2375-2384

Darken RS, Scola AM, Rakeman AS, Das G, Mlodzik M & Wilson PA (2002) The planar cell polarity gene strabismus regulates convergent extension movements in Xenopus. *EMBO J* **21**: 976-985

Du SJ, Purcell SM, Christian JL, McGrew LL, Moon RT (1995) Identification of Distinct Classes and Functional Domains of Wnts through Expression of Wild-Type and Chimeric Proteins in Xenopus Embryos. ***Mol Cell Biol* 15**: 2625-2634

Eissenberg JC, Ma J, Gerber MA, Christensen A, Kennison JA & Shilatifardi A (2002) dELL is an essential RNA polymerase II elongation factor with a general role in development. ***Proc Natl Acad Sci USA* 99**: 9894-9899

Guo S, Yamaguchi Y, Schilbach S, Wada T, Lee J, Goddard A, French D, Handa H & Rosenthal

A (2000) A regulator of transcriptional elongation controls neuronal development. ***Nature*** **408**: 366-369

Hollyday M, McMahon JA, McMahon AP (1995) Wnt expression patterns in chick embryo nervous system. ***Mech Dev*** **52**: 9-25

Keegan BR, Feldman JL, Lee DH, Koos DS, Ho RK, Stainier DYR & Yelon D (2002) The elongation factors Pandora/Spt6 and Foggy/Spt5 promote transcription in the zebrafish embryo. *Development* **129**: 1623-1632

Kiecker C, Niehrs C (2001) A morphogen gradient of Wnt/β-catenin signaling regulates anteroposterior neural patterning in Xenopus. ***Development*** **128**: 4189-4201

Kühl M, Sheldahl LC, Park M, Miller JR, Moon RT (2000a) The Wnt/Ca^{2+} Pathway a new vertebrate Wnt signaling pathway takes shape. ***Trends Genet*** **16**: 279-283

Kühl M, Sheldahl LC, Malbon CC, Moon RT (2000b) Ca^{2+}/Calmodulin-dependent Protein Kinase II is Stimulated by Wnt and Frizzled Homologs and Promotes Ventral Cell Fates in Xenopus. ***J Biol Chem*** **275**: 12701-12711

Li M, Wu X, Zhuang F, Jiang S, Jiang M & Liu YH (2003) Expression of murine ELL-associated factor 2 (EAF2) is developmentally regulated. ***Dev Dynam*** **228**: 273-280

Liu T, DeConstanzo AJ, Liu X, Wang H, Hallaghan S, Moon RT & Malbon CC (2001) G protein signaling from activated rat frizzled-1 to the beta-catenin-Lef-Tcf pathway. *Science* 292: 1718-1722

Liu X, Liu T, Slusarski DC, Yang-Snyder DC, Malbon CC, Moon RT & Wang H (1999) Activation of a frizzled-2/beta-adrenergic receptor chimera promotes Wnt signaling and differentiation of mouse F9 teratocarcinoma cells via Galphao and Galphat. *Proc Natl Acad Sci USA* **96**: 14383-14388

Lyuksyutova AI, Lu CC, Milanesio N, King LA, Guo N, Wang Y, Nathans J, Tessier-Lavigne M, Zou Y (2003) Anterior-posterior guidance of commissural axons by Wnt-frizzled signaling. ***Science*** **302**: 1984-1988

Mathers PH, Grinberg A, Mahon KA, Jamrich M (1997) The Rx homeobox gene is essential for vertebrate eye development. ***Nature*** **387**: 603-607

McGrew LL, Otte AP, Moon RT (1992) Analysis of Xwnt-4 in embryos of Xenopus laevis: A Wnt family member expressed in the brain and floor plate. ***Development*** **115**: 463-473

Mlodzik M (1999) Planar polarity in the Drosophila eye: a multifaceted view of signaling specificity and cross-talk. ***EMBO J*** **18**: 6873-6879

Naylor S, Smalley MJ, Robertson D, Gusteros BA, Edwards PAW, Dale TC (2000) Retroviral expression of Wnt-1 and Wnt-7b produces different effects in mouse mammary epithelium. ***J Cell Sci*** **113**: 2129-2138

Neumann CJ, Cohen SM (1997) Long-range action of Wingless organizes the dorso-ventral axis of the Drosophila wing. ***Development*** **124**: 871-880

Nieuwkoop PD, Faber J (1967) ***Normal table of Xenopus laevis (Daudin)***, North-Holland Publishing Company, Amsterdam, The Netherlands

Parr BA, Shea MJ, Vassileva G, McMahon AP (1993) Mouse Wnt genes exhibit discrete domains of expression in the early embryonic CNS and limb buds. ***Development*** **119**: 247-261

Rasmussen JT, Deardorff MA, Tan C, Rao MS, Klein PS, Vetter ML (2001) Regulation of eye development by frizzled signaling in Xenopus. ***Proc Natl Acad Sci USA*** **98**: 3861-3866

Rosso SB, Sussmann D, Wanshaw-Boris A, Salinas PC (2005) Wnt signaling through Dishevelled, Rac and JNK regulates dendritic development. ***Nature Neurosci.*** **8**: 34-42

Royet J and Finklstein R (1997) Establishing primordia in the Drosophila eye-antennal imaginal disc: the roles of decapentaplegic, wingless, and hedgehog. ***Development*** **124**: 4793-4800

Saulnier DME, Ghanbari H, Brändli AW (2002) Essential Function of Wnt-4 for Tubulogenesis in the Xenopus Pronephric Kidney. ***Dev Biol*** **248**: 13-28

Shilatifard A, Conaway RC & Conaway JW (2003) The RNA polymerase II elongation complex. *Annu Rev Biochem* **72**: 693-715

Simone F, Luo RT, Polak PE, Kaberlien JJ, Thirman MJ (2003) ELL-associated factor 2 (EAF2), a functional homolog of EAF1 with alternative ELL binding properties. ***Neoplasia*** **101**: 2355-2362

Stark K, Vainio S, Vassileva G, McMahon AP (1994) Epithelial transformation of metanephric

mesenchyme in the developing kidney regulated by Wnt-4. ***Nature*** **372**: 679-683

Stump RJW, Ang S, Chen Y, von Bahr T, Lovicu FJ, Pinson K, de Iongh RU, Yamaguchi TP, Sassoon DA, McAvoy JW (2003) A role for Wnt/β-catenin signaling in lens epithelial differentiation. ***Dev Biol*** **259**: 48-61

Veeman, MT, Axelrod, JD, Moon RT (2003) A Second Canon: Functions and Mechanisms of β-Catenin-Independent Wnt Signaling. ***Dev Cell*** **5**:367-77

Weston CR, Wong A, Hall JP, Goad MEP, Flavell RA, Davis RJ (2003) JNK initiates a cytokine cascade that causes Pax2 expression and closure of the optic fissure. ***Genes Dev*** **17**: 1271-1280

Logan CY & Nusse R (2004) The Wnt signaling pathway in development and disease. ***Annu Rev Cell Dev Biol*** **20**: 781-810

Wolda SL, Moon RT (1992) Cloning and developmental expression in Xenopus laevis of seven additional members of the Wnt family. ***Oncogene*** **7**: 761-766

Zecca M, Basler K, Struhl G (1996) Direct and long-range action of wingless morphogen gradient. ***Cell*** **87**: 833-844

Zhang L, Mathers PH, Jamrich M (2000) Function of rx, but not pax6, is essential for the formation of retinal progenitor cells in mice. ***Genesis*** **28**: 135-142

Zuber ME, Gestri G, Viczian AS, Barsacchi G, Harris WA (2003) Specification of the vertebrate eye by a network of eye field transcription factors. ***Development*** **130**: 5155-5167

4. Conclusions and perspectives

The present PhD thesis has focused on elucidating the role and mechanisms of Wnt/Frizzled signaling during pronephric kidney organogenesis during *Xenopus* development. I first identified fzd3, fzd6, and fzd8 as potential receptors for wnt proteins acting during pronephric development. My work also suggests crescent and sfrp2 as modulators of wnt signaling in proximal tubule development. I failed however to identify new wnt genes with expression in the pronephric kidney. However, it was recently demonstrated that wnt9a is expressed in the developing pronephric kidney (Garriock et al., 2007). Wnt9b has a similar temporal and spatial expression pattern as fzd6. Interestingly, the expression occurs also along the entire nephron from stage 29 onwards. My data indicates that fzd3 and fzd8 provide the necessary instructive signals to specify pronephric cells towards distinct pronephric tubule cell fates. The specification of proximal tubule cells depends on fzd3 function, while differentiation of intermediate, distal, and connecting tubules cells requires fzd8 gene function. Modulation of the activity of these genes affects the proximal, intermediate, distal, and connecting tubule cell populations. The signaling pathways mediating these effects could not be established with certainty. Nevertheless, the planar cell polarity pathway was necessary for the acquisition of terminal differentiation characteristics of the intermediate, distal, and connecting tubules cell populations. This suggests a requirement for fzd8/PCP signaling pathway in intermediate, distal, and connecting tubule maturation. In addition, active canonical Wnt pathway was able to both repress distal and promote proximal tubule cell fates.

4.1. Engineering of embryonic stem cells for stem cell-based therapy

The results reported above will be useful in future tissue engineering studies aiming to produce specific renal epithelial cell types for therapeutic applications. Indeed, embryonic stem (ES) cells could be engineered to conditionally express fzd3 or fzd8 under the control of inducible promoters. The engineered ES cells could then be differentiated *in vitro* to generate renal progenitors by treatment with retinoic acid, activin, and BMP7 (Kim and Dressler, 2005). The renal progenitor cells are expected to express renal marker genes such as expression of pax2, pax8, and lim1. Subsequently, these nephric cells could be specifically induced toward the proximal tubule or intermediate, distal, and connecting tubules fate by inducting fzd3 or fzd8 expression, respectively. Stimulation by soluble Wnt4 would then promote differentiation of Fzd3-expressing renal progenitor cells towards proximal tubules fates. Two therapeutic strategies could be envisaged. Either the $pax2^{+}$, $pax8^{+}$, $lim1^{+}$ renal progenitor cells are transplanted into patients suffering from tubular loss. In this case, Fzd gene expression could be induced *in vivo*. Nevertheless, *in vivo* accessibility of the inducer to the engineered cells might be limited. Thus, induction could be performed *in vitro* just before engraftment. It is anticipated that, the engrafted cells could contribute only to proximal or more distal tubule structures. In the last years, several groups have demonstrated the capacity of pluripotent stem cells to contribute to

kidney structures *in situ* (Mollura et al., 2003; Dekel and Reisner, 2004; Hammerman, 2004a; Hammerman, 2004b; Kim and Dressler, 2005). A more challenging *in vitro* approach would be to develop a fully differentiated organ fulfilling kidney functions or at least the filtration functions. Challenges inherent to *in vitro* kidney organ culture resides in the complexity of the organ itself. Kidneys are composed of several structures, such as the glomerulus and the nephron, which contain more than 20 different cell types organized in a precise three dimensional pattern. If kidneys could be developed *in vitro*, they could then be transplanted into patients. Interestingly, while this work provides tools to direct cells specification toward renal fate, other studies performed in the laboratory provide numerous molecular tools to characterize the induced organs (Raciti, 2007; Reggiani, 2007).

4.2. New avenues to study pronephric kidney development

The knowledge gained during my PhD studies provides a basis for further experiments aimed at understanding better pronephric development in further details. First, fzd6 expression during pronephros development coincides with the first signs of nephron epithelialization (Nieuwkoop and Faber, 1956; Vize et al., 2003). Unfortunately, we failed to identify a function for fzd6 in pronephros. Nevertheless, an alternative approach would be to deplete wnt9a from the pronephric lineage by injecting antisense MO targeted against *Xenopus* wnt9a. Afterwards, the resulting embryos could be analyzed for effects on pronephric development using the panel of marker genes described here. Furthermore, lab members have identified two transcription factors, sim2 and irx3, whose expression is dependent on fz8 gene function. Sim2 and irx3 function has been studied by other lab members (Bordoli, 2006; Regiani, 2007). They reported that irx3 regulates intermediate tubule specification. sim2 controls intermediate tubule compartment size. Thus, it would be interesting to determine whether sim2 and/or irx3 can partially rescue the phenotypes caused by fzd8 knockdown in the intermediate segment.

Follow up studies could be focused on defining the signaling relationships between wnt and notch signaling during nephron formation. Indeed, Notch signaling has been implicated in cell fate determination during both *Xenopus* pronephros and mouse metanephros tubulogenesis (McLaughlin et al., 2000; Taelman et al., 2006; Cheng et al., 2007). There Notch signaling functions to inhibit duct (intermediate, distal and connecting tubules) differentiation in the dorsoanterior region of the anlage where cells are normally fated to form (proximal) tubules. The transcription factor, ecotropic viral integration site 1 (evi1), has also been implicated in proximo-distal patterning of the pronephros and is repressed by Notch signaling (Van Campenhout et al., 2006). There, evi1 is required to promote distal tubules polarization. Thus, it is conceivable that evi1 is downstream of fzd8/PCP signaling in intermediate, distal, and connecting tubules. Hypothetically, fzd3 could promote notch signaling in the proximal segments, while fzd8 could inhibit Notch signaling from the intermediate and distal segments. A first step toward understanding Wnt/Notch relationship during pronephric kidney development in *Xenopus* would be to apply the same gain- and loss-of-function as well as pharmacological

pathways interference that I used in this thesis. Then, analyze the effects triggered on Notch signaling pathway components expression. It would also be possible to perform gain- and loss-of-function of notch genes and their receptors, delta and analyze effects on wnt4, fzd3, and fzd8 expression.

4.3. Development of Wnt signaling pathway reporter Xenopus lines

In order to better characterize the Wnt signaling pathways involved during pronephros development, I propose the development of transgenic *Xenopus* frog lines. Transgenic animals would be engineered to stably integrated genes encoding for fluorescent or enzymatic reporter genes under the control of appropriate Wnt signaling pathway-specific promoters. These tools would be valuable both to understand the endogenous pathways used during pronephric organogenesis and to characterize the effects triggered by gene function manipulations. To visualize the canonical Wnt pathway activity, the use a lef/tcf specific responsive promoter has been shown to be efficient (Korinek et al., 1997; Geng et al., 2003; Denayer et al., 2006). With regard to the calcium-dependent pathway, one could take advantage of NF-AT responsive elements (Szabo et al., 1993). Importantly, I would suggest the use of the diploid *Xenopus tropicalis* model organism instead of the historical pseudotetraploid *Xenopus laevis* species. Indeed, *Xenopus tropicalis* frogs need about three times less time to become adult and fertile. Thus, the generation time is shortened. Importantly, studies have shown that it is possible to use lef/tcf responsive elements to efficiently report canonical wnt signaling active areas in *Xenopus* embryos (Denayer et al., 2006). Notably, using this method wnt canonical activity was reported in the pronephros at stage 46. Nevertheless, the production of stable transgenic frog lines would ease functional experiments aimed to monitor changes in Wnt canonical signaling activities. Another line of research would be to identify target genes regulated during *Xenopus* pronephric kidney development by employing microarrays (Kimelman, 2006). One prerequisite is to be able to apply gain- and loss-of-function techniques in the context of an homogenous cell population. This can be achieved by the using pronephric the animal cap cultures (Asashima et al., 2000). Preliminary results indicate that both ectopic expression as well as loss-of-function of fzd3 led to an absence of proximal tubule marker genes expression in animal caps (C. Héligon, unpublished data). Several efforts have been directed towards the development of specific inhibitors of the canonical Wnt pathway (Lepourcelet et al., 2004). However to my knowledge, no molecule has entered clinical studies. It is of major scientific and therapeutic interest to carry on these efforts to develop drugs able to inhibit canonical Wnt signaling, which is implicated in numerous cancer types such as colon cancer carcinoma and mammary gland cancer (Brennan and Brown, 2004; Clevers, 2006).

4.4. Analysis of fzd3 function during *Xenopus* eye organogenesis

I have also demonstrated that wnt4 function is required during both pronephros and eye development upstream of EAF2 (Maurus et al., 2005). Interestingly, in both organs, fzd3 transcripts are detected (Shi et al., 1998). These observations suggest conservation of wnt4/ fzd3 signaling, both in pronephric kidney and eye development. In *Xenopus*, fzd3 function is sufficient to induce eye organogenesis (Rasmussen et al., 2001). Nevertheless, the precise role of fzd3 during eye organogenesis in *Xenopus* still remains to be established. Potentially, an antisense morpholino oligonucleotide strategy as described here could be used to elucidate fzd3 function during eye development.

4.5. Studies of fzd3 and fzd8 functions during *Xenopus* otic vesicle organogenesis

Overexpressions of fzd3 and fzd8 results in specific and distinct pronephric kidney defects, when the V2 blastomere was targeted in 8-cell stage embryos. Interestingly, when improper targeting happened into animal blastomeres, whose progeny give rise to the otic vesicle, I observed defects in the otic vesicle (C. Héligon, unpublished data). Using pax2 as a marker for the otic vesicle, I noticed that fzd3 overexpression led to formation of multiple smaller otic vesicles instead of one vesicle in control embryos. In contrast, fzd8 overexpression induced the formation of several ectopic otic vesicles without affecting the size of the endogenous one. In some cases, the ectopic vesicles were fused forming a line of fused circles. Taken together, this data suggests that fzd3 and fzd8 can trigger different cellular responses when expressed in otic vesicle precursor cells. Notably, fzd3 expression has been reported during otic vesicle formation (Shi et al., 1998). Furthermore, fzd3 and fzd6 double knockout mice lead to defects in inner hair cells polarity (Wang et al., 2006). Interestingly, we showed that fzd6 expression is highly expressed in the developing otic vesicle. Thus, one could speculate that fzd3 and fzd6 function during ear development is conserved in amphibians and mammals. Double knockdown strategies could be applied to the frog system to assess the degree of conservation of Wnt/Fzd signaling in amphibians. pax2, fzd6, gata3, gata4 as well as some slc genes could be used as marker genes (Raciti, 2007).

References

Asashima M, Ariizumi T, Malacinski GM. 2000. In vitro control of organogenesis and body patterning by activin during early amphibian development. Comp Biochem Physiol B Biochem Mol Biol 126:169-178.

Brennan KR, Brown AM. 2004. Wnt proteins in mammary development and cancer. J Mammary Gland Biol Neoplasia 9:119-131.

Cheng HT, Kim M, Valerius MT, Surendran K, Schuster-Gossler K, Gossler A, McMahon AP, Kopan R. 2007. Notch2, but not Notch1, is required for proximal fate acquisition in the mammalian nephron. Development 134:801-811.

Clevers H. 2006. Wnt/beta-catenin signaling in development and disease. Cell 127:469-480.

Dekel B, Reisner Y. 2004. Engraftment of human early kidney precursors. Transpl Immunol 12:241-247.

Denayer T, Van Roy F, Vleminckx K. 2006. In vivo tracing of canonical Wnt signaling in Xenopus tadpoles by means of an inducible transgenic reporter tool. FEBS Lett 580:393-398.

Garriock RJ, Warkman AS, Meadows SM, D'Agostino S, Krieg PA. 2007. Census of vertebrate Wnt genes: Isolation and developmental expression of Xenopus Wnt2, Wnt3, Wnt9a, Wnt9b, Wnt10a, and Wnt16. Dev Dyn 236:1249-1258.

Geng X, Xiao L, Lin GF, Hu R, Wang JH, Rupp RA, Ding X. 2003. Lef/Tcf-dependent Wnt/beta-catenin signaling during Xenopus axis specification. FEBS Lett 547:1-6.

Hammerman MR. 2004a. Growing new kidneys in situ. Clin Exp Nephrol 8:169-177.

Hammerman MR. 2004b. Organogenesis of kidneys following transplantation of renal progenitor cells. Transpl Immunol 12:229-239.

Kim D, Dressler GR. 2005. Nephrogenic factors promote differentiation of mouse embryonic stem cells into renal epithelia. J Am Soc Nephrol 16:3527-3534.

Kimelman D. 2006. Mesoderm induction: from caps to chips. Nat Rev Genet 7:360-372.

Korinek V, Barker N, Morin PJ, van Wichen D, de Weger R, Kinzler KW, Vogelstein B, Clevers H. 1997. Constitutive transcriptional activation by a beta-catenin-Tcf complex in APC-/- colon carcinoma. Science 275:1784-1787.

Lepourcelet M, Chen YN, France DS, Wang H, Crews P, Petersen F, Bruseo C, Wood AW, Shivdasani RA. 2004. Small-molecule antagonists of the oncogenic Tcf/beta-catenin protein complex. Cancer Cell 5:91-102.

Maurus D, Heligon C, Burger-Schwarzler A, Brändli AW, Kuhl M. 2005. Noncanonical Wnt-4 signaling and EAF2 are required for eye development in Xenopus laevis. Embo J 24:1181-1191.

McLaughlin KA, Rones MS, Mercola M. 2000. Notch regulates cell fate in the developing pronephros. Dev Biol 227:567-580.

Mollura DJ, Hare JM, Rabb H. 2003. Stem-cell therapy for renal diseases. Am J Kidney Dis 42:891-905.

Nieuwkoop PD, Faber J. 1956. Normal table of Xenopus laevis (Daudin): a systematical and chronological survey of the development from the fertilized egg till the end of metamorphosis.: North-Holland Publishing Company, Amsterdam.

Raciti D. 2007. A large-scale gene discovery screen identifies over hundred solute carrier (SLC) genes with organ specific expression patterns in the *Xenopus* embryo. In: Department of Chemistry and Applied Biosciences. Zürich: Swiss Federal Institute of Technology.

Rasmussen JT, Deardorff MA, Tan C, Rao MS, Klein PS, Vetter ML. 2001. Regulation of eye development by frizzled signaling in Xenopus. Proc Natl Acad Sci U S A 98:3861-

3866.

Reggiani L. 2007. Irx, Emx, and Sim transcription factors control distinct aspects of nephrogenesis in Xenopus. In: Department of Chemistry and Applied Biosciences. Zürich: Swiss Federal Institute of Technology.

Shi DL, Goisset C, Boucaut JC. 1998. Expression of Xfz3, a Xenopus frizzled family member, is restricted to the early nervous system. Mech Dev 70:35-47.

Szabo SJ, Gold JS, Murphy TL, Murphy KM. 1993. Identification of cis-acting regulatory elements controlling interleukin-4 gene expression in T cells: roles for NF-Y and NF-ATc. Mol Cell Biol 13:4793-4805.

Taelman V, Van Campenhout C, Solter M, Pieler T, Bellefroid EJ. 2006. The Notch-effector HRT1 gene plays a role in glomerular development and patterning of the Xenopus pronephros anlagen. Development 133:2961-2971.

Van Campenhout C, Nichane M, Antoniou A, Pendeville H, Bronchain OJ, Marine JC, Mazabraud A, Voz ML, Bellefroid EJ. 2006. Evi1 is specifically expressed in the distal tubule and duct of the Xenopus pronephros and plays a role in its formation. Dev Biol 294:203-219.

Vize PD, Woolf AS, Bard JBL. 2003. The kidney : from normal development to congenital disease. San Diego, Calif. London: Academic. xiii, 519 p. pp.

Wang Y, Guo N, Nathans J. 2006. The Role of Frizzled3 and Frizzled6 in Neural Tube Closure and in the Planar Polarity of Inner-Ear Sensory Hair Cells. J. Neurosci. 26:2147-2156.

5. Acknowledgments

I want to thank Prof. André Brändli for giving me the opportunity to work on exciting projects ranging from basic developmental biology to drug development. I am also grateful to him for his support, encouragements, and interest in my projects.

I am very grateful to Prof. Dario Neri for the knowledge I gained from the interesting meetings we had together and for accepting to be my co-examiner.

I want to thank Prof. Christoph Niehrs for accepting to be my co-examiner.

I would like to cordially thank all former and present lab members: Samer Eid, Hedhych Ghanbari, Roland Kälin, Vasili Dabouras, Daniela Raciti, Luca Regiani, Martin Kretz, Rita Lecca, Monica Walker, Titus Obanor, Mauro Imperiali, Florian Retchfeld, Andrea Meyer, Irena Senn, Astrid Subrizzi, Franziska Nötzli, Monika Hebeisen, Ivonne Miralles, Xavi Segui, Mattia Bordoli, and Francesca Bacchion. They all contributed in a way or another to my scientific and personal achievements.

I also thank the numerous people of the Institute of Pharmaceutical Sciences, especially from Prof. Wunderli's group for the nice atmosphere and their help and support.

I especially enjoyed sharing all these years in the lab with Daniela, Rita (also), Luca, Martin, Roland and Vasili. I learned a lot from them, in any situations.

I have special gratitude toward my-whole-PhD-colleague, Vasili. He is an exceptional person.

Finalement, je veux remercier ma famille :

Tout d'abord, mes parents, du plus profond de moi-même, pour leur soutient, leurs sacrifices et surtout leur amour.

Je dédie cette thèse à ma femme, Anne-Hélène, et ma fille, Maewenn, pour leur amour et pour toutes ces choses que l'ont partage au quotidien, qui me rendent heureux.

Curriculum vitae

Christophe HELIGON
15, rue Jean Moulin
F-68730 Blotzheim
France

e-m@il: christopheheligon@hotmail.com

Laboratory ☎ : +41-44-633 71 48 (Switzerland)
Cellphone ☎ : +33-6-89 55 62 27 (France)
French - 29 years - Married

EDUCATION

Dec. 2001 – May 2007 **PhD student in Biology**
Topic : **Wnt/Fzd signaling during pronephric kidney development**
Therapeutic Technologies group – Prof. Brändli
Swiss Federal Institute of Technology - Zürich (ETHZ, Switzerland)

2000 - 2001 **Master of Science in Biology and Health** (DEA)
Specialities : **molecular genetic and endocrinology** – Université de Rennes 1

1999 - 2000 **Bachelor of Science in Cellular Biology and Physiology**
Speciality : **molecular genetic** – Université de Rennes 1 (France)

1995 - 1998 **DEUG Life Sciences**– Université de Rennes 1 (France)
Specialities : **organic chemistry and microbiology**

1995 **High school scientific degree**

Languages **French**: native speaker
English: fluent
Spanish: read, written, spoken
German: basic knowledge

IT **IT manager for the Therapeutic Technologies group (2001-2007)**
MS Windows, Mac OS (9, X), LINUX
MS Office, LaTex, Adobe Creative Suite, Filemaker
HTML, FTP, Turbo Pascal

RESEARCH EXPERIENCES

2003 - 2004 **Collaboration with *The Genetics Company*, Schliren, Switzerland**
Project: Assays development and tests for in vivo validation of pharmaceutical lead compounds.

2000 - 2001 **Master's research project - CNRS unit #6026** – Université de Rennes 1
Topic: role of IGF-1R during the early development of xenopus embryos using morpholino oligonucleotides antisense strategy.

April to July 2000 **Bachelor's research project - CNRS unit #6026** – Université de Rennes 1
Topic: cloning and characterisation of Shc, an IRS-like molecule of *Xenopus laevis* oocytes.

AWARDS AND HONORS

Spring 2003 **Wander price for best oral presentation** at the "Doktorandentag" of the institute of pharmaceutical sciences of ETH Zürich.

OTHER

1995 to 1998 High school teaching.

Hobbies IT, Soccer, Fishing, 8-pool

PUBLICATIONS

2005 Ny A, Koch M, Schneider M, Neven E, Tong RT, Maity S, Fischer C, Plaisance S, Lambrechts D, **Heligon C**, Terclavers S, Ciesiolka M, Kalin R, Man WY, Senn I, Wyns S, Lupu F, Brandli A, Vleminckx K, Collen D, Dewerchin M, Conway EM, Moons L, Jain RK, Carmeliet P.
A genetic Xenopus laevis tadpole model to study lymphangiogenesis.
Nat Med (2005) 11:998-1004.

2005 Maurus D, **Heligon C**, Burger-Schwarzler A, Brandli AW, Kuhl M.
Noncanonical Wnt-4 signaling and EAF2 are required for eye development in Xenopus laevis.
Embo J (2005) 24:1181-1191.

2003 Chesnel F, **Heligon C**, Richard-Parpaillon L, Boujard D.
Molecular cloning and characterization of an adaptor protein Shc isoform from Xenopus laevis oocytes.
Biol Cell (2003) 95:311-320.

2002 Richard-Parpaillon L, **Heligon C**, Chesnel F, Boujard D, Philpott A. 2002.
The IGF pathway regulates head formation by inhibiting Wnt signaling in Xenopus.
Dev Biol (2002) 244:407-417.

Appendix

A genetic *Xenopus laevis* tadpole model to study lymphangiogenesis

A genetic *Xenopus laevis* tadpole model to study lymphangiogenesis

Annelii Ny[1,5], Marta Koch[1,5], Martin Schneider[1,5], Elke Neven[1,5], Ricky T Tong[2,5], Sunit Maity[1], Christian Fischer[1], Stephane Plaisance[1], Diether Lambrechts[1], Christophe Héligon[3], Sven Terclavers[1], Malgorzata Ciesiolka[1], Roland Kälin[3], Wing Yan Man[1], Irena Senn[3], Sabine Wyns[1], Florea Lupu[4], André Brändli[3], Kris Vleminckx[1], De´sire´ Collen[1], Mieke Dewerchin[1], Edward M Conway[1], Lieve Moons[1], Rakesh K Jain[2] & Peter Carmeliet[1]

[1]Flanders Interuniversity Institute for Biotechnology, Center for Transgene Technology and Gene Therapy, Campus Gasthuisberg O&N, Herestraat 49, KULeuven,
Leuven, B-3000 and Department of Molecular Biomedical Research, University of Ghent, Technology Park 927, Ghent, B-9052, Belgium.
[2]Harvard Medical School, Edwin L. Steele Laboratory for Tumor Biology, Department of Radiation Oncology, Massachusetts General Hospital, 55 Fruit Street, Boston, Massachusetts 02114, USA.
[3]Institute of Pharmaceutical Sciences, Department of Chemistry and Applied Biosciences, Swiss Federal Institute of Technology, Wolfgang-Pauli Strasse 10, HCI, CH-8057 Zurich, Switzerland.
[4]Cardiovascular Biology Research Program, Oklahoma Medical Research Foundation, 825 NE 13th Street, Oklahoma City, Oklahoma 73104, USA.
[5]These authors contributed equally to this work.

Correspondence should be addressed to P.C. (peter.carmeliet@med.kuleuven.be).

Nature Medicine **11**, 998 - 1004 (2005)

Abstract

Lymph vessels control fluid homeostasis, immunity and metastasis. Unraveling the molecular basis of lymphangiogenesis has been hampered by the lack of a small animal model that can be genetically manipulated. Here, we show that *Xenopus* tadpoles develop lymph vessels from lymphangioblasts or, through transdifferentiation, from venous endothelial cells. Lymphangiography showed that these lymph vessels drain lymph, through the lymph heart, to the venous circulation. Morpholino-mediated knockdown of the lymphangiogenic factor Prox1 caused lymph vessel defects and lymphedema by impairing lymphatic commitment. Knockdown of vascular endothelial growth factor C (VEGF-C) also induced lymph vessel defects and lymphedema, but primarily by affecting migration of lymphatic endothelial cells. Knockdown of VEGF-C also resulted in aberrant blood vessel formation in tadpoles. This tadpole model offers opportunities for the discovery of new regulators of lymphangiogenesis.

Introduction

Lymph vessels are involved in the absorption of fluid and fat, participate in inflammation and immunity and facilitate metastatic spread of tumor cells[1,2,3]. Insufficiency of lymph vessels results in lymphedema. Putative lymph vessels were documented as early as 1627 (ref. 4), yet lymphangiogenesis remains poorly understood for two reasons. First, the lack of specific markers precluded the identification of lymph vessels until recently. Second, researchers are lacking a small animal model that can be genetically manipulated to discover the function of novel lymphangiogenic candidates—similar to zebrafish for angiogenesis research[5]. Unfortunately, zebrafish lack a well-established lymphatic vasculature. Lizards and chick embryos have lymph vessels[6,7], but cannot be easily genetically manipulated. We therefore analyzed whether the frog might be useful for lymphangiogenesis research. Though the adult frog has lymph hearts[8,9], little is known about lymphatic development in the tadpole. In a few studies, dating from 1905 and earlier, the putative lymphatic network in tadpoles was visualized by injection of dyes[10,11]. But their 'true' molecular lymphatic identity was never established. Here, we characterized the *Xenopus* tadpole as a new genetic model to unravel the function of candidate genes involved in lymphangiogenesis.

Results

Development of the lymphatic vasculature in tadpoles

To identify lymph vessels, we stained *Xenopus laevis* tadpoles for Prox1, a transcription factor that is crucial for lymphatic commitment and selectively marks lymph but not blood vessels[12,13]. In the lymphatic system, Prox1 was expressed at three sites: the head where the rostral lymph sacs develop, the anterior trunk where the lymph hearts develop and the posterior trunk where the caudal lymph vessels form (Fig. 1a-d). These lymph vessels were distinct from blood vessels, which expressed typical blood vascular markers such as the mesenchyme-associated serpentine receptor (Msr)[14] (Fig. 1a-d) and the transcription factor Fli[15]. For clarity, a schematic overview of blood and lymph vessel development is shown in Figure 1e-h.

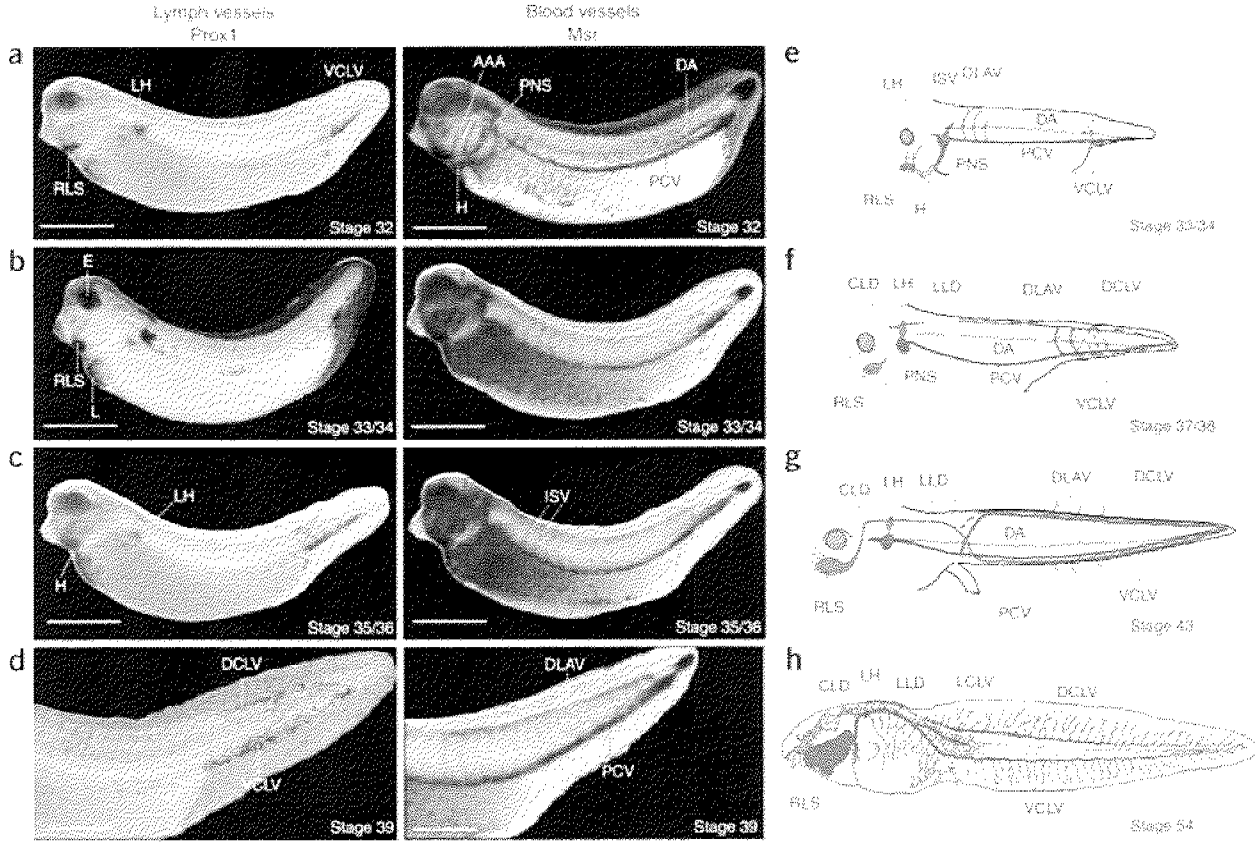

Figure 1. Expression of Prox1 and Msr in early tadpoles. (**a**–**d**) *In situ* hybridization for Prox1 (left panels) or Msr (right panels). Prox1 is expressed in the head where the rostral lymph sacs (RLS) develop; in the anterior trunk adjacent to the pronephric sinus (PNS), where the lymph hearts (LH) form; and in the posterior trunk, adjacent to the PCV where the VCLV forms. (**e**–**h**) Scheme of vascular development in tadpoles: veins shown in blue, arteries in red and lymph vessels in green. (**e**) At stage 33/34, lymphatic endothelial cells in the trunk region detach from the PCV to form the VCLV and migrate dorsally. (**f**) At stage 37/38, the RLS and LH enlarged, and the cephalic lymph duct (CLD) and lateral lymph duct (LLD) elongated from the LH into the head and trunk, respectively. In the posterior trunk, lymphatic cells at the dorsal roof coalesced into the DCLV. Additional lymphatic commitment sites emerged in the DLAV. (**g**) At stage 43, the RLS and periorbital lymph vessels drain, through the CLD, into the LH, which connects, through the PNS, to the venous circulation. In the trunk, the DCLV and VCLV are merging into the LLD, which drains into the LH. (**h**) Scheme of the lymphatic network at stage 54, adapted from ref. 10. The lymphatic network expands by sprouting in various regions. A superficial lymph vascular plexus gives rise to the LCLV. Scale bar in **a**–**c**, 1 mm; in **d**, 500 μm. H, heart; DA, dorsal aorta; PNS, pronephric sinus; ISV, intersomitic vessels; L, liver diverticle; AAA, aortic arch artery.

Development of rostral lymph sacs in tadpoles

From stage 28 onward, Prox1 was detectable in the head (Fig. 1a-c). Analysis of transverse sections of stage 30–32 tadpoles showed that cells in the lateral plate mesoderm adjacent to the cardiogenic region expressed Prox1 (Fig. 2a) and VEGFR-3 (Supplementary Fig. 1 online). These Prox1$^+$ cell clusters initially coexpressed Msr (Fig. 2a and Supplementary Fig. 1 online), indicating that they shared common markers with angioblasts. At later stages, the Prox1$^+$ cells became spatially restricted to the subectodermal regions, flanking the ventral aorta and heart tube, and progressively lost Msr expression (Supplementary Fig. 1 online). These lymphangioblasts could be clearly distinguished from angioblasts in the medially located cardiogenic region, which expressed only Msr and Fli but not Prox1 (Fig. 2a and Supplementary Fig. 1 online). Thus, putative lymphangioblasts, sharing a common origin with vascular progenitors, give rise to the embryonic anlage of the rostral lymph sacs.

Formation of lymph hearts in tadpoles

The second site of Prox1 expression was in the anterior trunk, where the lymph hearts develop (Fig. 1a-c). This is the region where, already by stage 30, VEGFR-2$^+$ angioblasts assemble into the anterior and posterior cardinal veins (PCV), which fuse into the pronephric sinus before draining through the common cardinal vein into the heart[15]. These vessels are the first lumenized venous structures and are perfused by stage 33/34, when the heart starts beating[16]. Endothelial cells at this site expressed Msr and Fli at stage 30, but initially no Prox1 (Fig. 1 and Fig. 2b). From stage 32 onward, some of these venous endothelial cells, particularly those at the dorsal margins, expressed Prox1 and VEGFR-3 and progressively lost Msr expression (Fig. 2b and Supplementary Fig. 1 online), indicating that they transdifferentiated to the lymphatic lineage. These lymphatic endothelial cells migrated to a more dorsolateral position, where they formed the lymph heart. From there, the cephalic lymphatic duct and lateral lymphatic duct extended in a posterior and anterior direction. At later stages, Prox1 was also expressed at the dorsolateral margin of the PCV at the midgut level, suggesting that venous-lymphatic transdifferentiation might also contribute to the formation of the lateral lymphatic duct (data not shown). Thus, development of these lymphatic structures occurred primarily through transdifferentiation of venous into lymphatic endothelial cells, similar to the mouse[12, 13].

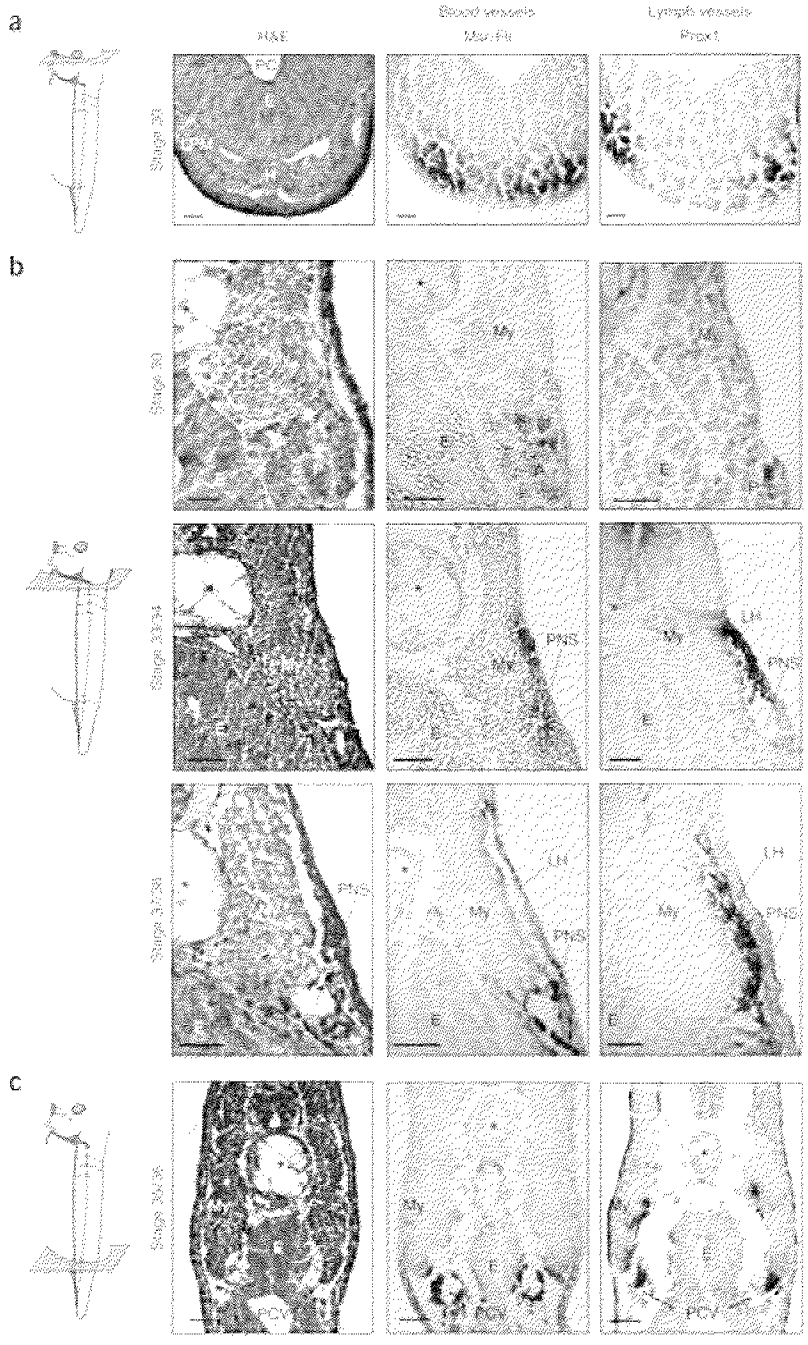

Figure 2. Development of the rostral lymph sac (RLS), lymph heart (LH) and caudal lymph vessels.

(**a**) Formation of RLS: at stage 30, putative lymphangioblasts in the lateral plate mesoderm (LPM), lateral to the heart (H) region, expressed Msr and Prox1. Msr was also expressed in the medial heart region. (**b**) Formation of the LH: at stage 30, Msr^+ angioblasts, which form the pronephric sinus (PNS), were present in the region dorsal to the pronephric tubule (P). Prox1 was only detectable in the pronephric tubule, but not in Msr^+ angioblasts. At stage 33/34, Fli was expressed in venous endothelial cells of the PNS and in $Prox1^+$ lymphatic endothelial cells of the LH. Only endothelial cells at the dorsal margin of the PNS expressed Prox1 and migrated dorsolaterally to form the LH. At this stage, only the PNS, but not the LH, acquired a lumen. At stage 37/38, endothelial cells of the LH expressed Prox1, but progressively lost Msr expression. (**c**) Formation of the caudal lymph vessels: by stage 35/36, Msr was expressed in the PCV, whereas $Prox1^+$ lymphatic endothelial cells migrated dorsally between the myotome (My) and endoderm (E) to form the prospective DCLV. Asterisk indicates notochord. Scale bar, 25 μm.

Development of the caudal lymph vessels in tadpoles

The third site of Prox1 expression in the early tadpole was in the posterior trunk at the level of the rectal diverticle—where the ventral caudal lymph vessel (VCLV) and dorsal caudal lymph vessel (DCLV) form (Fig. 1a-d). Beyond stage 24, VEGFR-2$^+$ endothelial cells in the anterior trunk assemble into paired PCVs, which subsequently extend to the tip of the tail by stage 33 (refs. 15,16). In the ventral region of the posterior trunk, where Msr$^+$ endothelial cells lined the PCVs (Fig. 1a-d), Prox1 was also detected by stage 32 (Fig. 1a). Sometimes, Prox1 was already detectable in endothelial cell clusters before the PCV had acquired a lumen, that is, in putative lymphangioblasts. Endothelial cells, lining the ventromedial PCV, expressed Prox1 (data not shown). These lymphatic cells detached from the PCV and formed initially a cord and subsequently a lumenized lymph vessel—the anlage of the VCLV (data not shown). Beyond stage 33/34, endothelial cells of the dorsal margin of the PCV also expressed Prox1 (Fig. 2c). These cells started to bud off from the PCV and to spread, in streaks, in a dorsal direction, through the somites and hindgut endoderm and near the neural tube (Fig. 2c and Supplementary Fig. 2 online). Budding and migration of Prox1$^+$ cells occurred in a polarized pattern. By stage 35/36, the lymphatic cells reached the dorsal roof, where they coalesced with neighboring cells into a longitudinal cord alongside the trunk axis. Lymphatic endothelial cells also migrated in the anterior and posterior direction. Lymphatic transdifferentiation initially occurred in the vicinity of the rectal diverticle, but subsequently also at more anterior and posterior locations. From stages 37/38 onward, endothelial cells of the dorsal longitudinal anastomosing vessel (DLAV), a vein draining blood to the heart[16], were also found to transdifferentiate into Prox1$^+$ cells (Supplementary Fig. 1 online). As a result, by stage 42, the ventral and dorsal Prox1$^+$ cords had extended in the anterior and posterior direction, thereby forming a lumenized VCLV and DCLV, respectively (Fig. 1d). These lymph vessels also expressed nuclear Prox1 protein (Fig. 3a) and VEGFR-3 (data not shown). Thus, venous endothelial cell transdifferentiation and lymphangioblast differentiation contributed to the formation of caudal lymph vessels.

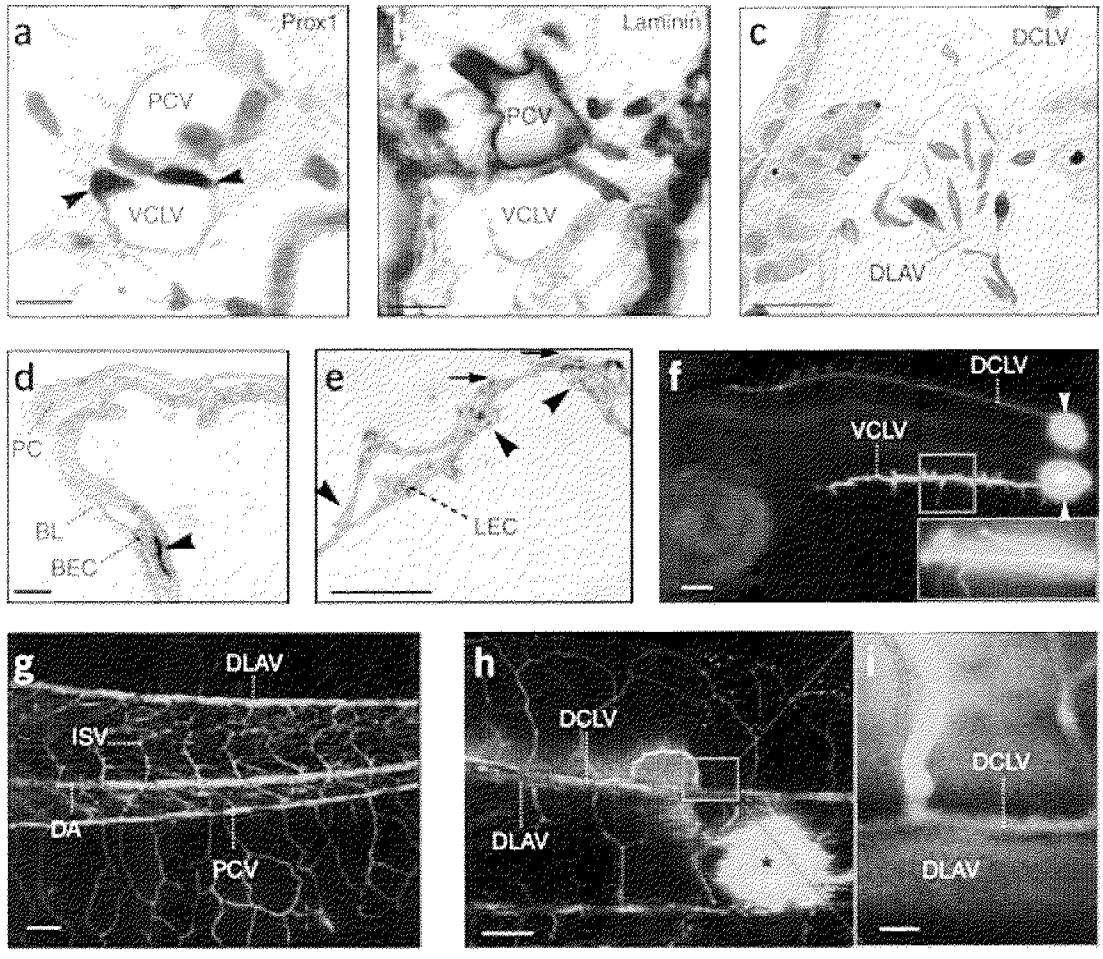

Figure 3. Lymphatic vascular development in tadpoles.

(**a**) Immunostaining of Prox1 in the VCLV but not the PCV. (**b**) Immunostaining of laminin, showing a basement membrane around the PCV but not the VCLV. (**c**) Semithin section, showing the DLAV with red blood cells and the adjacent DCLV. Scale bar in **a**–**c**, 10 μm. (**d**) Electron micrograph, showing a blood vessel consisting of blood vascular endothelial cells (BEC), which are interconnected by tight junctions (arrowhead) and covered by a pericyte (PC), all embedded in a basal lamina (BL). (**e**) In contrast, the VCLV contains thin elongated lymphatic endothelial cells (LEC) without adhesive junctions, basement membrane or pericyte coverage, but overlapping cell boundaries (arrowhead) and anchoring filaments (arrows). Scale bar in **d** and **e**, 1 μm. (**f**) Lymphangiography with FITC-dextran, showing the injection sites (arrowhead) and filling of the DCLV and VCLV in the tail trunk. Inset shows lymphatic sprouts, branching off from the large lymph trunk vessels. Scale bar, 250 μm. (**g**) Angiography with tetramethyl-rhodamine-dextran (red), showing the axial blood vessels, ISVs and side branches in stage 54 tadpoles. (**h**,**i**) Combined angiography with tetramethyl-rhodamine-dextran (red) and lymphangiography with FITC-dextran (green), showing the DLAV and DCLV. The asterisk denotes the injection site. Scale bar in **g** and **h**, 100 μm; in **i**, 20 μm.

Specificity of lymph vessel identity

Lymph vessels, unlike blood vessels, lack a basement membrane[1]. Consistent herewith, only the PCV, but not the VCLV, was immunoreactive for laminin (Fig. 3b). Endothelial cells in blood vessels were closely juxtaposed, surrounded by pericytes and formed tight intercellular junctions (Fig. 3c-d). In contrast, endothelial cells in lymph vessels were thin, elongated and irregular, had overlapping boundaries without well-established adhesive junctions, and lacked pericytes and a basement membrane, but instead had anchoring filaments (Fig. 3c,e). All these characteristics are typical features of lymph vessels, allowing intercellular transfer of fluids and macromolecules. Furthermore, we detected red blood cells in blood but not in lymph vessels (Fig. 3c and Supplementary Fig. 3 and Supplementary Movie 1 online). We further confirmed the identity of the lymph vessels by their weak expression of CD31 and von Willebrand factor (data not shown).

The lymphatic vasculature is functional

We determined whether lymph vessels in tadpoles were capable of draining interstitial fluid and macromolecules by subcutaneously injecting FITC-dextran into live tadpoles. In stage 46 tadpoles, both the DCLV and VCLV drained the dye in an anterior direction toward the beating lymph heart at a speed of ~100 μm/s, which is slower than red blood cell velocity in large blood vessels (1,370 ±196 μm/s in the DLAV; Fig. 3f). Side branches in the dorsal and ventral fin were also filled (Fig. 3f), suggesting that they lack functional valves at these junctions. By stage 54, tadpoles developed paired lateral caudal lymph vessels with many side branches (Supplementary Fig. 3 online). These lateral caudal lymph vessels were only visible when FITC-dextran was injected in the anterior but not in the posterior part of the tadpoles. The flow rate in lateral caudal lymph vessels is much slower than in the other two lymph vessels, at a speed of ~50 μm/min. We labeled the dorsal aorta, PCV, DLAV and intersomitic vessels (ISV) and side branches in the fins using angiography (Fig. 3g). Subsequent lymphangiography in the same tadpole showed that blood vessels and lymph vessels were distinct, nonoverlapping structures (Fig. 3h, i). Lymph vessels also drained dyes, which leaked out from blood vessels (Supplementary Fig. 3 online). Upon injection, FITC-dextran was transported to the lymph heart and ejected by these lymph hearts as jet-like streams through a set of valves into the pronephric sinuses (Supplementary Fig. 3 and Supplementary Movie 2 online). Generally, the lymphatic circulation was functional beyond stage 42.

Prox1 knockdown impairs lymphangiogenesis

To explore whether the tadpole model is useful to study the role of lymphangiogenic genes, we knocked down, as a positive control, the expression of Prox1, as it is a key regulator of this process[12,13]. Lymphatic endothelial cell differentiation and migration were scored by morphometrically measuring Prox1$^+$ 'area 1' and 'area 2' in the posterior trunk, which are ventral and dorsal, respectively, to the dorsal margin of the endoderm (Fig. 4a). Area 1 is a measure of lymphatic commitment and area 2 is a parameter of lymphatic endothelial cell budding, migration and sprouting; it also reflects branching of lymphatic endothelial cells into the DCLV. In addition, we measured the maximal distance over which lymphatic endothelial cells migrated from their ventral site of origin to their most dorsal position in the posterior trunk (Fig. 4a). Microscopic inspection of the posterior trunk showed that fewer Prox1$^+$ cells were present in Prox1 knockdown (Prox1^{KD}) tadpoles, injected with 25 ng morpholino (Fig. 4a and Supplementary Figs. 4 and 5 and Supplementary Note online). Morphometric analysis further indicated that knock down of Prox1 impaired lymphatic commitment in area 1 and migration of lymphatic endothelial cells into area 2 (Fig. 4b, c). By lymphangiography, lymph vessels in Prox1^{KD} tadpoles were underdeveloped, had a thin and irregular shape, were hypoperfused or even absent, and ruptured more easily upon dye injection (Fig. 4d). Moreover, compared to control tadpoles, more Prox1^{KD} tadpoles developed lymphedema by stage 45 (2% in controls versus 46% in Prox1^{KD}; $P < 0.001$ by chi-squared test; Fig. 4e). We also scored angiogenesis by counting the percentage of Msr$^+$ ISVs, reaching the dorsal roof, in the anterior trunk (stage 33/34) and by angiography (stage 45). Both in control and Prox1^{KD} embryos, a similar percentage of ISVs was completely formed by stage 33/34 (68 ±8% in controls versus 65 ±8% in Prox1^{KD} embryos). By angiography, blood vessels in Prox1^{KD} embryos formed normally in number, size, shape and pattern (Fig. 4f). Similar results were obtained when Prox1 expression was knocked down by a splice site-specific Prox1 morpholino (Supplementary Fig. 6 online). The selective lymphangiogenic but not angiogenic defects in Prox1^{KD} tadpoles phenocopy those observed in Prox1-null mice[12,13].

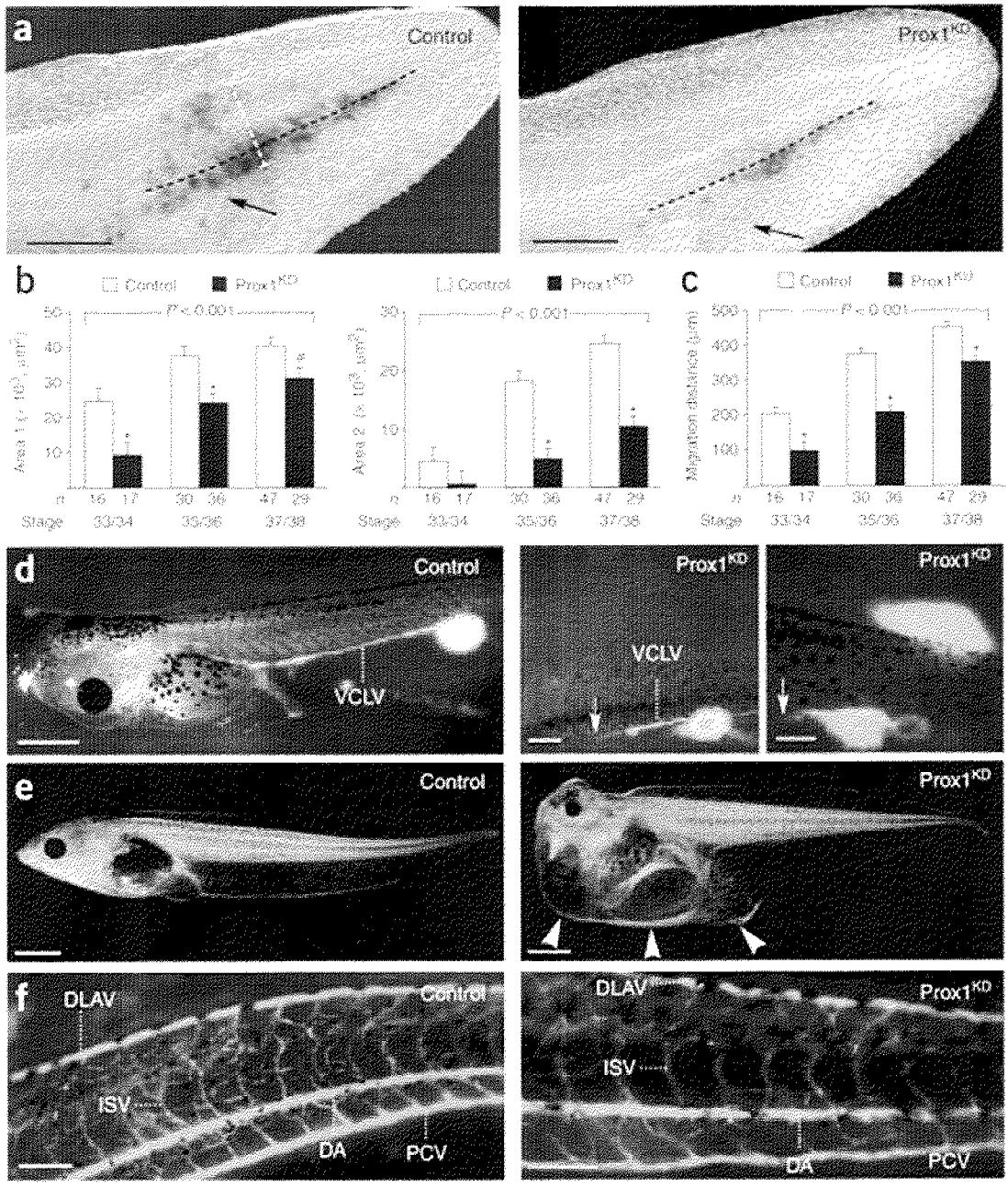

Figure 4. Impaired lymph vessel development in Prox1^{KD} tadpoles.

(**a**) Prox1 *in situ* hybridization (stage 35/36), showing fewer Prox1^{+} lymphatic endothelial cells in area 1 and 2 in the posterior trunk in Prox1^{KD}-morphant (right) than control (left) tadpoles. The black dashed line in the anteroposterior axis denotes the dorsal margin of the endoderm (separating area 1 from 2); the white dashed line in the ventrodorsal axis denotes the maximal migration distance; the rectal diverticle (arrow) is the anterior border of area 1 and 2. Scale bar, 250 µm. (**b**,**c**) Morphometric measurement of area 1 (**b**, left), area 2 (**b**, right) and the migration distance (**c**) in Prox1-stained tadpoles at the indicated stage. *P* value above the bar graphs: overall genotypic difference over the three stages (univariate analysis). * $P < 0.05$ versus control, $^{\#}$ $P = 0.058$ versus control. The number of tadpoles (*n*) is indicated. (**d**) Lymphangiography in stage 45 tadpoles, showing normal filling of the VCLV in control tadpoles, but only incomplete filling (arrow in middle panel) or no (arrow in right panel) filling in Prox1^{KD} morphant embryos. Scale bar in left panel, 1 mm; in middle and right panels, 250 µm. (**e**) Normal control stage 45 tadpole (left) versus Prox1^{KD} tadpole with severe lymphedema ('balloon disease'; arrowheads, right). Scale bar, 1 mm. (**f**) Angiography in stage 45 tadpoles, showing normal patterning, number and size of

blood vessels in the trunk of control (left) and Prox1^{KD} (right) tadpoles. Black spider dots: pigment cells. Scale bar, 100 μm.

Lymphatic defects after knockdown of VEGF-C

To further validate the tadpole model, we also knocked down the expression of VEGF-C (Supplementary Figs. 4 and 5 online). At a maximal dose (50 ng), the VEGF-C morpholino did not affect lymphatic commitment in area 1, but inhibited migration and sprouting of lymphatic endothelial cells into area 2 and thereby impaired formation of the DCLV (Fig. 5a-e). As a result, lymph vessels in VEGF-C knockdown (VEGF-C^{KD}) embryos showed various lymphangiographic defects: they were hypoplastic, had an irregular shape, slowly filled with injected dye, incompletely developed alongside the anterioposterior axis, or were simply absent (Fig. 5f). The majority of VEGF-C^{KD} embryos also developed lymphedema beyond stage 42 (2% in controls versus 81% in VEGF-C^{KD}; $P < 0.001$ by chi-squared test; Fig. 5g). Live screening further showed that blood flow in the DLAV and ISVs was disturbed, absent or reversed in VEGF-C^{KD} tadpoles. *In situ* hybridization of stage 33/34 embryos for Msr showed that up to 65 ±15% of the ISVs reached the dorsal roof in the anterior trunk in control embryos, whereas in VEGF-C^{KD} embryos, by contrast, ISVs branched from the aorta, but only 7 ±5% of them reached the dorsal roof ($P < 0.05$; Supplementary Fig. 6 online). Msr staining further showed that the vitelline vascular plexus was hypoplastic and abnormally remodeled in VEGF-C^{KD} embryos (data not shown). By angiography of stage 45 VEGF-C^{KD} embryos, the dorsal aorta and PCV were present, but ISVs were irregularly patterned, regularly missed branches and were heterogeneously dilated or thin (Fig. 5h). In addition, the DLAV, which develops from the ISVs, was incompletely formed and hypoperfused.

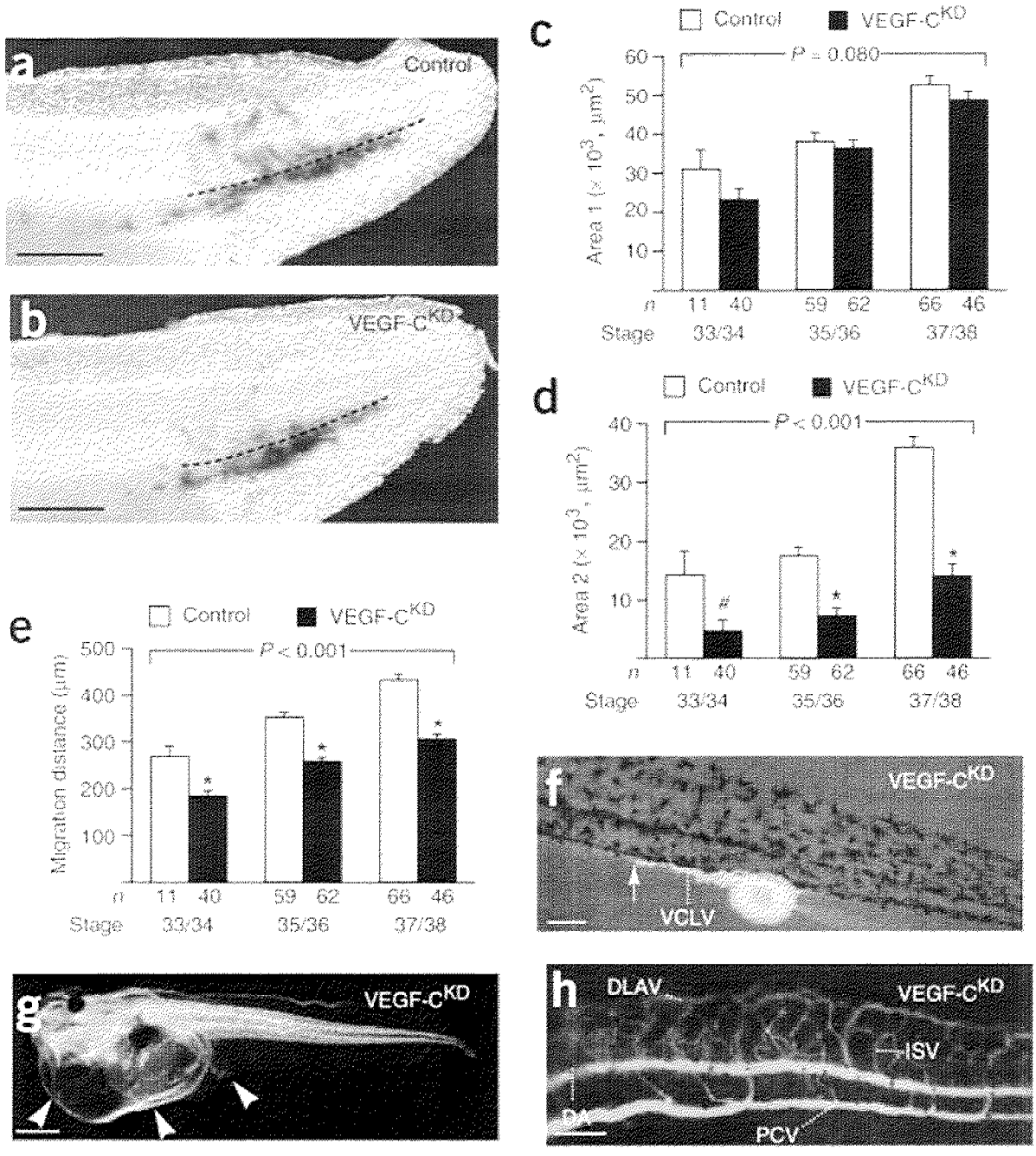

Figure 5. Impaired lymph vessel development in VEGF-C^{KD} tadpoles.

(**a**,**b**) Prox1 *in situ* hybridization of stage 35/36 tadpoles, showing fewer Prox1^{+} lymphatic endothelial cells in area 2 in VEGF-C^{KD}-morphant (**b**) than in control (**a**) tadpoles. Black dashed line indicates dorsal margin of the endoderm. Scale bar, 250 μm. (**c**–**e**) Morphometric measurement of area 1 (**c**), area 2 (**d**) and the migration distance (**e**) in Prox1-stained tadpoles at the indicated stage. *P* value above graphs: overall genotypic difference over the three stages (univariate analysis). **P* < 0.05 versus control, # *P* = 0.08. The number of tadpoles (*n*) is indicated. (**f**) Lymphangiography in stage 45 VEGF-C^{KD} tadpole, showing incomplete filling of VCLV (arrow); control is shown in Fig. 4d. Scale bar, 250 μm. (**g**) Severe lymphedema (arrowheads) in stage 45 VEGF-C^{KD} tadpole; control is shown in Fig. 4e. Scale bar, 1 mm. (**h**) Angiography in stage 45 VEGF-C^{KD} tadpoles, showing various blood vessel abnormalities: irregular size and shape of dorsal aorta (DA) and PCV, underdeveloped DLAV and misrouted, hypobranching or absent ISVs. Control is shown in Fig. 4f. Scale bar, 100 μm.

Discussion

Using morphological, molecular and functional criteria, we show here that tadpoles develop lymph vessels. Lymphatic endothelial cells have been proposed to arise by transdifferentiation from venous endothelial cells or by differentiation of lymphangioblasts—the former in mammals[12, 13], the latter in avian species[7]. In the tadpole, both mechanisms seem to contribute to lymph vessel development and can thus also be studied in this model. Furthermore, the tadpole model offers opportunities to study the role of lymphangiogenic candidates, as evidenced by the similarities in lymphatic phenotypes in knockdown tadpoles and knockout mice lacking Prox1 or VEGF-C. Indeed, similar to mice[13], Prox1 was crucial for lymphatic commitment and subsequent formation of lymph vessels in tadpoles. In VEGF-C–null mice, endothelial cells transdifferentiate to lymphatic endothelial cells, but sprouting and budding of these lymphatic endothelial cells is impaired[17]. Likewise, knockdown of VEGF-C in tadpoles did not prevent lymphatic commitment, but impaired the directional migration and budding of lymphatic endothelial cells. Moreover, similar to mice[18], loss of VEGF-D in tadpoles does not prevent the formation of a functional lymphatic vasculature (M.K. *et al.*, unpublished data).

The tadpole model also allows the simultaneous study of blood and lymph vessels—zebrafish do not offer this opportunity, as they lack lymph vessels. This is relevant, as lymphangiogenic molecules could affect angiogenesis as well. For instance, VEGF-C not only binds VEGFR-3 on lymph vessels but also VEGFR-2 (though with a lower affinity) on blood vessels[19, 20]. Whereas overexpression of VEGF-C stimulates angiogenesis[21], loss of VEGF-C did not abrogate the specification of arteries and veins in mice[17] and tadpoles. But similar to zebrafish[22], knockdown of VEGF-C in tadpoles impaired sprouting, branching and remodeling of blood vessels.

For more than a century, the morphology and function of lymph vessels have been studied in swine, dogs, cats, lizards, toads, chicken, mice and other species[6, 11, 23]. Genetics in the mouse allow a molecular dissection of lymphangiogenesis[12, 17], but the generation and phenotyping of gene-targeted mice is time-consuming, labor-intensive and still largely based on a gene-by-gene approach. The availability of a genetic tadpole model offers an unprecedented potential for future discovery of lymphangiogenic gene candidates.

Methods

For detailed methods, please see Supplementary Methods online.

Animals and morpholino injections.

We fertilized eggs of *X. laevis* frogs, dejellied them and incubated them in 0.1 ×Marc's modified Ringer's solution (10 mM NaCl, 0.2 mM KCl, 0.1 mM $MgSO_4$, 0.2 mM $CaCl_2$, 0.5

mM Hepes, pH 7.4)[24]. We injected embryos in the one-cell stage with morpholinos (Gene Tools, LLC) against the *Prox1* sequence 5'-CAGGCATCACTGGACTGTTATTGTG-3', the *Vegfc* sequence 5'-GCTCCCTCCAGCAAGTACATTTTCC-3' and the control sequence 5'-CCTCTTACCTCAGTTACAATTTATA-3'. We cultured embryos in 0.1 ×MMR at 18 °C until stage 12.5 and thereafter at 22 °C. Developmental stages of tadpoles were determined as previously described[25].

Histology, *in situ* hybridization and immunostaining.

We performed *in situ* hybridization as described[26], using digoxigenin-labeled RNA probes and BM Purple dye. Probes were: *Prox1* (nucleotides +190 to +1,139; with reference to ATG start codon); *Flt4* (encoding VEGFR-3, nucleotides -1,740 to -1 and +212 to +2,583; with reference to the first codon of the transmembrane domain; yielding similar results); *Pecam* (encoding CD31; 5' untranslated region + open reading frame), open reading frames of genes encoding Fli and Msr (gift of A. Ciau-Uitz, University of Nottingham, UK). Only antisense probes yielded specific signals. For double *in situ* hybridization, we used an additional fluorescein RNA probe and Fast red, after which we bleached tadpoles, refixed them in Memfa fixative, embedded them in 2% agarose and collected vibratome sections (40–60 μm). For immunostaining, we fixed tadpoles in Memfa fixative, embedded them in paraffin, used 0.2% trypsin to digest 10 μm sections and incubated them with a rabbit antibody to Prox1 (gift from S. Tomarev, National Eye Institute, National Institutes of Health, USA; dilution 1:50) or rabbit antibody to laminin (Sigma; dilution 1:50). We stained sections with peroxidase-labeled rabbit-specific swine IgG, and then amplified with the tyramide signal amplification system, and developed the sections with 3,3'-diaminobenzidine. We processed, imaged and performed ultrastructural analysis by transmission electron microscopy as previously described[27].

Morphometric analysis of Prox1-positive area.

We analyzed Prox1-stained areas in the tadpole tail as follows: in the anterioposterior axis, we defined each region from the location of the rectal diverticle to the tip of the tail; in the ventrodorsal axis, we defined area 1 from the ventral border of the trunk to the dorsal margin of the endoderm, and defined area 2 from the dorsal margin of the endoderm to the dorsal border of the trunk. We scored migration of lymphatic cells by measuring the maximal distance that $Prox1^+$ cells migrated from the PCV to the dorsal roof. We scored blood vessel formation by counting the percentage of fully formed Msr-positive ISVs (that is, reaching to the dorsal roof and forming a DLAV) in the anterior trunk and by angiography. All analyses were performed by investigators blinded to the genotype or experimental procedure on tadpoles matched for their stage and tail length (measured from the rectal diverticle until the tail tip). In each experiment, we always tested control and gene-specific morpholinos.

Angiography, lymphangiography and intravital video microscopy.

We anesthetized stage 42–54 tadpoles in 0.02% 3-aminobenzoic acid ethyl ester dissolved in 0.1 ×MMR and placed them on agarose gel. We performed dye injection with glass capillaries using a micromanipulator. We injected Evans Blue dye to obtain bright-field images, and tetramethyl-rhodamine-dextran (molecular weight, 2×10^6 Da) and FITC-dextran (molecular weight, 2×10^6 Da) to label functional blood and lymph vessels, respectively; we used multiphoton microscopy for imaging[28]. To measure red blood cell velocity in blood vessels, we used the line scan method. We measured lymph flow rate by taking serial images. To document red blood cell flow, we imaged stage 47 tadpoles by intravital phase-contrast video microscopy.

Statistical analysis.

We used absolute values to calculate means and s.e.m. We always compared each gene-specific morpholino to the control morpholino in every experiment. We calculated significance levels with the General Linear Model multivariate and univariate statistical model (full factorial), considering area 1, area 2 and maximal migration distance as dependent variables, and morpholino dose, morpholino type (control or gene-specific) and tadpole stage as fixed factors. For each knockdown, the overall multivariate P value was highly significant ($P < 0.001$). We used univariate analysis to determine whether the gene-specific morpholino induced a dose-dependent effect. Pairwise comparisons between the three different doses, after Bonferroni correction for multiple testing, showed that the highest dose was always significantly different from the lowest dose ($P < 0.001$). Because the highest dose of morpholino always induced the largest effect with maximal penetrance, we presented this dose in the text. We calculated overall P values over all three stages by univariate analysis for each parameter and have indicated them in the figures. The asterisks on the figures represent the genotypic difference per stage at a significance level of $P < 0.05$. To determine the degree of lymphedema, we counted the number of tadpoles exhibiting the morphant phenotype. We used chi-square analysis to determine whether this fraction differed between control and knockdown groups. We used SPSS 11.0 to perform all statistical analyses.

Note: Supplementary information is available on the Nature Medicine website.

Acknowledgments

A.N. is sponsored by a EU Sixth Framework Programme Marie Curie Intra European Fellowship; E.N. by the Fund for Scientific Research-Flanders (FWO); M.K. by the FCT (grant SFRH/BD/9349/2002, Portugal); M.S. and C.F. by the Deutsche Forschungsgemeinschaft (Germany). This work is supported, in part, by grant G.0567.05 from the FWO, by an unrestricted Bristol-Myers-Squibb grant, by a grant GOA2001/09 from Concerted Research Activities, Belgium and by grant CA-85140 from the US National Cancer Institute. The authors thank S. Tomarev and A. Ciau-Uitz for providing the rabbit anti-mouse Prox1 antibody and the *Xenopus* Fli and Msr cDNA, respectively, and K. Brepoels, A. Bouché, A. Claeys, M. De Mol, B. Hermans, S. Jansen, L. Kieckens, S. Louwette, A. Manderveld, W. Martens, L. Notebaert, A. Van Nuffelen, B. Vanwetswinkel (Leuven) and D. Fukumura (Boston) for their contribution.

References

1. Saharinen, P., Tammela, T., Karkkainen, M.J. & Alitalo, K. Lymphatic vasculature:

development, molecular regulation and role in tumor metastasis and inflammation. Trends Immunol. 25, 387–395 (2004).

2. Jain, R.K. Angiogenesis and lymphangiogenesis in tumors: insights from intravital microscopy. Cold Spring Harb. Symp. Quant. Biol. 67, 239–248 (2002).
3. Alitalo, K. & Carmeliet, P. Molecular mechanisms of lymphangiogenesis in health and disease. Cancer Cell 1, 219–227 (2002).
4. Asellius, G. Asellii Cremonensis antomici ticiensis qua sententiae anatomicae multae, nel perperam receptae illustrantur. De Lacteibus sive lacteis venis Quarto Vasorum Mesaroicum genere novo invente Gasp. (Mediolani, Milan, 1627).
5. Lawson, N.D. & Weinstein, B.M. Arteries and veins: making a difference with zebrafish. Nat. Rev. Genet. 3, 674–682 (2002).
6. Daniels, C.B. et al. Regenerating lizard tails: a new model for investigating lymphangiogenesis. FASEB J. 17, 479–481 (2003).
7. Wilting, J., Schneider, M., Papoutski, M., Alitalo, K. & Christ, B. An avian model for studies of embryonic lymphangiogenesis. Lymphology 33, 81–94 (2000).
8. Olszewski, W. Regulation of water balance between blood and lymph in the frog, Rana pipiens. Lymphology 26, 154–155 (1993).
9. Liu, Z.Y. & Casley-Smith, J.R. The fine structure of the amphibian lymph sac. Lymphology 22, 31–35 (1989).
10. Hoyer, M. Untersuchungen ueber das Lymphgefaessystem der Froschlarven. Bull. Acad. Cracov. Teill II, 451–464 (1905).
11. Sabin, F.R. On the origin of the lymphatic system from the veins and the development of the lymph hearts and thoracic duct in the pig. Am. J. Anat. 1, 367–389 (1902).
12. Wigle, J.T. & Oliver, G. Prox1 function is required for the development of the murine lymphatic system. Cell 98, 769–778 (1999).
13. Wigle, J.T. et al. An essential role for Prox1 in the induction of the lymphatic endothelial cell phenotype. EMBO J. 21, 1505–1513 (2002).
14. Devic, E., Paquereau, L., Vernier, P., Knibiehler, B. & Audigier, Y. Expression of a new G protein-coupled receptor X-msr is associated with an endothelial lineage in Xenopus laevis. Mech. Dev. 59, 129–140 (1996).
15. Cleaver, O., Tonissen, K.F., Saha, M.S. & Krieg, P.A. Neovascularization of the Xenopus embryo. Dev. Dyn. 210, 66–77 (1997).
16. Levine, A.J., Munoz-Sanjuan, I., Bell, E., North, A.J. & Brivanlou, A.H. Fluorescent labeling of endothelial cells allows in vivo, continuous characterization of the vascular development of Xenopus laevis. Dev. Biol. 254, 50–67 (2003).
17. Karkkainen, M.J. et al. Vascular endothelial growth factor C is required for sprouting of the first lymphatic vessels from embryonic veins. Nat. Immunol. 5, 74–80 (2004).
18. Baldwin, M.E. et al. Vascular endothelial growth factor D is dispensable for development of the lymphatic system. Mol. Cell. Biol. 25, 2441–2449 (2005).

19. Achen, M.G. et al. Vascular endothelial growth factor D (VEGF-D) is a ligand for the tyrosine kinases VEGF receptor 2 (Flk1) and VEGF receptor 3 (Flt4). Proc. Natl. Acad. Sci. USA 95, 548–553 (1998).
20. Joukov, V. et al. A novel vascular endothelial growth factor, VEGF-C, is a ligand for the Flt4 (VEGFR-3) and KDR (VEGFR-2) receptor tyrosine kinases. EMBO J. 15, 290–298 (1996).
21. Saaristo, A. et al. Adenoviral VEGF-C overexpression induces blood vessel enlargement, tortuosity, and leakiness but no sprouting angiogenesis in the skin or mucous membranes. FASEB J. 16, 1041–1049 (2002).
22. Ober, E.A. et al. VEGF-C is required for vascular development and endoderm morphogenesis in zebrafish. EMBO Rep. 5, 78–84 (2004).
23. Wilting, J. et al. Development of the avian lymphatic system. Microsc. Res. Tech. 55, 81–91 (2001).
24. Newport, J. & Kirschner, M. A major developmental transition in early Xenopus embryos: II. Control of the onset of transcription. Cell 30, 687–696 (1982).
25. Nieuwkoop, P.J. & Faber, J. Normal table of Xenopus laevis (Daudin): A systematical and chronological survey of the development from the fertilized egg till the end of metamorphosis (Garand Publishing, New York, 1994).
26. Harland, R.M. In situ hybridization: an improved whole-mount method for Xenopus embryos. Methods Cell Biol. 36, 685–695 (1991).
27. Carmeliet, P. et al. Urokinase-generated plasmin activates matrix metalloproteinases during aneurysm formation. Nat. Genet. 17, 439–444 (1997).
28. Padera, T.P. et al. Lymphatic metastasis in the absence of functional intratumor lymphatics. Science 296, 1883–1886 (2002).

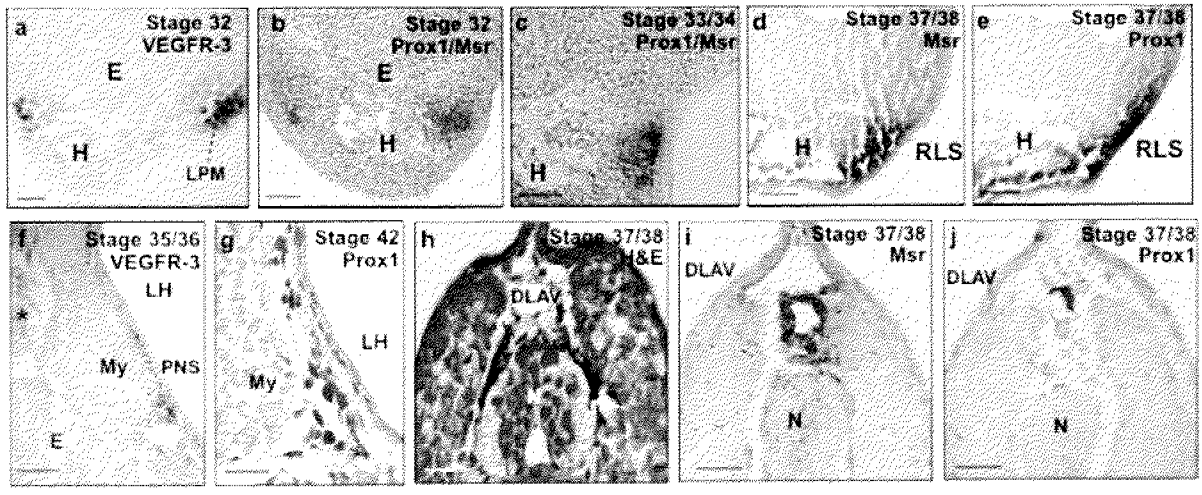

SUPPLEMENTARY FIGURE 1: Development of the rostral lymph sac and lymph heart.
a-e, Formation of rostral lymph sacs (RLS) in the head region. a, At stage 32, putative lymphangioblasts in the lateral plate mesoderm (LPM) adjacent to the heart (H) expressed VEGFR-3. E: endoderm. b,c, Double in situ hybridization for Prox1 (blue) and Msr (red) at stage 32, revealing that the LPM co-expressed Prox1 and Msr, whereas the heart region (H) expressed only Msr (panel b). From stage 33/34 onwards, Prox1-positive lymphangioblasts of the LPM became restricted to more superficial sites (panel c). d, At stage 37/38, Msr was expressed in blood vascular endothelial cells of the aortic arches close to the heart (H). e, The subectodermal compartment, where the superficial RLS form, was strongly Prox1-positive, but lost Msr expression. As expected, the myocardium was also Prox1-positive at stage 37/38. f,g, Lymphatic endothelial cells of the developing lymph heart expressed VEGFR-3 (f; in situ hybridization) and Prox1 protein (g; immunostaining). h-j, At stage 37/38, transdifferentiation of venous endothelial cells occured also in the dorsal longitudinal anastomosing vessel (DLAV). Panel h: H&E staining of a transverse section at the midgut level, revealing the DLAV dorsal of the neural tube (N). Panel i: DLAV endothelial cells expressed Msr. Panel j: Only a fraction of endothelial cells at the dorsal margin of the DLAV stained positive for Prox1. Magnification bar: 50 µm in panels d,e; 25 µm in panels a-c,f,h-j; 12.5 µm in panel g.

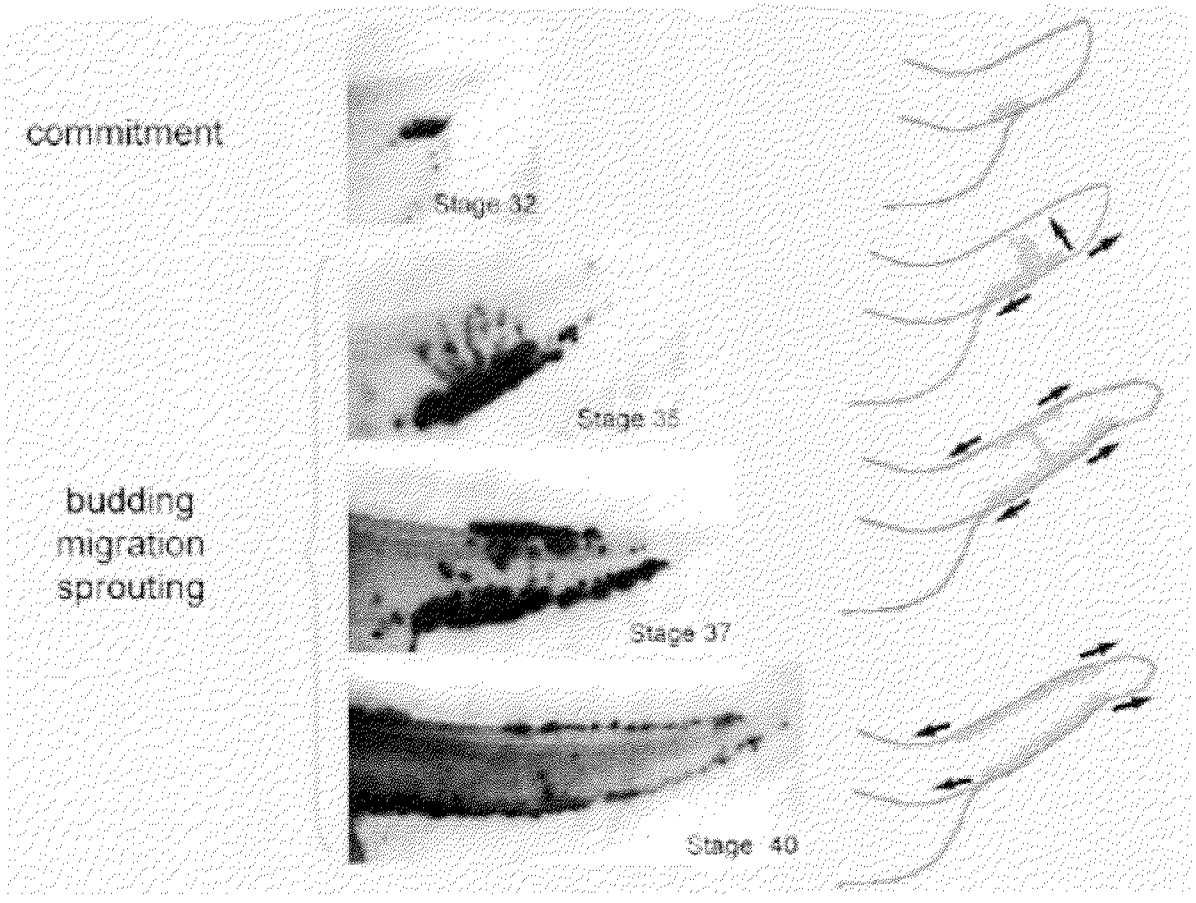

SUPPLEMENTARY FIGURE 2: Scheme of lymphatic cell migration
Whole mount in situ hybridization for Prox1, revealing the various stages of lymphatic development in the posterior trunk: commitment of Prox1-positive lymphatic endothelial cells is followed by migration of these cells, in streaks, to the dorsal roof, where they subsequently coalesce to form the DCLV. In the ventral trunk, the Prox1-positive cells coalesce to establish the VCLV. The cartoon schematically depicts these different steps. The arrows denote the migration of the lymphatic cells.

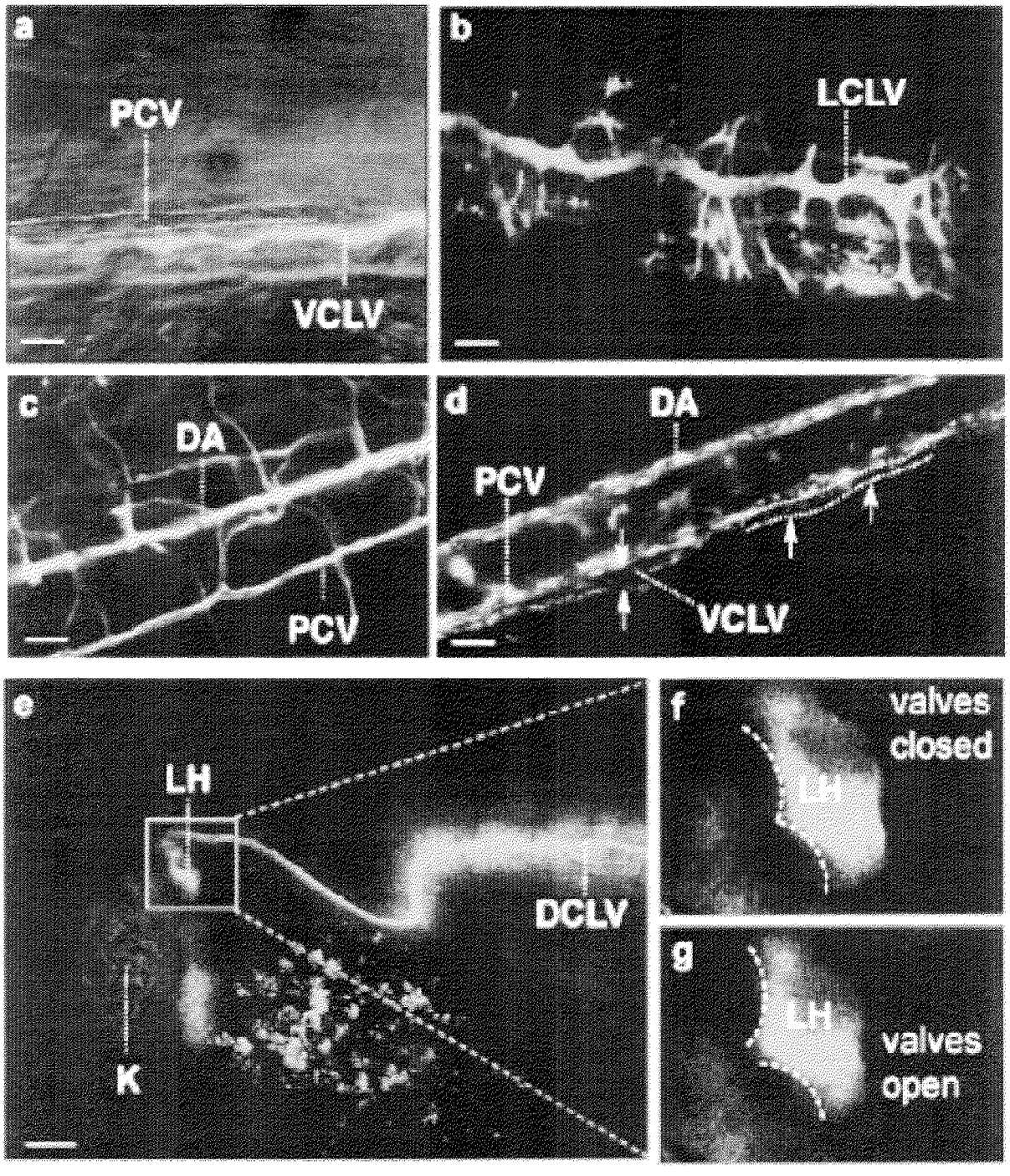
a
PCV
VCLV
b
LCLV
c
DA
PCV
d
DA
PCV
VCLV
e
LH
DCLV
K
f
valves
closed
LH
g
LH
valves
open

SUPPLEMENTARY FIGURE 3: Identity and functionality of lymph vessels and heart
a, Snap shot of Supplementary Movie 1 to indicate the position of the PCV and the adjacent VCLV, which was visualized by lymphangiography (injection of FITC-dextran). Supplementary Movie 1 shows fluorescent dye uptake by the VCLV and red blood cell flow in the PCV in a live tadpole. b, Lymphangiography with FITC-dextran, revealing the lateral caudal lymph vessel (LCLV) with numerous side branches in stage 54 tadpoles. c,d, To establish whether blood-borne macromolecules are reabsorbed by lymph vessels after leaking out from blood vessels, we intracardially injected tadpoles with Alexa 568 labeled-isolectin B4, which binds to endothelial cells but also slowly extravasates from blood vessels. Time-lapse videomicroscopy revealed that, within seconds after intracardial injection, the PCV was labeled (panel c). After 10 min, some of the extravasated Alexa568-labeled Isolectin B4 was reabsorbed by the VCLV (panel d: for clarity, a short fragment of this lymph vessel was traced by a white broken line). e, Lymphangiography with FITC-dextran, revealing the DCLV entering into the lymphatic heart (LH), which on its turn ejects the fluorescent dye into the venous Duct of Cuvier (not visible on this photo as it is hidden by the developing kidney (K)). f,g, Higher magnification snap shots of the multi-photon microscopy of the FITC-dextran lymphangiography, revealing the lymphatic heart valves (denoted by the white dashed line) in a closed (f) and open (g) state. Supplementary Movie 2 shows the ejection of the fluorescent lymph by the pumping lymph heart in a live tadpole. Notably, FITC-dextran injected in the trunk never reached the rostral head region and, conversely, when injected into the head region, the dye was never detected in the trunk, suggesting that a valve in the lymph heart prevented backflow. VCLV: ventral caudal lymph vessel; DA: dorsal aorta; PCV: posterior cardinal vein; DCLV: dorsal caudal lymph vessel; VCLV: ventral caudal lymph vessel; K: kidney. Magnification bar: 200 µm in panel e; 50 µm in panels c,d; 20 µm in panels a,b.

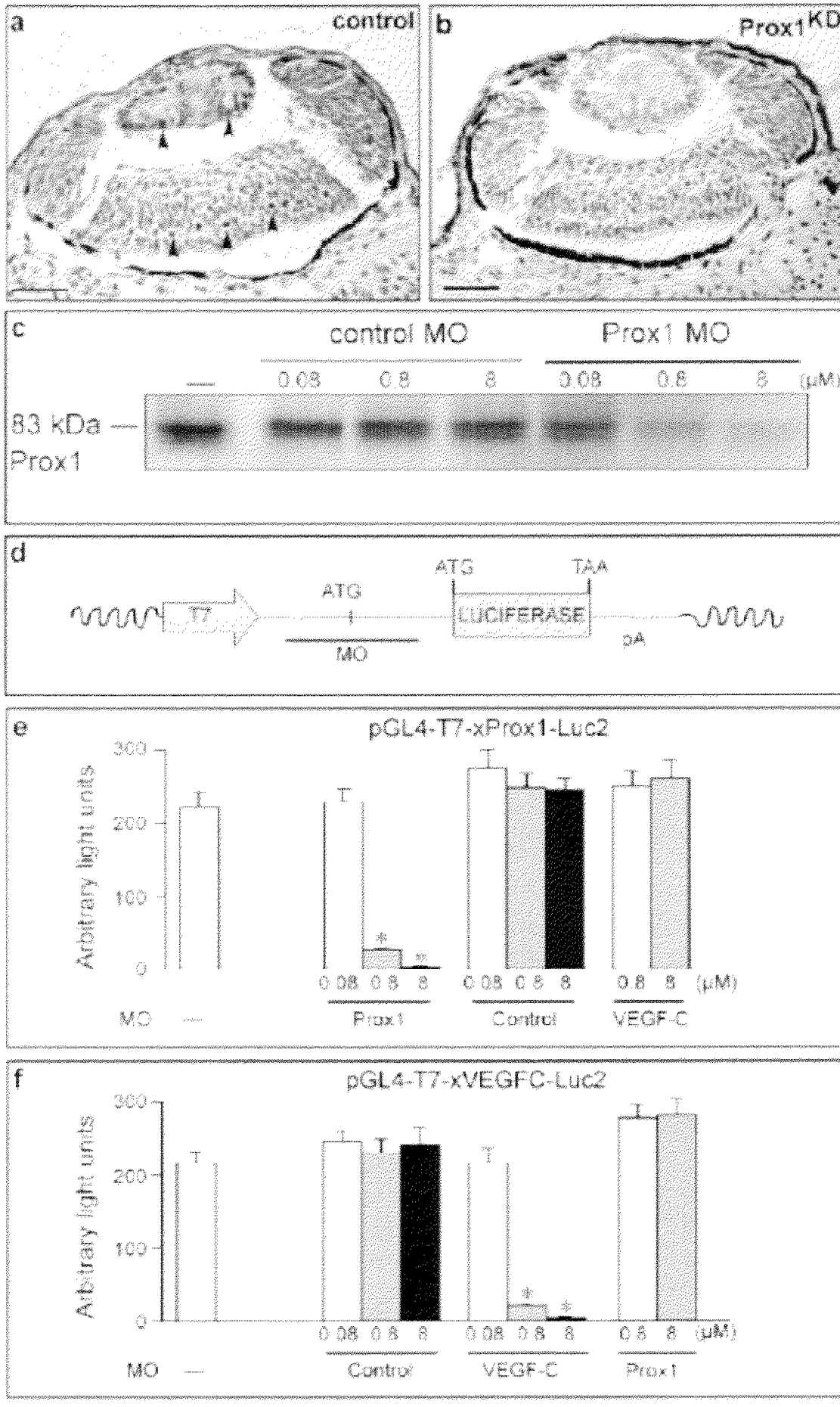
a
control
b
Prox1KD
c
control MO
Prox1 MO
0.08
0.8
8
(μM)
83 kDa
Prox1
d
T7
ATG
MO
ATG
TAA
LUCIFERASE
pA
e
pGL4-T7-xProx1-Luc2
Arbitrary light units
300
200
100
0
MO
Prox1
Control
VEGF-C
f
pGL4-T7-xVEGFC-Luc2
Arbitrary light units
MO
Control
VEGF-C
Prox1

SUPPLEMENTARY FIGURE 4: Morpholinos block translation of Prox1 and VEGF-C
a,b, Immunostaining for Prox1, revealing strong Prox1 expression in the lens epithelial cells and in the inner nuclear layer of the developing retina (arrowheads) of a stage 35/36 tadpole injected with control morpholino (*a*); in contrast, Prox1 staining is undetectable in the eye of a Prox1KD tadpole (*b*). ***c-f,*** Two methods were used to show that the morpholinos (MO), specific for Prox1 or VEGF-C, but not the control morpholino, dosedependently inhibited translation of *Xenopus* Prox1 or VEGF-C protein, respectively. ***c,*** First, the reticulocyte lysate assay (Promega) was used to translate protein, using constructs in which the T7 promotor was cloned upstream of the full length Prox1 or VEGF-C cDNA, respectively. As shown, the morpholinos, specific for Prox1, but not the control morpholino, dose-dependently inhibited translation of the *Xenopus* Prox1 protein. At the highest concentration, the gene-specific morpholino completely blocked protein expression. Presumably because of secondary RNA structures, *Xenopus* VEGF-C protein was only minimally translated, precluding reliable analysis of the activity of the morpholino (not shown). ***d,e,*** Secondly, a reporter plasmid (pGL4-T7-xProx1-Luc2; panel *d*) was constructed, consisting of, from 5' to 3', the T7 promotor, a short sequence of the *Xenopus* Prox1 sequence (33 nct upstream and 45 nct downstream of the ATG), the luciferase open reading frame and a SV40 poly-adenylation signal. Translation of pGL4-T7-xProx1-Luc2, using the reticulocyte lysate assay, resulted in the production of a chimeric protein, containing 15 amino acid residues of *Xenopus* Prox1 and an intact full length luciferase, the activity of which was used as a measure of the translation efficiency. Notably, translation of pGL4-T7-xProx1-Luc2 was dose-dependently inhibited by the Prox1 specific morpholino, but not by the control morpholino or by morpholinos specific for VEGF-C (panel *e*). ***f,*** To demonstrate that the VEGF-C morpholino inhibited translation, we cloned an analogous plasmid (pGL4-T7-xVEGFC-Luc2), containing 40 nct upstream and 34 nct downstream of the ATG of the *Xenopus* VEGF-C sequence. Translation of pGL4-T7-xVEGFC-Luc2 in the reticulocyte lysate assay resulted in high luciferase activity, which was dose-dependently inhibited by the VEGF-C specific morpholino, but not by the control morpholino or by morpholinos specific for Prox1. Magnification bar: 50 µm in panels *a,b*.

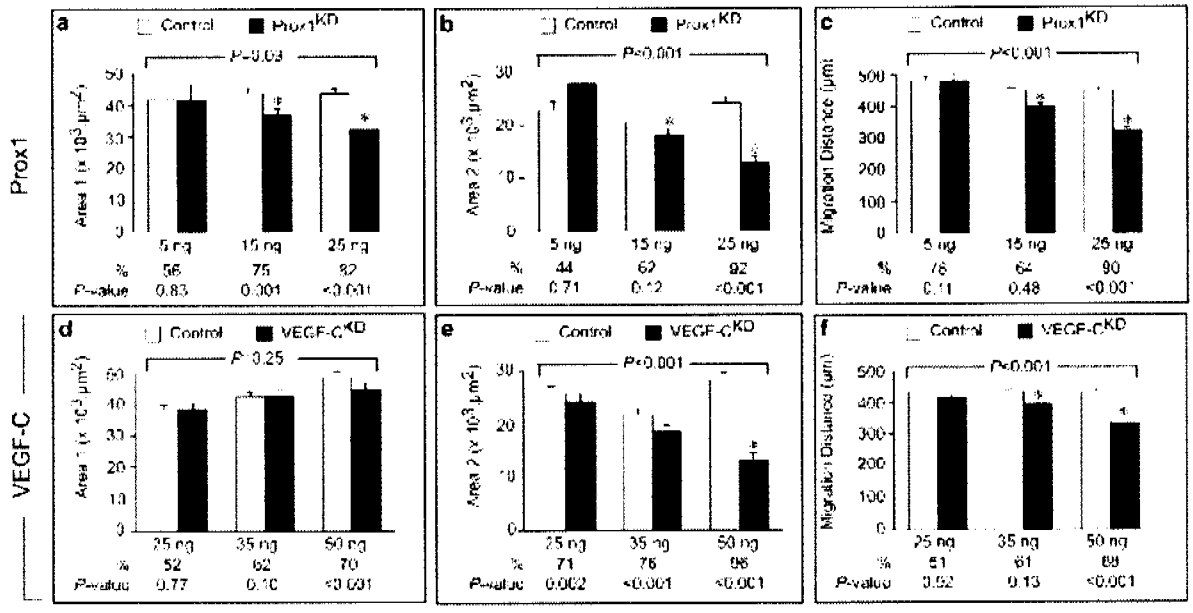

SUPPLEMENTARY FIGURE 5: Dose-dependence of Prox1 or VEGF-C knockdown
Dose-dependence pilot studies were first performed to determine the optimal dose of the Prox1 or VEGF-C morpholino, yielding the most informative and penetrant phenotype; for reasons of brevity, only the latter is shown in the main text. For all panels: The bar graphs represent the means ± SEM, as calculated by multivariate analysis of the area 1, area 2 and migration distance and considering the type of morpholino, the stage and morpholino dose as fixed factors (stage-corrected means for stage 37/38 tadpoles). The dose of morpholino is indicated below each pair of bar graphs. The *P*-value above the bar graphs denotes the overall significance of the dose-response effect. The percentage of tadpoles, exhibiting a lower value of the morphometric parameter than the average value in the control group (a measure of the penetrance of the phenotype), and the *P*-value of the Chi-square analysis comparing this percentage in control and knockdown groups, are indicated below the bar graphs. Note that the phenotype as well as its penetrance increased dose-dependently for each gene-specific morpholino. *: $P<0.05$ versus control. ***a-c,*** Dose-dependence of the Prox1 morpholino, using 240 control and 168 Prox1KD tadpoles. Injection of an increasing dose of the Prox1 morpholino dosedependently reduced area 1 and 2, as well as the maximal migration distance. ***d-f,*** Dose-dependence of the VEGF-C morpholino, using 422 control and 310 VEGF-CKD tadpoles. Injection of an increasing dose of the VEGF-C morpholino dose-dependently reduced area 2, as well as the maximal migration distance.

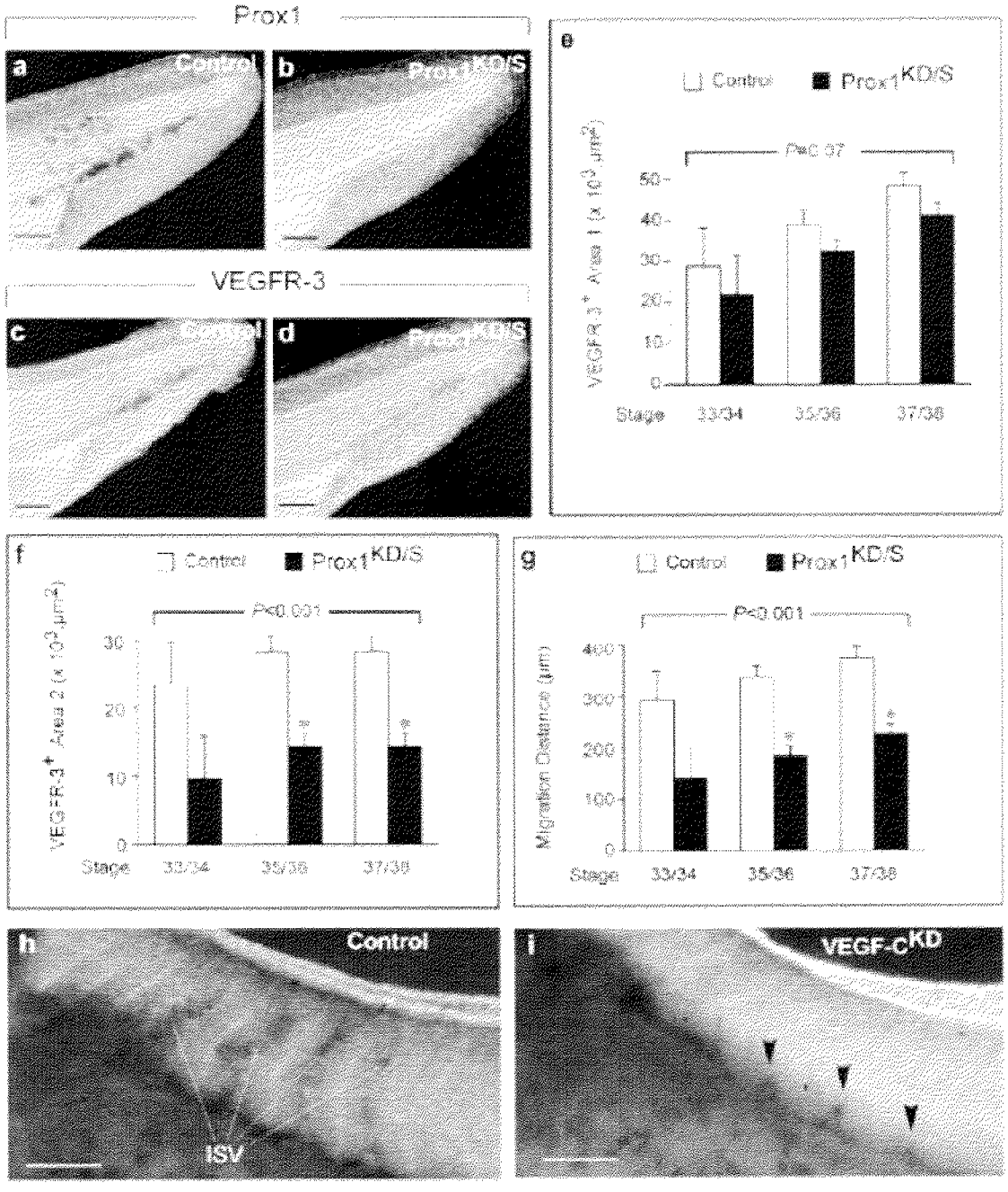
Prox1
a
Control
b
Prox1KD/S
VEGFR-3
c
Control
d
Prox1KD/S
e
Control
Prox1KD/S
P<0.01
VEGFR-3+ Area 1 (x 10³ µm²)
50
40
30
20
10
0
Stage
33/34
35/36
37/38
f
Control
Prox1KD/S
P<0.001
VEGFR-3+ Area 2 (x 10³ µm²)
30
20
10
0
Stage
33/34
35/36
37/38
g
Control
Prox1KD/S
P<0.001
Migration Distance (µm)
400
300
200
100
0
Stage
33/34
35/36
37/38
h
Control
ISV
i
VEGF-CKD

SUPPLEMENTARY FIGURE 6: Prox1 knockdown using the splice site morpholino
For panels a-g: Prox1KD/S indicates knockdown of Prox1 by the splice site morpholino. ***a,b,*** In situ hybridization for Prox1: Prox1 expression is detectable in tadpoles, injected with control morpholino, but undetectable in tadpoles after injection of 25 ng splice site Prox1-specific morpholino, indicating that this morpholino lowered *Xenopus* Prox1 mRNA levels. RT-PCR analysis of RNA, extracted from tadpoles, confirmed that *Xenopus* Prox1 mRNA levels were reduced by the splice site morpholino (copies Prox1 per 103 copies elongation factor-1alpha: 3.9 ± 0.5 for control versus 0.02 ± 0.01 for morpholino; $P<0.05$). The following primers were used for qRT-PCR of Prox1: forward primer: 5'-gtcggagtgcggagacatg-3'; reverse primer: 5'-ggccttttcaagtgatttgga-3'; probe: 5'-FAMaagatatgtctgatatctcaccttattcgggaagtgc-TAMRA-3'; for elongation factor-1 alpha: forward primer: 5'-gaaccatcgaaaagttcgagaag-3'; reverse primer: 5'-tccaagacccaggcatacttg-3'; probe: 5'-FAMaggagccttttcccatctcagcagctt-TAMRA-3'. ***c-g,*** As the Prox1 splice site morpholino reduced Prox1 mRNA levels, in situ hybridization for VEGFR-3 was used to identify the lymphatic endothelial cells. Injection of a maximal dose of the Prox1 splice site morpholino did not affect area 1 in the posterior tail (*d,e*), but significantly reduced area 2 (*d,f*) and the migration distance (*d,g*) of the VEGFR3-positive lymphatic endothelial cells. The effect on area 1 is only borderline significant (p=0.07), presumably because Prox1 knockdown does not affect blood vessel development and VEGFR-3 marks both lymphatic and blood vascular endothelial cells. Presumably, the VEGFR3-positive cells in area 2 represent a more pure population of lymphatic endothelial cells. *P*-values above each panel: the statistical significance of the univariate analysis; *: $P<0.05$ versus control. These defects were functionally important, as Prox1KD/S tadpoles developed lymphedema by stage 45. ***h,i,*** In situ hybridization for Msr, revealing that sprouting ISVs reached the dorsal floor plate, where they branched and formed the DLAV in control embryos at stage 33/34 (panel *h*). In contrast, ISVs (arrowheads) failed to reach the dorsal roof and to form the DLAV in morphant VEGF-CKD embryos by stage 33/34 (panel *i*). Bar: 250 µm in panels *a-d*; 100 µm in panels *h,i*.

SUPPLEMENTARY NOTE: To analyze whether the Prox1 morpholino affected Prox1 mRNA transcript levels, human embryonic kidney 293 cells, which endogenously express Prox1, were transfected with a Prox1 morpholino, by electroporation using the Easyject+ device of EquiBio (Immunosource, Belgium; single pulse of 250 V, 750 µF; 4 mm cuvette; 20 µM morpholino). After 36 hours, mRNA levels of human Prox1 were quantified by RT-PCR using the following primers for Prox1: forward primer: 5'-gtgctttggcgacgtcatc-3'; reverse primer: 5'-tcagtggaactggccatctg-3'; probe: 5'-FAM-ttccgaacccccctggacacctttg-TAMRA-3'; and for GADPH: forward primer: 5'-ccacccatggcaaattc-3'; reverse primer: 5'-tgggatttccattgatgac aag-3': probe: 5'-FAM-cgttctcagccttgacggtgcca-TAMRA-3'): mRNA copies Prox1 per 103 mRNA copies GAPDH were: 3.2 ± 0.3 after control morpholino versus 4.7 ± 0.3 after Prox1ATG morpholino(*P*=NS).

SUPPLEMENTARY METHODS

Animals and morpholino injections

Sexually mature adult frogs were purchased from Nasco Biology (Fort Atkinson, WI). *Xenopus* eggs were fertilized by standard methods 24, dejellied with 2% cysteine (pH 8.0), rinsed and incubated in 0.1 x MMR (10 mM NaCl, 0.2 mM KCl, 0.1 mM MgSO4, 0.2 mM CaCl2, 0.5 mM Hepes, pH 7.4). One cell stage embryos were placed in 1 x MMR containing 5% Ficoll, and injected with various doses of specific or control morpholino (Gene Tools, LLC). The morpholino oligonucleotides were designed based on published GenBank *Xenopus laevis* sequences of Prox1 (#AB008773) and VEGF-C (#CA973641); when unavailable, the upstream sequence up to the ATG start codon was obtained by 5' RACE. Sequences of the morpholinos, targeted to the sequence around the ATG start codon, were: for xProx1: 5'-CAG GCA TCA CTG GAC TGT TAT TGTG-3'; xVEGF-C: 5'-GCT CCC TCC AGC AAG TAC ATT TTCC-3'; and standard control morpholino: 5'-CCT CTT ACC TCA GTT ACA ATT TATA-3'. The sequence of the splice site Prox1 morpholino was 5'-AGC CAG GTT ACT TAC TCA GGG AAAG-3'. One hour after injection, embryos were transferred to 0.1 x MMR and cultured at 18°C until they reached stage 12.5, whereafter embryos were grown at 22°C. Live screening of general development, heart beating, blood flow and the presence or absence of edema was performed by inspection of tadpoles at various stages using an inverted microscope (Zeiss). Developmental stages of tadpoles were determined according to the published table of *Xenopus laevis* development [25].

Histology, in situ hybridization and immunostaining

For in situ hybridization, embryos were fixed in Memfa fixative and used for whole-mount in situ hybridization, according to Harland's protocol [26]. RNA probes were labeled with digoxigenin and BM-purple staining dye (1442074; Roche) was used as substrate. For double in situ hybridization, we used an additional fluorescein RNA probe and Fast red (1496549 Roche). The following orthologue *Xenopus* sequences were used as probes: Prox1 (nct +190 till +1139; in reference to ATG start codon); VEGFR-3 (fragment –1740 to –1 and fragment + 212 till +2583; in reference to the first codon of the transmembrane domain; yielding similar results); CD31 (5'UTR + open reading frame), Fli (open reading frame; gift of Dr. A. Ciau-Uitz) and Msr (open reading frame; gift of Dr. A. Ciau-Uitz). After in situ hybridization, the embryos where bleached, cleared and stored in glycerol until further analysis. Only antisense (not sense) probes yielded specific signals. For morphological analysis of tadpole sections after in situ hybridization, embryos were rinsed in PBS to remove the glycerol, dehydrated in graded series of ethanol, embedded in paraffin and cut into 10 µm transverse sections, which were counterstained with nuclear fast red. After double in situ hybridization, tadpoles were bleached, refixed in Memfa fixative (overnight at 4°C or 2 hrs at room temperature), washed with PBS and embedded in 2% agarose. Vibratome sections (40-60 µm) were collected on microscope slides and mounted in PBS. For immunostaining, tadpoles were fixed in Memfa fixative overnight at 4°C or 2 hrs at room temperature, dehydrated, embedded in paraffin, and sectioned at 10 µm thickness. After deparaffinization and rehydration, sections were digested with 0.2% trypsin (Sigma), blocked and incubated overnight with a rabbit anti-mouse Prox1 antibody (gift from Dr. S. Tomarev; dilution 1/50) or with a rabbit anti-laminin (Sigma; dilution 1/50). Sections were subsequently incubated with peroxidase-labeled swine anti-rabbit IgG, followed by amplification with the tyramide signal amplification system (Perkin Elmer, Life Sciences). Sections were developed with 3,3'-diaminobenzidine (DAB, Sigma) as a chromogen substrate and counterstained with Harris Hematoxilin. Microscopic analysis was performed with a Zeiss Axioplan 2 imaging microscope. For whole mount immunostaining, tadpoles were fixed in ice-cold Dent's fixative (20% DMSO, 80% methanol), blocked with 2% TBS/BSA and incubated overnight with a rabbit antihuman vWF antibody (Dako; dilution 1/100), followed by FITC-labeled goat anti-rabbit IgG (Rockland Immunochemicals). Embryos were then extensively washed with PBS-Tween and visualized on a Zeiss Axioplan 2 imaging microscope or a Zeiss LSM510 confocal laser scanning microscope. Processing, imaging and ultrastructural analysis by

transmission electron microscopy was performed as described [27].

Morphometric analysis of Prox1-positive area

Analysis of Prox1-stained areas after whole mount in situ labeling was performed in the tail of the tadpoles using a Zeiss Axioplan 2 imaging microscope, equipped with a Axiocam HrC camera and KS300 morphometry software (Zeiss). The development of lymphatic structures was quantified by measuring the area containing Prox1-positive cells in two regions, defined as follows: in the anterio-posterior axis, each region was defined from the location of the rectal diverticle to the tip of the tail; in the ventro-dorsal axis, area 1 was defined from the ventral border of the trunk to the dorsal margin of the endoderm (a readily recognizable anatomical reference structure upon microscopic inspection), while area 2 was defined from the dorsal margin of the endoderm to the dorsal border of the trunk. Migration of lymphatic endothelial cells was scored by measuring the maximal distance, which the Prox1-positive cells had migrated from the PCV towards the dorsal roof. Blood vessel formation was scored by counting the percentage of fully formed Msr-positive ISVs (i.e. reaching to the dorsal roof and forming a DLAV) in the anterior trunk and by angiography (see below). All analyses were performed by investigators, blinded for the genotype or experimental procedure, on tadpoles, matched for their stage and tail length (measured from the cloaca until the tail tip, fin excluded). In each experiment, control and gene-specific morpholinos were always tested.

Angiography, lymphangiography and intravital video-microscopy

For angiography and lymphangiography, stage 42-54 tadpoles were anesthetized in 0.02% of 3-aminobenzoic acid ethyl ester (MS-222: Sigma, St. Louis, Missouri), dissolved in 0.1x MMR, and placed on Agarose gel in a petri-dish. Glass capillaries were pulled with a micropipette puller (Narishige, Japan), broken at a tip size of 20 µm under light microscopy and sharpened for 30 minutes using a micropipette beveller (Sutter Instrument, California). Dye injection was performed using a micromanipulator at a rate of 0.5 µl/min. Evan's Blue Dye (Sigma) was injected to obtain bright field images, and tetramethylrhodamine-dextran (Mr 2x106 Da) and FITC-dextran (Mr 2x106 Da) were injected to label functional blood and lymph vessels, respectively. The fluorescent images, obtained within 10 minutes of injection to avoid extravasation, were either captured by a digital camera through the eyepiece or by using multi-photon microscopy [28]. To measure red blood cell velocity in blood vessels, the line scan method was used. Lymph flow rate was measured by taking serial (temporal) images of lymph vessels immediately after injection. To analyze whether lymph vessels reabsorbed extravasated macromolecules, anesthesized stage 45-47 tadpoles were injected intracardially with Alexa568-labeled Isolectin B4 (Molecular Probes) and fixed in Dent's fixative immediately (i.e. before the dye extravasated) or after 10 min (i.e. when the extravasated dye was reabsorbed by the lymph vessels). Embryos were then analysed by fluorescent microscopy (Axioplan 2 imaging microscope). To document red blood cell flow in blood vessels, anesthetized stage 47/48 tadpoles were imaged by intravital phase-contrast videomicroscopy, using a Plan NeoFluar 20x PH2-objective (Zeiss) on an Axioplan 2 imaging microscope (Zeiss), to which a Digital Handycam (Sony) was attached for image acquisition. Final video-editing was performed using the Final Cut Express software (Apple).